ICR

ANNUAL REPORT 1999

Kyoto University
Institute for Chemical Research

Volume 6

***ICR* ANNUAL REPORT 1999 (Volume 6)**
For the calendar year 1 January 1999 to 31 December 1999

Editors:
Professor Toshinobu YOKO (Editor in chief)
Professor Minoru KANEHISA
Professor Nobuyoshi ESAKI

Managing editor:
Haruo NAKAGAWA

Published and distributed by:
Institute for Chemical Research (*ICR*), Kyoto University

Note: *ICR* Annual Report available from the *ICR* Library,
Institute for Chemical Research, Kyoto University,
Uji, Kyoto 611-0011, Japan.
Tel: +81-(0)774-38-3009
Fax: +81-(0)774-38-4370

ISSN 1342-0321

Printed by
Nakanishi Printing Co., Ltd.
Shimodachiuti-dori Higashi-iru, Kamigyo-ku, Kyoto 602-8048, Japan.
TEL:+81-(0)75-441-3155. FAX:+81-(0)75-417-2050;441-3159.
E-mail:info@nacos.com
HP URL http://www.nacos.com/

31 March 2000

Front cover

The figures shown on the front cover represent a schematic diagram of Gas Scintillation Proportional Counter (hereafter abbreviated as GSPC) and pulse height spectra (Mn Kα, β) obtained by GSPC. The GSPC is a parallel-mesh type one as shown schematically in the upper figure. The instruments and conditions in experimental are presented in Table1. The entrance window consists of 50 μm thick Be of 30 mmø area. The outer surface of Be is coated with a dotite for electrical conductivity. The counter is filled with Xe gas which is introduced for the purification for rare gases.

An X-ray photon absorbed in the first region produces a cluster of primary electrons. Theseelectrons drift towards the first mesh held at a potential V_1. This region is called the drift region. In the second region, the electrons are accelerated towards the second mesh at a potential V_2, and generate a number of photons, whose total number is proportional to the energy of the incoming X-ray photon. This is called the accelerating region. The performance of the counter is determined by the high voltage values V1 and V2 and the gas pressure p. We operate the counter with V_1 = 340 V, V_2 = 5660 V and p = 1.5 atm. As an X-ray source, Mn K X-rays (Radio-Isotope ^{55}Fe) were used. In the laboratory, GSPC has been developed for the observations of the fluorescence x-rays below 1 keV.

CONTENTS

Preface

In 1999, the first transplant of an organ from a brain-dead donor was performed since the Organ Transplant Law was passed. This has brought science under scrutiny from the ethical side. As well as the leading edge such as information, life sciences, and earth sciences, science and technology for mankind and for a better society and quality of life probably become to active field of development.

The government's plan to turn national universities into "agencies" provides that they are allowed to continue to give priority to education and research. The move would add Japan's 99 national universities to a list of government-run institutions including national museums and research institutes, that are transformed into semiautonomous agencies. The plans are part of the government's bid to increase administractive efficiency by placing the institutions under the control of a separate management system. Rather than complying with the government's agency bill, which sets targets based on the rationalization plan, Monbusho is asking for a separate bill for universities to maintain the standard of research and education. According to the proposed bill, performance-related targets would be reviewed every five years, and the evaluation would be carried out by an independent assessment body that Monbusho plans to set up this April. Indeed, this plan is serious problem as for national universities.

The ICR Annual Report continues to strive to provide timely and important information on the scientific activities of the ICR. At the end of March, 1999, Professor A.Ohno of the Laboratory of Bioorganic Reaction Theory retired from the ICR and was appointed to a Professorship at Fukui Technology University. Professor M.Matsui of the Laboratory of Separation Chemistry, who has contributed a great deal to environmental protection of the ICR, also retired from the ICR. In addition, Professor M.Inoue of the Laboratory of Beams and Fundamental Reactions moved to the Research Reactor Institute as Director, and Professor S.Takahashi of the Laboratory of Biopolymer Structure moved to Kyoto Women's University. We have appointed Drs. S.Goto and K.Mibu as Associate Professors of the ICR. At the present stage, 23 full professors. 27 associate professors, and 39 instructors work in the ICR, and about 240 graduate students study at the ICR.

Finally, I would like to congratulate Professor K.Tamao for the Chemical Society of Japan Award, and also Associate Professor J.Hiratake for the Japan Bioscience, Biotechnology and Agrochemistry Society Award for the Encouragement of Young Scientists.

January, 2000

Yukio Sugiura
DIRECTOR

TOPIC AND INTRODUCTORY COLUMNS OF LABORATORIES

Key to headline in the columns

RESEARCH DIVISION – Laboratory (Subdivision)*

*** See also "Organization and Staff" on pages 90 and 91.**

Abbreviations used in the columns

Prof Em	Professor Emeritus
Prof	Professor
Vis Prof	Visiting Professor
Assoc Prof	Associate Professor
Lect	Lecturer
Lect(pt)	Lecturer (part-time)
Instr	Instructor
Assoc Instr	Associate Instructor
Techn	Technician
Guest Scholar	Guest Scholar
Guest Res Assoc	Guest Research Associate
Univ	University

GS	Graduate Student
DC	Doctor Course (Program)
MC	Master Course (Program)
UG	Undergraduate Student
RF	Research Fellow
RS	Research Student

D Sc	Doctor of Science
D Eng	Doctor of Engineering
D Agr	Doctor of Agricultural Science
D Pharm Sc	Doctor of Pharmaceutial Science
D Med Sc	Doctor of Medical Science

Development of Gas Scintillation Proportional Counter

Nobuyuki Shigeoka, Kohei Mutaguchi, Yoshikazu Nakanishi, Yoshiaki Ito and Takeshi Mukoyama

Properties of gas scintillation proportional counter are investigated for Mn K X-ray spectra. The energy resolution (8.9%) on this type of the counter has twice as good as that (19%) of Xe gas sealed proportional counter. In the counter, a distortion of the pulse-height distribution due to a low-energy tail is observed. This fact can be attributed to the penetration of high energy X-rays in the accelerating region. Therefore, it is considerable that the tail may be enhanced for higher energy photons.

Keywords:Gas Scintillation / Proportional counter / Mn K X-ray / Pulse-height distribution

Proportional counters have been most commonly used in various field of research due to the structural simplicity and the high quantum efficiency. The energy resolution of the proportional counter is about 40 % and insufficient for resolving characteristic emission lines for Al Kα. On the other hand, X-ray spectrometers are limited in use for wavelength dispersion. Therefore, gas scintillation proportional counters (hereafter abbreviated as GSPC) have a good potential for X-ray characteristics in the material sciences and X-ray astronomy. The physical processes which underlie the functioning of the GSPC are described elsewhere[1].

We have developed GSPC for the observations of the fluorescence X-rays below 1 keV. This energy region including L emission lines in 3d elements is recently being watched with keen interest. In this paper, we present the properties of Xe gas sealed proportional counter (as PC) and GSPC for Mn K X-rays. A distortion of the pulse-height distribution in low energy side appeared in GSPC. This phenomenon is discussed.

The GSPC used in this work is a parallel-mesh type one as shown schematically on **Figure 1**. The entrance window consists of 50μm thick Be of 30mm ϕ area. The outer surface of Be is coated with a dotite for electrical conductivity. The counter is filled with Xe gas which is purification for rare gases.

An X-ray photon absorbed in the first region produces a cluster of primary electrons. These electrons drift to-

STATES AND STRUCTURES — Atomic and Molecular Physics —

Scope of Research

In order to obtain fundamental information on the property and structure of materials, the electronic states of atoms and molecules are investigated in detail using X-ray, SR, ion beam from accelerator and nuclear radiation from radioisotopes. Theoretical analysis of the electronic states and development of new radiation detectors are also performed.

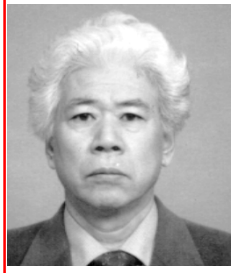

Professor
MUKOYAMA,
Takeshi
(D ENG)

Assoc. Prof
ITO,
Yoshiaki
(D Sc)

Instructor
KATANO,
Rintaro
(D Eng)

Instructor
NAKAMATSU,
Hirohide
(D Sc)

students:
YAMAGUCHI, Koichiro
SHIGEMI, Akio (DC)
TOCHIO, Tatsunori (DC)
VLAICU, A. Mihai(DC)
MASAOKA, Sei (DC)
ITO, Kunio (MC)
SHIGEOKA, Nobuyuki (MC)
MUTAGUCHI, Kohei (MC)
OHASHI, Hirofumi (MC)
NAKANISHI, Yoshikazu (RF)

wards the first mesh held at a potential V_1. This region is called the drift region. In the second region, the electrons are accelerated towards the second mesh at a potential V_2, and generate a number of photons, whose total number is proportional to the energy of the incoming X-ray photon. This is called the accelerating region. The performance of the counter is determined by the high voltage values V_1 and V_2, the gas pressure p[2]. We operate the counter with V_1=340 V, V_2=5660 V and p=1.5 atm. These values were constant during the course of the present study. As an X-ray source, Mn K X-rays (Radio-Isotope ^{55}Fe) was used. A sealed PC was prepared in this work for a comparison. A mixture of 97% Xe and 3% CO_2 at 250 torr was used for PC.

Mn K X-rays were used in order to evaluate the properties of the GSPC and PC.Pulse-height spectra for almost mono-energetic X-ray taken with the GSPC and PC are shown in **Figure 2**. The pulse-height spectrum is expressed in keV. Relative intensity and FWHM of Mn K photon energies are presented in **Table 1**. From this table, it is found that GSPC has twice as good an energy resolution as that of PC.

A characteristic feature in GSPC is that the pulse-height spectra reveal a taiil towards lower pulse-heghts as seen in **Figure 2** and **Table 1**. This phenomenon is not observed in PC. It is considerable that the tail may be attributed to the penetration of X-rays, and also influence the peak position of the spectrum in the fitting method.

The fact gives the suggestion that the high energy photons pass through the drift region and reach the accelerating region. Therefore, in near future, we attempt to explain the phenomenon in terms of the variation in the drift and acceleraing region.

References

1. R.D.Andresen, E.A.Leimann and A.Peacock: *Nucl.Instr.Meth.*,**140**,371(1977)
2. H.Inoue, K.Koyama, M.Matsuoka. et al.: *Nucl.Instr.Meth.*,**157**,295(1978)

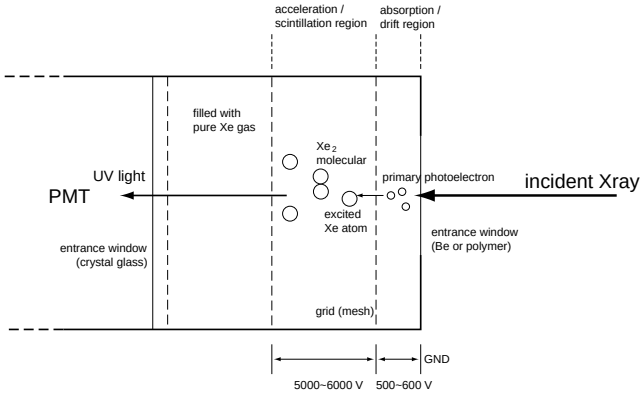

Figure 1. Schematic Diagram of GSPC

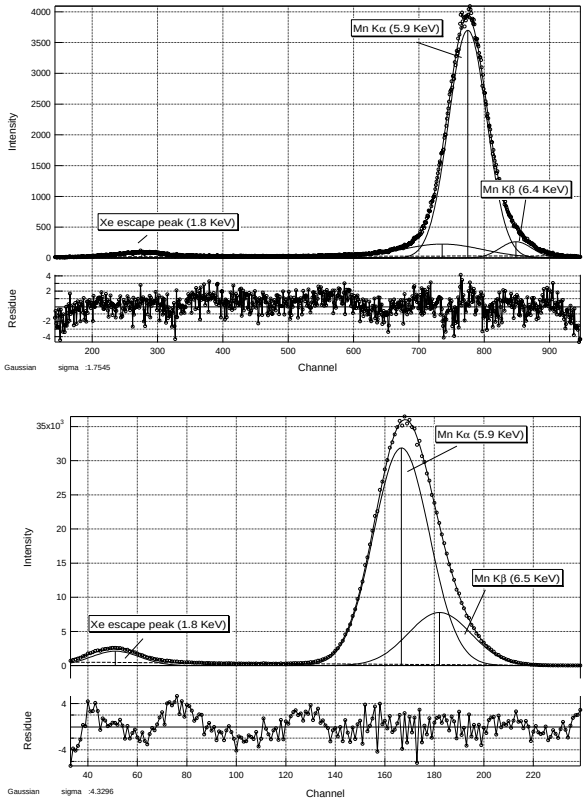

Figure 2. Pulse-height spectrum obtained by GSPC (up) and Sealed PC (down)

Detector	Peak (split by gaussian fitting)	FWHM (channel)	Relative Intensity(Integral)
GSPC	Mn Kα	8.9 %	100
	Mn Kβ	6.7 %	5.9
	Xe escape peak	33 %	2.5
	low energy tail	20 %	13
SPC	Mn Kα	16 %	100
	Mn Kβ	16 %	27
	Xe escape peak	45 %	5.7

Table 1. FWHM and relative intensity of eachpeak obtained by GSPC and Sealed PC

TEM Analysis of Pt-particles Embedded on TiO_2 Exhibiting High Photocatalytic Activity

Masahiko Tsujimoto, Sakumi Moriguchi, Seiji Isoda, Takashi Kobayashi and Teruo Komatsu

For fine particles of semiconductive rutile TiO_2 supporting ultra-fine particles of Pt which were prepared by decomposing a colloidal organic-Pt complex, the structural aspects of the high photoactivity were examined by high resolution imaging, X-ray mapping by energy dispersive spectroscopy and electron energy-loss spectroscopy. As a result, the Pt particles with nm-sizes were found to grow epitaxially on rutile, which supports an expected mechanism that the photo-excited electrons efficiently transfer from TiO_2 to Pt and promote the reduction of O_2 to O_2^-.

Keywords: Decomposing organic-platinum colloid/ Epitaxial growth/ Analytical electron microscopy

A photocatalytic reaction is induced at surfaces of semiconductors being related with the generation of electrons and holes photo-excited by light irradiation. Their high chemical activities cause reduction or oxidation of reaction system. In the photocatalytic effect of the semiconductor, the activity usually increases with increasing surface area, and also it is possible to improve the reaction rate and the selectivity of reaction by changing metal species [1].

The effect of embedding of metal particles is considered to depend on the exchange of the electron or the positive hole at the boundary between the semiconductor surface and metal particle. Recently Komatsu *et al*. have proposed a new method to embed fine metal particles on TiO_2 by decomposing colloidal organic-metal complexes [2]. The enhancement in photocatalytic activity was considered to be due to the increase in numbers of surface reaction sites, and also the photo-excited electrons transfer mainly from TiO_2 to metal at the surface of ultra-fine particles. However, the boundary structure has not been made clear. Therefore, in the present study, the Pt ultra-fine particles embedded on TiO_2 were studied by transmission electron microscopy (TEM) including high resolution imaging (HR-imaging), elemental mapping by energy-dispersive X-ray spectroscopy and electron energy-loss spectroscopy analyses.

The TiO_2 embedded with ultra-fine particles of Pt was prepared following the decomposing method already reported [2]. HR-images were taken with a high resolution high voltage TEM (HRHVTEM, JEOL ARM-1000) and elemental mapping with characteristic X-ray was carried out with a JEM-2010F scanning transmission electron microscope (STEM) equipped with a field emission gun at 200kV. Electron energy-loss spectroscopy (EELS) and

STATES AND STRUCTURES — Crystal Information Analysis —

Scope of research

Structures of materials and their structural transition associated with chemical reactions are studied through the direct observation of atomic or molecular imaging by high resolution spectro-microscopy. It aims to explore new methods for imaging with high resolution and for obtaining more detailed chemical information. The following subjects are studied: direct structure analysis of ultrafine crystallites and ultrathin films, crystal growth and adsorption states of organic materials, and development on high resolution energy filtered imaging as well as electron energy-loss spectroscopy.

Prof KOBAYASHI, Takashi (D Sc)

Assoc Prof ISODA, Seiji (D Sc)

Instr OGAWA, Tetsuya (D Sc)

Instr NEMOTO, Takashi (D Sc)

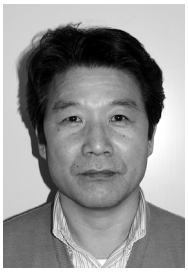

Assoc Instr MORIGUCHI, Sakumi

Students:
KUWAMOTO, Kiyoshi (DC)
KOSHINO, Masanori (DC)
YAJI, Toyonari (DC)
SUGA, Takeo (DC)
FUJIWARA, Eiichi (DC)
TSUJIMOTO, Masahiko (MC)
YOSHIDA, Kaname (MC)
FURUKAWA, Chieko (MC)
ADACHI, Yoshio (MC)
KANEYAMA, Syutetsu (MC)
HASEGAWA, Yuko(MC)

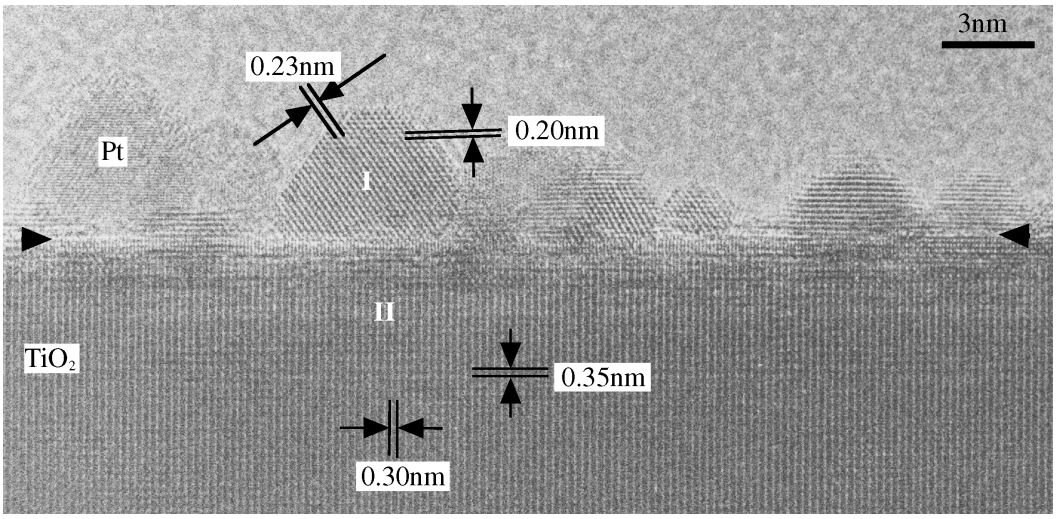

Figure 1. A typical HR-image taken along the [110] of rutile TiO_2, on which the Pt particles are concluded to grow epitaxially. The (110)-plane surface of TiO_2 is indicated with the horizontal two arrowheads.

energy filtered imaging were carried out with a GIF attached to the HRHVTEM.

From TEM observation, the TiO_2 particles were found to be embedded with smaller Pt particles of about 3nm. The specimen was examined with a STEM, EELS and energy filtered-image with a GIF in HRHVTEM to analyze the elemental distribution in the specimen.

The structure of the boundary between the TiO_2 particle and the embedded Pt particle was observed by HR-imaging (Fig. 1). The image is a projection of rutile TiO_2 along the [110], whose (110)-surface indicated by the two black arrowheads is almost parallel to the incident electron beam. In this case, all observed Pt particles are embedded on the (110)-surface of TiO_2. In the Pt particles, lattice fringes with the spacings of d=0.23nm and 0.20nm are observed, which correspond to the (111)- and (002)-spacings of f.c.c. Pt, respectively. Based on the above results, the orientation of the Pt particles in the figure is almost along the [110]-projection of f.c.c. Pt. On the other hand, in the TiO_2, the lattice fringes of d=0.30nm and 0.35nm are observed, which correspond to the lattice spacing of (001)- and (110)-planes of rutile TiO_2, respectively. Consequently, the image of TiO_2 was taken along the [110]-direction of rutile-type structure.

The image of Fig. 1 indicates a specific orientation relation of Pt particles with respect to TiO_2. In other words, the image was taken as a projection along the [110] of Pt and also along the [110] of TiO_2. This crystallographic relation is achieved by epitaxial growth of f.c.c. Pt on tetragonal rutile TiO_2.

Based on the above results, we will discuss here the growth mechanism of Pt on TiO_2. The epitaxy is usually controlled by lattice misfit at the boundary [3]. The fundamental spacings of d=0.296nm and d=0.268nm on TiO_2 (110) are the low-indexed Fourier-components in the Fourier series of two-dimensional surface potential. Lattice planes of Pt having the similar spacings to 0.296nm and 0.268nm of TiO_2 are the candidates to match with the basic lattice of TiO_2 surface. From the values of misfit, the smallest two cases are sellected; (110) of Pt // (001) of TiO_2 and (110) of Pt // $(1\bar{1}1)$ of TiO_2, which may realize the lower interfacial energy due to lower distortion of lattices at the boundary. However, the sign of misfit in the latter case is positive. This designates that the lattice spacing of overlying Pt ultra-fine particle should be compressed at the boundary from that in bulk, but such situation is not favorable. Accordingly, the former case with negative sign of the misfit value may lead to relatively lower interfacial energy than that in the latter case, though the misfit value is slightly larger. Actually observed epitaxial orientation of Pt particles is (110) of Pt // (001) of TiO_2.

In conclusion, the Pt ultra-fine particles grow epitaxially on TiO_2 surface by decomposing method of colloidal organic Pt complex, which indicates a regular interface between Pt and TiO_2. Such regular boundary works as a good transfer region for electrons and holes. Consequently the Pt ultra-fine particles contribute to separate distinctly the charges of electrons and holes generated in TiO_2 by light irradiation as well as to enlarge surface area which relates with higher reaction efficiency.

References

1. Fujii M, Kawai T and Kawai N: *Oyobutsuri* **33**, 916-933 (1984).
2. Doi H, Komatsu T, Karasawa T, Akai I, Kobayashi T and Okamoto Y: *Proc. 2nd Asia Symp. Condensed Matter Photophys.* 177-181 (1996).
3. Hoshino A, Isoda S, Kurata H and Kobayashi T: *J. Appl. Phys.* **76**, 4113-4120 (1994).

Swelling Behavior of Polybutadiene Networks in Nematic Liquid Crystal Solvents

Kenji Urayama, Mousumi De Sarkar, Takanobu Kawamura and Shinzo Kohjiya

Degree of equilibrium swelling (Q) of polybutadiene networks in four nematic liquid crystals (LCs) has been investigated as a function of temperature by cross-polarized microscopy. Phase behavior of the LCs in the networks has also been observed. It has been found that the nematic-to-isotropic phase transition temperatures of the LCs in the networks (T_{NI}^{g}) are slightly (ca. 1K) lower than the ones of the corresponding pure LCs (T_{NI}^{o}), and that the depression degrees of T_{NI} in each system are comparable in spite of large differences in Q between every system. In the temperature regions of $T_{NI}^{g}<T<T_{NI}^{o}$ where the LC phases inside and outside gel are different, Q is almost constant against temperature change.

Keywords : Swelling/ Polymer network/ Polymer gel/ Liquid crystal/ Nematic-to-isotropic phase transition

Swelling is an interesting property specific to polymer gels together with rubber elasticity. Degree of swelling of polymer gels significantly depends on the environments such as the nature of swelling solvents, temperature etc. which influence the thermodynamic interaction between the constituent polymer and the solvent. Most of the earlier studies are focused on the swelling in conventional isotropic solvents, but few studies on the polymer gels swollen in anisotropic solvents, i.e., liquid crystal (LC) solvents are reported so far. Polymer network swollen in LC solvent is expected to exhibit some unique physical properties originating from nematic-to-isotropic phase transition and nematic character of the LC solvents. Especially, the effect of the nematic-to-isotropic phase transition of LC (as swelling solvent) on the degree of equilibrium swelling (Q) is an interesting subject. In the present study, we have critically investigated the temperature dependence of Q especially in the close vicinity of nematic-to-isotropic phase transition temperature (T_{NI}) using four chemically stable LC solvents with varying structure [1].

Cylindrical polybutadiene (PB) gels with a diameter of less than 1mm were immersed in the LC solvents in an optical cell at certain temperatures until the equilibrium swelling was achieved. Four LC solvents, 4-octyl-4-biphenyl carbonitrile (**I**), 4-(*trans*-4-pentyl-cyclohexyl) benzonitrile (**II**), 4-(cyanophenyl-4-heptyl) benzoate (**III**) and 4-4'-diheptyl azoxybenzene (**IV**) were used as swelling solvents. The phase and swelling behaviors were examined with Nikon cross-polarized microscope equipped with Mettler Hot stage FP-82 under nitrogen atmosphere. T_{NI} of LC solvent was determined as the temperature at which the nematic texture appears in the cooling process. The degree of equilibrium swelling (Q), defined as the ratio of the gel volumes in the dry (V_o) and equilibrium swollen state (V), was calculated from the diameter of the gels in the dry (d_0) and swollen state (d) under the assumption of isotropic swelling using the relationship, $Q = V/V_o = (d/d_o)^3$.

Cross-polarized microscopic observation reveals that the LC solvents outside or inside the gels have different

STATES AND STRUCTURES — Polymer Condensed States —

Scope of research

Attempts have been made to elucidate the molecular arrangement and the mechanism of structural formation/change in crystalline polymer solids, polymer gels and elastomers, polymer liquid crystals, and polymer composites, mainly by electron microscopy and/or X-ray diffraction/scattering. The major subjects are: synthesis and structural analysis of polymer composite materials, preparation and characterization of polymer gels and elastomeric materials, structural analysis of crystalline polymer solids by direct observation at molecular level resolution, and in situ *studies on structural formation/change in crystalline polymer solids.*

Prof KOHJIYA, Shinzo (D Eng)

Assoc Prof TSUJI, Masaki (D Eng)

Instr URAYAMA, Kenji (D Eng)

Instr TOSAKA, Masatoshi (D Eng)

Instr MURAKAMI, Syozo (D Eng)

Guest Research Associate:
DE SARKAR, Mousumi (Ph D); TUEBKE, Jens (Ph D); MA, Shi Ping (D Eng)
Students:
SHIMIZU, Toshiki (DC); MURAKAMI, Takeshi (DC); BEDIA, Elinor L.(DC); FUJITA, Masahiro (DC); KAWAMURA, Takanobu (DC); NAKAO, Toshio (DC); YOKOYAMA, Keisuke (MC); HAMASHIMA Taro (MC); KITADE Taku (MC); ENDO, Yoshiyuki (MC); YASUDA, Takashi (UG)
Research Fellow:
ASAEDA, Eitaro; OHARA, Masayoshi

T_{NI} for all the systems studied. The LC solvent outside the gel corresponds to the pure LC solvent. T_{NI} of the LC inside and outside gel, designated as T_{NI}^{g} and T_{NI}^{O} respectively, are displayed in Table 1. T_{NI}^{g} of all the systems are 0.7~0.9 degree lower than T_{NI}^{O}. In the temperature range $T_{NI}^{g} < T < T_{NI}^{O}$, the LCs outside or inside the domain of gels form two different phases: nematic and isotropic respectively. The corresponding appearance of the surrounding solvents and gel remain bright and dark, respectively, under cross-polarized microscope. The slightly lower T_{NI}^{g} compared to T_{NI}^{O} can be qualitatively explained by taking into account of the impurity effects of the polymer backbone of the gels on the phase transition of the LCs. However, it is noteworthy that the degrees of depression in T_{NI}^{g} in each system are comparable (0.7 to 0.9 degree) regardless of the considerable differences in Q values (impurity content) at T_{NI}^{g} between every system. For example, the polymer volume fractions in the gels (ϕ=1/Q) containing **II** and **III** at T_{NI}^{g} are ca. 0.14 and ca. 0.49, respectively, corresponding minimum and maximum among the four systems. In our previous communication, we reported that T_{NI}^{g} of the PB gels in a nematic LC (EBBA) was much higher than T_{NI} of the uncrosslinked PB solution of EBBA with the same PB content, i.e., T_{NI}^{g} was not so much depressed as expected from the impurity content [2]. In the present study, the independence of T_{NI}^{g} values on ϕ observed also implies that the depression in T_{NI}^{g} can not be simply explained in terms of only the impurity effect. Interaction between LC solvents outside and inside gel leading to promote the nematic phase formation inside gel, if present, may explain the unexpected non-sensitivity of T_{NI}^{g} to ϕ for the present systems. The study for this problem is now in progress.

Temperature (T) dependence of the degree of equilibrium swelling (Q) for the PB gel in LC **I** is shown in figure 1. In general, Q tends to increase with increase in temperature. The magnitude of Q in the isotropic phase is larger than that in the nematic phase. The following features for the T dependence of Q around T_{NI} are commonly observed for all the systems as evidenced by the inset of the figure: (i) The Q-T curves show plateau regions at around T_{NI} with no appreciable change in Q; (ii) A finite abrupt (discontinuous-like) change in Q values is observed at certain temperatures around T_{NI}.

In the temperature range of $T_{NI}^{g} < T < T_{NI}^{O}$ which is characterized by a plateau region for Q, the LC solvents inside the gel are isotropic, whereas the solvents outside are in their nematic phase. It appears that such a phase difference prevents the flow of LC solvents between outside and inside the gels and the swelling practically stops showing almost constant value of Q against the temperature change. The discontinuous-like change in Q is observed at certain temperatures for all the systems. But the degree of discontinuity is much smaller than that observed in some gels showing typical volume phase transition. Without application of any external fields, LC in the nematic phase has poly-domain nematic structure where the anisotropic nature of nematic LC is macroscopically cancelled out. The slight discontinuity of volume change should be attributed to the screening effect of poly-domain nematic structure on the anisotropic characters of nematic LC molecules. However, the effect of the formation of the poly-domain nematic structure on the thermodynamic interaction between the PB and LC is still large enough to cause an appreciable, though small, discontinuous-like change in gel volume. Formation of mono-domain nematic structure, under the application of external field, where the LC molecules are macroscopically aligned in a unique direction is expected to induce significant change in thermodynamical interaction leading to large discontinuous volume change. Swelling in a mono-domain nematic LC solvent using external electric field is our future subject to study.

References

1. De Sarkar M, Urayama K, Kawamura T and Kohjiya S, *Liquid Crystals*, in press.
2. Urayama K, Luo Z, Kawamura T and Kohjiya S, *Chem. Phys. Lett.*, **287**, 342 (1998).

Table 1. Nematic-to-isotropic phase transition temperatures of liquid crystalline solvents outside (T_{NI}^{O}) and inside (T_{NI}^{g}) poly(butadiene) gel, and polymer volume fraction (ϕ) in the gels at T_{NI}^{g}.

LC	T_{NI}^{o}/K	T_{NI}^{g}/K	ΔT_{NI}/K	ϕ at T_{NI}^{g}
I	313.6	312.9	0.7	0.26
II	327.3	326.4	0.9	0.14
III	328.1	327.4	0.7	0.49
IV	343.5	342.6	0.9	0.32

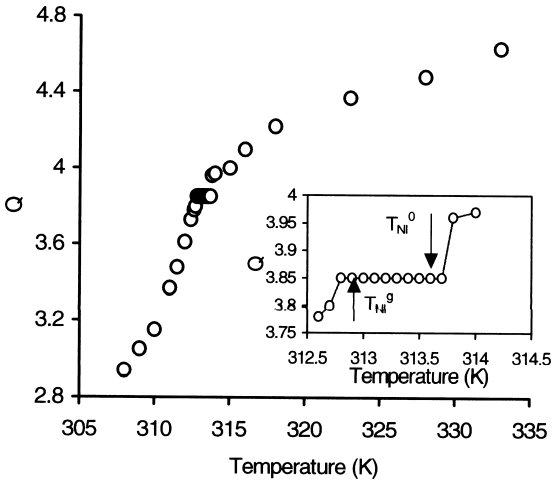

Figure 1. Temperature dependence of degree of equilibrium swelling (Q) of PB gel in LC **I**. The inset is for the vicinity of T_{NI}.

In-situ NMR Study of Hydrothermal Reactions of Hazardous Chlorinated Organic Compounds: CH_2Cl_2

Chihiro Wakai, Masaru Nakahara, Yasuo Tsujino and Nobuyuki Matubayasi

Hydrothermal decomposition of a hazardous chlorinated organic compound, dichloromethane, has been investigated using *in-situ* NMR spectroscopy. It is found that the hydrolysis of dichloromethane yields methanediol as an intermediate. Methanediol is a hydrated form of formaldehyde and easily transformed into methanol and formic acid under basic conditions. In the temperature range of 70-140 °C, the Cannizzaro-type reaction occurs: methanediol produces the reduced form, methanol and the oxydized form, formic acid. At higher temperatures between 200 and 250 °C, on the other hand, two methanediol molecules form glycolic acid which has a new C-C bond. The reaction rate constants and activation energies for the dechlorination and the Cannizzaro-type reactions have been obtained.

Keywords : Hydrothermal reaction / *in-situ* NMR spectroscopy / dichloromethane / dechlorination / Cannizzaro reaction

Recently we are alerted that many useful chlorinated organic compounds are biologically and environmentally hazardous. It is thus a main goal of environmental chemistry to establish a reaction scheme which provides nontoxic and recyclable organic compounds from chlorinated organic compounds by reducing the C-Cl bonds as shown in Fig. 1. To achieve this goal, high-temperature and high-pressure water is a desirable medium since it is clean and safe and able to dissolve organic compounds. In order to convert hazardous chlorinated compounds to recyclable compounds, the reduction process in supercritical water (SCWR) is more preferable than the oxidation process (SCWO), as shown in Fig. 1. By the SCWO method, organic compounds are oxidized completely and any useful compounds are not recovered. In contrast, the hydrothermal dechlorination enables one to recycle hazardous chlorinated compounds under milder conditions. In order to develop an optimal process for recycling hazardous chlorinated compounds, it is essential to understand the dechlorination mechanism. The purpose of this report is to show the power of *in-situ* NMR spectroscopy for gaining insights into the reaction mechanism. By this method, the formation and breakage of chemical bonds can be observed in real time and it is possible to simultaneously characterize not only products but also reaction intermediates. Here we focus on the *in-situ* NMR observation of the hydrothermal reactions of CH_2Cl_2.

CH_2Cl_2 supplied by Nacalai was used after the stabilizer and impurity were removed. NaOH of guaranteed reagent grade obtained from Nacalai was used without further purification. Water was purified using a Milli-Q Labo. filter system (Milli-Q Pore). Aqueous NaOH solution was prepared by weight; the concentration

INTERFACE SCIENCE — Solutions and Interfaces —

Scope of research

Structure and dynamics of a variety of ionic and nonionic solutions of physical, chemical, and biological interests are systematically studied by NMR under extreme conditions. High pressures and high temperatures are employed to shed light on microscopic controlling factors for the structure and dynamics of solutions. Vibrational spectroscopic studies are carried out to elucidate structure and orientations of organic and water molecules in ultra-thin films. Crystallization of protein monolayers, advanced dispersion systems at liquid-liquid interfaces, and biomembranes are also investigated.

Prof
NAKAHARA, Masaru
(D Sc)

Assoc Prof
UMEMURA, Junzo
(D Sc)

Instr
MATSUMOTO, Mutsuo
(D Sc)

Instr
MATUBAYASI, Nobuyuki
(Ph D)

Assoc Instr
OKAMURA, Emiko
(D Pharm Sci)

Assoc Instr
WAKAI, Chihiro
(D Sc)

Lecturer(part-time)
BOSSEV,
Dobrin (D Sc)
Students
KONISHI,
Hirofumi (DC)
KIMURA,
Tomohiro (DC)
MCNAMEE,
Cathy (DC)
TOYA, Hiroshi (MC)
IMADA,
Tomokatsu (MC)
KAWAI,
Kunichika (MC)
TSUJINO,
Yasuo (MC)
KAKITSUBO,
Ryou (MC)
NAKAO,
Naoko(MC)
NAGAI,
Yasuharu(MC)
MURAKAMI,
Takashi(MC)

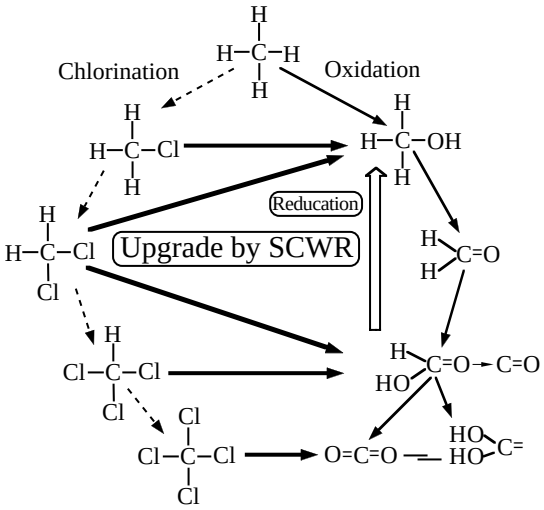

Figure 1. Sub- and supercritical C_1 chemistry of chlorinated organic compounds. For example, CH_2Cl_2 can be converted to useful organic compounds by reduction and oxidation before reaching to the final oxidation states, H_2O and CO_2.

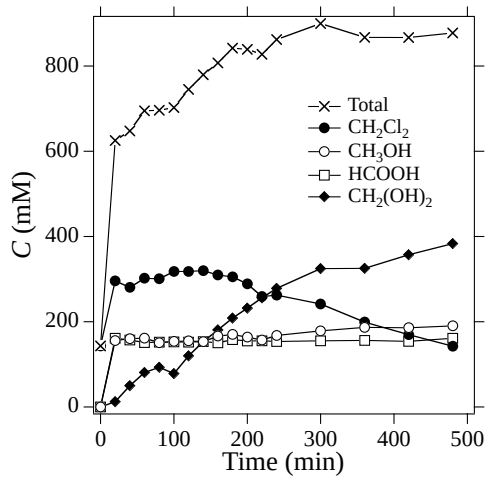

Figure 2. Time dependence of the concentrations of the reactant and products of the hydrothermal reaction of CH_2Cl_2(0.8 M) in aqueous NaOH solution (1.6 M) at 140 °C.

was 0.5-2.0 M. An amount of CH_2Cl_2 corresponding to 0.8-1.0 M solution was put in a quartz tube, the outer and inner diameters of which were 4.0 and 2.5 mm, respectively, and then water or aqueous NaOH solution was added by using a micro-syringe. The tube was sealed to a length of 7 cm. We used an NMR spectrometer (JNM-EX270, JEOL; 6.35 T) equipped with a high-temperature probe previously applied to the study of supercritical water. We measured ^1H and ^{13}C spectra as functions of temperature and NaOH concentration; it took ~10 min to heat the system up to 250 °C. CH_2Cl_2 and CH_3OH were used as reference materials for the ^1H and ^{13}C chemical shift measurements. The free induction decay signal was accumulated 8-16 times for ^1H and 25000 times for ^{13}C.

The main reaction of methanediol in the temperature range of 70-140 °C is

$$2CH_2(OH)_2 + OH^- \xrightarrow{\text{Cannizzaro}} HCOO^- + CH_3OH + 2H_2O.$$

At higher temperatures (200 and 250 °C), on the other hand, we have found another reaction path of methanediol. From the chemical shifts of ^1H and ^{13}C, it is clear that the new product is glycolic acid ($CH_2(OH)COOH$), and the reaction path of the formation of glycolic acid is considered as follows:

$$2CH_2(OH)_2 \xrightarrow[-2H_2O]{} CH_2(OH)CHO \xrightarrow[\text{Oxidized}]{} CH_2(OH)COOH\,.$$

According to the time dependence of the concentrations of the intermediate and products at 80 °C, the concentration of methanediol quickly increases and reaches a plateau. The concentrations of methanol and formic acid increase linearly with the time. This indicates that the dechlorination reaction is the rate-determining step and that the Cannizzaro reaction occurs immediately after the dechlorination. In other words, $CH_2(OH)_2$ is further evidenced as an intermediate of the hydrothermal decomposition of CH_2Cl_2. It is in addition shown at 80 °C that the reaction rate of the Cannizzaro reaction increases with the concentration of OH^-.

It is depicted in Fig. 2 how the concentrations of the reactant and products vary with time at 140 °C: at 120 and 130 °C, the time dependences are very similar to that at 140 °C. As expected, the dechlorination at 140 °C is much faster than that at 80 °C. The plateau values for the concentrations of the products indicate that the Cannizzaro reaction is quickly finished. The stationary concentrations of methanol and formic acid produced are almost the same (~170 mM) at 120, 130, and 140 °C. Methanediol increases monotonously with time. When more than 300 min has passed, the concentration of methanol is larger than that of formic acid. This is caused by the cross Cannizzaro-type reaction between methanediol and formic acid, which produces methanol and carbon dioxide as clarified in the previous work on the hydrothermal decomposition of *s*-trioxane.

We also determined the rate constants as functions of the $[OH^-]$ concentration at 80 °C according to the following reaction scheme:

$$CH_2Cl_2 + 2OH^- \xrightarrow{k_1} CH_2(OH)_2 + 2Cl^-,$$

$$2CH_2(OH)_2 + OH^- \xrightarrow{k_2} HCOO^- + CH_3OH + 2H_2O\,.$$

In the low concentration range, the rate constant for the Cannizzaro reaction is almost independent of $[OH^-]$: k_2 = 5.6×10^{-3} and 6.2×10^{-3} M^{-2} s^{-1} at 0.5 and 1.0 M, respectively. In 2.0 M solution, on the other hand, k_2 is 15×10^{-3} M^{-2} s^{-1} and ~3 times larger than those in 0.5 and 1.0 M solutions. It has been reported that the rate constant is proportional not to $[OH^-]$ but to $[OH^-]^2$ at high concentrations due to the existence of the second ionized state, $CH_2(O^-)_2$, of methanediol: the ability to make the hydride ion H^- is much higher for $CH_2(O^-)_2$ than for $CH_2(OH)O^-$.

It is therefore concluded that the hydrothermal dechlorination of dichloromethane can be achieved efficiently at 250 °C in the presence of a base (NaOH). Such a high temperature is required to compensate for the solubility drop due to the base and to accelerate the rate of the transformation to useful compounds.

A Molecular Design towards a Highly Amphoteric and Polar Molecule (HAPM) to Assemble Novel Organic Solid-State Structures

Naoki Sato, Ikuo Kawamoto, Taro Sakuma and Hiroyuki Yoshida

A molecular design towards a highly amphoteric and polar molecules (HAPM) to fabricate a novel molecular assembly with notable electronic properties is proposed. This design stresses the combination of electron-donating and accepting segments with a pseudo-delocalized π-electron system. To examine the suggested contrivance, 2-(4-dicyanomethylenecyclohexa-2,5-dienylidene)-4,5-ethylenedithio-1,3-dithiole, **1**, was designed and synthesized as a test molecule. Results from semiempirical MO calculations and several kinds of experiments imply most characteristics expected for HAPM in principle.

Keywords: *Amphoteric molecule/ Intramolecular charge transfer/ Intermolecular charge transfer/ Dipole moment/Molecular packing*

A single molecule which works as both an electron donor (D) and an electron acceptor (A) is called an amphoteric molecule. The amphotericity is connected with, *e.g.*, a small energy gap between HOMO and LUMO and is noteworthy in organic materials science. Nevertheless, only a few studies to produce a highly amphoteric molecule have been reported so far, *e.g.*, an approach with tuning electronic levels of a polycyclic aromatic hydrocarbon (PAH) to stabilize its LUMO and also to destabilize its HOMO as demonstrated by pentaleno[1,2,3-*cd*:4,5,6-*c'd'*]diphenalene (PDPL), while they have not taken the control of molecular aggregation form into account as such a molecule has no peculiar clue for intermolecular interaction.

Here we propose another approach based on the combination of D and A segments with a pseudo-delocalized electron system to realize an amphoteric nature with controllability of molecular arrangements via charge transfer interactions leading to novel electronic properties. A molecule thus-designed is expected to have a high polarity, however, is different from the conventional 'push-pull' type of molecules.

This molecular design of a highly amphoteric and polar molecule (HAPM) lays stress on the choice of a chemical link between D and A segments; this is influential to both intramolecular and intermolecular charge-transfer degrees [1]. When a non-conjugated bonding like a saturated hydrocarbon chain is applied, two segments are fixed at both ends with no through-bond interaction. Conversely, an intramolecular charge transfer will rigorously be induced to form nearly zwitterionic charge distribution in the molecule when an efficiently delocalized π-electron system such as a charge resonance one is employed; this could depress a controllability of molecular arrangements by a balance between intramolecular and intermolecular charge-transfer interactions.

Thus, a bonding system permitting a moderately high degree of π-electron delocalization is expected to keep

INTERFACE SCIENCE — Molecular Aggregates —

Scope of research

The research at this subdivision is devoted to correlation studies on structures and properties of both natural and artificial molecular aggregates from two main standpoints: photoelectric and dielectric properties. The electronic structure of organic thin films is studied using photoemission and inverse photoemission spectroscopies in connection with the former, and its results are applied to create novel molecular systems with characteristic electronic functions. The latter is concerned with heterogeneous structures in microcapsules, biopolymers, biological membranes and biological cells, and the nonlinearity in their dielectric properties is also studied in relation to molecular motions.

Professor
SATO, Naoki
(D Sc)

Associate Professor
ASAMI, Koji
(D Sc)

Instructor
KITA, Yasuo
(D Sc)

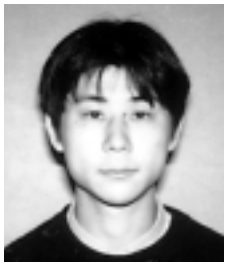

Instructor
YOSHIDA, Hiroyuki
(D Sc)

Students
SAKUMA, Taro (DC)
TSUTSUMI, Kiyohiko (DC)
TAKAHASHI, Ryo (MC)
YOKOI, Tomoko (MC)
OKAZAKI, Takashi (MC)

the electronic nature of each segment nearly unchanged, so that intermolecular charge-transfer interactions could further work in the condensed phase. Besides, not only electronic factor above but also steric one should be considered to choose the system to realize a variety of molecular packing manners. HAPM fulfilling these requirements may be crystallized with gross polarization due to molecular dipole moments arranged in the same direction if the resulting electrostatic instability is suppressed by the intermolecular interaction; such a specific structure could exhibit notable electronic properties.

With bearing these discussions in mind, to test the promise of HAPM by our approach the following molecule has been designed and synthesized: 2-(4-dicyanomethylenecyclohexa-2,5-dienylidene)-4,5-ethylenedithio-1,3-dithiole,**1**, by connecting a 4,5-ethylenedithio-1,3-dithiolylidene group as D segment and a dicyanomethylene group as A segment with a quinoid structure, which is expected to show a possible heterovalent resonance through the electron conjugation resulting in a moderately high degree of intramolecular π-electron delocalization. This is largely predicted by semiempirical MO calculations.

The electronic absorption spectrum of **1** in a chloroform solution exhibits an intense band at λ_{max} = 670 nm ($h\nu \approx$ 1.85 eV) with the oscillator strength f = 0.75. Such a large value can be understood by considering the intramolecular charge transfer to be enhanced by optical excitation; this is consistent with the calculated results of the dipole moments in the ground and excited states. It is notable that the λ_{max} value is much larger than that calculated by the ZINDO/S method, 406 nm (3.05 eV), even if a possible influence by solvent is taken into account.

Cyclic voltammetry gives the difference between the first oxidation potential and the first reduction one, Δ_1E, which indicates the magnitude of electrochemical amphotericity. Although Δ_1E = 1.615 V for **1** is larger than that of PDPL (0.99 V), it is slightly smaller than that (1.65 V) of a derivative of bis[1,2,5]thiadiazolo-*p*-quinobis(1,3-dithiole) known as a single-component organic semiconductor with a remarkably narrow energy gap. It should be noted that it is much smaller than that of dibenzo[*cd*,*lm*]perylene (2.29 V), a PAH with a similar size to PDPL.

Thus, the above results can support feasibility of our molecular design towards HAPM, while aggregation forms of its test molecules are to be examined.

This work has been performed partly in cooperation with the late Professor E. A. Silinsh and Dr. A. J. Jurgis.

Reference

1. Sato N, Kawamoto I, Sakuma T, Silinsh E A and Jurgis A J, *Mol. Cryst. Liq. Cryst.*, **333**, 243 (1999).

Real-Time Monitoring of Cell Cycle Progression by Dielectric Spectroscopy

Koji Asami, Eugen Gheorghiu[†1] and Takeshi Yonezawa[†2]

A dielectric technique has been developed for monitoring of cell cycle progression in synchronized culture, which would be a promising tool for cell cycle analysis in cell biology and biotechnology.

Keywords: Dielectric relaxation/ Yeast/ Synchronized culture/ Septum formation/ Cdc mutant

Synchronized cell culture is an indispensable technique in cell cycle research. In order to assay synchronous cell growth, cells are sampled at a regular interval over a few cell cycles, and the changes in morphology and DNA content are examined by optical microscopy and flow cytometry, respectively. Unfortunately, the examinations are time-consuming and laborious task, and therefore alternative methods capable of real-time and in situ measurement become increasingly important for precise analysis of cell cycle progression and for screening mutants. Dielectric spectroscopy can be a most suitable method for this purpose because of the non-invasive and rapid measurement sensitive to the morphological and electrical properties of cells.

We have applied dielectric spectroscopy to real-time monitoring of cell cycle progression in synchronized yeast cell culture [1]. The dielectric monitoring is based on the electromagnetic induction method, regarded as a non-electrode method, which has resolved the problems encountered in measurements with metal electrodes, namely, electrode polarization and bubble formation on electrodes. In the synchronized culture with temperature-sensitive cell division cycle mutants, the permittivity of the culture broth showed cyclic changes at low frequencies below 300 kHz. The increase and decrease in the cyclic permittivity changes correspond to the increase in cell length and bud size (S-phase to M-phase) and to the septum formation between mother and daughter cells (M-phase to G1-phase), respectively.

[†1]NIB-UNESCO Center of Biodynamics, Calea Plevnei 46-48, 77102 Bucharest 1, Romania. [†2]Production Division I, Suntory, Shimamoto-cho, Osaka 618-0001.

Reference

1. Asami K, Gheorghiu E and Yonezawa T, *Biophysical J.*, **76**, 3345 (1999).

Improved Extraction-Separation Utilizing Macrocyclic Ionophores as Ion-Size Selective Masking Reagents

Shigeo Umetani

Improved extraction-separation could be achieved in the extraction of alkaline earths with 1-phenyl-3-methyl-4-benzoyl-5-pyrazolone and tri-n-octylphosphine oxide by adding macrocyclic ionophore such as 18-crown-6 or cryptand [2.2.2] to the aqueous phase as an ion-size selective masking reagent. The larger the ionic radius is, the higher pH region the extraction moved to. Consequently, the separation among the metal ions was enhanced markedly.

Keywords: Solvent extraction / Separation / Masking effect / Macrocyclic ionophore / Ion-size selectivity

Application of a masking effect to the solvent extraction method is an effective means for a selective separation of metal ions. In the solvent extraction of alkali, alkaline earth and lanthanide metal ions with the chelating reagents, metal ions having smaller ionic radii exhibit higher extractability. On the other hand, the stability in the complex formation between the macrocyclic ionophores and the above mentioned metal ions exhibits a quite different tendency. Thus, the solvent extraction system of high selectivity could possibly be developed by the combination of the chelating reagents and the macrocyclic ionophores. 18-Crown-6 and cryptand [2.2.2] have been shown to be useful ion-size selective masking reagents in the synergistic extraction of alkaline earths into cyclohexane with 1-phenyl-3-methyl-4-benzoyl-5-pyrazolone (HPMBP) and tri-n-octylphosphine oxide (TOPO).[1-4] In the present work, a novel macrocycle application has been proposed.

Extraction of alkaline earths in the presence of 18-crown-6. The results for the extraction of alkaline earths with 0.05 M HPMBP and 0.01 M TOPO into cyclohexane in the absence (blank symbols) and presence (solid symbols) of 18-crown-6 (0.03 M) are shown in Figure 1. Alkaline earths were extracted in the order, Mg>Ca>Sr>Ba, which is the same order that the ionic radius decreases. When 0.03 M 18-crown-6 was added to the aqueous phase, the extractions were made in the higher pH region. The larger the ionic radius is, the higher pH region the extraction moved to. As a result, the separation among alkaline earths especially for Ca/Sr and Sr/Ba has been improved. It is clear that 18-crown-6 works as an ion-size selective masking reagent in the aqueous phase.

In the synergistic extraction of alkaline earths (M^{2+}) with HPMBP (HA) and TOPO (L), the extraction equilibrium and the extraction constant, $K_{ex,s}$, can be written as follows:

$$M^{2+} + 2HA_o + sL_o = MA_2L_{s,o} + 2H^+ \quad (1)$$

$$K_{ex,s} = D[H^+]^2 / [HA]_o^2 [L]_o^s \quad (2)$$

INTERFACE SCIENCE — Separation Chemistry —

Scope of research

Our research activities are concerned in selective complex formation systems. Major subjects of the research are followings: (1) Design and synthesis of the selective complex formation systems. Ligands that have novel functions in separation of metal ions and guest molecules are designed and synthesized. Their functions are analyzed basing on structures of the ligands and complexes. (2) Biogeochemistry of trace elements in the hydrosphere. Novel analytical methods for trace elements are developed. The behavior of trace elements in the hydrosphere is explored.

Assoc Prof
UMETANI, Shigeo
(D Sc)

Instr
SASAKI, Yoshihiro
(D Sc)

Instr
Hasegawa, Hiroshi
(D Sc)

Techn
SUZUKI, Mitsuko
(D Sc)

Students

MITO, Saeko (DC)
AZUMA, Yohei (DC)
NAITO, Kanako (DC)
NORISUE, Kazuhiro (DC)
FUKUI, Yoshiharu (MC)
KOHYAMA, Haruhiko (MC)
OOHASHI, Chikako (MC)
ITO, Makoto (MC)
SHIMOJO, Shinichiro (MC)
SHINOURA, Misato (MC)

where subscript o denotes the species in the organic phase and D is defined as $[MA_2L_s]_o/[M^{2+}]$.

The distribution ratio in the presence of 18-crown-6 (CE), D*, can be expressed in eq 3.

$$D^* = [MA_2L_s]_o / \{[M^{2+}] + [M(CE)^{2+}]\}$$
$$= K_{ex,s}[HA]_o^2[L]_o^s / [H^+]^2\{1+ß[CE]\} \quad (3)$$

The separation factor, SF, between two metal ions, M1 and M2, is defined as the difference of the logarithmic value of the respective distribution ratio.

$$SF = \log (D_{M1}/D_{M2}) = \log (K_{ex,s,M1}/K_{ex,s,M2}) \quad (4)$$

The separation factor in the presence of crown ether, SF* {(defined as $\log (D^*_{M1}/D^*_{M2})$}, is written in eq 5 when s1 and s2 are the same and [CE] is high enough.

$$SF^* = \log (K_{ex,s,M1}/K_{ex,s,M2})(ß_{M2}/ß_{M1}) \quad (5)$$

Comparing eqs 5 and 6, the separation factor can be improved as much as $ß_{M2}/ß_{M1}$. Separation factors in the presence and absence of crown ether are seen in ref. 2.

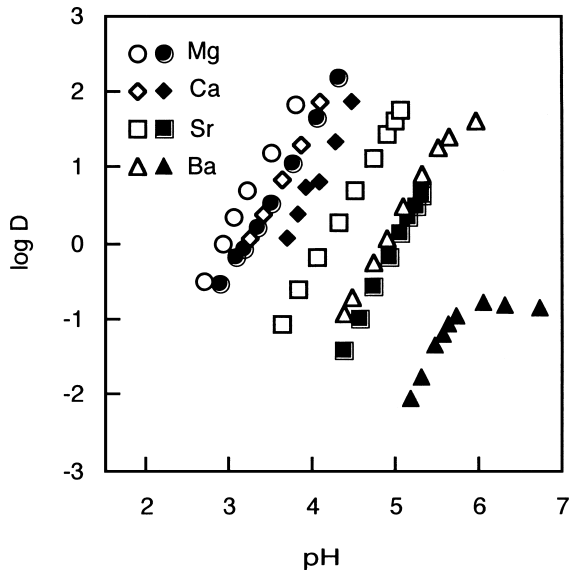

Figure 1 Extraction of alkaline earths in the absence and presence of 18-crown-6.

Extraction of alkaline earths in the presence of cryptand [2.2.2]. Diazapolyoxabicyclic ligands (cryptands) exhibit a prominent selectivity for alkali and alkaline earth metals. They are soluble in water and their stability in complexation is large enough for using as a practical masking reagent. Incorporating nitrogens as an element constituting the ring structure, the masking effect of cryptands depends on a pH unlike crown ethers such as 18-crown-6. Cryptand [2.2.2] should be the most suitable masking reagent for separating Ca and Sr in the series of alkaline earths. The extraction with 0.01 M HPMBP and 0.01 M TOPO into cyclohexane in the absence and presence of 0.01 M cryptand [2.2.2] has been examined. The extraction behaviors for Mg and Ca in the presence of cryptand [2.2.2] are quite similar to those in the absence of cryptand [2.2.2]. The log D values for Sr in the presence of cryptand [2.2.2] increase as the pH increases similarly to those in the absence of cryptand [2.2.2], then begin to decrease over pH 5. The log D values for Ba in the presence of cryptand [2.2.2] deviate from those in the absence of cryptand [2.2.2] over pH 4.5.

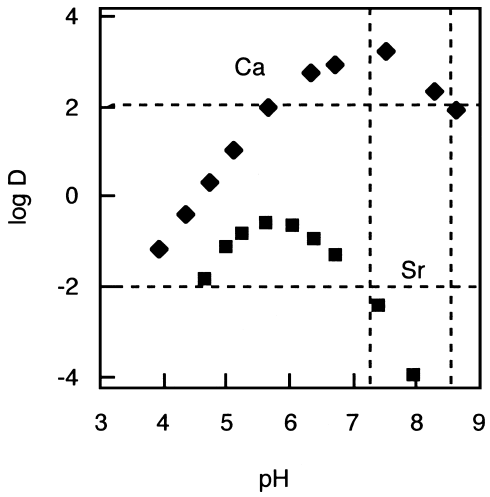

Figure 2 Quantitative extraction-separation of calcium from strontium.

The results obtained indicate that the masking effect by cryptand depends on the stability in complexation and on the pH. The extraction behaviors in the presence and absence of cryptand can be predicted by taking the above equilibrium and the concentrations of the reagents into consideration. In order to establish the quantitative extraction-separation system for Ca and Sr, the extraction was made reducing the concentrations of HPMBP and TOPO to $4x10^{-3}$ M keeping the initial concentration of cryptand at $1x10^{-2}$ M. As shown in Fig. 2, the distribution ratio of Sr decreases rapidly over pH 5.6 as expected, while that of Ca still increases by pH 7.5. Ca can be separated from Sr quantitatively at the pH range 7.2 to 8.6 where more than 99% of Ca (log D > 2) is extracted into cyclohexane, while more than 99% of Sr (log D < -2) remains in the aqueous phase at the same time. A careful control of pH at 7.8 could lead to the best separation; 99.9% extraction of Ca (log D > 3) remaining 99.9% of Sr (log D < -3) in the aqueous phase.

References

1. Umetani S, Matsui M, and Tsurubou S, *J. Chem. Soc., Chem. Commun.*, 914-916 (1993).
2. Tsurubou S, Mizutani M, Kadota Y, Yamamoto T, Umetani S, Sasaki T, Le T. H. Q, and Matsui M, *Anal. Chem.*, **67**, 1465-1469 (1995).
3. Sasaki T, Umetani S, Matsui M, and Tsurubou S, *Chem. Lett.*, 1195-1198 (1994).
4. Tsurubou S, Umetani S and Komatsu Y, *Anal. Chim. Acta*, **394**, 317-324 (1999).

Electric Resistance of Magnetic Domain Wall in NiFe Wires with CoSm Pinning Pads

Taro Nagahama, Ko Mibu and Teruya Shinjo

A NiFe wire of 1μm width with hard magnetic CoSm pinning pads and Cu electrodes was prepared by electron-beam lithography and lift-off technique. Using the exchange interaction between the NiFe wire and CoSm pads, magnetic structures with and without magentic domain walls were realizecd at zero external field. The electric resistance of the wall state was smaller than that of the no-wall state. The difference of the resistance can be explained by the anisotropic magnetoresistance effect in the domain walls.

keywords: Submicron magnetic wire/ Exchange-spring bilayer/ Magnetic domain wall/ Hysteresis curve/ Anisotropic magnetoresistance

Recently electric transport properties through magnetic domain walls have been attracting much attention. Here we report an experiment using NiFe wires partially pinned by hard magnetic CoSm pads. The wire is magnetically composed of two parts; one is magnetically free areas that have a small coercive field and the other is pinned areas that have a large coercive field. In a weak magnetic field, only the magnetization in the free parts changes the direction, and therefore 2*N* magnetic domain walls are nucleated at the boundary between two different areas (Here, *N* is the number of pinning pads). The resistance was compared for the no-wall state and 2*N*-wall state at zero external field.

The sample was composed of a NiFe wire (thickness : 200 Å, width : 1 μm, length : 300 μm) and CoSm pinning pads. A schematic image of the sample is shown in Fig.1(a). Every part, i.e., a NiFe wire, CoSm pads, and Cu electrodes, was prepared by a lift-off technique. The deposition and lift-off processes were repeated three times to prepare the sample.

Figure 2 shows a minor hysteresis loop of the MR curve for a NiFe wire with three CoSm pinning pads. The starting point was the magnetically saturated state in a negative applied field (Fig.1(b)). When a magnetic field was applied to the opposite direction, the resistance decreased abruptly at a certain magnetic field (H_n). Then,

SOLID STATE CHEMISTRY — Artificial Lattice Alloys —

Scope of research

By using vaccum deposition method, artificial multilayers have been prepared by combining various metallic elements. The recent major subject is an interplay of magnetism and electric transport phenomena such as the giant magnetoresistance effect. Fundamental magnetic properties of metallic multilayers have been studied by various techniques including Mössbauer spectroscopy using Fe-57, Sn-119, Eu-151 and Au-197 as microprobes, and neutron diffration. Microstructured films such as wires and dots were successfully prepared by electron-beam lithography and novel magnetic and transport properties are investigated.

Prof
SHINJO, Teruya
(D Sc)

Assoc Prof
HOSOITO, Nobuyoshi
(D Sc)

Techn
KUSUDA, Toshiyuki

Guest Research Associate:
BACZEWSKI, L. Tomasz(D Sc)
HASSDORF, Ralf (D Sc)
Students:
NAGAHAMA, Taro (DC)
SHIGETO, Kunji (DC)
ALMOKHTAR, A. M. M. (DC)
FUJIMOTO, Tatsuya (MC)
OKUNO, Takuya(MC)
Research Fellow:
HAMADA, Sunao

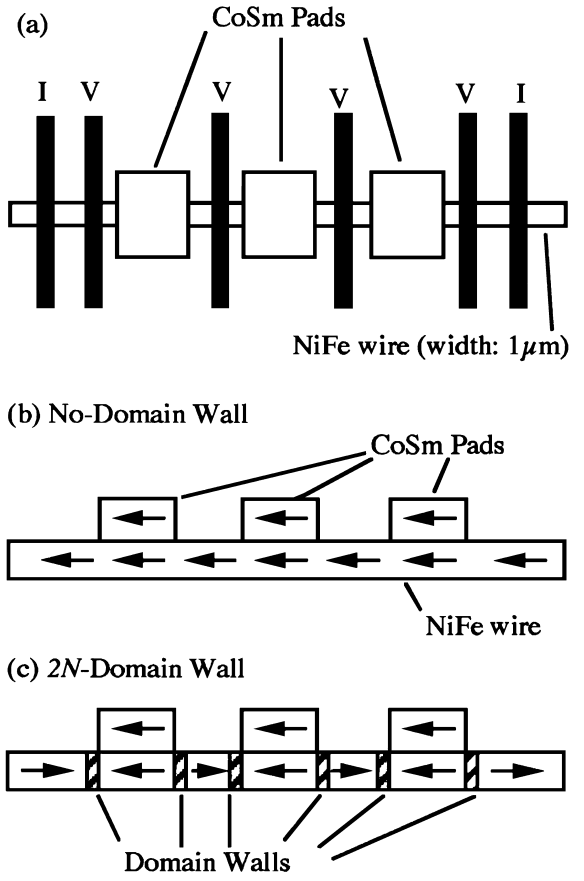

Figure 1. The schematic image of (a) a typical sample (top view), (b) no-wall state (magnetically saturated state)(side view), and (c) 2*N*-wall state (side view).

the resistance slightly increased, and started to decrease again at H_b. When the magnetic field was decreased from 800 Oe, the resistance first changed almost reversibly down to H_n. The resistance decreased slightly until the magnetic field went across zero, and returned to the saturated value abruptly at H_r. This change in MR curve is understood as follows: At H_n, antiparallel magnetic domains were nucleated in the NiFe wire, with the magnetic domain walls situated at the boundary between the pinned area and the free area (Fig.1 (c)). When the magnetic field exceeded H_b, the magnetic moments of the NiFe layer in the pinned area started to rotate gradually like soft magnetic layers in exchange-spring bilayers [1]. When the magnetic field was reversed, the magnetization returned reversibly down to H_b. The magnetic domain walls remained down to H_r, and at H_r they were annihilated. The reason why the resistance decreases from H_b to H_r is not clear, but that can be concerned with the magnetic structure of domain walls

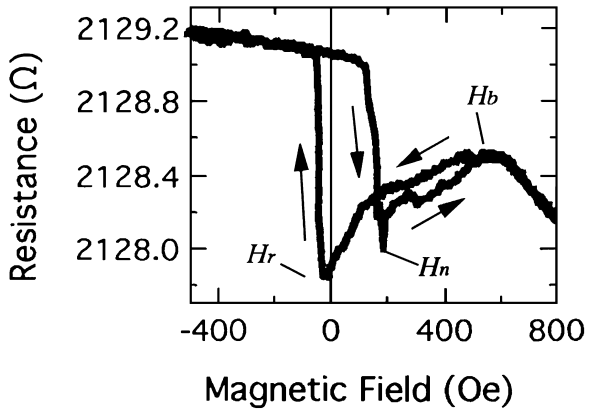

Figure 2. The minor loop of the magnetoresistance of a NiFe(200Å) wire with three CoSm(400Å) pads at 5 K.

that changes slightly in this field range. If the magnetic structure does not change, the resistance should be kept constant.

Obviously there is a difference of resistance (ΔR) between the 2*N*-wall state and the no-wall state; the 2*N*-wall state has a smaller resistance than the no-wall state. This result shows that the domain wall contributes to negative magnetoresistance. We calculated the length of the domain wall under the assumption that ΔR is totally due to anisotropic magnetoresistance (AMR) originating from the magnetic moments that make certain angles with the electric current direction. For simplicity, the angle of the magnetic moment in the wall was assumed to change linearly. Then the length of the domain wall was estimated to be about 1 μm. This value seems too long because usually the width of a domain wall is several hundreds Å. However, in a head-on-head wall in a nanowire, a longer and complex domain wall structure was observed by MFM measurement [2]. In this way, the observed decrease in magnetoresistance can be explained by the AMR effect in the domain walls.

References

1. T.Nagahama, K.Mibu and T.Shinjo, J. Phys. D: Appl. Phys. 31(1998)43.
2. Y.Nozaki, K.Matsuyama, T.Ono and H.Miyajima, Jpn. J. Appl. Phys. 38(1999)6282.

Spin Correlation in $La_{2-x}Sr_xCuO_4$ Studied by Neutron Scattering Measurement

M. Fujita and K. Yamada

Systematic elastic neutron scattering study was performed on several single crystals of $La_{2-x}Sr_xCuO_4$ in the wide hole concentration. Incommensurate spin modulation in the CuO_2 plane exists in both the insulating and superconducting phases, however, the direction of modulaton vectors are different by 45degrees from each other. Both type of spin modulation possibly coexist around the lower critical concentration (x≈0.055) for superconductivity.

Keywords: static spin correlation/ neutron scattering/ high-Tc superconductor

The intimate connection between superconductivity and magnetism in the high-T_c copper oxide superconductors is one of the key issues to understand the mechanism of hith-T_c superconductivity. In order to clarify the relationship between the two, we have performed systematic elastic neutron scattering study on several single crystals of $La_{2-x}Sr_xCuO_4$ in the wide hole concentration range. Our recent research focusing on the spin correlation near the insulaor-superconductor phase boundary revealed a qualitative change in the direction of spin modulation.

In the insulating sample (x=0.053), we observed so-called diagonal magnetic component corresponding to the magnetic correlations modulated along the diagonal direction of the CuO_2 square lattice, consistent with our recent work.[1] On the other hand, all the superconductiong samples (x=0.056,0.06,0.07) show so-called parallel magnetic component corresponding to the modulation parallel to Cu-O-Cu line.[2-4] As a remarkable feature, the superconduntingsample in narrow concentration above the insulator-superconductor boundary exhibits the "diagonal" component in addition to the "parallel" one. For both the "diagonal" and "parallel" components, the incommensurability parameter δ, defined as the distance between the incommensurate the (π,π) positions in reciprocal lattice units of the "tetragonal" structure, follows a linear relation δ=x regardlessly of the insulator-superconductor boundary.

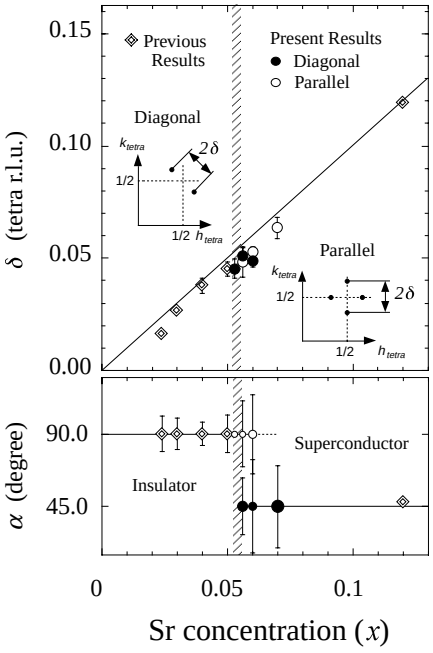

SOLID STATE CHEMISTRY — Quantum spin Fluids —

Scope of research

Quantum spin oxide system such as high-T_c superconducting cuprates, $La_{2-x}Sr_xCuO_4$ and $Nd_{2-x}Ce_xCuO_4$ are synthesized in the form of single crystals using traveling-solvent-floating-zone method. Detailed equilibrium phase diagram of Bi cuprate systems is investigated. Main subjects and techniques are: mechanism of high-T_c superconductivity: origin of quantum phase separation in strongly correlated electron systems: spin excitations in quantum spin systems: interplay between spin and charge flow in doped spin system: neutron scattering by using triple-axis as well as time-of flight techniques.

Prof
YAMADA,
Kazuyoshi
(D Sc)

Assoc Prof
MIBU,
Ko
(D Sc)

Instr
IKEDA,
Yasunori

Techni
FUJITA,
Masaki
(D Sc)

Students:

UEFUJI, Tetsuji (MC)
GOKA, Hideto (MC)

Magnetic Excitations in the Electron-Doped Superconductor $Nd_{1.85}Ce_{0.15}CuO_4$

K. Yamada, K. Kurahashi, M. Fujita and Y. Ikeda

Neutron scattering on electron-doped high-Tc superconductor firstly observed well-defind spin flucations in the superconducting state. Similar to the hole-doped system, the spin excitations are gapped with the energy-gap of about 4 meV. However, the spacial spin correlation is commensurate in contrast to the incommensurate one in the hole-doped system.

Keywords: spin fluctuations/ neutron scattering/ electron-doping/ high-Tc superconductor

For the hole-doped high-T_c superconductor it is now established that the spin fluctuations coexist and closely correlate with the superconductivity. For the electron-doped system, however, many key experiments have been missing possibly due to the difficulty in growing single crystal and in preparing the superconducting sample by the post-growth heat treatment. In fact, previous neutron scattering measurements so far performed observed no well-defined magnetic signal in the superconducting (SC) phase.

We have succeeded in growing large single crystals of $Nd_{1.85}Ce_{0.15}CuO_4$ by using a TSFZ method. The as-grown crystal is antiferromagnetic insulator. With the heat treatment of the crystal bulk superconductivity appears below T_c=18 K. Neutron scattering experiments have been performed for both the antiferromagnetic (AF) insulating and the superconducting (SC) phases in (h k 0) zone. For the AF sample, we monitored (3/2 1/2 0) magnetic reflection in the tetragonal lattice to study the long range antiferromagnetic order. At low temperature below around 10 K the intensity of (3/2 1/2 0) reflection starts to increase rapidly due to the participation of Nd^{3+} spins in the magnetic order. As shown in Fig.1 (a), a sharp commensurate magnetic inelastic scattering peak was observed for AF sample at (1/2 1/2 0). For the SC sample, we newly observed a commensurate inelastic scattering peak at (1/2 1/2 0) . Compared with Fig.1(a) , the q-width of the peak is substantially broader than that of the AF phase. However, the q-integrated peak intensities of both samples are comparable except at low temperatures. Even in the SC phase, we observed a Bragg peak at (3/2 1/2 0) though the intensity is much weaker than that in the AF phase.

If the observed commensurate peak in the SC sample originates from the residual AF phase with the reduced volume and no magnetic intensity exists in the SC phase as in the previous work, it is very unlikely to observe comparable magnetic intensity as in the as-grown AF phase. Therefore, the commensurate peak is considered to be associated with the SC phase. However, the nature of the residual AF phase should be studied in more detail. The temperature dependence of the spin fluctuations is quite different between AF and SC phases. For the SC phase, *the energy as well as temperature dependence indicate an energy-gap of about 4 meV in the SC state.*

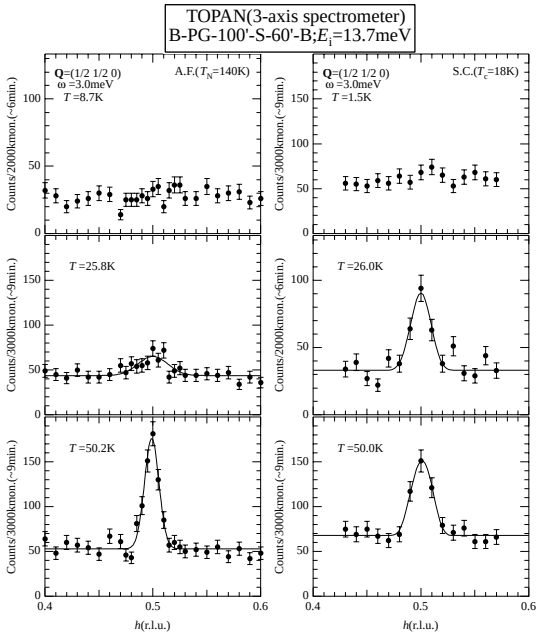

Both works were done in collaboration with Tohoku University(Y.Endoh, K.Hirota, H.Hiraka), MIT(R.J.Birgeneau, M.A.Kastner, S.Wakimoto), BNL(G.Shirane), NIST(Y.S.Lee, S.H.Lee, P.M.Gehring) and RIKEN(M.Matsuda) group.

References

1. S.Wakimoto, G.Shirane, Y.Endoh, K.Hirota, S.Ueki, K.Yamada, R.J.Birgeneau, M.A.Kaster, Y.S.Lee, P.M.Gehring, and S.H.Lee, Phys. Rev. **60**, R769 (1999)

2.J.M.Tranquada, B.J.Sternlieb, J.D.Axe, Y.Nakamura, and S.Uchida, Nature **375**, 561 (1995)

3. T.Suzuki, T.Goto, K.Chiba, T.Shinoda, T.Fukase, H.Kimura, K.Yamada, M.Ohashi, and Y.Yamaguchi, Phys. Rev. B **57**, 3229 (1998)

4.H.Kimura, K.Hirota, H.Matsushita, K.Yamada, Y.Endoh, S.H.Lee, C.F.Majkrzak, R.Erwin, G.Shirane, M.Greven, T.S.Lee, M.A.Kastner, and R.J.Birgeneau, Phys. Rev. B **59**, 6517 (1999)

Single Crystal Growth at High Pressure

Masaki Azuma, Takashi Saito and Mikio Takano

Single crystals of a spin-1/2 Heisenberg alternating chain compound, high pressure phase of $(VO)_2P_2O_7$, was grown by slowly cooling the melt at 3 GPa. Powder XRD study at high pressure using synchrotron radiation was performed in advance to observe the formation and the melting of this compound.

Keywords: High pressure synthesis/ Synchrotron radiation XRD/ Single crystal growth

High pressure synthesis is a powerful technique to search for new materials. Various quantum spin compounds including high T_c superconductors and quantum spin ladders [1] have been found using this method in a past decade. However, the limitation of the sample space and the difficulty in the direct observation of high pressure reactions made it difficult to grow single crystals of such compounds.

The high pressure phase of $(VO)_2P_2O_7$ (HP-VOPO) is a spin-1/2 Heisenberg alternating chain compound with a spin gap stabilized at 2GPa and 700 °C[2]. We have succeeded in growing single crystals of this compound by slowly cooling the melt at 3GPa [3]. High pressure powder X-ray diffraction (XRD) was performed using a cubic-anvil type high pressure apparatus (SMAP 1800) installed at BT14B1 of SPring-8, Japan Synchrotron Radiation Research Institute, to determine the melting temperature. White beam X-ray from the synchrotron radiation was irradiated to the sample in a platinum capsule through the high pressure cell and was detected by the solid state detector fixed at $2\theta = 4°$. Figure 1 shows the XRD patterns taken at 3GPa and at various temperatures. When the pressure was applied, the peak shifted to the high energy direction indicating a shrinkage of the lattice. The peak broadening was due to strains in the particles. The peaks sharpened again with increasing the temperature and new peaks corresponding to (2 2 1), (1 1 3) and (2 3 1) reflections of the HP phase appeared at 500°C. This clearly showed that the transition to the HP phase took place between 400 and 500°C. Finally at 1150°C the sample melted and all the peaks disappeared expect for those of characteristic X-rays of lead.

Single crystals were grown by slowly cooing the melt at 3GPa. About 2 g of the ambient pressure phase sample was packed in a platinum capsule of 9.6 mm in diameter and 15 mm height and compressed using a cubic anvil type high pressure apparatus. The sample was first heated to 1200°C and then cooled to 600°C in 60 h. Green transparent crystals of a typical size of 1 mm × 0.5 mm × 0.2 mm were obtained. A magnified view of obtained crystals is shown in Fig. 2.

References

1. M. Azuma, Z. Hiroi, M. Takano, K. Ishida and Y. Kitaoka, Phys. Rev. Lett. **73**, 3468 (1994).

2. M. Azuma, T. Saito, Y. Fujishiro, Z. Hiroi, M. Takano, F. Izumi, T. Kamiyama, T. Ikeda, Y. Narumi and K. Kindo, Phys. Rev. B **60**, 10145 (1999).

3. T. Saito, M. Azuma, M. Takano, T. Goto, H. Ohta, W. Uthumi, P. Bordet and D. C. Johnston, preprint.

SOLID STATE CHEMISTRY — Multicomponent Materials —

Scope of research

Novel 3d transition-metal oxides showing exotic electrical and magnetic properties are being searched for using different synthesizing techniques like high pressure syntesis (5 GPa and 1000°C, typically) and epitaxial film growth. Recent topics are:

- *High T_c superconductivity.*
- *Low-dimensional spin systems like ladders showing dramatic quantum effects.*
- *Oxides of late 3d transition metals like $SrFeO_3$ with strong oxygen-hole character.*

Prof
TAKANO, Mikio
(D Sc)

Assoc Prof
TERASHIMA, Takahito
(D Sc)

Instr
AZUMA, Masaki
(D Sc)

Students:

YAMADA, Takahiro (DC)
FURUBAYASHI, Yutaka (DC)
HAYASHI, Naoaki (DC)
SAITO, Takashi (DC)
ISHIWATA, Shintaro (MC)
ODAKA, Tomoori (MC)
TERASHIMA, Takashi (MC)
MASUNO, Atsunobu (MC)

Research Fellow:
KAWASAKI, Shuji

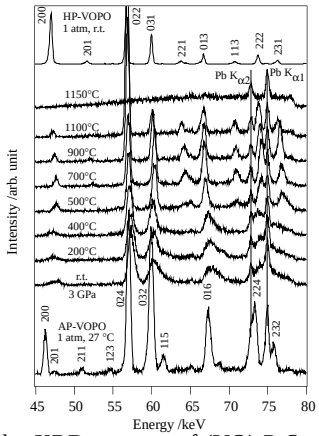

Figure 1 Powder XRD patterns of $(VO)_2P_2O_7$ taken at 3 GPa and various temperatures.

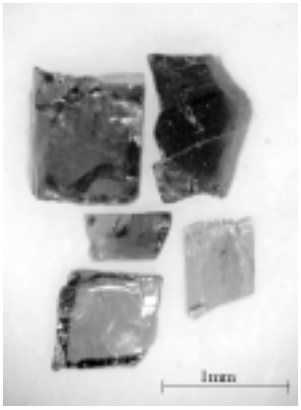

Figure 2 Single crystals of HP $(VO)_2P_2O_7$ grown at 3 GPa.

Epitaxial Growth of $Fe^{4+}(3d^4)$-Perovskite Oxides Thin Films

T. Terashima, N. Hayashi and M. Takano

Epitaxial films of $SrFeO_3$ containing high valent $Fe^{4+}(3d^4)$ were successfully grown by the pulsed laser ablation and subsequent ozone annealing. The film showed good crystallinity and lower resistivity than a bulk sample.

Keywords: Fe^{4+}/ Perovskite oxides/ Thin film/ Epitaxial growth/ Laser ablation

Perovskite-type oxides containing high valent $Fe^{4+}(3d^4)$ are prototypical systems to study electronic properties dominated by oxygen-hole character. $SrFeO_3$ (SFO) is a broad band metal down to the lowest temperature. Although the electronic state of SFO has attracted much attention, detailed transport properties have not been clarified due to the difficulty of the preparation of a single crystal. The high pressure treatment is required to oxidize Fe to Fe^{4+} state. The epitaxial growth is an alternative way to prepare a metastable substance. We report a successful growth of the epitaxial thin films of SFO by the pulsed laser deposition and subsequent ozone oxidation.

The films were grown by the pulsed laser deposition with KrF eximer laser (λ=248nm). The deposition conditions are the following: The substrate temperature was 650˚C and the oxygen pressure during the deposition was 500mTorr. The substrate was LSAT ($(LaAlO_3)_{0.3}(SrAl_{0.5}Ta_{0.5}O_3)_{0.7}$) (100) which has a good lattice matching with SFO. After the deposition the film was cooled with blowing partially ozonized oxygen.

The epitaxial growth was confirmed by the reflection high-energy electron diffraction measurement. An equi-intensity contour map of X-ray scattering around (203) point for the SFO film is displayed in Fig.1. The narrow peak widths of the SFO film comparable to those of the substrate show good crystallinity of the film. The calculated in-plane and out-of plane lattice spacings are 3.865Å and 3.837Å, respectively, revealing a pseudo tetragonal structure of the film caused by an elastic strain.

Figure 2 shows the temperature dependence of the resistivity for the SFO film. The film exhibited metallic behavior with much lower resistivity than bulk sample prepared by high-pressure synthesis. A change in dR/dT is seen at 100K, which would be correlated to a magnetic ordering. Measurements of the transport properties, such as Hall effect and magnetoresistance, of the SFO film are now in progress.

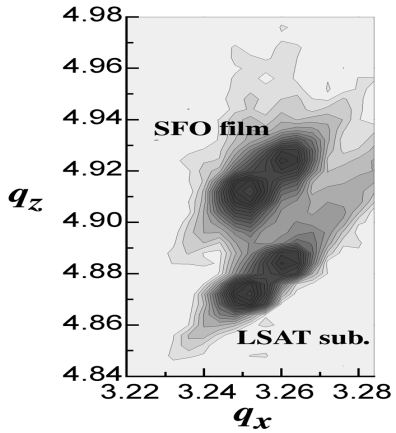

Figure 1. Equi-intensity contour map of X-ray scattering around the (203) point for the SFO thin film.

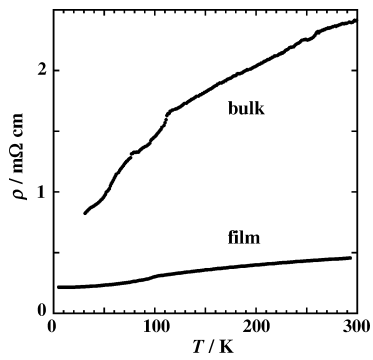

Figure 2. Temperature dependence of the resistivity for the SFO thin film and bulk.

Structure and Formation Mechanism of Ge Related Paramagnetic Centers in Ge-Doped Silica Glass

Takashi Uchino, Masahide Takahashi, Jisun Jin and Toshinobu Yoko

We have performed ab initio quantum chemical calculations on clusters of atoms modeling a divalent Ge defect in Ge-doped SiO_2 glasses. It has been found that the divalent Ge defect interacts with a nearby GeO_4 tetrahedron, forming complex structural units that are responsible for the observed photoabsorption band at ~ 5eV. We have shown that these structural units can be transformed into two equivalent Ge E' centers by way of the positively charged defect center.

Keywords : Silica Glass / Paramagnetic defect centers/ Photostructural changes / Quantum chemical calculations

Photosensitivity and photoinduced holographic Bragg gratings were discovered in Ge-doped SiO_2 glasses about 20 years ago [1]. Presently photoinduced Bragg fiber- and planar waveguide gratings in the glasses are widely used in telecommunication technology for wavelength-divided multiplexing, signal shaping, fiber lasers and amplifiers, etc [2]. In contrast to these spectacular advances in practical applications, however, the fundamental understanding of the respective photoinduced processes in glass is very incomplete. In Ge-doped SiO_2 glasses, there exists an intense photoabsorption band at 5 eV, which is believed to be related to oxygen deficiency. Although the defect center associated with the 5-eV band most likely plays an important role in the photorefractive index change induced by ultraviolet (uv) irradiation, the details of the processes and mechanisms involved have remained obscure.

In this paper, we, therefore, investigate the formation mechanism of Ge E´ centers from the divalent Ge defect in Ge-doped SiO_2 glasses by using ab initio cluster model calculations at the Hartree-Fock (HF) level. It has been demonstrated that ab initio quantum-chemical cluster approaches are useful to investigate the structure and vibrational properties of glassy systems [3]. In particular, since the defect states in glasses are in general quite localized, their structure and energy states will be reasonably modeled by the cluster calculations. Appropriate cluster models hence allow us to investigate the geometries and electronic structures of the defect centers in glasses, and the calculated results will shed new light on the unsolved problem concerning the formation mechanism of Ge E´ centers associated with the photo-bleaching of the 5.16-eV band and other photoinduced phenomena of interest in Ge-doped SiO_2 glasses.

SOLID STATE CHEMISTRY — Amorphous Materials —

Scope of Research

Inorganic amorphous materials with various functions are the targets of research in this laboratory. (1) To obtain a clear view of glass materials and the bases for designing functional glasses, we investigate the structure of glasses using X-ray and neutron diffraction analysis, high resolution MAS-NMR, and ab initio MO calculation. (2) To develop materials with high optical nonlinearity, we search heavy metal oxide-based glasses and transition metal oxide thin films, and evaluate the nonlinear optical properties by Z-scan methods. (3) Photosensitivity of glasses for optical fibers and waveguides is investigated to design efficient fiber gratings and optical nonlinear materials. (4)Using sol-gel method, synthesis and microstructure control are carried out on various functional oxide thin films.

Prof
YOKO, Toshinobu
(D Eng)

Assoc Prof
UCHINO, Takashi
(D Eng)

Instr
TAKAHASHI, Masahide
(D Sc)

Assoc. Instr
JIN, Jisun
(D Eng)

Students:
TAKAISHI, Taigo (DC)
TOKUDA, Youmei (DC)
NIIDA, Haruki (DC)
DORJPALAM, Enkhtuvshin (DC)
MORI, Ryohei ((DC)
KONDO, Yuki (DC)
KAJITA, Daisuke (MC)
HIROSE, Motoyuki (MC)
TSUKIGI, Kaori (MC)
TAKEUCHI, Toshihiro (MC)
ICHII, Kentaro (UG)
KONDO, Shoichi (UG)
UENAKA, Shin-ichiro (RF)

In this work, we used a cluster of atoms modeling a divalent Ge atom in silica glass (model 1, see Fig. 1a). The geometry of the ground-state singlet (S_0) structure of the cluster was fully optimized at the HF level of theory with the polarized 6-311G(d) basis set by using analytical gradient methods. All ab initio MO calculations were carried out using the GAUSSIAN 94 computer program [4] on a supercomputer CRAY T94/4128. In order to obtain excitation energies for model 1, we employed time-dependent density-functional response theory (TD-DFRT). The TD-DFRT excitation energies were calculated for the HF/6-311G(d) geometries at the Becke's 1993 hybrid exchange functional with the Lee-Yang-Parr correlation energy functional (B3LYP) level with the 6-311G(d) basis set augmented by two sets of diffuse s and p functions on Ge1. The first transition energy was calculated to be 5.29 eV, which is in reasonable agreement with the observed transition at 5.16 eV.

The high-power density irradiation such as an excimer laser results in the photo-bleaching of the 5.16-eV band. Because of the high-power density of the laser pulses, electrons in the valence orbital will be excited to the conduction band via two photon processes, and, accordingly, a positively charged defect center is expected to be formed. It is hence interesting to reoptimize the geometry of model 1 by assuming a total charge of +1 for the cluster. We did not impose any structural constraint in optimizing the geometry of this positively charged cluster, which will be referred to as model 2 (see Fig. 1b). The Ge1–O1 (1.710 Å) and Ge1–O2 (1.725 Å) bond distances in model 2 are considerably shorter than the corresponding bond distances in model 1, and there exists no substantial interaction between O2 and Ge2 in model 2. It should also be noted that the Ge1–O3 bond distance in model 2 (1.903 Å) is shorter than that in model 1 (3.038 Å), indicating that the interaction between Ge1 and O3 becomes stronger as a result of the ionization process. The atomic spin density on Ge1 in model 2 is ~0.9, and its atomic charge is larger than that in models 1a and 1b by ~0.5. Thus, the center Ge1 atom in model 2 can be regarded as a positively charged defect center, and the shorter Ge1–O3 bond mentioned above can be interpreted in terms of the stronger Coulomb interaction between Ge1 and O3 as compared with that in model 1.

What happens when this positively charged cluster is neutralized ? In order to simulate such a process, we then optimized the geometry of model 2 by assuming a triplet state at the restricted open HF level. The optimized geometry of the triplet state, which we call model 3, is illustrated in Fig. 1c. It is quite interesting to note that the resultant geometry of model 3 is completely different from that of the previous clusters. We see from Fig. 3 that the distance between Ge2 and O3 tends to become wide apart, resulting in two almost equivalent GeO_3 units. The atomic spin densities for Ge1 and Ge2 in model 3 are calculated to be 0.897 and 0.882, respectively, indicating that these two GeO_3 units are unambiguously Ge E´ centers.

In conclusion, the present calculations have shown that

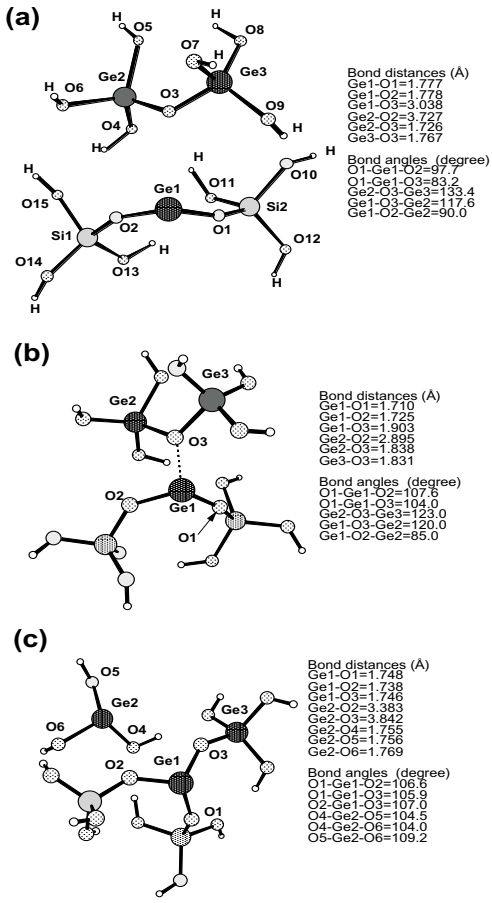

Figure 1. Equilibrium geometries for (a) a ground state singlet $Ge_3Si_2O_{15}H_{12}$ (b) a doublet $(Ge_3Si_2O_{15}H_{12})^+$, and (c) a triplet $Ge_3Si_2O_{15}H_{12}$ optimized at the HF/6-311G(d) level. Principal bond distances and angles are also shown.

the divalent Ge defect and its adjacent GeO_4 unit interact with each other, forming the combined structural units shown in Fig 1. We have further demonstrated that these structural units can be transformed into two equivalent GeO_3 units having an unpaired electron, namely, Ge E´ centers, via positively charged defect centers. We consider that the structural conversion mechanism proposed in this study plays a vital role in the refractive index changes of Ge-doped SiO_2 glasses induced by high-power uv irradiation. More detailed results will be given in a forthcoming paper [5].

References

1. K. O. Hill, Y. Fujii, D. C. Johnson and B. S. Kawasaki, Appl. Phys. Lett. **32**, 647 (1978).
2. K. Schwartz, *The Physics of Optical Recording* (Springer-Verlag, Berlin, 1993).
3. T. Uchino et al., Phys. Rev. B **58**, 5322 (1998); T. Uchino and T. Yoko, J. Chem. Phys. **108**, 8130 (1998); T. Uchino and T. Yoko, J. Phys. Chem. B **102**, 8372 (1998).
4. M. J. Frisch et al. Gaussian 94 (Gaussian Inc., Pittsburgh, 1995).
5. T. Uchino, M. Takahashi and T. Yoko, Phys. Rev. Lett. **84**, 1475 (2000)

Nonlinear Rheology and Flow-Induced Structure in a Concentrated Spherical Silica Suspension

Hiroshi Watanabe, Tadashi Inoue and Kunihiro Osaki

In hard-sphere suspensions of solid particles, the stress has the Brownian (thermodynamic) and hydrodynamic components σ_B and σ_H, the former reflecting the anisotropy of the particle distribution while the latter being determined by the hydrodynamic interaction between the particles. These two components exhibit nonlinearities under steady shear flow with different mechanisms. The nonlinearity of σ_B results from the particle distribution insensitive to the shear rate, while σ_H becomes nonlinear due to flow-induced clustering of the particles. These structural origins of the nonlinearities were confirmed from flow-SANS experiments.

Keywords: hard-sphere suspension/ Brownian stress/ hydrodynamic stress/ shear-thinning/ shear-thickening/ small angle neutron scattering

Hard-sphere suspensions of solid particles having no long-ranged potentials provide a rich field in current rheological research. At equilibrium, the particles have a liquid-like, isotropic spatial distribution. On application of strain/flow, this distribution is distorted and the particles exhibit stresses having Brownian and hydrodynamic components σ_B and σ_H [1]. Under small strain/slow shear flow, the particle distribution is only slightly distorted to exhibit the linear viscoelasticity, i.e., increases of σ_B and σ_H in proportion to the strain (γ) and/or shear rate ($\dot{\gamma}$). Large strains/fast flow considerably distort the particle distribution thereby inducing nonlinearities of σ_B and σ_H.

Recently, we investigated nonlinear rheological behavior of a concentrated hard-sphere suspension of monodisperse silica particles in an ethylene glycol/glycerol mixture (2.27/1 wt/wt) [2]. The particle radius was 40 nm, and the particle concentration was 50 wt%. For large step strains γ, the nonlinear relaxation modulus $G(t,\gamma)$ of this suspension exhibited strong damping and obeyed the time-strain separability at long times. This damping, seen under absence of flow and not attributable to changes in the hydrodynamic σ_H, was related to the nonlinearity of the Brownian σ_B. Under flow, the same suspension showed thinning and thickening of the viscosity $\eta(\dot{\gamma})$ at low and high $\dot{\gamma}$.

Structural origins of these thinning and thickening were examined through a rheological approach that uti-

FUNDAMENTAL MATERIAL PROPERTIES — Molecular Rheology —

Scope of research

The molecular origin of various rheological properties of materials is studied. Depending on time and temperature, homogeneous polymeric materials exhibit typical features of glass, rubber, and viscous fluids while heterogeneous polymeric systems exhibit plasticity in addition to these features. For a basic understanding of the features, the molecular motion and structures of various scales are studied for polymeric systems in deformed state. Measurements are performed of rheological properties with various rheometers, of isochronal molecular orientation with flow birefringence, and of autocorrelation of the orientation with dynamic dielectric spectroscopy.

Prof
OSAKI, Kunihiro
(D Eng)

Assoc Prof
WATANABE, Hiroshi
(D Sc)

Instr
INOUE, Tadashi
(D Eng)

Techn
OKADA, Shinichi

Students:
SATO, Tomohiro (DC)
KAKIUCHI, Munetaka (DC)
MATSUMIYA, Yumi (DC)
ISOMURA, Takenori (MC)
NISHIMURA, Masaki (MC)
OGAWA, Takeshi (MC)
UEMATSU, Takehiko (MC)
NOMURA, Soichiro (UG)

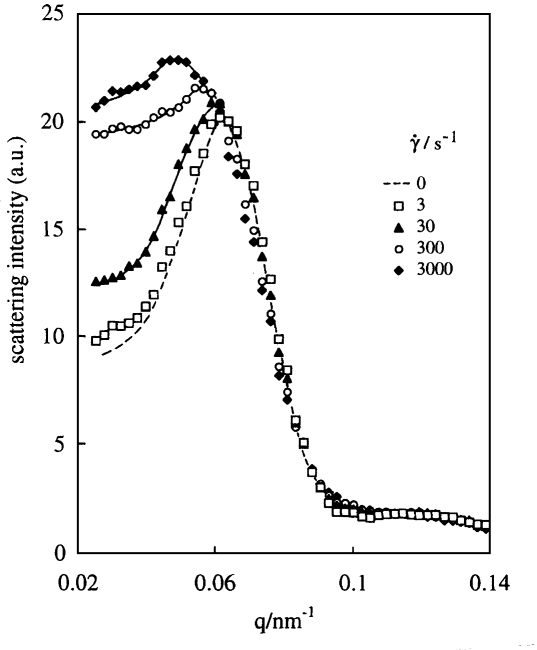

Figure 1. Scattering profile of the silica suspension at 25 ˚C detected along the velocity direction in the velocity-vorticity plane.

lized a BKZ-type constitutive equation incorporating the G(t,γ) data [2]. This equation successfully described the $\eta(\dot{\gamma})$ data in the thinning regime. Thus the thinning of $\eta(\dot{\gamma})$ and damping of G(t,γ) were commonly attributed to the nonlinearity of σ_B due to γ- and $\dot{\gamma}$-insensitive particle distribution under moderately large strain/flow [2].

In contrast, the BKZ equation failed in describing the $\eta(\dot{\gamma})$ data in the thickening regime [2]. From this result, the thickening was related to the nonlinearity of σ_H not incorporated in the equation. This nonlinearity was attributed to dynamic clustering of the particles under the flow faster than the Brownian motion of the particles.

Neutron scattering experiments were carried out for the suspension under flow to test the above structural arguments for the thinning/thickening behavior [3]. The experiments were conducted with the 30 m SANS machine on the NG3 beam line at the National Institute of Standards and Technology (NIST) at Gaithersburg, Maryland, USA, with a generous help by Prof. N. Balsara at Polytechnic University and Dr. B. Hammouda at NIST. Figure 1 shows the scattering profile at 25 ˚C detected along the velocity axis in the velocity-vorticity plane (radial view). The corresponding $\eta(\dot{\gamma})$ data are shown in Figure 2.

As seen in Figure 1, the suspension in the quiescent state ($\dot{\gamma}$ = 0 s^{-1}) exhibits a peak at the scattering vector q ≅ 0.06 nm^{-1}. This peak corresponds to the liquid-like, nearest neighbor order of the particles in this state. (This

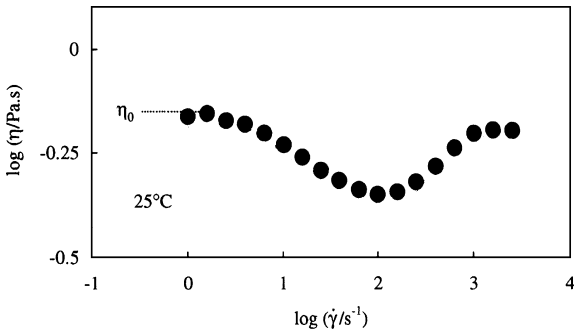

Figure 2. Steady state viscosity of the silica suspension at 25˚C. (The data were obtained in the Couette geometry.)

scattering profile was isotropic). In the shear-thinning regime ($\dot{\gamma}$ < 100 s^{-1}; Figure 2), the scattering profile is distorted from this quiescent profile only a little. Small, corresponding changes were observed in the vorticity as well as shear gradient directions. Thus the particle distribution is rather insensitive to the flow in this regime, lending support to the thinning mechanism explained earlier.

In contrast, in the thickening regime ($\dot{\gamma}$ > 100 s^{-1}; Figure 2), the scattering profile in the velocity direction is largely distorted. Specifically, the peak shifts to a lower q side and increases its intensity, indicating that large clusters of the particles are formed under the flow in this regime. Changes in the profiles detected in the other directions suggested that the clusters of anisotropic shape were formed. (A detailed analysis of this cluster structure was described in [4].) The quiescent profile was recovered in all directions on cessation of the flow, demonstrating the dynamic (non-permanent) nature of the clusters. All these results are in harmony with the thickening mechanism deduced from our rheological approach [2].

References

[1] J. F. Brady, *J. Chem. Phys.*, **1993**, *99*, 567.

[2] H. Watanabe, M.-L. Yao, A. Yamagishi, K. Osaki, T. Shikata, H. Niwa, and Y. Morishima, *Rheol. Acta*, **1996**, *35*, 433.

[3] H. Watanabe, M.-L. Yao, K. Osaki, T. Shikata, H. Niwa, Y. Morishima, N. P. Balsara, and H. Wang, *Rheol. Acta*, **1998**, *37*, 1.

[4] M. C. Newstein, H. Wang, N. P. Balsara, A. A. Lefebvre, Y. Shnidman, H. Watanabe, K. Osaki, T. Shikata, H. Niwa, and Y. Morishima, *J. Chem. Phys.*, **1999**, *111*, 4827.

Conformational Change and Orientation Fluctuations Prior to Crystallization of Crystalline Polystyrenes

Go Matsuba, Keisuke Kaji, Koji Nishida, Toshiji Kanaya and Masayuki Imai

Aiming to clarify the cause of a spinodal decomposition (SD) type microphase separation occuring during the induction period of polymer crystallization, we have made quantitative investigations about the conformational changes using FT-IR spectroscopy as well as the orientation fluctuations of the polymer rigid segments using depolarized light scattering (DPLS) . It is confirmed for syndiotactic and isotactic polystyrenes (sPS and iPS) that during the induction period, the polymer chains first transform partially from the amorpous to the crystalline conformation, involving in the increase of length of the rigid segments, which makes the system unstable to induce the orientation fluctuations of the SD type. Thus, the intensity of orientation fluctuations evloved exponentially with annealing time.

Keywords: Polymer Crystallization / Polystyrenes / Induction Period / Spinodal Decomposition / Conformational Change / Orientation Fluctuations

In the previous papers [1,2], we have reviewed the crystallization processes of poly(ethylene terephthalate) (PET) when it was crystallized directly from the melt, called 'melt crystallization' as well as from the glass, called 'glass crystallization'. It was discovered that a new peak in small-angle X-ray scattering (SAXS) appears from the very early stage of the induction period before nucleation. The detailed analysis of this new peak revealed a surprising result that a spinodal decomposition (SD) type microphase separation occurs during the induction period of crystallization. Such SD can be understood based on the kinetic theory for the isotropic-to-nematic transition of polymer liquid crystals by Doi et al.[3]; it is caused by parallel ordering of polymer rigid segments. This prediction was actually confirmed by depolarized light scattering (DPLS) . However, the origin of such orientation fluctuations is unclear. We suppose that the polymer stiff segments corresponds to crystalline segments and their extension causes the increase of their excluded volumes to make the system unstable and trigger the SD. In this study we therefore verify this hypothesis. For this purpose, the time-resolved Fourier transform infrared (FT-IR) spectroscopy and DPLS measurements during the induction period have been performed on syndiotactic polystyrene (sPS) and isotactic polystyrene (iPS) when they are crystallized by jumping the temperature to 120 °C for sPS, and to 135 °C for iPS from the glass [4,5].

Experimental

The samples used for this study were iPS and sPS with number-average molecular weights M_n = 4.0 x 10^5 and 2.9 x 10^5, respectively. The polydispersity, M_w / M_n, for the both samples is 2.0. The glass transition temperatures were determined by DSC measurements to be 100 °C for both iPS and sPS. Amorphous thin films of iPS and sPS were obtained by quenching their melts into ice-water after hot-pressed *i.e.* at 290 °C and 330 °C, respectively, for 5 min.

The time-resolved FT-IR measurements were per-

FUNDAMENTAL MATERIAL PROPERTIES — Polymer Materials Science —

Scope of research

The structure and molecular motion of polymer substances are studied using mainly scattering methods such as neutron, X-ray and light with the intention of solving fundamentally important problems in polymer science. The main projects are: the mechanism of structural development in crystalline polymers from the glassy or molten state to spherulites; the dynamics in disordered polymer materials including low-energy excitation or excess heat capacity at low temperatures, glass transition and local segmental motions; formation process and structure of polymer gels; the structure and molecular motion of polyelectrolyte solutions; the structure of polymer liquid crystals.

Prof
KAJI, Keisuke
(D Eng)

Assoc Prof
KANAYA, Toshiji
(D Eng)

Instr
NISHIDA, Koji

Students
MATSUBA, Go (DC)
YAMAMOTO, Hiroyoshi (MC)
YAMASHITA, Ryoji (MC)
SAITO, Mitsuru (MC)
TAKAHASHI, Nobuaki (MC)
KITO, Takashi (UG)
KONISHI, Takashi (UG)
OKUYAMA, Tomohiro (UG)

formed on the melt-quenched sample under an isothermal condition in a home-made temperature-control cell. The IR absorption spectra were recorded at 3.0 min intervals. The time-resolved DPLS measurements were also carried out under the same condition of the FT-IR measurements. The samples were irradiated by a plane-polarized He-Ne laser beam (λ = 632.8 nm) on a hot-stage and the scattered light intensity under depolarized conditions was recorded by a photodiode array system at 0.5 min intervals.

Results and Discussion

FT-IR It is absolutely necessary that the concerned IR bands of the sample polymers should be well characterized. Fortunately, crystalline polystyrenes, both isotactic and syndiotactic, have been done in terms of sequences of *trans* and *gauche* by Kobayashi et al. [6] Here, we aimed at bands of sPS and iPS related to crystalline conformations and measured the time dependence of their absorbance. In case of sPS, the increase in absorbance of successive *trans* conformations (TT) was observed immediately after the jump to a crystallization temperature from the glass, indicating that sPS chains begin to assume the crystalline extended conformations and that the stiff segments of sPS may be lengthened even in the very early stage of the induction period of crystallization. On the other hand, the crystalline conformation of iPS is a 3/1 helix consisting of alternate *trans* and *gauche* (TG) conformations. In this case the time-resolved FT-IR measurements showed increase in absorbance of TG conformation bands after a similar temperature jump. Furthermore, as seen from Figure 1, the bands concerned with the length of 3/1 helix also increase during the induction period of 70 min, which is indicated with a solid line in the figure. This supports that iPS chains start to assume the crystalline conformation of 3/1 helix before crystallization. From these results, we calculated critical lengths that trigger parallel ordering of polymer stiff segments using the Doi's theory. In case of the amorphous state, the persistence length is 1.88 nm for sPS or 1.32 nm for iPS [7]. In case of sPS, we calculated the critical length to be 2.51 nm, corresponding to 10 TT monomers. The parallel ordering begins when the stiff segments expand only by 0.7 nm, i.e. 2.5 monomers. The critical length is calculated to be 2.24 nm for iPS, corresponding to 3/1 helix consisting of 11 monomers. Figure 1 shows that the absorbance of 3/1 helix not longer than 10 monomers increases with time during the induction period while the band of helix not shorter than 16 monomers hardly grows. This means that the critical value of the stiff segments is between 10 and 16 monomers because at the critical value a further extension may be suppressed due to the unstable state of the system, agreeing with the prediction of 11 monomers.

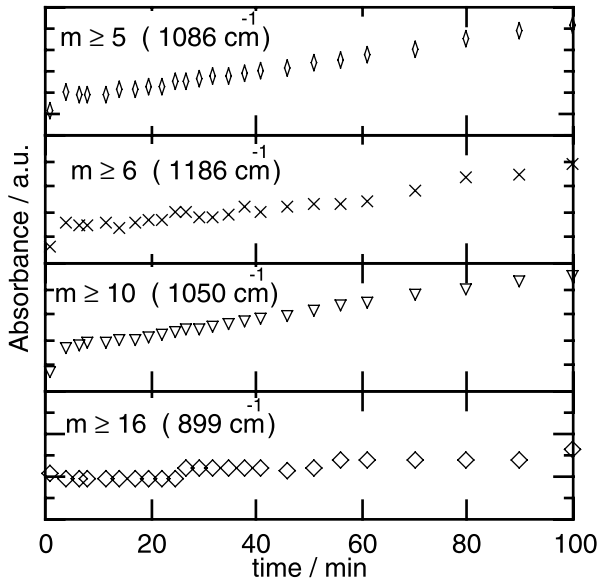

Figure 1. Time dependence of the absorbance of 3/1 helix bands of iPS annealed at 135 °C. Induction period 70 min.

DPLS The total intensity of DPLS increased with annealing time during the induction period and the scattering profiles were almost independent of scattering vector, *q*, for both the polystyrenes. These facts indicate that the sizes of the oriented domains or their aggregates are much smaller than the laser wavelength or the sizes corresponding to the measured *q*-range between 2.0 and 5.0 μm^{-1}. In the crystal growing period, however, the scattering profile becomes *q*-dependent; the intensity increases with decreasing *q*, which means that the sizes of the oriented domains or their aggregates become comparable with those of the examined *q*-range by crystal growth probably because of formation of spherulites of iPS and sPS.

We calculated the integrated intensity for the orientation fluctuations, I_{VH}, of iPS and sPS within the present *q*-range. In the first stage until 3 min, the growth rate of the integrated intensity was very slow, while the crystalline conformation (3/1 helix) suddenly grows at the very initial stage as seen from in Figure 1. For sPS the first stage of the induction period is much shorter than that for iPS at any annealing temperatures. This suggests that conformational change, that is, extension of polymer segments emerges first of all. In conclusion we have proved the hypothesis that the microphase separation is triggered by extension of polymer segments. After the first stage, we can observe the exponential growth of the integrated intensity of DPLS for each polystyrene, which is one of characteristic features of SD. Hence it has as well been confirmed in the case of crystallization of PS's as in PET that the SD-like phase separation actually emerges during the induction period.

References

[1] Imai M, Kaji K and Kanaya T, *ICR Annual Report*, **1**, 26 (1994).

[2] Kaji K, Matsunaga S, Matsuba G, Kanaya T, Nishida K and Imai M, *ICR Annual Report*, **5**, 26 (1998).

[3] Doi M and Edwards S F, *The Theory of Polymer Dynamics*, Oxford, Chapter 9 and 10 (1986).

[4] Matsuba G, Kaji K, Nishida K, Kanaya T and Imai M, *Macromolecules*, **32**, 8932 (1999).

[5] Matsuba G, Kaji K, Nishida K, Kanaya T and Imai M, *Polymer J.*, **31**, 722 (1999).

[6] Kobayashi M, Akita K and Tadokoro H, *Makromol. Chem.*, **118**, 324 (1968).

[7] Yamakawa H, *Ann. Rev. Phys. Chem*, **35**, 23 (1984).

Cellulose Assemblies Produced by *Acetobacter Xylinum*

Asako Hirai and Fumitaka Horii

Structures of cellulose assemblies produced by *Acetobacter xylinum* under various conditions have been studied mainly by transmission electron microscopy. Native cellulose crystals are composites of cellulose I_α and I_β. Twisted-ribbn cellulose assemblies produced in the HS medium at 28 ˚C were rich in cellulose I_α. On the contrary, splayed microfibrils produced in the presence of CMC at 28 ˚C were rich in I_β. Not only the ribbon assembly but also the bundle of splayed microfibrils was determined to twist in the right-handed manner. When the bacteria were incubated at 4 ˚C, two kinds of band-like assemblies, “dense” and “coarse”, were extruded perpendicularly to the long axis of bacterial cells. The number of cellulose chains produced by one bacterium was different between “dense” and “coarse” assemblies. The “dense” assembly gave the electron diffraction pattern of cellulose II. In certain cases the transition region from dense to coarse portions was observed in one assembly. Initially a “dense” portion was produced and thereafter a “coarse” portion was produced. The number of cellulose synthesis sites seems to decrease, because a bacterium becomes less active after a certain period of time at 4 ˚C.

Keywords: Bacterial cellulose/ Ribbon assembly/ Band-like assembly/ Cellulose I_α and I_β/ Cellulose II / CP/MAS ^{13}C NMR

It is known that native cellulose crystals are composites of two allomorphs, cellulose I_α and I_β. The ratio of cellulose I_α to I_β greatly differs from species to species[1]. Why do two allomorphs exist and why does the ratio vary, in nature? To answer these questions, we have studied the crystallization process for a cellulose-producing bacterium, *Acetobacter xylinum*, as a model system, because the biosynthesis of cellulose with the bacterium has been relatively well studied and the ratio is changed depending on the culture conditions, *e.g.* additives and temperature[2-4]. Recently we have found that two kinds of band-like cellulose assemblies, “dense” and “coarse”, are produced when incubated at 4 ºC [5,6]. The “dense” assembly gives the electron diffraction pattern of cellulose II.

This paper reports structures of cellulose assemblies produced by *Acetobacter xylinum* under various conditions, as revealed by transmission electron microscopy (TEM).

Cell suspensions prepared from smooth colonies isolated from *Acetobacter xylinum* ATCC 23769 were stored at 4 ºC in the Hestrin-Schramm (HS) medium or in the phosphate buffer (pH7) until use. A drop of cell suspension at 4 ºC was put on a formvar/carbon-coated Cu grid for TEM (TEM grid). After incubation for a desired period of time at 28 ºC or 4 ºC, the specimen on the TEM grid was washed with water and was negatively stained with 1% aqueous uranyl acetate containing bacitracin of 0.5 mg/ml. Some specimens on the grids were not stained but shadowed with Pt-Pd. All observations and electron diffraction (ED) experiments were carried out with a JEOL JEM-200CS transmission electron microscope operated at 200 kV. For ED, specimens were mounted on carbon-coated Cu grids. In order to suppress electron irradiation damage, appropriate specimen areas were searched with the help of a TV system, Gatan Model 622SC+ 663, and

FUNDAMENTAL MATERIAL PROPERTIES — Molecular Dynamic Characteristics —

The research activities in this subdivision cover structural studies and molecular motion analyses of polymers and related low molecular weight compounds in the crystalline, glassy, liquid crystalline, solution, and frozen solution states by high-resolution solid-state NMR, dynamic light scattering, electron microscopy, X-ray diffractometry, and so on, in order to obtain basic theories for the development of high-performance polymer materials. The processes of biosynthesis, crystallization, and higher-ordered structure formation are also studied for bacterial cellulose.

Prof
HORII
Fumitaka
(D Eng)

Assoc Prof
TSUNASHIMA
Yoshisuke
(D Eng)

Instr
KAJI
Hironori
(D Eng)

Assoc Instr
HIRAI
Asako
(D Eng)

Techn
OHMINE
Kyoko

Guest Scholar:
HU, Shaohua (Ph.D)
Students:
ISHIDA, Hiroyuki (DC)
KAWANISHI, Hiroyuki (DC)
KUWABARA, Kazuhiro (DC)
OHIRA, Yasumasa (DC)
MASUDA, Kenji (DC)
MURAKAMI, Miwa (DC)
MIYAZAKI, Masayuki (MC)
MORIMOTO, Hidetoshi (MC)
MAEKAWA, Yasushi (MC)
YAMADA, Shusaku (MC)
FUKE, Kazunori (UG)
KOJIMA, Makoto (RF)

selected-area ED patterns were recorded onto photo-films. CP/MAS ^{13}C NMR spectra were measured on a JEOL GSX-200 spectrometer operating under 4.7 T.

Figure 1a is a typical TEM photograph of a negatively stained ribbon assembly produced from a bacterial cell when grown in the HS medium at 28 °C. Figure 1b shows a model of ribbon assembly. The ribbon assembly is 40-60 nm wide and has a twist with a periodicity of 0.6-1.0 μm. The twist sense was determined to be right-handed, judging from ribbon assemblies shadowed with Pt-Pd [7]. Ribbon assemblies were found by CP/MAS ^{13}C NMR to contain both I_α and I_β crystals, with I_α being dominant (64%) [1]. On the contrary, splayed microfibrils were rich in I_β (80%) when produced in the presence of 1% CMC with DP=80 and DS=0.57 at 28 °C [3]. Compared to the twisted ribbon assembly, the splayed microfibrils formed a rather loose bundle and the bundle itself exhibited a right-handed twist sense. From these results we assume that the twisted ribbon assembly is produced while the bacterium travels translationally along its longitudinal axis with rotating around its axis.

When the bacteria are incubated at 4 °C, two kinds of band-like cellulose assemblies, "dense" and "coarse", are produced [5,6]. Figure 2 shows a "dense" assembly which is extruded directly from a bacterium during 20 min incubation at 4 °C. For comparison, a "coarse" assembly produced during 3 h incubation is shown in Figure 3. Both of the band-like assemblies are extruded perpendicularly to the long axis of the cell and appear to be wavy and coiled. It seems that at 4 °C the translational and rotational movements of the cells are suppressed. The number of cellulose chains produced by one bacterium is different between "dense" and "coarse" assemblies. The "dense" assembly gave the ED pattern of cellulose II. In contrast, the "coarse" one gave diffuse scattering. Even though a folded-chain "antiparallel" structure has been proposed for the band-like assembly [8], how to arrange "parallel" cellulose chains, when produced from a bacterium, into cellulose II with so-called "antiparallel" packing is a problem to be solved. In certain cases, the transition region from "dense" to "coarse" portions was observed in one assembly. Initially a "dense" portion was produced and thereafter a "coarse" portion was produced. It is assumed that the number of cellulose synthesis sites decreases, because a bacterium becomes less active after a certain period of time at 4 °C.

When a cell producing a "dense" band-like assembly at 4 °C was transferred into an incubator thermostated at 28 °C, a ribbon assembly (cellulose I) was produced after formation of the "dense" band-like assembly (cellulose II). When a cell producing a ribbon assembly at 28 °C was transferred into an incubator thermostated at 4 °C, a "coarse" band-like assembly began to form and the ribbon was pushed away from the cell. These results suggest that the movements of the bacterial cell are responsible for the crystallization of cellulose I or cellulose II in the bacterial system.

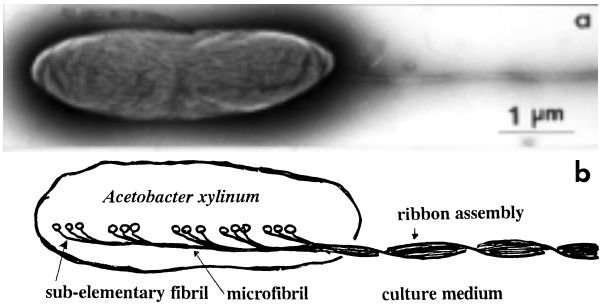

Figure 1. (a) Ribbon assembly (negatively stained). (b) A model of ribbon assembly in *A. xylinum*.

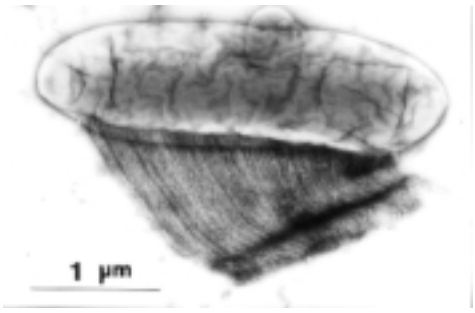

Figure 2. "Dense" band-like assembly (negatively stained).

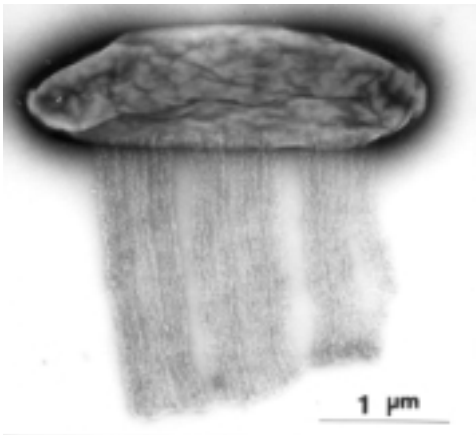

Figure 3. "Coarse" band-like assembly (negatively stained).

References

1. F. Horii, H. Yamamoto, and A. Hirai, *Macromol. Symp.*, **120**, 197-205 (1997).
2. H. Yamamoto and F. Horii, *Cellulose*, **1**, 57-66 (1994).
3. H. Yamamoto, F. Horii, and A. Hirai, *Cellulose*, **3**, 229-242 (1996).
4. A. Hirai, M. Tsuji, H. Yamamoto, and F. Horii, *Cellulose*, **5**, 201-213 (1998).
5. A. Hirai, M. Tsuji, and F. Horii, *Cellulose*, **4**, 239-245 (1997).
6. A. Hirai, M. Tsuji, and F. Horii, Preprints of *'99 Cellulose R&D*, 64-65 (1999).
7. A. Hirai, M. Tsuji, and F. Horii, *Sen'i Gakkaishi*, **54**, 506-510 (1998).
8 . S. Kuga, A. Takagi, and R. M. Brown, Jr., *Polymer*, **34**, 3293-3297 (1993).

Surface Interaction Forces of Well-Defined, High-Density Polymer Brushes Studied by Atomic Force Microscopy

Yoshinobu Tsujii, Shinpei Yamamoto, Muhammad Ejaz, Takeshi Fukuda and Takeaki Miyamoto

Direct force measurements were made by atomic force microscopy (AFM) at surfaces of polymer brushes comprising low-polydispersity poly(methyl methacrylate) chains densely end-grafted on a silicon substrate by living radical polymerization. These brushes are characterized by an exceptionally high graft density. The AFM force measurements revealed that the repulsive force rapidly increased with decreasing separation in toluene. The equilibrium thickness of the brushes was found to be proportional to the chain contour length. This indicates formation of a homogeneous polymer layer with highly stretched graft chains. Unlike the previously reported results for lower density polymer brushes, longer brushes were more resistant to compression. It is believed that these are the first observations of "polymer brushes" in the true sense of the words.

Keywords: Atomic force microscopy / Living radical polymerization / Polymer brush / Steric repulsion

Polymers densely end-grafted on a solid surface will be obliged to stretch away from the surface, forming a so-called "polymer brush". Because of their important role in many areas of science and technology, e.g., colloid stabilization, adhesion, lubrication, tribology and rheology, polymer brushes in a solvent have been extensively studied theoretically and experimentally. Most of the polymer brushes experimentally studied so far were prepared by end-functionalized polymers or block copolymers with terminal group or one block selectively adsorbed on the surface. Such systems, however, had a rather low graft density due to the steric hindrance of preadsorbed chains. Theoretical analyses of polymer brushes with higher graft densities predict that the repulsive force steeply increases with increasing graft density. By the adsorption method, however, it is difficult to obtain such high graft densities. An alternative method is the graft polymerization starting with initiating sites fixed on a surface, but it usually results in a poor control of chain length and its distribution.

We firstly succeeded in applying a living radical polymerization technique to the graft polymerization and densely grafting low-polydispersity poly(methyl methacrylate) (PMMA)[1]. In this work, we have made an AFM study on the structure and interaction forces of such dense PMMA brushes in toluene[2]. The graft density σ was estimated to be as high as 0.4 chains/nm^2, which is one of the highest ever reported values, being an order of magnitude larger than those of the polymer brushes prepared by the adsorption method. The characteristics of the brushes are given in Table 1.

The interaction forces F were measured in toluene as a

ORGANIC MATERIALS CHEMISTRY — Polymeric Materials —

Scope of research

Basic studies have been conducted for better understandings of the structure/property or structure/function relations of polymeric materials and for the development of various types of polymers with controlled structure and/or novel functions. Among those have been the studies on (1) the mechanism and kinetics of "living" radical polymerization and its applications to the synthesis of well-defined polymers and copolymers of varying architecture, (2) the synthesis and properties of cellulose- and oligosaccharide-based functional polymers, and (3) the structure of polymer gels, ultrathin films and polymer alloys.

Prof MIYAMOTO, Takeaki (D Eng)

Assoc Prof FUKUDA, Takeshi (D Eng)

Instr TSUJII, Yoshinobu (D Eng)

Instr MINODA, Masahiko (D Eng)

Assoc Instr WATAOKA, Isao (D Eng)

Students:
YAMAMOTO, Shinpei (DC)
EJAZ, Muhammad (DC)
GOTO, Atsushi (DC)
ENDO, Masaki (MC)
MARUMOTO, Yasuhiro (MC)
MIWA, Nobuhiro (MC)
SATO, Koichi (MC)
NISHIMURA, Taichiro (UG)
YOSHIKAWA, Chiaki (UG)
YAMAGUCHI, Toshinori (RF)
ZHOU, Qi (RF)

Table 1. Characteristics of PMMA Brushes

code	d [a] (nm)	M_n [b]	M_w/M_n [b]
C1	12	23000	1.36
C2	20	35900	1.36
C3	44	70500	1.34
C4	87	121700	1.39
C5	102	171400	1.56

a) Thickness in dry state measured by ellipsometry.
b) Values for free polymers produced in the polymerization system.

function of separation D using AFM while the brushes were compressed by a silica sphere probe attached on an AFM cantilever. The measured force F can be reduced to the free energy G_f of interactions between two parallel plates according to the Derjaguin approximation, $F/R = 2\pi G_f$, where R is the radius of the probe sphere. Figure 1 shows the F/R vs D curves. We note that the true distance D between the substrate surface and the silica probe, which usually is difficult to define in AFM experiments, was successfully determined by AFM-imaging across the boundary of a scratched and an unscratched region of the sample surface. The most notable feature of the F/R vs D curves is a rapid increase of the repulsive force with decreasing D. The observed repulsive forces originate from the steric interaction between the solvent-swollen brush and the probe sphere.

The equilibrium thickness L_e of the solvent-swollen brushes was determined as the critical distance from the substrate surface beyond which no repulsive force was detectable (cf. Figure 1). The scaling and self-consistent mean field approaches predict that L_e varies like

$$L_e \propto L_c \sigma^{1/3} \quad (1)$$

where L_c is the contour length of the graft chain. This relationship was confirmed by other theoretical calculations as well as by some experimental data. In Figure 2, L_e is plotted against L_c on logarithmic scale, where L_c is the number-average value calculated from the M_n value. The figure gives a linear line with a slope of 0.95, confirming eq.1. It should be noted that the ratio of L_e to L_c in our system gives a nearly constant value, $L_e/L_c = 0.8$, independent of L_c. This indicates that in our system, the graft chains are highly stretched in toluene as compared with those prepared by the adsorption of block copolymers, in which the graft densities are much lower, e.g., $L_e/L_c = 0.3$.

Using the scaling approach, de Gennes derived the equation concerning the interaction force between two parallel plates with a "moderately dense" polymer brush layer, in which graft chains overlap each other but the volume fraction of polymer in the layer is still low. This predicts that the F/R value should be scaled by D/L_e for the polymer brushes with the same graft density. The results for the block copolymer brushes were reported to be nearly consistent to this scaling theory. Our system, however, was poorly represented by this scaling theory. This indicates that the graft density in our system is so high that the scaling theory is no more applicable. In the case of the shortest graft chain, the brush layer was compressible nearly to the dry thickness ($D/L_e = 0.3$). With increasing chain length, the scaled force curve becomes steeper, meaning that the brush layer becomes more and more difficult to be compressed. The system with the longest graft chain was compressible only to $D/L_e = 0.8$, which is about three times larger than the dry thickness. This strong resistance against compression must be characteristic of polymer brushes with an extremely high graft density.

In conclusion, we succeeded in preparing low-polydispersity PMMA brushes with an exceptionally high graft density. AFM force measurements revealed that these polymer brushes have properties quite different and unpredictable from the "moderately dense" polymer brushes previously studied. Most notably, the chains in these high-density brushes were highly extended, nearly to their full lengths, and highly resistant against compression. It is believed that these were virtually the first observations of the "real" polymer brush behavior.

References

1. Ejaz, M.; Yamamoto, S.; Ohno, K.; Tsujii, Y.; Fukuda, T. *Macromolecules* **1998**, 31, 5934.
2. Yamamoto, S.; Ejaz, M.; Tsujii, Y.; Fukuda, T. *Macromolecules*, submitted.

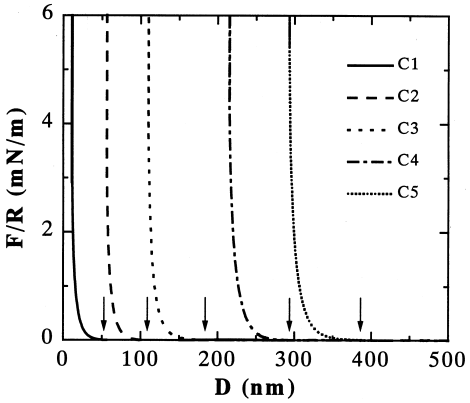

Figure 1. F/R vs D curves. The arrowheads indicate L_e.

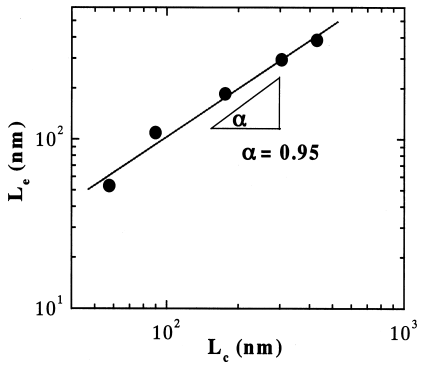

Figure 2. Plot of L_e vs L_c.

π-Conjugated Radical Cations Stabilized by Surrounding Bicyclic σ-Frameworks

Koichi Komatsu, Tohru Nishinaga, Akira Matsuura and Atsushi Wakamiya

Benzene **1**, naphthalene **2**, biphenylene **3**, and anthracene **4**, fully annelated with bicyclo[2.2.2]octene were transformed into the corresponding radical cations, and their structures were clarified by X-ray crystallography. The remarkable stability of these salts are ascribed to the electronic and steric effects of the bicyclic frameworks. 1,4-Dithiin **5** annelated with the same bicyclic units was also oxidized into the stable salt of the radical cation, and the structure examined by X-ray crystallography. The ESR study indicated that the spin is effectively delocalized into the bicyclic frameworks. Dithiin **5** was further oxidized into the dication, which was shown to be 6π aromatic by the NMR and theoretical studies.

Keywords: cyclic voltammetry / X-ray crystallography / ESR / molecular orbital calculations

Organic radical cations have been of fundamental interest to organic as well as physical chemists in a variety of contexts. Their stabilization have in general been achieved by the extension of the π-conjugated system. In our group, however, it has been clarified that the remarkable stabilization of such a positively charged π-conjugated system can be attained by structural modification with σ-frameworks. Typical examples are demonstrated by the following studies.

1. Radical Cations of Benzenoid Aromatics.

A series of benzenoid aromatics, benzene **1** [1], naphthalene **2** [2], biphenylene **3** [3], and anthracene **4** [4], fully annelated with bicyclo[2.2.2]octene (abbreveated as BCO) exhibited reversible oxidation waves at remarkably

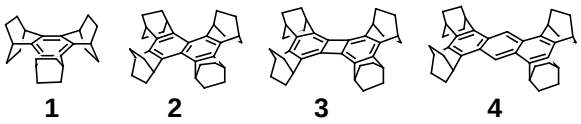

low potentials (+1.08, +0.33, +0.25, and +0.17 V in tetrachloroethane vs Fc / Fc^{+}, respectively). Accordingly these hydrocarbons were readily converted to the corresponding radical cation salts, $Ar^{\cdot+}SbCl_6^{-}$, quantitatively by one-electron oxidation with 1.5 equivalents of $SbCl_5$.

The salts were isolated as ruby red (**1**$^{\cdot+}$), dark green (**2**$^{\cdot+}$), blue violet (**3**$^{\cdot+}$), and dark green (**4**$^{\cdot+}$) crystals, which were stable in air at room temperature. This is the first examples of the isolation of the radical cation salts of alkyl-substituted benzene, naphthalene, and biphenylene as stable crystals. This stability is ascribed

ORGANIC MATERIALS CHEMISTRY — High-Pressure Organic Chemistry —

Scope of Research

Fundamental studies are being conducted for creation of new functional materials with novel structures and properties and for utilization of high pressure in organic synthesis. The major subjects are: synthetic and structural studies on novel cyclic π-systems having σ-π conjugation; synthesis of redox-active dehydroannulenes; chemical transformation of fullerene C_{60}; mechanochemical reactions of fullerenes.

Prof
KOMATSU
Koichi
(D Eng)

Instr
MORI
Sadayuki
(D Eng)

Instr
NISHINAGA
Tohru
(D Eng)

Instr
MURATA
Yasujiro
(D Eng)

Students:
MATSUURA, Akira (DC)
FUJIWARA, Koichi (DC)
IZUKAWA, Yoshiteru (DC)
KATO, Noriyuki (MC)
WAKAMIYA, Atsushi (MC)
ITO, Miho (MC)
NODERA, Nobutake (MC)
INOUE, Ryouta (UG)
SUZUKI, Mitsuharu (UG)

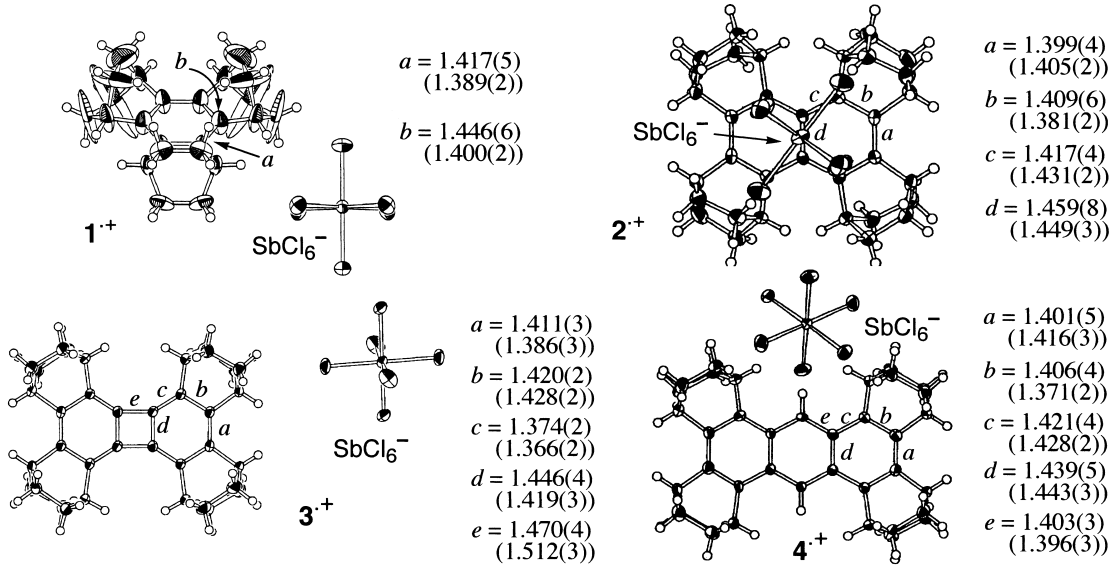

Figure The X-ray crystal structures of $\mathbf{1}^{\cdot+}SbCl_6^-$ – $\mathbf{4}^{\cdot+}SbCl_6^-$ with the averaged bond lengths. The values in the parentheses are the bond lengths of the neutral molecules.

to both the electronic effects, such as inductive and σ-π conjugative effects, and the steric effects, such as steric and "Bredt's rule" protection, of the rigid bicyclic σ-frameworks surrounding the π-system.

The X-ray crystallography was conducted for these radical cation salts to give the results shown in Figure. Here the change in bond lengths upon one-electron oxidation of **2**–**4** is related to the coefficients of the relevant carbons' HOMO of the neutral molecule: the bonds with the bonding nature in HOMO were elongated and those with antibonding in HOMO were shortened. The benzene radical cation appears to be subjected to the static Jahn-Tellar distortion, although the effect of crystal packing force can not be completely ruled out.

2. Radical Cation and Dication of 1,4-Dithiin [5, 6].

The 1,4-dithiin is a π-conjngated system isoelectronic to cyclooctatetraene, and its derivative annelated with BCO (**5**) is highly susceptible to the consecutive one-electron oxidation as shown by the oxidation potential in dichloromethane: $E_{1/2}$ (1) +0.0 V, $E_{1/2}$ (2) 0.82 V vs Fc / Fc^+.

The oxidation with $SbCl_5$ afforded the radical cation salt $\mathbf{5}^{\cdot+}SbCl_6^-$ as brown-colored crystals, which were characterized by X-ray crystallography.

The ESR spectrum of $\mathbf{5}^{\cdot+}$ exhibited a 9-line signal due to the coupling with 8 anti-methylene protons (a_H 0.080 mT) and also a weak coupling with ^{33}S (natural abundance 0.75%) (a_S 9.86 mT). The a_S value was even smaller than the value reported for the thianthrene radical cation (**6**). This is supported by the spin density calculated (B3LYP / 6-31G*) for these two sulfur atoms (spin density 0.2869 for $\mathbf{5}^{\cdot+}$, 0.2874 for $\mathbf{6}^{\cdot+}$), and indicates that the bicyclic σ-framework is even more effective for spin delocalization than the annelated benzene π-system [5].

The treatment of dithiin **5** with an excess amount of a stronger oxidant, SbF_5, in CD_2Cl_2 caused the formation of dication $\mathbf{5}^{2+}$ as examined by ^1H and ^{13}C NMR spectroscopy. The downfield shift (Δδ 2.02 ppm) of the bridgehead proton of the BCO unit clearly demonstrates the presence of 6π-electron aromaticity in dication $\mathbf{5}^{2+}$. This was further supported by the value of nucleus independent chemical shift (NICS) of -8.8 calculated for $\mathbf{5}^{2+}$ (GIAO / HF / 6-31+G* // B3LYP / 6-31G*) [6].

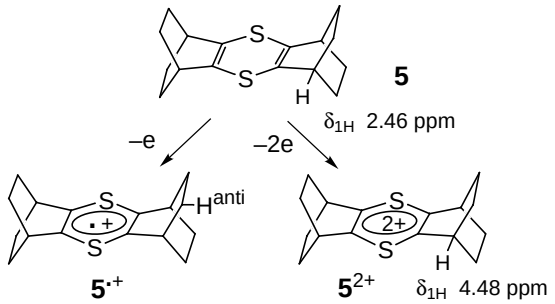

References

1. Komatsu K, Aonuma S, Jinbu Y, Tsuji R, Hirosawa C and Takeuchi K, *J. Org. Chem*., **56**, 195 (1991).
2. Matsuura A, Nishinaga T and Komatsu K, *Tetrahedron Lett*., **40**, 123 (1999).
3. Matsuura A, Nishinaga T and Komatsu K, *Tetrahedron Lett*., **38**, 4125 (1997).
4. Matsuura A, Nishinaga T and Komatsu K, *Tetrahedron Lett*., **38**, 3427 (1997).
5. Nishinaga T, Wakamiya A and Komatsu K, *Tetrahedron Lett*., **40**, 4375 (1999).
6. Nishinaga T, Wakamiya A and Komatsu K, *Chem. Commun*., **1999**, 777.

Reaction of Hypercoordinate Dichlorosilanes Bearing 8-(Dimethylamino)-1-naphthyl Group(s) with Magnesium: Formation of the 1,2-Disilaacenaphthene Skeleton

Kohei Tamao, Masahiro Asahara, Tomoyuki Saeki and Akio Toshimitsu

The reaction of a hypercoordinate dichlorosilane bearing an 8-(dimethylamino)-1-naphthyl group(s) with magnesium affords a dimeric product that contains a 1,2-disilaacenaphthene skeleton arising from silicon–silicon and silicon–naphthyl carbon bond formation and amino group migration from the naphthyl carbon atom to the coordinated silicon atom.

keywords: 1,2-disilaacenaphthene / hypervalent compounds / magnesium / silicon / rearrangements

We have clarified that a pentacoordinate monochlorosilane **1** containing the 8-dimethylamino-1-naphthyl group undergoes reductive coupling with magnesium to afford **2**, which provides a new procedure for the direct interconnection of pentacoordinate silicon atoms (Scheme 1).[1] We anticipated that a similar magnesium reduction of a pentacoordinate dichlorosilane containing the same aminonaphthyl group would give polysilanes in which all the silicon atoms are pentacoordinate [eq. (1)]. However, contrary to our expectation, the reaction actually afforded

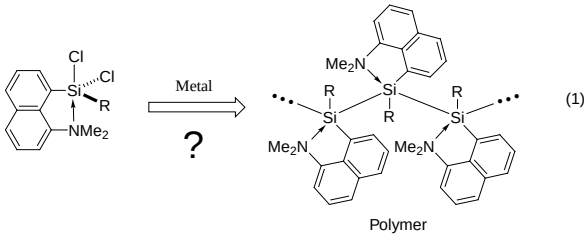

(1)

no polysilanes but only a dimeric product that contained a 1,2-disilaacenaphthene skeleton arising from Si—Si and Si—C bond formation and amino group migration from the naphthyl carbon atom to silicon atom (Scheme 2).[2]

The pentacoordinate dichlorosilane **3** bearing an 8-(dimethylamino)-1-naphthyl group was treated with 2 g-atom amounts of magnesium. After quenching with isopropyl alcohol, the dimerized product 1-isopropoxy-1,2-disilaacenaphthene (**4**) bearing only one 8-(dimethylamino)-1-naphthyl group, was obtained as a mixture of

Scheme 1.

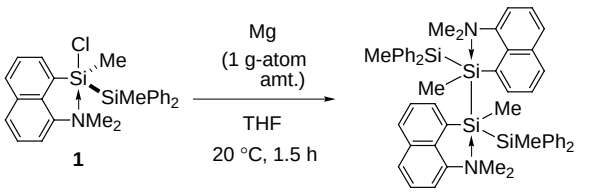

SYNTHETIC ORGANIC CHEMISTRY — Synthetic Design —

Scope of research

(1) Synthesis, structural studies, and synthetic applications of organosilicon compounds, such as pentacoordinate silicon compounds, functionalized silyl anions, and functionalized oligosilanes. (2) Design and synthesis of novel π-conjugated polymers containing silacyclopentadiene (silole) rings, based on new cyclization reactions and carbon-carbon bond formations mediated by the main group and transition metals. (3) Chiral transformations and asymmetric synthesis via organosulfur and selenium compounds, especially via chiral episulfoniun and episelenonium ions.

Prof TAMAO, Kohei (D Eng)

Assoc Prof TOSHIMITSU, Akio (D Eng)

Instr KAWACHI, Atsushi (D Eng)

Instr YAMAGUCHI, Shigehiro (D Eng)

RANGAPPA, Kanchugarakoppal Subbegowda (Guest Scholar); KATKEVICS, Martins (Guest Res Assoc); JIN, Ren-Zhi (Guest Res Assoc); CHO, Yeon Seok (Guest Res Assoc); NAKAMURA, Hiroshi (D Eng); NAKAMOTO, Masaaki (D Eng); AKIYAMA, Seiji (DC); MAEDA, Hirofumi (DC); TSUJI, Hayato (DC); SHIRASAKA, Toshiaki (DC); ITAMI, Yujiro (DC); GOTO, Tomoyuki (MC); SAEKI, Tomoyuki (MC); HIRAO, Shino (MC); MINAMIMOTO, Takashi (MC); MATSUDA, Ryotaro(UG); MIKI, Takashi (UG)

stereoisomers (*cis*:*trans* = 2:1). The structure of this quite unexpected product was confirmed by X-ray crystallography on *cis*-**4** (Figure 1) and by ^{1}H, ^{13}C, and ^{29}Si-NMR spectra of *cis*- and *trans*-**4**. It is noteworthy that the coordination number of one of the two silicon atoms is lowered from five to four.

Scheme 2.

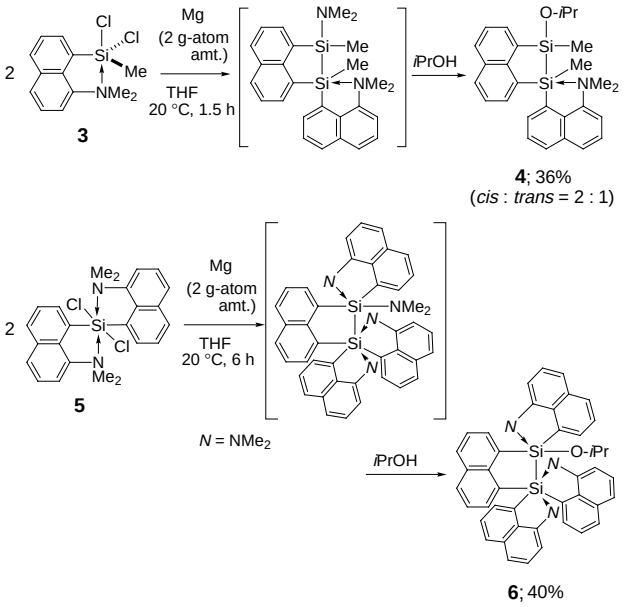

Hexacoordinate dichlorosilane **5** bearing two 8-(dimethylamino)-1-naphthyl groups also reacted with magnesium to afford, after treatment with isopropyl alcohol, 1-isopropoxy-1,2-disilaacenaphthene (**6**), which bears three 8-(dimethylamino)-1-naphthyl groups as the major product (Scheme 2). The structure of this crowded molecule was also determined by X-ray crystallography (Figure 2). One silicon atom is again pentacoordinate while the other is hexacoordinate. Compound **6** is the first disilane composed of hexacoordinate and pentacoordinate silicon centers.

Interestingly, in these reactions, one silicon atom became bonded to the naphthyl carbon atom that bore the amino group. The amino group migrated to the coordinated

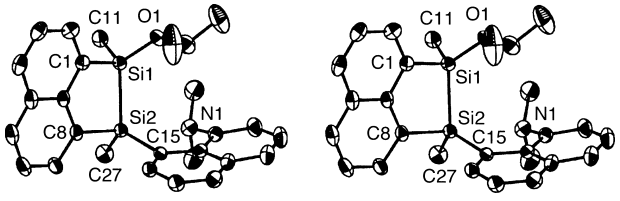

Figure 1. X-ray structure of *cis*-**4** drawn in stereoview at 30% probability level. All hydrogen atoms were omitted for clarity. Selected distances (Å) and angles (deg): Si1—Si2, 2.3469(8); Si2···N1, 2.828(2); N1···Si2—C8, 177.16(8); Si1—Si2—C8, 89.43(8); Si1—Si2—C15, 113.56(7); Si1—Si2—C27, 119.14(9); Si2—Si1—O1, 122.01(7); Si2—Si1—C1, 93.75(7); Si2—Si1—C11, 114.07(9).

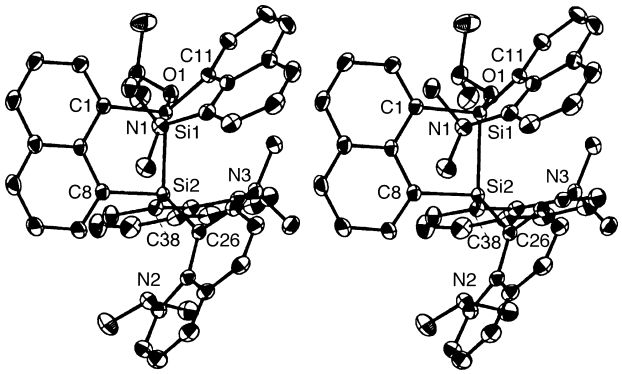

Figure 2. X-ray structure of **6** drawn in stereoview at 30% probability level. All hydrogen atoms were omitted for clarity. Selected distances (Å) and angles (deg): Si1—Si2, 2.3641(6); Si1···N1, 3.078(2); Si2···N2, 3.147(2); Si2···N3, 2.970(2); O1—Si1···N1, 168.06(6); Si2—Si1—O1, 107.17(5); Si2—Si1—C1, 94.35(6); Si2—Si1—C11, 127.54(6); Si1—Si2···N2, 171.97(4); N3···Si2—C8, 175.84(7); Si1—Si2—C8, 89.14(6); Si1—Si2—C26, 122.15(6); Si1—Si2—C38, 104.17(6).

silicon atom to afford an aminosilane with a lower coordination number and was finally substituted by the isopropoxy group during workup with isopropyl alcohol.

Two types of reactions of hypercoordinate dihalosilanes with alkali or alkali earth metals have been reported. One is the conventional silicon—silicon bond formation observed by Beltzner et al. in the reaction of a hypercoordinate dichlorosilane bearing 2-[(dimethylamino)methyl]phenyl group(s) with magnesium to afford the corresponding cyclic trisilane.[3] The other is cyclization by silicon—benzyl carbon bond formation and migration of the amino group from the benzyl carbon atom to the silicon atom without silicon—silicon bond formation. Thus, Corriu, Auner et al. reported the reaction of a pentacoordinate difluorosilane bearing the 8-[(dimethylamino)methyl]-1-naphthyl group with lithium or lithium naphthalenide to afford a 1-silaacenaphthene derivative.[4] In our case, both silicon—silicon bond formation and amino-group migration proceeded concomitantly and selectively in the reaction of **3** and **5** with magnesium to afford the 1-amino-1,2-disilaacenaphthene derivatives. These results indicate that the course of reaction depends on the structure of the aminoaryl groups and suggest the possibility of developing new types of reactions by the introduction of new intramolecular coordinating groups.

References

1. Tamao K. Asahara M. Saeki T. and Toshimitsu A. *Chem. Lett.*, 335 (1999),
2. Tamao K. Asahara M. Saeki T. and Toshimitsu A. *Angew. Chem. Int. Ed. Engl.*, **38**, 3316 (1999).
3. a) Belzner J. *J. Organomet. Chem.*, **430**, C51 (1992). b) Belzner J. Dehnert U. Ihmels H. Hübner M. Müller P. and Usón I. *Chem. Eur. J.*, **4**, 852 (1998).
4. Corriu R. Lanneau G. Priou C. Soulairol F. Auner N. Probst R. Conlin R.and Tan C. *J. Organomet. Chem.*, **466**, 55 (1994).

Visualization of Molecular Length of α,ω-Diamines and Temperature by a Receptor Based on Phenolphthalein and Crown Ether

Kaoru Fuji, Kazunori Tsubaki, Kiyoshi Tanaka, Noriyuki Hayashi, Tadamune Otsubo and Takayoshi Kinoshita

The hybrid molecule **1** consisting of phenolphthalein and crown ether moieties can discriminate the chain length of the α,ω-diamines by color change, while **2** can not. Thus, it is suggested that two crown ether part are necessary to visualize the chain length by the color. The pink color faded at 50 °C and reappeared at 20 °C, which could repeated more than 10 times.

Key words: Chromgenic receptor/ Molecular recognition/ Phenolphthalein

Supramolecular chemistry based on molecular recognition has become attractive not only for organic chemists but also for researchers in other academic fields, and remarkable progress has recently been made in this area. If the weak signals derived from such molecular interaction could be transformed into visual information, more information could be directly available. Here, we report the visual determination of the chain length of linear diamines using a functional molecule **1** consisting of phenolphthalein (**3**) and two loops of crown ether. Visualization of the "length" of a guest molecule as well as "temperature" is possible using **1** [1].

Interactions of host compounds (**1** and **2**) and phenolphthalein (**3**) with a terminal diamine **4** (n = 8) and nonylamine (**5**) were examined by taking UV-visible spectra in MeOH at 25 ˚C (Fig. 1). While diamine **4** (n = 8) developed no color change with **3**, a slight color change was observed with **2**. In contrast, dramatic color change

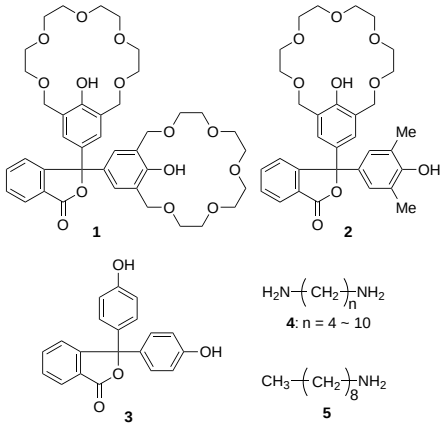

SYNTHETIC ORGANIC CHEMISTRY — Fine Organic Synthesis —

Scope of Research

The research interests of the laboratory include the development of new synthetic methodology, molecular recognition, and total synthesis of natural products. Programs are active in the areas of use of chiral leaving groups for an asymmetric induction, asymmetric alkylation of carbonyl compounds based on "memory of chirality", development of new type of chiral nucleophilic catalysts, utilization of 8,8'-disubstituted 1,1'-binaphthyls as a chiral controller, visualization of molecular length by functionalized phenolphthalein, use of homooxacalixarene for molecular recognition, syntheses of molecular switch.

Professor FUJI Kaoru (D Pharm SC)

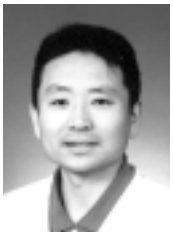

Assoc Prof KAWABATA Takeo (D Pharm SC)

Instructor TSUBAKI Kazunori (D Pharm SC)

Technician TERADA Tomoko

Secretary:
IZAWA, Yukako
Lecturer (part-time):
BAGUL, Trusar D. (Ph. D)
Guest Research Associate:
MARX, Karsten H. (Ph. D); CHEN, Jianyong (Ph. D); WANG, Bingui (Ph. D); CHANCHARUNEE, Sirirat (Ph. D)
Students:
MOMOSE, Yashima (DC); OHNISHI, Hiroshi (DC); NURUZZAMAN, Mohammad (DC); FUJII Kunihiko (MC); HAYASHI, Noriyuki (MC); OTSUBO, Tadamune (MC); YOSHIDA, Hiroshi (MC); TANAKA, Hiroyuki (MC); SUZUKI, Ryutaro (MC) MUKOYOSHI, Koichiro (MC)

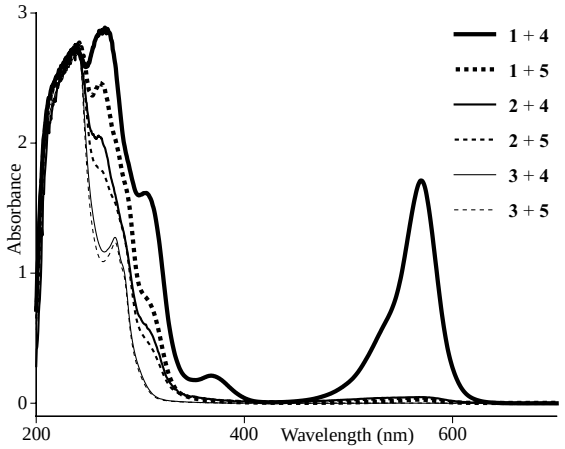

Figure 1. UV-visible spectra of **1, 2** and **3** with the diamine **4** (n = 8) (solid lines) and with nonylamine (**5**) (dotted lines) in MeOH at 25 °C. The concentrations are 2.5 x 10^{-4} M for the hosts and 2.5 x 10^{-3} M for the guests.

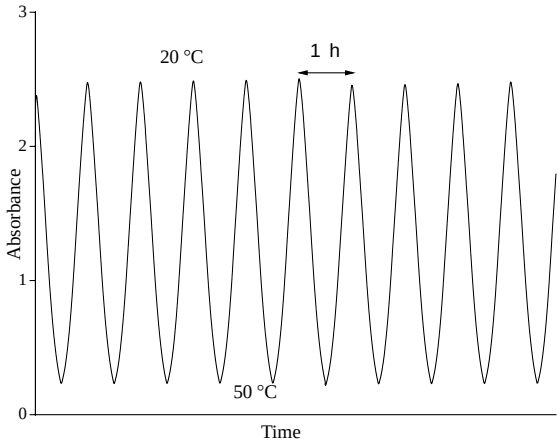

Figure 2. Temperature dependence of the absorbance of **1** (5.0 x 10^{-4} M) in the presence of **4** (n = 9, 1.0 x 10^{-3} M).

Table 1. The Apparent Association Constant (K') of the complexes of **1** with diamines **4** and Molar Absorption Coefficients (ε).

diamine **4**	K' (M^{-1})	ε
n = 7	910 ± 60	5830 ± 120
n = 8	1270 ± 50	8930 ± 100
n = 9	2020 ± 100	7940 ± 130
n = 10	1370 ± 80	5280 ± 70

was seen with compound **1**. The change in color depends upon the length of the diamine. The color development by **1** and amines was greatest with guest diamines of n = 8 and 9. Diamines shorter than 1,5-diaminopentane gave no coloration that could be detected by the naked eye.

The degree of color development by **1** and diamines **4** is quite sensitive to temperature. The absorbance at 571 nm by the complex of **1** and diamine **4** (n = 9) decreases with a rise in temperature. The reversibility and reproducibility of this change were confirmed as follows. The temperature of the mixture was gradually increased from 20 ˚C to 50 ˚C over 30 min and then dropped to 20 ˚C over another 30 min. This temperature profile was repeated more than 10 times while monitoring the UV-visible spectrum at 571 nm (Fig. 2). In the ^{1}H NMR spectrum of the complex, the signal of the α-methylene of the diamine at δ 2.47 ppm was broad at 22 ˚C, but sharpened to a triplet at 60 ˚C. These experiments show that the diamine **4** (n = 9) dissociates from the host molecule **1** to show free rotation at a higher temperature. Thus, color development due to complex formation reflects changes in temperature.

To better understand the above phenomena, the structure of the colored complex of **1** and diamine **4** (n = 9) was investigated in detail. The values of pK_a1' and pK_a2' in 50% aqueous methanol at 30 °C were 10.4 and 11.1 for **1**, and 9.6 and 11.3 for **3**. These data suggest that there is no correlation between the coloration of **1** and the difference in p*K*a' values. Tamura and his coworkers reported that the colored complex of phenolphthalein (**3**) exists in a dianionic form [2]. The colored complex of **1** and diamines is also considered a dianion. A Job plot using UV-visible spectra suggested that the host-guest ratio in the colored complex of **1** and diamine **4** (n = 9) was not 1:1, but rather 1:2, 2:3, or some intermediate ratio. These findings indicate that one molecule of the diamine is bridged between two crown rings and the other serves as a counter cation of the carboxylate, derived from ring-opening of the γ-lactone of **1**. Therefore, a new system was designed in which a large excess of *N*-ethylpiperidine exists together with the diamine to act as a counter cation for the carboxylate anion. *N*-Ethylpiperidine itself gave no color without a diamine. The Job plot of **1** and diamines **4** (n = 7-10) in the presence of *N*-ethylpiperidine clearly showed a 1:1 correlation between them. Thus, the colored complex consists of **1**, diamine and *N*-ethylpiperidine in the ratio of 1:1:1 in this system. The apparent association constant (K') of the complexes and molar absorption coefficients (ε) were determined by UV-visible titration. The results listed in Table 1 show that the degree of coloration caused by the interaction between **1** and diamines depends not only on the apparent association constants but also molar absorption coefficients.

References

1. Fuji, K.; Tsubaki, K.; Tanaka, K.; Hayashi, N.; Otsubo, T.; Kinoshita, T. *J. Am. Chem. Soc.*, **1999,** *121,* 3807.
2. Tamura, Z.; Abe, S. Ito, K.; Maeda, M. *Anal. Sci.*, **1996**, *12*, 927.

Stereoselection Controlled by Electronic Effect of a Carbonyl Group in Oxidation of NAD(P)H Model

Seiji Oda and Norimasa Yamazaki

Newly synthesized NAD(P)H model compound (1,4,6,7-tetrahydro-1,6,11-trimethyl-5-oxo-5*H*-benzo[*c*]pyrido[2,3-*e*]azepin; 11Me-MMPAH) has an axial chirality with respect to carbonyl dipole in the side chain amide group. The orientation of carbonyl dipole is fixed with sticking out of the dihydropyridine ring. In oxidation of this compound with a series of *p*-benzoquinone derivatives, we investigated the relationship between the orientation of carbonyl dipole in nicotinamide and the stereochemistry of the reactions of NAD(P)H

Keywords: NAD(P)H model compound/ (net) hydride transfer/ stereochemistry/ carbonyl dipole/ oxidation

The pyridine nucleotide coenzymes NADH and NADPH are ubiquitous in all living systems. They are required for the redox reactions of more than 370 different kinds of enzymes. Although pyridinium/dihydropyridine moieties in $NAD(P)^+$ / NAD(P)H coenzymes are achiral, *re*- and *si*-faces of the molecules are recognized by a substrate when they are set in a pocket of an enzyme. Formally, a hydride ion is transferred stereospecifically and reversibly between the 4-position of $NAD(P)^+$ or NAD(P)H and substrate. From the viewpoint of chemical evolution of an enzyme, the difference in stereochemistry as well as the mechanism of the redox reactions involved is an interesting subject.

It is considered that the stereochemistry of the reactions of NAD(P)H is influenced by the orientation of the carbonyl dipole in the side-chain amide group. To clarify this relationship, we designed and synthesized new NAD(P)H model compound (11Me-MMPAH) [1]. In this compound, the methyl substituent at 11-position in an *o*-phenylene group prevents a flipping of the *o*-phenylene moiety, and, therefore, a flipping of the carbonyl group at room temperature. At the same time, in the oxidized form (11Me-$MMPA^+I^-$), the axial chirality with respect to the orientation of the carbonyl dipole in 11Me-MMPAH is sophisticatedly preserved. This model fixing the orientation of carbonyl dipole with sticking out of the dihydropyridine ring, we can readily investigate the relationship between the orientation of carbonyl dipole in nicotinamide and the stereochemistry of the reactions of 11Me-MMPAH.

In order to investigate the selectivity of the faces in which a (net) hydride is transferred, oxidations of 11Me-MMPAH, which are predominantly

BIOORGANIC CHEMISTRY — Bioorganic Reaction Theory —

Scope of research

Biochemical reactions are studied from the viewpoint for physical organic chemistry. Specifically, the reaction mechanism and stereochemistry of NAD-dependent oxidoreductases are explored. Stereospecific redox transformations mediated by certain biocatalysts such as microbes, enzymes, cultured tissues are also studied. The results will be applied to develop new organic reactions.

Assoc Prof NAKAMURA, Kaoru (D Sc)

Instr SUGIYAMA, Takashi (D Sc)

Instr KAWAI, Yasushi (D Sc)

Assoc Instr YAMAZAKI, Norimasa (D Sc)

Techn HIRANO, Toshiko

Students
KINOSHITA, Masamichi (RF, D Sc)
HIDA, Kouichi (DC)
TAKENAKA, Keishi (DC)
INABA, Yoshikazu (DC)
MATSUDA, Tomoko (DC)
MATSUO, Takashi (DC)
MISAWA, Ibuki (DC)
ODA, Seiji (DC)
HAYASHI, Motoko (DC)
ITOH, Kenji (DC)
YAMAGUCHI, Hitomi (DC)
TAKEUCHI, Minoru (MC)
UMEMOTO, Shin'ichi (MC)
YAMANAKA, Rio (MC)
OOTA, Mitsuko (MC)
SASAKI, Takayo (MC)
DAO, Duc Hai (RS)

deuterated the *syn*- and *anti*-hydrogen with respect to carbonyl dipole respectively, with a series of *p*-benzoquinone derivatives in the absence and presence of Mg^{2+} were studied [2,3]. Without Mg^{2+}, relative reactivity ratio for *syn*- and *anti*-hydrogens with respect to carbonyl dipole in 11Me-MMPAH indicated uniformly high *anti*-selectivity in oxidation with all quinones; *anti*-hydrogen is 3-32 times more reactive than *syn*-hydrogen. On the other hand, a dramatic change in the *syn*/*anti* selectivity was observed when Mg^{2+} was present in the system.

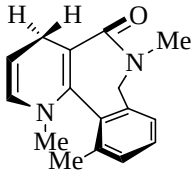

11Me-MMPAH

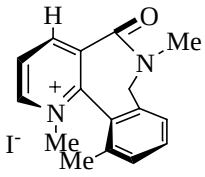

11Me-MMPA$^{+}I^{-}$

In addition, as the reduction potential of *p*-benzoquinone derivative decreases, the reactivity of the *syn*-hydrogen becomes larger. This tendency is emphasized in the reaction with a weakly oxidizing agent such as 2,6-dimethyl-*p*-benzoquinone; *syn*-hydrogen is 5 times more reactive than *anti*-hydrogen.

These observed selectivity in the absence and presence of Mg^{2+} can be explained by the contribution of initial electron transfer process prior to the proton transfer. In the *syn*-hydrogen transfer reaction, the carbonyl oxygen points toward the pairing *p*-benzoquinone derivative, whereas the pairing *p*-benzoquinone derivative sits itself in the opposite side of the carbonyl oxygen in the *anti*-hydrogen-transfer reaction. In the absence of Mg^{2+}, the transfer of the *anti*-hydrogen takes place easier than that of the *syn*-hydrogen because the *anti*-face is electronically more favored than the other; electrostatic repulsion of the *syn*-side between the carbonyl dipole of radical cation of 11Me-MMPAH and the radical anion and/or carbonyl dipole of quinone is much larger than that of *anti*-side (Fig. 1(a)). The change in the reactivity of the *syn*/*anti*-hydrogen strongly suggests an important contribution of Mg^{2+} in the pre-association complex for determining the stereochemistry of the reaction. There is no doubt that Mg^{2+} play the role of a Lewis acid catalyst to promote the reaction, because a weakly oxidizing quinone such as 2,6-dimethyl-*p*-benzoquinone can not oxidize 11Me-MMPAH without Mg^{2+}. The reactivity of relative weakly oxidizing agent is not sufficient to abstract an electron from 11Me-MMPAH in the model-quinone binary complex, or the reactant and quinone not to bring them into closer face-to-face contact in the *syn*-face without catalytic assistance of Mg^{2+}. Thus, in the oxidation with relative weakly oxidizing agent, catalytic contribution of Mg^{2+} becomes large to undergo the reaction and, therefore, the *syn*-hydrogen is inevitably involves a model-Mg^{2+}-quinone ternary complex as a pre-association intermediate (Fig. 1(b)).

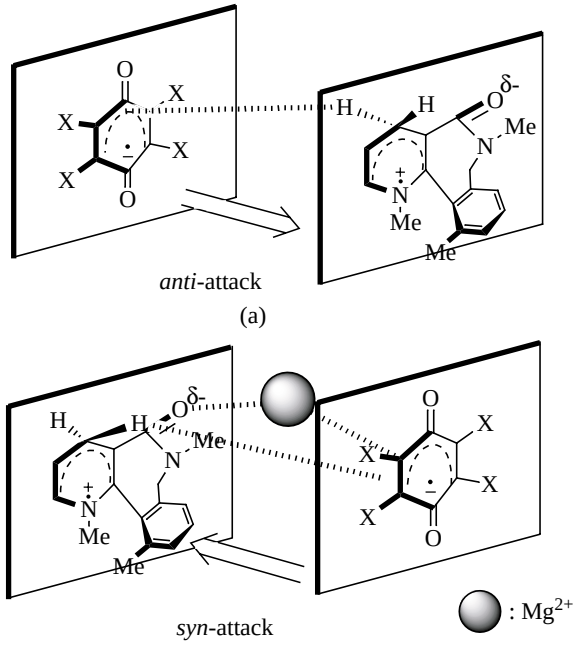

Figure 1. Pre-association complex between NAD(P)H model and quinone without Mg^{2+} (a) and with Mg^{2+} (b) from initial electron transfer.

We showed that the orientation of carbonyl dipole in model compound as well as the presence or absence of Mg^{2+} controls the stereochemistry of oxidation of an NAD(P)H model compound with *p*-benzoquinone derivative. Such a strong control of the stereochemistry by an electronic(nonsteric) effect may be a mimic of stereochemical controls in biological reactions catalyzed by archaic enzymes, where structural sophistication was insufficient to exert a perfect control of the stereochemistry.

References

1. Ohno A, Tsutsumi A, Yamazaki N, Okamura M, Mikata Y, Fujii M, *Bull. Chem. Soc. Jpn.*, **69**, 1679, (1996).
2. Ohno A, Ishikawa Y, Yamazaki N, Okamura M, Kawai Y, *J. Am. Chem. Soc.*, **120**, 1186, (1998).
3. Ohno A, Oda S, Yamazaki N, *Tetrahedron Lett.*, **40**, 4577, (1999).

Structural Basis for Reaction Mechanism and Drug Delivery System of Chromoprotein Antitumor Antibiotic C-1027

Yasushi Okuno and Yukio Sugiura

Antitumor antibiotic C-1027 that is regarded as a natural model of drug delivery system, consists of a carrier apoprotein (Apo) and an enediyne chromophore (Chr). We have compared three solution structures of the DNA-Chr complex, Apo-Chr complex, and free Chr determined by high-resolution NMR experiments. The guest molecule, C-1027 chromophore, showed two distinct binding modes fitted to binding sites of the hosts (target DNA and carrier Apo). The novel Chr interacts with DNA through its benzoxazolinate and aminosugar moieties, and also with Apo through the benzoxazolinate and macrocyclic moieties. The superposition of Chrs in these three states clearly revealed conformational deviation of the 16-membered macrocyclic moiety containing intra-chlorophenol ring. *Ab initio* calculations supported good correlation between the reactivity and the conformational alteration of Chr induced in hosts. The present results provide molecular basis and implication for the host-recognition mode, the reaction mechanism, and drug delivery system of chromoprotein C-1027.

Key words: Antitumor antibiotic/ Enediyne/ Drug delivery system/ NMR structure/ DNA cleavage

To understand the molecular basis for unique biological activity of C-1027, three-dimensional structures of DNA-Chr complex, Apo-Chr complex, and free Chr are essential. We clarified solution structures of free Chr and the complex formed between the drug and DNAoligomer by NMR techniques. The NOESY measurements of Chr-DNA oligomer complex yielded a total of 144 DNA intramolecular, 33 drug-intramolecular, and 36 DNA-drug intermolecular NOEs that we were able to clearly assign. Free Chr in D_2O solution provided 14 intramolecular ROES in the ROESY. The solution structures of DNA-Chr complex and free Chr obtained with distance-restrained molecular dynamics computations gave relevant modeds that are fully consistent with the observed NMR-derived distance date. In the unbound state, restrained molecular dynamics simulation illustrated that free Chr can't fix its benzoxazolinate (BO) and aminosugar (AS) moieties in one specific monfomation without characteristic interaction. Indeed, ROEs of the BO and AS parts were

BIOORGANIC CHEMISTRY — Bioactive Chemistry —

Scope of research

The major goal of our laboratory is to elucidate the molecular basis of the activity of various bioactive substances by biochemical, physicochemical, and synthetic approaches. These include studies on the mechanism of sequence-specific DNA cleavage by antitumor or carcinogenic molecules, studies on the DNA recognition of zinc-finger proteins, and model studies on the action of ion channels. In addition, artificial designed peptides have also been developed as useful tools in molecular biology and potentially in human medicine.

Prof
SUGIURA,Yukio
(D Pharm Sci)

Assoc Prof
FUTAKI, Shiro
(D Pharm Sci)

Instr
NAGAOKA, Makoto
(D Pharm Sci)

Assoc Instr
OKUNO, Yasushi

Students
ARAKI, Michihiro (DC)
IMANISHI, Miki (DC)
MATSUSHITA, Keizo (DC)
OMOTE, Masayuki (MC)
KAJI, Tamaki (MC)
MIYAGAWA, Naoko (MC)
SUZUKI , Tomoki (MC)
UNO, Yumiko (MC)
OHHASHI, Wakana (MC)
TAKADA, Naoko (MC)
HORI, Yuichiro (MC)
KIWATA, Tatsuto (UG)
NOMURA, Wataru (UG)

rarely detected. Since most of observed intra-ROEs of Chr arose from the 16-membered macrocyclic part (MC), the conformation of MC was restrained. Average pairwise RMS deviations among final structures were 0.75 Å for the DNA-Chr complex and 0.77 Å for free Chr. The generated structures of DNA-Chr complex and free Chr were averaged and energy-minimized.

In the Chr-DNA heptamer complex, the inter-NOEs of BO and AS moieties with DNA were in the majority (75%) of all observed intermolecular peaks. The proton chemical shit perturbations of these functionla moieties were also large upon binding to DNA. Thus, both the BO and AS parts play important roles for the recognition and binding of Chr to DNA. The DNA-Chr complex model evidently revealed that C1027-Chr interacts with each tetranucleotide of the d(C3C4A5T6)/d(A0T10G11G12) duplex through unique intercalation of the BOmoiety at the d(C3C4)/d(G11G12) step and also minor groove binding of the AS part at d(A5T6)/d(Q9T10G11). This complex is stabilized by the stacking interaction through intercalation and by the backbone helical and minor groove contacts through van der Waals interactions. The intercalation of the BO moiety was demonstrated by the NOEs connecting 1''-NH with H6, H1', H2', 2'' of C3 and H6, NH_2 of C4; OMe with H8, H1, H1' of G11; H6'' with H3' of G12. One of the two six-membered rings of C3 and C4, while the one containing methoxy group stacks on the purine rings of G11 and G12. The protruding methoxy group of BO moiety makeds van der Waals contacts with H1' of G11 sugar. Furhermore, the inter-NOEs of the AS moiety with the DNA oligomer were obzerved connecting of β-Hs (H2', H3', H4', and 5'-Meβ) with H1' and H4' of T6 and H2 of A5; α-Hs (4'-NMe and 5'-Meα) with H2 of A9, H1' and H4' of T10 and H4', H5', and H5'' of G11. There are backbone heical sugur-phosphate backbones of A5T6 and A9T10G11strands on other side. The orientation of the AS moiety permits its α^1Hs and β^1HS to face toward the A9T10-strand and A5T6-strand, respectively. A set of contacts between Chr and DNA minor groove floor was detected. These contacts include van der Waals interaction of AS H3' with DNA A5(H2) and A9(H2) and a hydrogen bond supports our previous data that the guanine 2-amino group of the central base in trinucleotide 5'-AGG plays a key role in the recognition of the DNA oligomerby by Chr. In addition, the observation of several NOEs showed the backbone helical binding between the aromatized AEB ring (H5,H6, and H8) and the DNA backbone [C4(H1'), A5 (H1' and H4'), and T6(H5')]. An intermolecular NOE cross peak between Chr-H6 and A5-H1' or -H4' revealed the prozimity of these protons. The Chr-H3 is situated close to H1' of G12, as indicated by the constructed model. Therefore, it is reasonably proposed that the DNA lesions caused by the C-1027 Chr are due to the abstraction of hydrogen atoms from A5-C1' or -C4' by the Chr-C6 radical and from G12--C1' by the Chr-C3 radical. In fact, our previous gel electrophoretic analysis evidently showed that the DNA domage occurs at CCA/TGG with a two nucleotide 3'-stagger of the reactive biradical atoms(C3 and C6) of the enediyne Chr to the vicinity of deoxyribose hydrogen atoms (H1' or H4') of the DNA backbone (A5 and G12). The AS assists in winding of the Chr around the minor groove of the DNA oligomer.

We evaluated the influence of spatial configuration of the neighboring aromatic ring on the reactivity of the biradical by an *ab initio* method (23,24). Recently, Chen and co-workers pointed out that the reactivity of p-benzyne type bieadicals depends upon the energy splitting between the singlet (S) ground state and triplet (T) excited state; the lager the S-T splitting becomes, the less reactive the singlet biradical dose. On the basis of this information, we istimated and conpared teh S-T splittings of both biradical-aromatic ring systems that are confomationally similar to C1027-Chrs in DNA and Apo. The S-T splitting of the biradical-aromaric ring system in DNA was slightly smaller than that in Apo (Table III). Accordingly, the p-benzyne type biradical in DNA is more reactive than that in Apo, because of the conformational alteration of the MC part containing chlirophenoling. It is possible for the drug to control the reactivity of hydrogen-abstraction reactions by subtle structural perturbation of the intramolecular cholorphenol ring adjacent to the reacting AEB system . On the other band, neocarzinostatin (NCS), esperamicin, calcheamicin, and kedarcidin require external cofactor (thiol) as trigger of the Bergmann reaction.

Nucleocytoplasmic Transport of Preintegration Complex and Viral mRNA in Retrovirus-Infected Cells

Yoshifumi Adachi

Active transport of proteins and mRNAs between the nucleus and cytoplasm is a major process in eukaryotic cells. Recently, factors that recognize transport substrates and mediate nuclear import or export have been characterized, revealing interactions that target substrates to the nuclear pore complexes, through which translocation occurs. In the first half of the report, nuclear import of the human immunodeficiency virus 1 (HIV-1) preintegration complex (PIC) is discussed. The second half describes recent information on the mechanistic details of nuclear export of viral mRNA so-called Rev-dependent *trans*-activation of viral genes.

Keywords : Retrovirus / Viral integration / Rev-dependent *trans*-activation / Nuclear import / Nuclear export / Nucleocytoplasmic transporter

The ability of HIV-1 to transport its preintegration complex (PIC) into the nucleus of an infected cell during interphase is a unique feature (1). A basic-type nuclear localization signal (NLS) was identified in the N-terminal region of the HIV-1 matrix protein (MA) and was found to regulate viral nuclear import and infection. Genetic analysis also implicated viral protein Vpr in the process of nuclear import of the HIV-1 PIC. But this protein does not have a classical NLS, and its role in nuclear import remained unclear until recently.

Recent studies identified that Vpr controls nuclear import through an importin α-independent mechanism (1). This result was consistent with resistance of Vpr-regulated viral nuclear import to competition by NLS peptides. The binding site of Vpr on importin α does not appear to overlap with the NLS-binding sites. In fact, importin α, Vpr, and MA can assemble into a trimer. As a result of Vpr binding to importin α, the affinity of interaction between the NLS and importin α was increased approximately 10-fold. This mechanism may be instrumental in increasing the karyophilic potential of the HIV-1 PIC.

It appears, therefore, that nuclear import of the HIV-1 PIC is controlled by two viral proteins, Vpr and MA (Fig. 1). While MA contributes its NLS which connect the PIC to importin α and cellular import machinery, Vpr functions as an enhancer of the MA-importin α interaction. In addition, Vpr was found to bind nucleoporins and was suggested on these grounds to function as an importin β analog. Although this hypothesis is consistent with the role of Vpr in docking of the HIV-1 PIC to the nuclear envelope, it is hard to imagine that a small protein, such as Vpr (with a molecular mass of only 14 kDa), can perform the function of a 97-kDa importin β. We therefore favor the notion that the effects of Vpr are mediated through the importin α/β pathway. Inactivation of either partner in the HIV-1 nuclear import (i.e., MA, Vpr, or importin α/β) results in the loss of

BIOORGANIC CHEMISTRY — Molecular Clinical Chemistry —

Scope of research

This laboratory was founded in 1994 with the aim of linking (bio)chemical research and clinical medicine. Thus, the scope of our research encompasses the structure, function and regulation of various biomolecules, the pathophysiological significance of bioreactions in relation to human diseases, and the application of molecular techniques to clinical diagnosis and therapy. Our current interest is focused on poly(ADP-ribosyl)ation, nucleocytoplasmic transport of proteins in association with leukemogenesis and apoptosis, and the molecular etiology of Alzheimer's disease and related disorders.

Prof
UEDA, Kunihiro
(D Med Sc)

Assoc Prof
TNAKA, Seigo
(D Med Sc)

Instr
ADACHI, Yoshifumi
(D Med Sc)

Guest Scholar:
BANASIK, Marek (D Med Sc)
Guest Research Associate:
STROSZNAJDER, Robert (Ph D)
Students:
MATOH, Naomi (DC)
CHU, Dong (DC)
TAKEHASHI, Masanori (DC)
BAHK, Songchul (DC)
TAKANO, Emiko (RF)
IIDA, Shinya (RS)

import function and virus inability to establish efficient infection in primary cells. These proteins, therefore, present an attractive target for development of novel anti-HIV therapeutics.

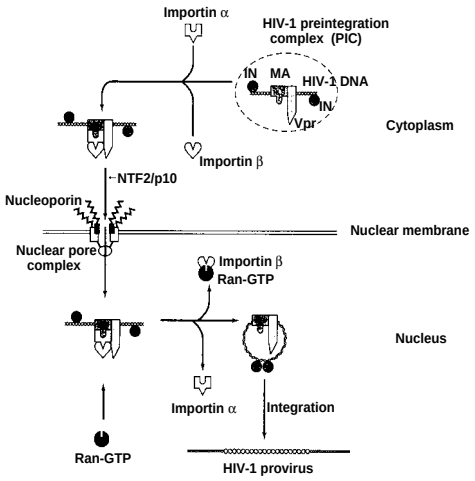

Figure 1. A model of nuclear import of the HIV-1 PIC.

HIV-1 encodes the regulatory protein Rev, which is absolutely required for viral replication (2,3). Rev promotes the nuclear export of incompletely spliced HIV-1 mRNA species containing the Rev response element (RRE). Rev interacts directly with a stem-loop within the RRE. Rev is a 116-amino acids phosphoprotein that has been shown to continuously shuttle between the nucleus and cytoplasm. Nuclear import of Rev is mediated by NLS embedded in the the RRE-binding domain. The NLS of Rev has been reported to associate with the conventional importin α/β heterodimer as well as a nucleolar shuttle protein B23. Nuclear export of Rev is mediated by the nuclear export signal (NES), which contains a conserved stretch of characteristically spaced leucine residues.

Recently, the highly conserved CRM1 protein was identified as a functional nuclear receptor for Rev NES and hence the protein was also renamed exportin 1 (4,5). Independent experiments showed that overexpression of CRM1 increased the export of nuclear-injected Rev protein. Moreover, the cytotoxin leptomycin B (LMB) inhibited *in vivo* export of both Rev protein and Rev-dependent RRE RNA export. This effect by LMB is direct because LMB binds to CRM1, and , in yeast, resistance to LMB maps to *crm 1* gene. Further support for CRM1 being an export receptor for NES-containing proteins is based on the observation that N-terminal region of CRM1 is homologous to the RanGTP-binding domain of importin β, placing CRM1 in the family of RanGTP-binding proteins that includes other known and putative import and export receptors. CRM1 has also been found in complex with at least two proteins associated with the human nuclear pore complex, namely the nucleoporins CAN/Nup214 and Nup88, and yeast two-hybrid analysis have demonstrated interactions between CRM1 and several nucleoporins as well as Rev and Ran (6).

The molecular details behind CRM1-mediated Rev export are still ambiguous. Our studies have been focused on the assembly of the RRE RNA-Rev-CRM1-RanGTP complex in greater detail *in vitro*. CRM1 interacts directly with full-length Rev independently of the conserved leucine residues within the core of the NES and the presence of RanGTP. This Ran-independent interaction is LMB insensitive. In contrast, formation of the ternary Rev-CRM1-RanGTP complex is highly sensitive to NES mutations and is readily dissociated *in vitro* by LMB or by hydrolysis of Ran GTP.

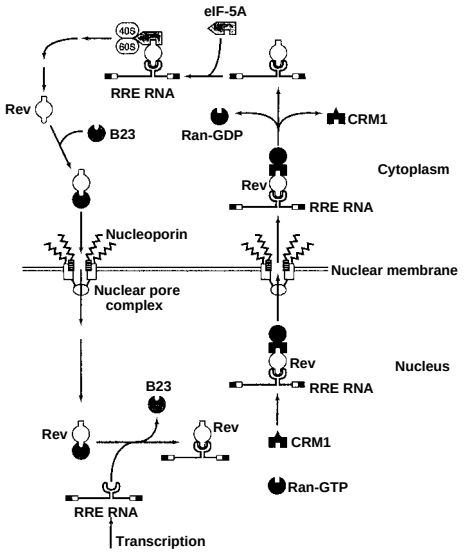

Figure 2. Mechanism of Rev-dependent nuclear export of viral mRNA.

As shown in Figure 2, Rev utilizes the cellular shuttle service to be imported into the nucleus as the Rev-B23 complex via the NLS/RRE-binding domain. As the RRE RNA has higher affinity for Rev than B23, the nuclear-imported complex is specifically dissociated by the RRE RNA. The RRE RNA-Rev complex binds to CRM1 via NES cooperatively with RanGTP and is subsequently translocated through the nuclear pore complex. In the cytoplasm, the RRE RNA-Rev-CRM1-RanGTP complex dissociates when Ran hydrolyzes GTP under the influence of RanBP or RanGAP.

References

1. Adachi, Y, *"Dynamism of Intracellular Traffic"* (Yoneda Y and Nakano A, eds), Springer-Verlag Tokyo, 32-39 (1999).
2. Adachi Y, Copeland TD, Hatanaka M and Oroszlan S, *J. Biol. Chem.* **268**, 13930-13934 (1993)
3. Kubota S, Adachi Y, Copeland TD and Oroszlan S, *Eur. J. Biochem.* **233**, 48-54 (1995).
4. Adachi Y, *Jpn. J. Clin. Chem.* **27**, 117-126 (1998)
5. Adachi Y, *Gene Med.* **2**, 632-637 (1998)
6. Minakuchi M and Adachi Y, *Kagaku to Seibutsu* **36**, 813-819 (1998)

Potent Transition-State Analogue Inhibitor of *Esherichia coli* Asparagine Synthetase A

Jun Hiratake, Mitsuteru Koizumi, Toru Nakatsu, Hiroaki Kato, and Jun'ichi Oda

A potent and slow-binding inhibitor of *E. coli* asparagine synthetase A (AS-A) was synthesized, and its inhibition behavior was characterized. The enzyme complexed with the inhibitor was analyzed by X-ray diffraction analysis to identify several key amino acid residues responsible for catalysis as well as for substrate recognition. AS-A catalyzes the formation of L-Asn from L-Asp and ammonia coupled with the hydrolysis of ATP to AMP and pyrophosphate. The reaction catalyzed by this enzyme is prototypic of mammalian asparagine synthetase (AS-B) which utilizes glutamine as a nitrogen source. In addition, asparagine synthetase is a potential target for chemotherapy to treat certain leukemias. We therefore designed and synthesized a transition-state analogue, *N*-adenylated *S*-methyl-L-cysteine sulfoximine **1**, based on the proposed reaction mechanisms of AS-A. The compound **1** strongly inhibited the *E. coli* AS-A in a time-dependent manner with an overall inhibition constant (K_i*) of 67 nM and with an onset rate of inactivation of 3.27 s^{-1} mM^{-1}. The inhibition was almost irreversible and no regain of enzyme activity was observed in 10 days after gel filtration. The inhibitor **1** was also used as a ligand for X-ray diffraction analysis of AS-A. The X-ray crystal structure of AS-A complexed with **1** revealed several key amino acid residues such as Arg 100, Gln 116 and Asp 46 responsible for catalysis as well as those for substrate recognition. An attempt to inhibit AS-A by each diastereomer of *S*-methyl-L-cysteine sulfoximine and ATP is also described. Since AS-A is prototypic of asparagine synthetases in terms of the chemistry in substrate activation, compound **1** should formulate a basis for future inhibitor design of asparagine synthetase B.

Keywords: Transition-state analogue inhibitor/ Asparagine synthetase A/ ATP-Dependent ligase/ Sulfoximine/ Slow-binding inhibition/ Irreversible inhibition/ X-Ray crystallography

L-Asparagine synthetase [L-aspartate: ammonia ligase (AMP-forming) EC 6.3.1.1] (AS-A) from *Escherichia coli* [1] is a typical member of ammonia-dependent asparagine synthetases and catalyzes the formation of L-Asn from L-Asp and ammonia with concomitant hydrolysis of ATP to AMP and pyrophosphate. The reaction catalyzed by AS-A is mechanistically prototypic of all the classes of ATP-utilizing C-N bond ligases in which the substrate carboxyl group is activated by adenylation followed by substitution by amine nucleophile. It is therefore highly desirable to obtain good transition-state analogue inhibitors of AS-A to probe the detailed reaction mechanisms and structure of asparagine synthetases and its mechanistically related ligases. We describe here the synthesis and characterization of a transition-state analogue, *N*-adenylated *S*-methyl-L-cysteine sulfoximine **1**.

The catalytic reaction of AS-A is thought to proceed by a two-step mechanism via an intermediate β-aspartyl adenylate; the first step is the formation of the intermediate, and the resulting adenylated β-carboxy is attacked

MOLECULAR BIOFUNCTION — Functional Molecular Conversion —

Scope of research

Our research aims are to elucidate the chemistry-function relationships of various biocatalysts (enzymes) in combination with organic chemistry, molecular biology and X-ray crystallography. The biochemical and physiological roles of enzymes and hormone receptors are also studied from the chemical point of view. Main subjects are (1) Chemical, biochemical and molecular biological studies on β-primeverosidase, a major tea aroma-producing β-glycosidase concerned with tea-manufacturing process, and on its original physiological roles in tea plants, (2) Design and synthesis of transition-state analogue inhibitors of ATP-dependent ligases and glycosidases, (3) Development of a new method for functional cloning of plant hormone receptors and biochemical studies on plant hormone biosynthesis, (4) X-Ray crystallography of firefly luciferases and pyruvate phosphate dikinase from Maize, (5) Development of a new types of lipase by evolutionary molecular engineering.


Prof
SAKATA, Kanzo
(D Agr)


Assoc Prof
HIRATAKE, Jun
(D Agr)


Instr
KATO, Hiroaki
(D Agr)


Instr
MIZUTANI, Masaharu
(D Agr)


Assoc Instr
NAKATSU, Toru
(D Agr)

INOUE, Makoto (DC), FUJII, Ryota (DC), MA, Seung-Jin (DC), FURUKAWA, Hiroshi (MC), TAKEGAWA, Mizuki (MC), EMA, Jun'ichi (MC), NAKANISHI, Tsugumi (MC), SATO, Tadashi (MC), GUO, Wenfei (PD), SHIMIZU, Tetsuya (MC, RS), KISHIMOTO, Masayuki (MC, RS), SHIMA, Masami (UG, RS), UEMURA, Miyuki (secretary)

Scheme 1

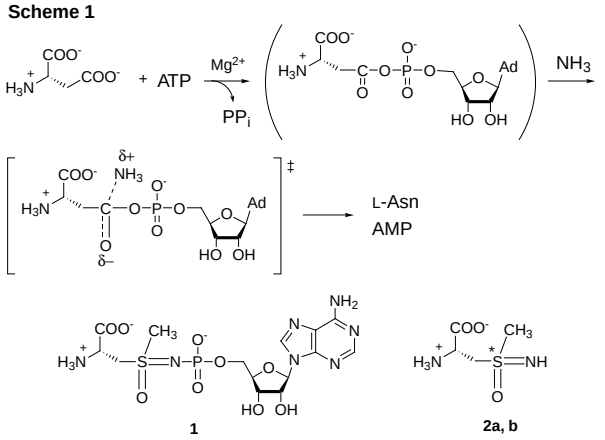

by ammonia in the second step to form L-Asn and AMP (Scheme 1). As a stable analogue of the transition state in the latter step, we designed *N*-adenylated *S*-methyl-L-cysteine sulfoximine **1** where the carbonyl to be attacked by ammonia is replaced by a tetrahedral sulfoximine sulfur atom with a methyl group mimicking ammonia. Compound **1** was synthesized in 9 steps from *S*-methyl-L-Cys via adenylation of sulfoximine nitrogen [2]. The resulting P-N bond was hydrolytically stable even under acidic conditions.

The *N*-adenylated sulfoximine **1** (1:1 mixture of diastereomers) was found to be an extremely potent slow-binding inhibitor that caused time-dependent inactivation of AS-A (Figure 1). The enzyme, for example, was totally inactivated in 15 min when 2.5 μM of **1** was present. The inhibition was virtually irreversible, and no regain of enzyme activity was observed after gel filtration. Since the inhibition was time-dependent, the onset rate of inactivation (k_{on}) was calculated from the progress curves and was found to be 3.27 s^{-1} mM^{-1}. The overall inhibition constant (K_i*) was calculated as 67 nM by measuring the inhibited enzyme activity after slow-binding inhibition equilibrium was reached. Considering that the kinetic constants for AS-A were K_m (Asp) = 1.69 mM, K_m (ATP) = 1.24 mM and k_0/K_m (Asp) = 28.5 $s^{-1}mM^{-1}$, the inhibitor **1** bound to the enzyme at a rate nine times as small as that of the enzymatic reaction, but with 25,000-fold higher affinity than its substrates.

We first attempted to inhibit AS-A with diastereomeric *S*-methyl-L-cysteine sulfoximine **2a**, **b** and ATP in the hope that a mechanism-based inactivation of AS-A might result by *in situ* adenylation of the sulfoximine by ATP within the enzyme active site. However, each diastereomer **2a** and **2b** was a poor and reversible inhibitor of AS-A with K_i = 3.27 and 0.76 mM, respectively, and no enzyme inactivation was observed after a prolonged incubation of the enzyme with **2a** or **2b** in the presence of ATP.

Since compound **1** was most likely to mimic the putative transition state, the enzyme complexed with **1** was crystallized and subjected to X-ray diffraction analysis [2]. The inhibitor **1** gave a very clear electron density in the enzyme active site, and several specific interactions were identified between the active site amino acid residues and the inhibitor **1** (Figure 2). Of particular interest is the interaction regarding the sulfoximine moiety. First, the sulfoximine oxygen (S=O) is hydrogen bonded to Arg 100 and Gln 116. Since S=O represents the oxyanion

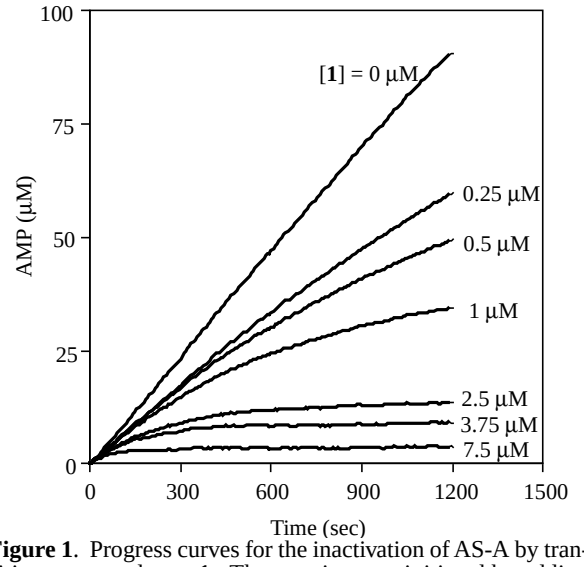

Figure 1. Progress curves for the inactivation of AS-A by transition-state analogue **1**. The reaction was initiated by adding the enzyme to an assay mixture containing L-Asp (1.5 mM), NH_4Cl (20 mM), ATP (3 mM) and the inhibitor **1** (0-7.5 μM) in 100 mM Tris-HCl (pH 7.8) at 37 °C.

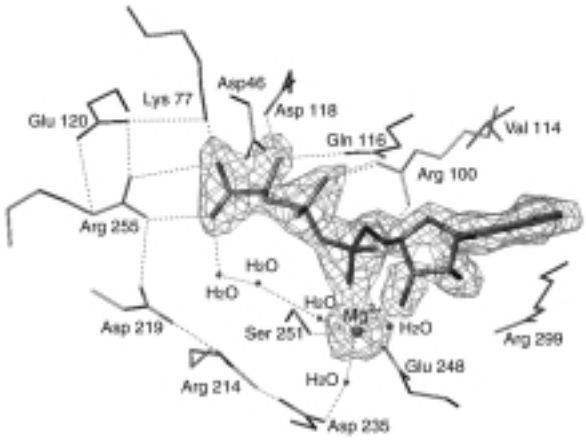

Figure 2. X-Ray crystal structure of *E. coli* AS-A active site complexed with the inhibitor **1**, showing the SIGMAA weighted F_O-F_c omit electron density map, superimposed with the refined structure of the inhibitor **1** and the active site amino acid residues. The contour level is 3.0 σ.

generated by nucleophilic attack of ammonia, these residues are most likely to be key catalytic residues responsible for stabilizing the tetrahedral oxyanion transition state or intermediate. Another point is the methyl attached to the sulfur atom. This methyl, which is supposed to mimic the -NH^{3+} moiety of the zwitterionic tetrahedral intermediate, was found to be 3.1 Å distant from Asp 46. This negatively charged residue probably plays a key role in the electrostatic stabilization of the -NH^{3+} part of the transition state or the intermediate and also acts as a base to abstract a proton from the tetrahedral intermediate completing the formation of the product asparagine.

References

(1) Sugiyama, A.; Kato, H.; Nishioka, T.; Oda, J. *Biosci. Biotech. Biochem.* **1992**, *56*, 376-379.

(2) Koizumi, M.; Hiratake, J.; Nakatsu, T.; Kato, H.; Oda, *J. J. Am. Chem. Soc.* **1999**, *121*, 5799-5800.

Reaction Mechanism of DL-2-Haloacid Dehalogenase from *Pseudomonas* sp. 113: Hydrolytic Dehalogenation Not Involving Enzyme-Substrate Ester Intermediate

Nobuyoshi Esaki, Tatsuo Kurihara, Kenji Soda, Vincenzo Nardi-Dei and Chung Park

DL-2-Haloacid dehalogenase from *Pseudomonas* sp. 113 (DL-DEX 113) catalyzes the hydrolytic dehalogenation of D- and L-2-haloalkanoic acids, producing the corresponding L- and D-2-hydroxyalkanoic acids, respectively. L-2-Haloacid dehalogenase, haloalkane dehalogenase, and 4-chlorobenzoyl-CoA dehalogenase, which catalyze the hydrolysis of various organohalogen compounds, have an active site carboxylate group that attacks the substrate carbon atom bound to the halogen atom, leading to the formation of an ester intermediate. This is subsequently hydrolyzed, resulting in the incorporation of an oxygen atom of the solvent water molecule into the carboxylate group of the enzyme. In the present study, we analyzed the reaction mechanism of DL-DEX 113. When a single turnover reaction of DL-DEX 113 was carried out with a large excess of the enzyme in $H_2{}^{18}O$ with either D- or L-2-chloropropionate, the major product was found to be ^{18}O-labeled lactate. After a multiple turnover reaction in $H_2{}^{18}O$, the enzyme was digested with proteases, and the molecular masses of the peptide fragments were measured. No peptide fragments contained ^{18}O. These results indicate that the $H_2{}^{18}O$ of the solvent directly attacks the α-carbon of 2-haloalkanoic acid to displace the halogen atom. This is the first example of an enzymatic hydrolytic dehalogenation that proceeds without formation of an ester intermediate.

Keywords: 2-Haloacid dehalogenase/ Ionspray mass spectrometry/ Reaction mechanism

Halidohydrolases catalyze hydrolytic cleavage of carbon-halogen bonds of various organohalolgen compounds. 2-Haloacid dehalogenases (EC 3.8.1.2), haloacetate dehalogenases (EC 3.8.1.3), haloalkane dehalogenases (EC 3.8.1.5), and 4-chlorobenzoyl-CoA dehalogenases (EC3.8.1.6) are included in this group of enzymes. 2-Haloacid dehalogenases are further classified into the following three groups: 1) L-2-Haloacid dehalogenase (L-DEX) catalyzes hydrolysis of L-2-haloalkanoic acids to produce the corresponding D-2-hydroxyalkanoic acids. 2) D-2-Haloacid dehalogenase (D-DEX) catalyzes the conversion of D-2-haloalkanoic acids into L-2- hydroxyalkanoic acids. 3) DL-2-Haloacid dehalogenase (DL-DEX) dehalogenates both D- and L-2-haloalkanoic

MOLECULAR BIOFUNCTION — Molecular Microbial Science —

Scope of research

Structure and function of biocatalysts, in particular, pyridoxal enzymes and enzymes acting on xenobiotic compounds, are studied to elucidate the dynamic aspects of the fine mechanism for their catalysis in the light of recent advances in gene technology, protein engineering and crystallography. In addition, the metabolism and biofunction of selenium and some other trace elements are investigated. Development and application of new biomolecular functions of microorganisms are also studied to open the door to new fields of biotechnology. For example, molecular structures and functions of psychrophilic enzymes and their application are under investigation.

Prof
ESAKI, Nobuyoshi
(D Agr)

Assoc Prof
YOSHIMURA, Tohru
(D Agr)

Instr
KURIHARA, Tatsuo
(D Eng)

Assoc Instr (part-time): MIHARA, Hisaaki **Technician:** SEKI, Mio; UTSUNOMIYA, Machiko **Guest Research Associate:** GALKIN, Andrey G.; MIROLIAEI, Mehran; LACOURCIERE, M. Gerard **Students:** WATANABE, Akira (DC); ICHIYAMA, Susumu (DC); KULAKOVA, Ljudmila B.(DC); UO, Takuma (DC); YOSHIMUNE, Kazuaki (DC); KATO, Shin-ichiro (DC); YOW, Geok-Yong (DC); ISUI Ayako (MC); NAKAYAMA Daisuke (MC); SAITO Mami (MC); TODO Fumiko (MC); WEI, Yun-Lin (MC); YAMAUCHI Takahiro (MC); KENNEDY, R. Alexander J. D. (MC); MORI, Kensuke (MC); NAKANO Michiko (MC); SAITO Megumi (MC); TAKAHATA, Hiroyuki (MC)

acids to produce the corresponding L- and D-2-hydroxyalkanoic acids, respectively. DL-DEX is similar to racemases and epimerases in that it acts on the chiral center of both D- and L-enantiomers indiscriminately. However, this enzyme is unique in that it catalyzes a chemical conversion on the chiral centers of both enantiomers.

Reactions catalyzed by L-DEX from *Pseudomonas* sp. YL (L-DEX YL), haloalkane dehalogenase from *Xanthobacter autotrophicus* GJ10, and 4-chlorobenzoyl-CoA dehalogenases from *Pseudomonas* sp. strain CBS3 and *Arthrobacter* sp. 4-CB1 have been shown to proceed as in Fig. 1 (A) [1]. These mechanisms resemble each other in that the reactions proceed through ester intermediates formed from catalytic acidic amino acid residues of the enzymes and their substrates. The ester intermediates are subsequently hydrolyzed releasing the products and restoring the carboxylate groups of the enzymes.

DL-DEXs have been purified from *Pseudomonas* sp. 113 (DL-DEX 113), *Pseudomonas putida* PP3, and *Rhizobium* sp. However, none of the reaction mechanisms of these DL-DEXs has been studied, and it has remained unknown whether the reaction mechanism of DL-DEX is similar to that of other halidohydrolases. We previously determined the primary structure of DL-DEX113, and found that it is similar to that of D-DEX from *Pseudomonas putida* AJ1 [2]. We also showed that DL-DEX 113 has a single and common catalytic site for both D- and L-enantiomers based on a site-directed mutagenesis experiment and kinetic analysis [2]. In the present study, we analyzed the reaction mechanism of DL-DEX 113 by means of ^{18}O incorporation experiments [3].

We conducted the single turnover reaction of DL-DEX 113 in $H_2{}^{18}O$ with D- or L-2-chloropropionate as a substrate, using an excess amount of the enzyme. We found that a majority of the lactate produced was labeled with ^{18}O. This makes a clear contrast with the results on the L-DEX YL reaction, which proceeds through the mechanism involving an ester intermediate (Fig. 1 (A)). Only 10% of the D-lactate produced from L-2-chloropropionate by L-DEX YL was labeled with ^{18}O. This suggests that in the DL-DEX 113 reaction an oxygen atom of the solvent water was directly incorporated into the product. While supporting the mechanism shown in Fig. 1 (B), this is not compatible with the mechanism in Fig. 1 (A), in which an oxygen atom of the solvent water is first incorporated into the enzyme.

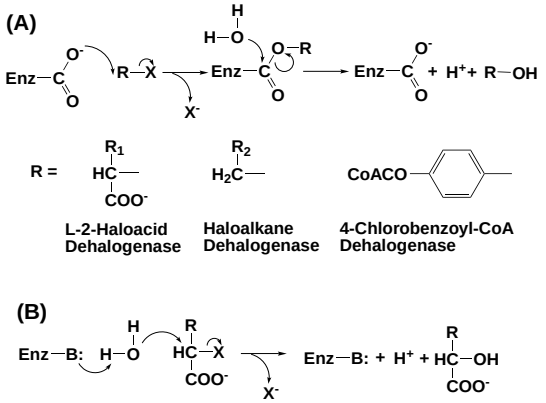

Figure 1. Reaction mechanisms of dehalogenases

A multiple turnover reaction of DL-DEX 113 was carried out in $H_2{}^{18}O$ with D- or L-2-chloropropionate as a substrate. After completion of the reaction, the enzyme was digested with TPCK-treated trypsin, and the resulting peptide fragments were separated on a reversed phase column interfaced with an ionspray mass spectrometer as a detector. If the reaction proceeds through the mechanism in Fig. 1 (B), ^{18}O should not be detected in the proteolytic fragments. The molecular masses of all peptides were virtually indistinguishable from the predicted ones whether the reaction was conducted with D- or L-2-chloropropionate. Since peptides containing amino acid residues 1, 106-107, 135-142, 181-183, 229-238, 250-254, 284-285, and 299-300 were not found in the trypsin-digested sample, we also analyzed lysyl endopeptidase-digested enzyme by the same method. Peptides 120-142, 232-285, and 299-306 were identified, and their molecular masses were virtually indistinguishable from the predicted ones.

In the above experiment, the molecular masses of the peptides containing amino acid residues 1, 106-107, 181-183 and 229-231 could not be measured. Therefore, we could not exclude the possibility that ^{18}O was incorporated into Asp or Glu in these peptides. However, among these peptides, only peptide 181-183 contains an acidic residue, Asp181. We replaced Asp181 with Ala, Arg, and Glu by site-directed mutagenesis to clarify whether Asp181 is involved in the catalytic reaction shown in Fig. 1 (A). The activities of these mutant enzymes were similar to that of the wild-type enzyme, indicating that Asp181 is not essential for the catalysis.

All the above results are consistent with the general base mechanism shown in Fig. 1 (B), but not with the mechanism shown in Fig. 1 (A). This applies to the dehalogenations of both enantiomers of 2-haloalkanoic acids because the results obtained for both enantiomers were virtually the same. We previously reported that DL-DEX 113 has a single and common catalytic site for both L- and D-enantiomers based on a site-directed mutagenesis experiment and kinetic analysis. This conclusion is supported by our present data showing that the enzymatic dehalogenations of both enantiomers proceed through the same mechanism as shown in Fig. 1 (B). DL-DEX 113 is unique in that its reaction does not involve the formation of an ester intermediate. Since D-DEX from *Pseudomonas putida* AJ1 shows sequence similarity with DL-DEX 113, the reaction of D-DEX probably proceeds through the mechanism shown in Fig. 1 (B). Although DL-DEX and L-DEX can catalyze the same reaction (hydrolysis of L-2-haloalkanoic acids), our present data clearly show that the reaction mechanisms of DL-DEX and L-DEX are completely different from each other.

References

1. Liu, J.-Q., Kurihara, T., Miyagi, M., Esaki, N. and Soda, K. (1995) J. Biol. Chem. 270, 18309-18312
2. Nardi-Dei, V., Kurihara, T., Park, C., Esaki, N. and Soda, K. (1997) J. Bacteriol. 179, 4232-4238
3. Nardi-Dei, V., Kurihara, T., Park, C., Miyagi, M., Tsunasawa, S., Soda, K. and Esaki, N. (1999) J. Biol. Chem. 274, 20977-20981

ADP and ATP Destabilize the *Escherichia coli* Chaperonin GroEL whereas Potassium Ion Does Not; Structural Evidence by the Solution Small Angle X-ray Scattering Measurements

Yuzuru Hiragi and Kaoru Ichimura

ATP, ADP and Mg^{2+} dependence of the denaturation by Guanidine Hydrochloride of the GroEL, a chaperonin originated from *Escherichia coli*, was investigated by the solution small-angle X-ray scattering (SAXS) measurements using synchrotron radiation source. Disappearance of the quaternary structure of the GroEL was observed by the Kratky plots of the scattered intensities. Disintegration of the quarternary structures occurred at Guanidine Hydrochloride (GdnHCl) concentration of 0.8M in the presence of Mg-ATP, 1.1M for Mg-ADP and 1.3M for K^+; decreasing curves of weight averaged molecular weights observed from forward scatterings are shown to be compatible with this results. The destabilization of GroEL by nucleotides was proved structurally.

Key words ; Small-angle X-ray scattering/ GroEL / GdnHCl denaturation / Nucleotides

E. coli GroEL is a member of chaperonin, a family of molecular chaperones which assist refolding of nonnative proteins. It consists of 14 subunits of molecular weight *ca*. 57,000 dalton. Seven subunits of the tetradecamer are arranged to form a ring. Two of the 7 member rings contact each other in back to back manner completing whole GroEL oligomer. Hydrolysis of adenosine triphosphate is required to assist the refolding of the nonnative substrate proteins.

Apart from the refolding mechanism of the substrate proteins, dissociation and reconstitution mechanism of GroEL itself is interesting in the scope of the constitution principle of the oligomeric proteins by estimating from their structural stability. In the case of denaturation by guanidine hydrochloride (GdnHCl), magnesium ion stabilizes GroEL, whereas magnesium-adenosine diphosphate (Mg-ADP) and triphosphate (Mg-ATP) destabilizes. We studied the structural change during the denaturation of GroEL by the method of solution small-angle scattering method (SAXS).

SAXS experiments were carried out at 25˚C with the optics and detector system of SAXES installed at the 2.5 GeV storage ring in the Photon Factory, KEK,Tsukuba, Japan. Scattering intensities at wave length of 1.49Å were registered in the range $0.013\ Å^{-1} < Q < 0.355\ Å^{-1}$, where Q denotes the amplitude of the scattering vector equal to $4\pi \sin(\theta/\lambda)$ and 2θ is the scattering angle. Specimen chamber was kept at 25 ˚C throughout the

MOLECULAR BIOLOGY AND INFORMATION — Biopolymer Structure —

Scope of research

Our research aims are to elucidate structure-function relationships of biological macromolecules, mainly proteins, by using physicochemical methods such as spectroscopic and X-ray diffraction methods. The following attempts have been mainly made in our laboratory for that purpose. (1) X-ray diffraction studies on protein structures in crystal and in solution are carried out by crystallographic and/or small-angle X-ray scattering techniques to elucidate structure-function relationships of proteins. (2) Molecular mechanism for myosin assembly is studied by proteolytic method, electron microscopy, and computer analysis of the amino acid sequence.

Assoc Prof
HATA,
Yasuo
(D Sc)

Instr
HIRAGI,
Yuzuru
(D Sc)

Instr
FUJII,
Tomomi
(D Sc)

Instr
AKUTAGAWA,
Tohru

Students:
HIDA, Kouichi (RF, D Sc)
KURIHARA, Eiji (MC)
SAKAI, Hisanobu (MC)
HASEGAWA, Junya (MC)

experiments. Net scattering intensities were calculated by subtracting the scattering intensities of a blank buffer solution from those of the assembly solution. Absorption of X-ray by chloride atoms was corrected.

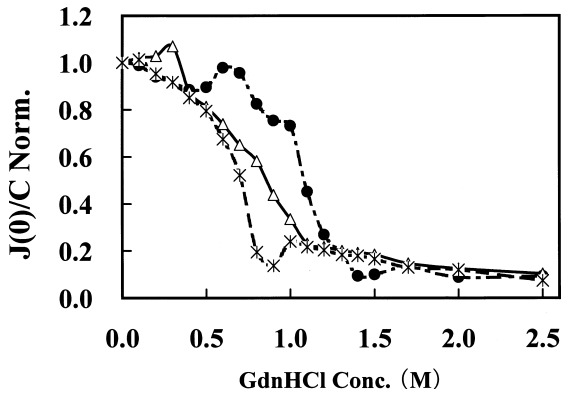

Figure 1. Change of *J(0)/C*, proportional to the weight average molecular weight against GdnHCl concentration; addition of potassium ion only (•), Mg-ADP (Δ), and Mg-ATP (*).

Fig. 1 shows the change of *J(0)/C*, against GdnHCl concentration with the addition of potassium ion only, Mg-ADP, and Mg-ATP. *J(0)* is scattered intensity extrapolated to scattering vector Q=0 and C is the concentration of the protein and is proportional to the weight average molecular weight. In the case of the process of the structural change, what observed are the mixture of intact and denatured particles. Consequently solution system is polydisperse. Molecular weights obtained here are, therefore, weight average molecular weight.

In the absence of nucleotides, decrease in the molecular weight proceeds slowly. When nucleotides were added, the denaturation was accelerated in both case. ATP seems to destabilize stronger than ADP. Probably hydration of ATP during measurements affected the protein stability.

Disappearance of quaternary structure is impossible to detect from the average molecular weight. This is easily observable by the Kratky plots, $J(Q)*Q^2$ *vs* Q, of the scattered curves. Fig. 2 shows the plots in different solution conditions. The first peak in low Q region is typical for globular proteins. The second peak around Q=0.075Å^{-1} derives from the proteins having the quaternary structure. As can be seen from Fig2. (a), the second peak together with first peak, disappeared at the GdnHCl concentration of 1.3M for potassium ion solution. Likewise the peaks did at 1.1M and 0.8M GdnHCl concentration in the presence of Mg-ADP (Fig.2 (b)) and ATP (Fig.2. (c)), respectively. As the first and the second peaks disappeared simultaneously, GroEL denatured directly to unfolded coil without passing the globular monomer structure in the equilibrium denaturation.

In the addition of ADP or ATP decrease in average molecular weight and disappearance of Kratky peaks proceeds in lower GdnHCl concentration. This is interpretable by the effects of nucleotides on the inter-subunit interaction of GroEL. Under the existence of nucleotides, large movement of apical domain is expectable even when GroES, the helper of chaperonin, does not exist. Increase in the flexibility in the subunit would contribute to the fragileness of the GroEL.

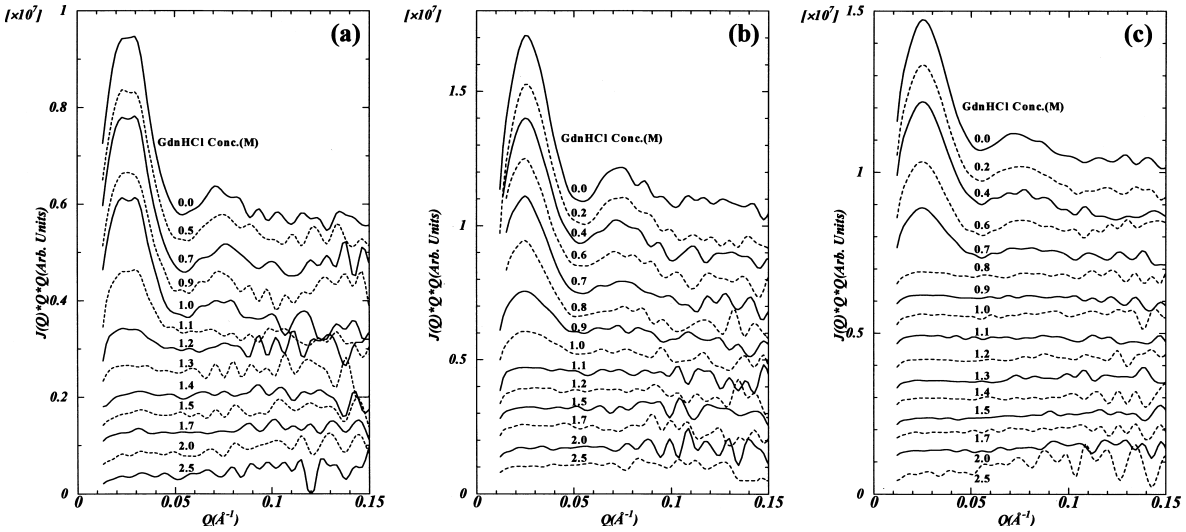

Figure 2. Change of Karatky plot patterns against GdnHCl concentration; (a):addition of potassium ion, (b):Mg-ADP., and (c):Mg-ATP.

Artificial Control in Transgenic Plants of the Activity of Transcription Factors

Takashi Aoyama, Maki Ohgishi, Takuya Muramoto, Mayumi Tukuda, and Atsuhiro Oka

For artificial control in transgenic plants of the activity of transcription factors, constructed was a DNA cassette encoding the transcriptional activation domain of Herpes Simplex viral protein VP16 and the hormone binding domain of rat glucocorticoid receptor. Combining with DNA segments coding for the DNA binding domain of transcription factors, the VG cassette produced fusion proteins whose activity can be induced in transgenic plants by the exogenous steroid hormone. Thus plant phenotypes specifically induced by the hormone give information on *in vivo* roles of the transcription factors. In addition, this system provides a tool by which we identifies direct target genes of the transcription factors. The *Arabidopsis* ATHB-1 and ATHB-2 transcription factors containing the homeodomain and leucine zipper motif have been studied with this system.

Keywords: Transcription/ Steroid hormone/ Homeodomain/ Transgenic plant

It is generally accepted that transcriptional initiation is the most critical step at which gene expression is regulated. In eukaryotic cells, transcription factors are largely involved in control of gene expression, and frequently play key roles in the regulation of cell differentiation, organ development, ontogenesis, and so on. However, their actual roles remain unclear in many cases, especially in higher eukaryotes because of the difficulty in the *in vivo* analysis of transcription factors. The purpose of this study is to construct a generally applicable tool for artificial control in transgenic plants of transcription factors, and then to apply it to functional analysis of the *Arabidopsis* transcription factors, ATHB-1 and ATHB-2. We developed a DNA cassette encoding a protein whose function of transcriptional activation can artificially be modulated, and fused it to another DNA segment that codes for a transcription factor or its portion containing the DNA-binding domain. To construct an artificially-regulable activator domain, we took advantage of well-characterized functional domains, the acidic domain of the Herpes Simplex viral protein VP16 [1] and the hormone binding domain of the rat glucocorticoid receptor (GRHBD) [2]. The VP16 domain is thought to act as a powerful transactivating domain in various organisms including plants by interacting with basal transcription factors [3-5]. The GRHBD domain suppresses the function of its neighboring domain in the absence of glucocorticoid, and the hormone binding to GRHBD results in release from the suppression [6-8]. As shown in Figure 1a, the DNA fragment encoding GRHBD was fused to the 3' end of the fragment encoding the VP16 domain in an in-frame manner. The restriction sites existing be-

MOLECULAR BIOLOGY AND INFORMATION — Molecular Biology —

Scope of research

Attempts have been made to elucidate structure-function relationships of genetic materials and various gene products. The major subjects are mechanisms involved in signal transduction and regulation of gene expression responsive to environmental stimuli, differentiation and development of plant organs, and plant-microbe interaction. As of December 1999, study is being concentrated on the roles of homeo domain proteins, MADS box proteins, and DDK response regulators of higher plants in developmental and signal transduction processes.

Prof
OKA, Atsuhiro
(D Sc)

Assoc Prof
AOYAMA, Takashi
(D Sc)

Instr
GOTO, Koji
(D Sc)

Students:
HOMMA, Takashi (DC)
OHGISHI, Maki (DC)
SAKAI, Hiroe (DC)
LIANG Yajie (DC)
YANO, Hiroyuki (DC)
OHASHI, Yohei (DC)
MURAMOTO, Takuya (RF, D Sc)

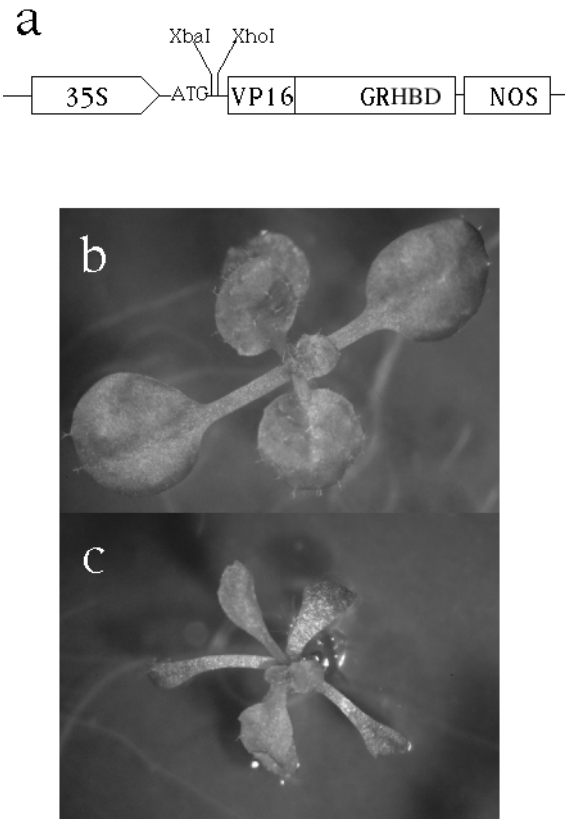

Figure 1. Architecture of the VG cassette vector (a), and phenotypes of *Arabidopsis* plants transgenic for 35S-HDZip1-VG grown under the absence (b) and presence (c) of hormone.

tween the translation initiation codon and the VP16 domain can be used for making a fusion protein with transcription factors or their DNA-binding domains. In the vector plasmid DNA, the VP16-GRHBD segment (VG cassette) is preceded by the cauliflower mosaic virus 35S promoter [9] and followed by the polyA-addition signal sequence of the nopaline synthase gene of the *Agrobacterium* Ti plasmid. This architecture of the cassette provides the expectancy that the resulting chimeric protein acts as a strong transcriptional activator only when glucocorticoid is exogenously supplied.

The *Arabidopsis* ATHB-1 and ATHB-2 [10-12] are transcription factors containing the homeodomain and leucin zipper motif. To analyze their function, the DNA segment encoding their DNA-binding domain (termed HDZip1 and HDZip2, respectively) was cloned into the VG cassette vector. The resulting chimeric genes (35S-HDZip1-VG and 35S-HDZip2-VG) were introduced into *Arabidopsis* for transgenic plants. In the absence of glucocorticoid, transgenic plants carrying either of 35S-HDZip1-VG and 35S-HDZip2-VG were indistinguishable from the wild-type plants (Figure 1b). On the other hand, treatment with dexamethasone, an agonist of glucocorticoid, led to transgene-specific phenotypes. On agar plates containing 10 μM of dexamethasone, seedlings carrying 35S-HDZip1-VG had very thin cotyledons. True leaves also showed similar thin phenotypes and lobes of leaves were extremely exaggerated (Figure 1c). From these phenotypes induced, ATHB-1 itself or genes recognized by its DNA-binding domain is thought to be involved in leaf development. 35S-HDZip2-VG seedlings under similar conditions had each a short and radially swollen hypocotyl and petioles (data not shown). Another transgenic plant simply overexpressing the native ATHB-2 gene, on the contrary, gave an opposite phenotype (data not shown). These results suggest that ATHB-2 itself acts originally as a repressor but not an activator, and that the opposite phenotype with 35S-HDZip2-VG is brought by inducible activation of transcription with the foreign VG domain. The specific inducible phenotypes described above indicate that the chimeric transcription factors were activated in transgenic plant cells inducibly by exogenously added dexamethasone.

This hormone-induction system is useful for analysis of the regulatory network of gene expression downstream from a transcription factor of interest. The most advantageous point of this system is no requirement of *de novo* protein synthesis for induction of transcriptional activation. Combining with an inhibitor of protein synthesis (e.g. cycloheximide), this system makes it possible to isolate mRNAs (or cDNAs) derived from genes that are directly activated by the transcription factors without secondary effects. In other words, the VG cassette system allows us to identify direct target genes of the transcription factor. We have actually found several candidates for the target of ATHB-1 and ATHB-2.

References

1. Triezenberg SJ, Kingsbury RC, and Mcknight SL, *Genes Dev.*, **2**, 718-729 (1988).
2. Rusconi S and Yamamoto KR, *EMBO J.*, **6**, 1309-1315 (1987).
3. Sadowski I, Ma J, Triezenberg S, and Ptashne M, *Nature*, **335**, 563-564 (1988).
4. Lin Y-S, Maldonado E, Reinberg D, and Green MR, *Nature*, **353**, 569-571 (1991).
5. Goodrich JA, Hoey T, Thut CJ, Admon A, and Tjian R, *Cell*, **75**, 519-530 (1993) .
6. Picard D, Salser SJ, and Yamamoto KR, *Cell*, **54**, 1073-1080 (1988).
7. Beato M, *Cell*, **56**, 335-344 (1989).
8. Picard D, *Trends Cell Biol.*, **3**, 278-280 (1993).
9. Odell JT, Nagy F, and Chua N-H, *Nature*, **313**, 810-812 (1985).
10. Ruberti I, Sessa G, Lucchetti S, and Morelli G, *EMBO J.*, **7**, 17871791 (1991).
11. Aoyama T, Dong C-H, Wu Y, Carabelli M, Sessa G, Ruberti I, Morelli G, and Chua N-H, *Plant Cell*, **7**, 1773-1785 (1995) .
12. Steindler C, MatteucciA, Sessa G., Weimar T, Ohgishi M, Aoyama T, Morelli G, and Ruberti I, *Development*, **126**, 4235-4245 (1999).

HMM Search for Apoptotic Domains

Masahiro Hattori and Minoru Kanehisa

For the purpose of analyzing apoptotic molecular interactions, we have developed a knowledge base, which consists of apoptotic molecular interactions, together with the WWW interface for it. This database and the user interface enabled us to find out entries containing various information about cell death. This information tells us that the apoptotic molecular interactions are likely to be controlled under a series of specific conserved domains. Thus, the viewpoint of domain seems to be more effective than the sequence similarity of the entire protein, when analyzing pathways, molecules, genes and genomes. In this study, we collected several hundred domain sequences of apoptotic interactions from our database, made 14 Hidden Markov Models (HMMs) for the domain groups, and searched against KEGG/GENES database with those HMMs to detect evolutionarily conserved domains.

Keywords: Apoptosis / Database / Hidden Markov Model / Bioinformatics

The characteristic form of cell death, which is accompanied with a cell shrinking, an active proteolysis and a nucleosome level DNA incision, has been observed[1]. Those dying cells show a specific process which is clearly different from the usual cell dying process. They are absorbed into other living cells around them and their biomaterials, for instance amino acids or nucleotides, seem to be recycled within those living cells. This type of cell death is called apoptosis, and is believed to play an important role in tissue and organ development in ontogenesis and homeostasis of living body. It is also known that apoptosis is related to some diseases such as autoimmune disease, virus infection and cancer. Furthermore many drugs such as anticancer agents take effect via induction of apoptosis in the target cells. With those background the studies on apoptosis have become popular and recently many experimental facts have been reported. In these studies the authors have found new apoptotic related genes or molecules and determined the relationships among those specific molecules. They also suggest that the cell death mechanism like apoptosis has been incorporated and diversified into animals during their evolutional history but its main system has been conserved from *C.elegans* to *H.sapiens*.

In this study, in order to analyze apoptotic pathways in the viewpoint of molecular interactions we have devel-

MOLECULAR BIOLOGY AND INFORMATION — Biological Information Science —

Scope of research

This laboratory aims at developing theoretical frameworks for understanding the information flow in biological systems in terms of genes, gene products, other biomolecules, and their interactions. Toward that end a new database is being organized for known molecular and genetic pathways in living organisms, and computational technologies are being developed for retrieval, inference and analysis. Other studies include: functional and structural prediction of proteins from sequence information and development of sequence analysis tools.

Prof
KANEHISA, Minoru
(D Sc)

Assoc Prof
GOTO, Susumu
(D Eng)

Students:
KIHARA, Daisuke (DC)
PARK, Keun-joon (DC)
HATTORI, Masahiro (DC)
BONO, Hidemasa (DC)
IGARASHI, Yoshinobu (DC)
KATAYAMA, Toshiaki (DC)
SATO, Kiminobu (DC)
KINJO, Fumi (DC)
NAKAO, Mitsuteru (DC)
YOSHIZAWA, Akiyasu (DC)
OKUJI, Yoshinori (MC)
KATO, Masaki (MC)
Research Fellow:
SATO, Kazushige (RF)
DANNO, Masaki (RF)
SHIRAISHI, Kotaro (RF)

oped a new knowledge base and the WWW interface for it, which focus on interactions among those apoptotic molecules[2]. We have also tried to analyze several apoptosis-specific domains with a Hidden Markov Model (HMM) technique because of the fact that the molecular interactions concerning with apoptosis are characterized by a set of domains[3].

At first we have collected information on domains or motifs concerning with apoptotic interactions from literature or databases, such as PROSITE or Pfam, and extracted those domain sequences from our database. After that we have obtained 409 sequences of 14 domain groups, which are originally derived from 200 protein entries of our database. The largest group has 66 sequences of extracellular cysteine repeat domain of tumor necrosis factor receptor (TNFR) superfamily, and the smallest has 2 sequences of C-terminus homologous region of CIDE superfamily. The average size is 29 sequences per domain, which seems enough for HMM learning and further sequence analyses. Secondly, we made the HMMs from those domain sequences by using HMMER2 programs (http://hmmer.wustl.edu/). Thus we got 14 HMMs for the domain groups. These HMMs are statistically tested in order to estimate their ability and efficiency of detection. Finally we looked for any homologous domains in KEGG/GENES database[4] by using those HMMs. Currently KEGG/GENES has 7 eukaryotes and 29 prokaryotes. It contains 24 complete genomes of 2 eukaryote and 22 prokaryotes. Our HMM-search procedure was done on each of the 36 species.

We could detect potentially interesting protein entries in *C.elegans*, *S.pombe* and *S.cerevisiae* as follows.(Table 1)

1) *C.elegans* has two BIR homologous peptides, C50B8.2 and T27F2.3, one caspase like peptidase, Y48E1B.13, and four death domain containing peptides, B0350.2A, B0350.2B, B0350.2C and B0350.2D. Here Y48E1B.13 has both His- and Cys-active sites of caspase, this seems to be a homologue of Ced-3 apart from its physiological function. Four B0350.2x are thought as the homologue to ankyrin, which is already known as a death domain containing protein. But the function of death domain has not yet been checked in ankyrin.

Species	Gene	detected motif
C.elegans	C50B8.2	two BIR domains
	T27F2.3	one BIR domain
	Y48E1B.13	caspase, Cys- & His-active site
	B0350.2A,B,C,D	death domain
S.pombe	SPAC2C6.16	two BIR domains
S.cerevisiae	YJR089W	one BIR domain

Table 1. HMM search results vs KEGG/GENES

2) *S.pombe* SPAC2C6.16 has two BIR domains and *S.cerevisiae* YJR089W has one. BIR domain is known to be necessary for an inhibition of apoptotic peptidase, and in higher animals three domains are usually found in one protein sequence. Then these two peptides in fungi might be an original type of inhibitor of apoptotic peptidase (IAP) family. Interestingly, these two sequences don't have an overall similarity to each other.

On the other hand, we could get no high scoring domains in prokaryotes but found that several peptides have weak homologies to apoptosis domains. We do not yet know the biological significance of these homologies.

Acknowledgments

This work was supported in part by a Grant-in-Aid for Scientific Research on Priority Areas ‘Genome Science’ from the Ministry of Education, Science, Sports and Culture in Japan. The computation time was provided by the Supercomputer Laboratory, Institute for Chemical Research, Kyoto University.

References

1. J.F. Kerr, A.H. Wyllie and A.R. Currie, Brit. J. Cancer, **26**, 239 - 257 (1972).
2. M. Hattori and M. Kanehisa, Genome Informatics, **8**, 276 - 277 (1997).
3. M. Hattori and M. Kanehisa, Genome Informatics, **10**, 267 - 268 (1999).
4. H. Ogata, S. Goto, K. Sato, W. Fujibuchi, H. Bono and M. Kanehisa, Nucleic Acids Research, **27**, 29 - 34 (1999).

Commissioning of the Electron Ring, KSR

Toshiyuki Shirai, Yoshihisa Iwashita, Takashi Sugimura, Hiromu Tonguu, Akira Noda and Hirokazu Fujita

KSR (Kaken Storage Ring) is a compact electron ring in Kyoto University. The circumference of KSR is 25.7 m and the maximum beam energy is 300 MeV. It is designed for the synchrotron light source and the electron pulse stretcher ring. The beam commissioning of KSR had started in September, 1999. In last October, the beam current of 3 mA was stored successfully. The beam parameter measurements and the machine parameter adjustments were carried out. At the end of 1999, the beam current is 10 mA. The typical beam lifetime is 1000 second.

Keywords : electron ring/ KSR/synchrotron radiation

A compact electron ring (Kaken Storage Ring, KSR) is now under construction at Institute for Chemical Research, Kyoto University. KSR has two operation modes, one is a beam storage mode and the other is a pulse stretcher mode. In the storage mode, the beam energy is 300 MeV and the design current is 100 mA. The critical wave length of the synchrotron radiation is 17 nm from the bending magnets. The design issue of the ring is to make 5 m straight sections where the dispersion is zero. One of the straight section is used for a beam injection, an extraction and an RF cavity. An electrostatic septum and a septum magnet for the stretcher mode are installed in this section. At the other section, an insertion device will be installed for the storage mode.

The beam commissioning had started from September, 1999. In last October, the beam current of 3 mA was stored successfully. The parameter measurements of

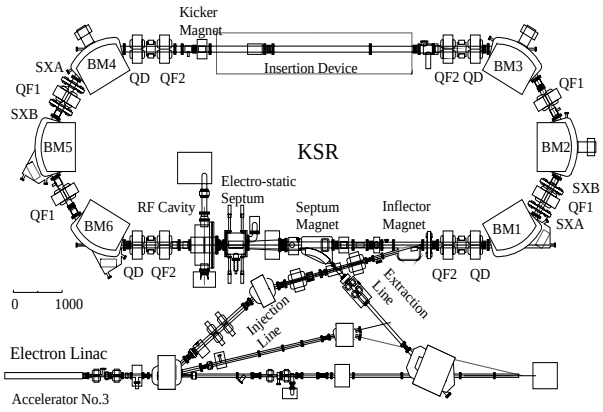

Figure 1. Layout of KSR, the injection and the extraction beam line.

NUCLEAR SCIENCE RESEARCH FACILITY — Particle and Photon Beams —

Scope of research

Particle and photon beams generated with accelerators and their instrumentations both for fundamental research and practical applications are studied. The following subjects are being studied: Beam dynamics related to space charge force in accelerators: Beam handling during the injection and extraction processes of the accelerator ring:radiation mechanism of photon by electrons in the magnetic field: R&D to realize a compact proton synchrotron dedicated for cancer therapy: Control of the shape of beam distribution with use of nonlinear magnetic field: and Irradiation of materials with particle and photon beams.

Prof
NODA, Akira
(D Sc)

Assoc Prof
IWASHITA, Yoshihisa
(D Sc)

Instr
SHIRAI, Toshiyuki

Techn
TONGUU, Hiromu

Lecturer(part-time):
NAKAJIMA, Kazuhisa (KEK)
Students:
MIZUMOTO, Motoharu
(RF, D Sc)
SUGIMURA, Takashi(DC)
KIHARA, Takahiro (DC)
FUJIEDA, Miho (DC)
URAKABE, Eriko (DC)
MORITA, Akio (MC)

This work is supported by Monbusho Grant-in-Aid A(2), No. 090304042

KSR were carried out using the stored beam. Table 1 shows the comparison between the simulation and the measurement results. The tune value is an important parameter to show the beam stability. It was measured using the RF electric field. The beam is perturbed strongly when the electric force of the RF field resonates with the transverse motion of the beam. The beam perturbation was measured from the deformation of the synchrotron radiation profile. Figure 2 shows the tune value at the operation point and the resonance line. The present tune is far from the resonance lines up to 6th order. At the injection time, the tune spreads due to the energy spread. It is compensated to be smaller than +/- 0.01 by the sextupole magnet correction not to cross the resonance line up to 4th order. The higher order resonance is not effective for the injection.

The β function agrees well to the simulation results within the measurement error. The natural chromaticity in the vertical direction is different from the design value. It is due to the effect of the sextupole components in the field of the bending magnet, especially in the fringe field. Including this effects, the chromaticity was corrected using 2 sets of sextupole magnets.

At the end of 1999, the beam stacking and the beam acceleration up to 300 MeV succeeded. Figure 3 shows the circulation beam current at the injection. The beam current is measured by a DC current transformer. The beam pulse is injected every 3.3 seconds from the linac. It corresponds to the horizontal dumping time. The beam are stacked about 20 times and the final storage current becomes 10 mA. It is limited by the scattering beam loss with the residual gas, especially, the gas induced by the synchrotron radiation. The conditioning process is going on now. The beam life also depends on the beam current strongly because of the same reason. The typical beam life is 1000 second with zero current and 400 sec with 3 mA.

References

[1] A.Noda, et al., "Electron Storage and Stretcher Ring, KSR", Proc. of the 5th European Particle Accelerator Conference, Sitges (Barcelona), Spain, 451-453 (1996)

Table 1. Comparison between the simulation and the measurement results of the beam parameters.

	Design	*Measurement*
Tune	*(2.300, 1.275)*	*(2.309, 1.270)*
Storage Current	*100 mA*	*10 mA*
Beam Life	---	*400 sec (at 3 mA)* *1000 sec (at 0 mA)*
β function at QF	*(7.1, 10.2)*	*(6.5, 10.3)*
Natural Chromaticity	*(2.4, -8.2)*	*(-2.6, -6.1)*
Chromaticity with Correction	*(0.0, 0.0)*	*(-0.1, -0.3)*
Dispersion at straight section	*0.0 m*	*< 0.05 m*

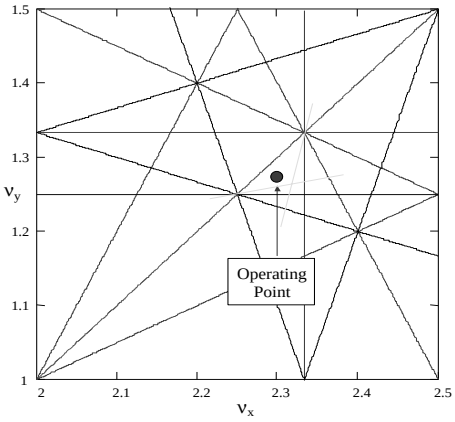

Figure 2. Operation point in the tune diagram. The lines show the resonance up to 6th order.

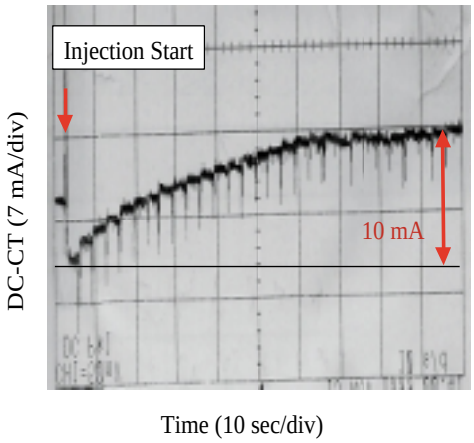

Figure 3. Stacking beam current at the injection. It is measured by the DC current transformer.

Selective Field-Ionization Electron Detector at Low Temperature of 10 mK Range

M. Shibata, M. Tada, Y. Kishimoto, C. Ooishi and S. Matsuki

Combined with a dilution refrigerator, selective field-ionization detection system with a channel electron multiplier optimized at 10 mK-range temperature was developed. The detection efficiency of the ionized electrons from the n~110 Rydberg states of Rb is 98% at the lowest achieved temperature of 12 mK.

Keywords : Dark matter/axion/Rydberg atoms/field ionization/channel electron multiplier

Highly excited atoms, so called Rydberg atoms, have been utilized for many fields in fundamental physics including cavity quantum electrodynamics, quantum computation, and the quantum measurements as well as their own spectroscopic studies. Recently important application of the Rydberg atoms has been forwarded to detect extremely low-power microwave photons in resonant cavities: indeed the detection of each single microwave photon in a resonant cavity with Rydberg atoms has been utilized to search for dark matter axions in the Universe [1-6]: in this scheme, the axion is first converted to single photon in the strong magnetic field (Primakoff process) and the microwave photons thus produced are absorbed by Rydberg atoms passed through the cavity and the excited Rydberg atoms are then selectively field-ionized and detected (Rydberg-atom cavity detector). The microwave power expected from the dark matter axions in the cavity is extremely small, less than 10^{-26} W.

One of the essential ingredients of the Rydberg-atom cavity detector is the selective field ionization (SFI) system. Specifically the cavity and the SFI system should be cooled down to 10 mK range in order to reduce the background thermal blackbody photons in the cavity, the number of which is still comparable with the expected axion-converted photon number. To our knowledge, no SFI detectors usefull at such low temperature have been developed so far.

The SFI detection system for the above requirement was developed with a channel electron multiplier (CEM) together with a dilution refrigerator of the modified Oxford Kelvinox 300. Overall view of the detection system is shown in Fig.1. The field ionization electrode of a few V/cm was located just outside of the microwave cavity, which is attached to the bottom plate of the mixing chamber of the dilution refrigerator, thus the cavity and the SFI detector being able to be cooled down to 10 mK range. Since the CEM dissipate much higher power (more than mW) than the cooling power of the dilution

NUCLEAR SCIENCE RESEARCH FACILITY — Beams and Fundamental Reaction —

Scope of research

Particle beams, accelerators and their applications are studied. Structure and reactions of fundamental substances are investigated through the interactions between beams and materials such as nuclear scattering. Tunable lasers are also applied to investigate the structure of unstable nuclei far from stability and to search for as yet unknown cosmological dark-matter particles in the Universe.

Prof
INOUE, Makoto
(D Sc)

Assoc Prof
MATSUKI, Seishi
(D Sc)

Students
KAPIN, Valeri (RF)
TADA, Masaru (DC)
KISHIMOTO, Yasuhiro (DC)
AO, Hiroyuki (DC)
SHIBATA, Masahiro (DC)
OOISHI, Chikara (MC)
SAIDA, Tomoya (MC)

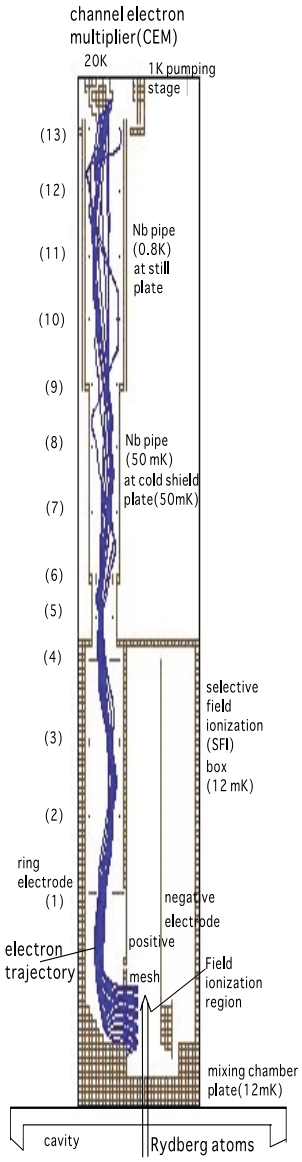

Figure 1. Overall view of the present system for the field ionization electron detector. Rydberg atoms passed through the detection cavity are ionized at the field ionization region shown in the figure. Field ionization electrode is set inside of a Nb box located at the mixing chamber plate of a dilution refrigerator of 12 mK temperature. The ionized electrons are transported to the channel electron multiplier (CEM) at the 1K pumping stage through a series of ring-electrodes of 13 elements. All the ring electrodes are surrounded by Nb pipes to expel out the external megnetic field (except the earth's field). The simulation of the electron transport was done by taking into account the earth's magnetic field as well as Nb pipes and other materials of ground potential. Typical electron trajectories are shown in the figure. Overall transport length of electrons is about 30 cm. The Nb pipes are anchored to the still plate (0.8K) and the cold-shield plate at the heat exchanger region (~50mK), respectively. The CEM electron detector (Channeltron) is heated up to ~ 20 K with a heating coil surrounding it.

refrigerator, the CEM channeltron was located at the 1K pumping stage which is about 30 cm apart from the mixing chamber plate. Thus the ionized electrons resulting from the field ionization process have to be transported with good efficiency from the ionized point to the detector region. A series of ring electrodes was adopted to transport electrons efficiently in the present system where the available space for the trasportation is very limited due to the structure of the dilution refrigerator system.

The ring electrodes are set inside of two Nb pipes and a field ionization box made of Nb, which are anchored to the still plate (0.8K), cold-plate shielding stage at the heat exchanger position (~50 mK), and the mixing chamber stage (~10 mK), respectively. The Nb pipes and box are chosen to expell out the external magnetic field to get rid of the complicated electron trajectories due to the strong external magnetic field applied for the axion conversion into photons. The overall electron trajectory was simulated with the ion trajectory code SIMION where all the relevant materials including the surrounding ground plates and the CEM detector potential were taken into account. In Fig. 1 also shown are typical electron trajectories.

Typical signal of the field-ionized electrons is shown in Fig.2, where the ionized electrons were detected as a function of the second laser wavelength to excite the n=110 Rydberg states of Rb atoms. The overall detection efficiency is 98 % at the lowest achieved temperature of 12 mK. Note that the CEM was heated up to ~ 20K in order to get enough amplification gain of electrons.

Although this SFI system and the CEM electron detector have been developed primarily for the dark matter axion detection, this detection scheme is general and applicable to more broad research area.

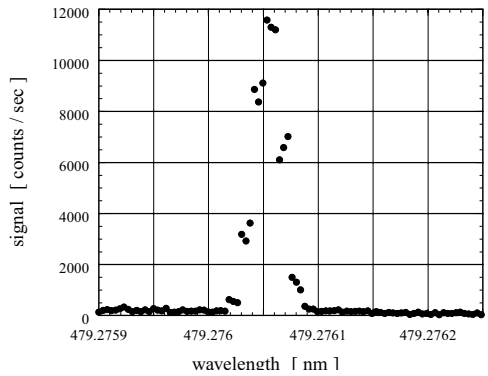

Figure 2. Typical field ionization signal of electrons from the n=110 Rydberg states of Rb measured with the present detector system at 12 mK temperature as a function of the second laser wavelength. The Rb Rydberg states are produced with two-step laser excitation.

References

1. S. Matsuki and K. Yamamoto, Phys. Lett. B263 (1991) 523.
2. I. Ogawa, S. Matsuki and K. Yamamoto, Phys. Rev. D53 (1996) R1740.
3. S. Matsuki, I. Ogawa, S. Nakamura, M. Tada, K. Yamamoto and A. Masaike, Nucl. Phys. B51 (1996) 213.
4. K. Yamamoto and S. Matsuki, Nucl. Phys. B72 (1998) 132.
5. M. Tada, Y. Kishimoto, K. Kominato, M. Shibata, H. Funahashi, K. Yamamoto, A. Masaike and S. Matsuki, Nucl. Phys. B72 (1998) 164.
6. S. Matsuki, M. Tada, Y. Kishimoto, M. Shibata, K. Kominato, C. Ooishi, H. Funahashi, K. Yamamoto and A. Masaike, Proceedings of the 2nd International Workshop on the Identification of Dark Matter in the Universe, Buxton UK, 1998 (World Scientific, Singapore, 1999) p.441.

Constructing Expression Pattern Database of Ascidian mRNAs

Shuichi Kawashima

MAGEST is a database for ascidian, *Halocynthia roretzi*, maternal mRNAs that have been newly identified by our cDNA project. We have collected 3' and 5' tag sequences of mRNAs and their expression data from whole mount *in situ* hybridization in early embryo. To date we determined more than 2,000 tag-sequences of *Halocynthia roretzi* cDNAs and deposited in the public databases. The tag sequences and the expression data with additional information can be obtained through MAGEST via the World Wide Web at URL http://www.genome.ad.jp/magest/.

keywords: maternal mRNA / Ascidian / Database / Bioinformatics

Fertilized eggs cleave many times to give rise to multicellular organisms. Within embryos, embryonic blastomeres develop into various types of tissues such as epidermis, muscles and nervous systems. In the processes of early embryogenesis, maternal factors stored in the egg cytoplasms are known to play various significant roles (1). Since the last century, ascidian egg has been well-known as a mosaic egg in which many blastomeres in the early embryo differentiate autonomously. Recent works have revealed that there exist cytoplasmic determinants that direct formation of epidermis, muscle and endoderm as well as cytoplasmic factors involved in axis specification of the embryo and in gastrulation(2,3). In addition, embryonic cell lineage is almost completely revealed by intracellular marking (4). For these reasons, we became interested in maternal mRNAs as candidates for the cytoplasmic determinants and initiated a cDNA project which collects mRNA tag-sequences and their expression data. The information regarding gene expression and localization is important for understanding the outline of gene functions in developmental mechanisms. Thus, we are constructing a database, named MAGEST— Maboya ,the Japanese ascidian, (*Halocynthia roretzi*) Gene Expression patterns and Sequence Tags— for analysis of the data produced in our project.

CONTENTS OF MAGEST

Currently MAGEST contains two types of data: the 3' and 5' ESTs by DNA sequencing and the gene expression

RESEARCH FACILITY OF NUCLEIC ACIDS

Scope of research

The following is the current major activities of this facility.

With emphasis on regulatory mechanisms of gene expression in higher organisms, the research activity has been focused on analysis of signal structures at the regulatory regions of transcriptional initiation and of molecular mechanisms involved in post-transcriptional modification by the use of eukaryotic systems appropriate for analysis. As of December 1994, studies are concentrated on the molecular mechanisms of RNA editing in mitochondria of kinetoplastids

Assoc Prof
SUGISAKI, Hiroyuki
(D Sc)

Instr
KAWASHIMA, Shuichi

Techn
YASUDA, Keiko

data by whole-mount *in situ* hybridization (WISH). Each cDNA clone is given a unique gene code consisting of 6 alphanumerical characters. This gene code reflects our way of handling plasmid DNAs by 384 (16 lines times 24 columns) well plate. For each clone, we remove cloning vector sequences and ambiguous regions that contain stretches of N (ambiguous nucleotide) from raw sequence data and register the processed sequences in the MAGEST database. These sequences are used as query sequences for BLAST homology searches against GenBank at the nuceotide sequence level and also against nr-aa, which is a non-redundant protein sequence database constructed from SWISS-PROT, PIR, PRF and GenPept (trunslated GenBank), at the amino acid sequence level. Up to ten entries above a given threshold are stored in MAGEST and they can be retrieved from the original databases by the DBGET/LinkDB system (5). All 3' EST sequences are compared with each other to examine the numbers of redundant genes. Because we use an unnormalized cDNA library, redundant genes may be considered to reflect the population of maternal mRNAs. Based on these search results, we annotate the EC number to a clone coding for an enzyme. Using the EC numbers, these clones are linked to the KEGG pathway map (6).

WISH was carried out for staged embryos to obtain informations about localization and/or expression sites of the clones during embryogenesis. We adopt three developmental stages: the 8-cell stage, the 110-cell stage and early tailbud (eTb) stage. At the 8-cell embryo, it is easy to identify the orientation of the embryo along the animal-vegetal and anterior-posterior axes which are utilized to see the distribution of maternal RNAs. In the 110-cell embryo, the developmental cell fate of every blastomere is almost completely restricted. The 110-cell embryo is used to see lineage-specificity of gene expression. In the eTb embryo, the basic body plan is established. Embryo at this stage is used to see tissue-specificity of gene expression. Many genes that are isolated from the cDNA library are zygotically expressed, and the data of both the maternal and/or the zygotic expression pattern of these genes are registered in MAGEST. We classify the expression data according to each blastmere or tissue. We classify the expression data according to each blastomere or tissue. This classification is based on the cell lineage analysis in ascidian embryo (4). A clone not showing a specific expression pattern is classified as "overall" when it is expressed over the entire embryo, or only "ISH_done" when no signal is detected. We provide the original images of WISH in addition to the classification data.

DATA RETRIEVAL SYSTEM

MAGEST is implemented in the Sybase relational database system, is accessible through the WWW. Its CGI programs are written in the Perl programming language with Sybperl, a Sybase extension module to Perl.

We provide several facilities for data retrieval. One can retrieve the data by using keywords or by specifying an entry identifier. A similar search can be performed against the 3' and 5' ESTs in MAGEST. In addition, we provide a unique data retrieval system using our classification of gene expression data derived from WISH.

FUTURE DIRECTIONS

In this project, we aim at all-inclusive and systematic description of maternal transcripts of Japanese ascidian fertilized eggs, *H. roretzi*: cDNA sequences from ca. 10,000 different genes and their expression patterns during embryogenesis. Currently we registered more than 2,000 cDNA clones in the public databases. From a survey of these data, we found several genes that may play important roles during early development. These clones include key elements for development such as some transcription factors, signal transducing molecules, or RNA binding proteins (7, 8, 9). Finally MAGEST will also enable us to understand molecular mechanisms for establishment of embryonic body plans of chordates and more generally the evolution from invertebrate to vertebrate.

REFERENCES

1 Satoh, N., (1994) Developmental Biology of Ascdians, CAMBRIDGE UNIVERSITY PRESS]

2 Conklin, E.G. (1905) *Biol.Bull*., 8, 205-230.

3 Nishida, H. (1997) *Int.Rev. Cytol.*, 176, 245-306.

4 Nishida, H. (1987) *Dev.Biol*.,121,526-541.

5 Fujibuchi, W., Goto, S., Migimatsu, H., Uchiyama, I., Ogiwara, A. Akiyama, Y. and Kanehisa, M. (1998) *Pacific Symposium on Biocomputing '98* (Altman, R. B., Dunker, A. K., Hunter, L. and Klein, T. E., eds.), World Scientific, 175-186.

6 Ogata, H., Goto, S., Sato, K., Fujibuchi, W., Bono,H., and Kanehisa, M. (1999) *Nucleic Acid Res*., 27, 29-34

7 Sasakura, Y., Ogasawara, M., and Makabe, K.W., (1998) *Int.J.Dev.Biol*. 42, 573-579

8 Sasakura,Y.,Ogasawara,M.,and Makabe,K.W.,(1998) *Mech.Dev*.,76,161-163

9 Kobayashi, A., Sasakura, Y., Ogasawara, M., and Makabe,K.W.,(1999) *Develop. Growth. Differ*. 41, 419-427

LABORATORIES OF VISITING PROFESSORS

SOLID STATE CHEMISTRY – Structure Analysis –

Vis Prof
MAEKAWA, Sadamichi
(D Sci)

Professor
MAEKAWA, Sadamichi (D Sci)
Institute for Materials Research, Tohoku University
(2-1-1 Katahira, Aoba-ku, Sendai 980-8577)

Lectures at *ICR*
Spin Liquid State around a doped Hole in Insulating Curates
Effect on Strips on Electronic States in Undoped $La_{2-x}Sr_xCuO_4$

Vis Prof
HOSONO, Hideo
(D Eng)

Professor
HOSONO, Hideo (D Eng)
Materials and Structures Laboratory
Tokyo Institute of Technology
(Nagatsuta, Midori-ku, Yokohama 226-8503)

Lectures at *ICR*
Modern Alchemy- A New Technique to Transform Transparent Insulators into Metals
Defect Engineering

FUNDAMENTAL MATERIAL PROPERTIES – Composite Material Properties –

Vis Prof
KAZUO, Matsuura
(D Sci)

Professor
KAZUO, Matsuura (D Sci)
Consultant, Technical Headquarters, Japan Polyolefins Co. Ltd.
(10-1 Chidori, Kawasaki-ku 210-0865)

Lectures at *ICR*
Innovation in Transition Metal Catalysis and Polyolefin Material Revolution
Progress in Heterogeneous Zeigler-Natta and Phillips Chromium Catalysis
Metallocenes and Post Metallocenes Catalysis
Progress in Polyolefin Manufacturing Process
New Specialized Polyolefin Materials

Vis Assoc Prof
HANABUSA, Kenji
(D Eng)

Associate Professor
HANABUSA, Kenji (D Eng)
Faculty of Textile Science & Technology, Shinshu University
(3-15-1, Tokida, Ueda , Nagano 386-8567)

Lectures at *ICR*
Development of New Organogelators and Their Gelation Mechanism
Development of New Organogelators and Application to Functional Materials

SYNTHETIC ORGANIC CHEMISTRY – Synthetic Theory –

Vis Prof
TANAKA, Hirokazu
(D Pharm Sci)

Professor
TANAKA, Hirokazu (D Pharm Sci)
Department of External Scientific Affairs, Fujisawa Pharmaceutical Co., LTD
(Yodogawa-ku, Osaka 532-8514)

Lectures at *ICR*
Strategies for the Drug Creation

Vis Assoc Prof
TOMOOKA, Katsuhiko
(D Eng)

Associate Professor
TOMOOKA, Katsuhiko (D Eng)
Department of Chemical Engineering, Tokyo Institute of Technology
(Meguro-ku, Tokyo 152-8552)

Lectures at *ICR*
Development and Progress in Carbanion [1,2]-Rearrangement

PUBLICATIONS

STATES AND STRUCTURES

I. Atomic and Molecular Physics

Suzuki C, Kawai J, Tanizawa J, Adachi H, Kawasaki S, Takano M and Mukoyama T: Local spin moment of $LaCoO_3$ probed by a core hole, *Chemical Physics*, **241**, 17-27 (1999)

Mukoyama T: Introduction to Relativistic Electronic Structure Calculation in "Studies on the Heavy Elements Research using the DV-DFS Method", *JAERI-Review (Japan Atomic Energy Research Institute, Tokai, 1999)*, **99-008**, 1-6 (1999) (in Japanese)

Mukoyama T, Song B and Taniguchi K: Relativistic Calculations of X-Ray Transition Energies and Emission Rates for Titanium Atoms, *X-Ray Spectrometry*, **28**, 99-104 (1999)

Bastug T, Vlaicu A. M, Nakamatsu H and Mukoyama T: Density functional calculation for N_2 adsorption on Ni(100), in *20. Arbeitsbericht, EAS-20 (Arbeitsgruppe Energiereiche Atomare Stosse, Kassel, 1999)*, 166-168 (1999)

Uda M, Yamamoto T, Takenaga T, Mochizuki M and Mukoyama T: Intensity estimation of He^+-ion-induced F K doubly ionized X-ray satellites emitted from alkali and alkaline-earth fluorides, *Nucl. Instr. and Meth. B*, **150**, 50-54 (1999)

Uda M, Kanno H and Mukoyama T: Preliminary report on porcelain in Meissen (Germany) and Arita (Japan), *Nucl. Instr. and Meth. B*, **150**, 597-600 (1999)

Mukoyama T: Inner-Shell Ionization in Ion-Atom Collisions - Beyond the First-Born Approximation -, *Nucl. Instr. and Meth. B*, **154**, 54-61 (1999)

Mukoyama T and Lin C. D: Saturation Effect of Projectile Excitation in Ion-Atom Collisions, *Physica Scripta T*, **80**, 396-397 (1999)

Mukoyama T and Uda M: A New Approach to Shake Process Accompanying Inner-Shell Vacancy Production, in *Abstracts, 18th Internat. Conf. on X-Ray and Inner-Shell Processes, Chicago (Argonne National Laboratory, Illinois, 1999)*, **August 23 - 27**, 95 (1999)

Tsuji J, Mukoyama T, Kojima K, Ikeda S and Taniguchi K: Studies of X-Ray Absorption Process in Various Sulfur Compounds, in *Abstracts, 18th Internat. Conf. on X-Ray and Inner-Shell Processes, Chicago (Argonne National Laboratory, Illinois, 1999)*, **August 23 - 27**, 201 (1999)

Yasui J, Mukoyama T, Nakamatsu H, Hock G and T. Shibuya: Analytical Expressions of Atomic Wave Functions and Molecular Integrals for the Calculation of the X-Ray Transition Probabilities of Molecules, *in Abstracts, 18th Internat. Conf. on X-Ray and Inner-Shell Processes, Chicago (Argonne National Laboratory, Illinois, 1999)*, **August 23 - 27**, 230 (1999)

Yamaguchi K and Mukoyama T: Higher order calculation of Compton excitation of nucleus, *in Abstracts, 18th Internat. Conf. on X-Ray and Inner-Shell Processes, Chicago (Argonne National Laboratory, Illinois, 1999)*, **August 23 - 27**, 306 (1999)

Suzuki C, Kawai J, Adachi H and Mukoyama T: Electronic structures of 3d transition metal (Ti-Cu) oxides probed by a core hole, *Chem. Phys.*, **247**, 453-470 (1999)

Roller-Lutz Z, Wang Y, Lutz H. O, Bastug T, Mukoyama T and Fricke B: Charge exchange in collisions of C_{60}^+ ions with laser-excited aligned Na atoms, *Phys. Letters A*, **262**, 66-71 (1999)

Mukoyama T, Ito Y and Taniguchi K: Atomic Excitation and Ionization as the Result of Inner-Shell Vacancy Creation, *X-Ray Spectrometry*, **28**, 491-496 (1999)

Vlaicu A. M, Ito Y and Mukoyama T: On the 74W L2 satellite, in *abstract of 18th International Conference on X-ray and Inner-shell Processes*, **A20**, August 23-27 (1999)

Ito Y, Tochio T, Ishizuka T, Vlaicu A. M and Mukoyama T: The resonant inelastic L x-ray emission spectra in Cr metal, in *abstract of 18th International Conference on X-ray and Inner-shell Processes*, **B31**, August 23-27 (1999)

Emura S, Ito Y, Takahashi M and Mukoyama T: A new type of fine structure in the x-ray absorption spectroscopy, in *abstract of 18th International Conference on X-ray and Inner-shell Processes*, **B32**, August 23-27 (1999)

Ito Y, Tochio T,Ishizuka T, Vlaicu A.M, Hayakawa S, Cohsi Y and Shoji T: K x-ray emission spectra of Ti, in *abstract of 18th International Conference on X-ray and Inner-shell Processes*, **B33**, August 23-27 (1999)

Ishizuka T, Tochio T, Vlaicu A.M, Ito Y, Mukoyama T, Hayakawa S, Gohsi Y and Shoji T: K x-ray emission spectra of Cu in copper metal, in *abstract of 18th International Conference on X-ray and Inner-shell Processes*, **B34**, August 23-27 (1999)

Tochio T, Ishizuka T, Vlaicu A.M, Ito Y, Mukoyama T, Hayakawa S, Gohsi Y and Shoji T: K x-ray emission spectra of Cr, in *abstract of 18th International Conference on X-ray and Inner-shell Processes*, **B35**, August 23-27 (1999)

Ito Y, Mukoyama T, Emura S and Takahashi M: On the multi-electron excitations in XAFS, in *abstract of 18th International Conference on X-ray and Inner-shell Processes*, **B36**, August 23-27 (1999)

Shigeoka N, Shigemi A, Tochio T, Ishizukab T, Vlaicu A. M, Ito Y, Mukoyama T and Gohshi Y: K X-ray Emission Spectra in The nickel (II) Shiff Base Complexes, in *abstract of 18th International Conference on X-ray and Inner-shell Processes*, **B54**, August 23-27 (1999)

Yamaguchi K, Ito Y, Mukoyama T, Takahashi M and Emura S: Inverse problem analysis of x-ray absorption fine structure, in *abstract of 18th International Conference on X-ray and Inner-shell Processes*, **C51**, August 23-27 (1999)

Ito Y, Tochio T, Vlaicu A. M, Ohsawa D,Mukoyama T, Muramatsu Y, Perera R.C.C, Grush M.M, Callcott T.A and Sherman E: The contribution of the ligands around Cr to the resonant inelastic L x-ray emission spectra, *J.Electron Spectros. Relat. Phenom.*, **101/103**, 851-858(1999)

Ishizuka T, Tochio T, Vlaicu A. M, Ohsawa D, Ito Y, Mukoyama T, Hayakawa S and Gohsi Y: K x-ray emission spectra and satellites in copper metal, *Advances in x-ray Chemical Analysis*, **30**,21-28(1999) (in Japanese)

Ishizuka T, Vlaicu A. M, Tochio T, Ito Y, Mukoyama T, Hayakawa S, Gohsi Y, Kawai S, Motoyama M and Shoji T: x-ray emission spectra by a simple-quasi-two crystal spectrometer, *Advances*

in x-ray Chemical Analysis, **30**, 29-40 (1999) (in Japanese)

Yamaguchi K, Ito Y, Mukoyama T, Takahashi M and Emura S: The regularization of the basic x-ray absorption spectrum fine structure equation via the wavelet-Galerkin method, *J.Phys.B*, **32**, 1393-1408 (1999)

Yamaguchi K, Ito Y, Mukoyama T, Takahashi M and Emura S: Linear inverse problem solution of the basic XAFS equation via the Wavelet-Galerkin method, *J.Synchrotron Rad.*, **6**, 249-250 (1999)

Ichihara J, Takahashi M, Emura S, Tochio T, Ito Y and Mukoyama T: Acceleration of halogen-exchange reaction of lead(II) fluoride in organic, *J.Synchrotron Rad.*, **6**, 602-603 (1999)

Ito Y: The contribution of multielectron transitions to x-ray absorption spectra (invited), in *Proceedings of International Workshop on Atomic and Molecular Physics at High Brilliance Synchrotron Radiation Facilities*, **November 4-6**, 225-237 (1998)

Shigeoka N, Mutaguchi K, Nakanishi Y, Ito Y, Mukoyama T, Shimizu K, Shoji T and Omote K: Development of Gas Scintillation Proportional Counter, *The Third International Symposium on Bio-PIXE*, **November 16-19** (1999)

Shigemi A, Tochio T, Ishizuka T, Shigeoka N, Ito K, Vlaicu A.M, Ito Y, Mukoyama T and Gohshi Y: K x-ray emission spectra of Ni in nikel (II) schiff base complexes, *x-ray spectrum*. **28**, 478-483 (1999)

Kurihara M, Hirata M, Sekine R, Onoe J, Nakamatsu H, Mukoyama T and Adachi H: Discrete-variational Dirac-Slater calculation on valence band XPS for UC, J. *Alloys Compounds*, **283**, 128-132 (1999)

Song B, Nakamatsu H, Shigemi A, Mukoyama T and Taniguchi K: Calculations of X-Ray Emission Spectra for Sulfur Dioxide by the DV-Xa Method, *X-Ray Spectrometry*, **28**, 94-98 (1999)

Ueda K, Muramatsu Y, Shimizu Y, Chiba H, Sato Y, Kitajima M, Tanaka H and Nakamatsu H: Quasi-isotropic fragmentation of PF5 following P 2p photoabsorption, *Chem. Phys. Lett.*, **308**, 45-50 (1999)

Muramatsu Y, Ueda K, himizu Y, Chiba H, Amano K, Sato Y and Nakamatsu H: Anisotropic fragmentation of CF4 following F 1s photoabsorption, *J. Phys. B*, **32**, L213-217 (1999)

II. Crystal Information Analysis

Yoshida K, Tsujimoto M, Isoda S, Kobayashi T, Kamata T and Matsuoka M: Selective On-top Crystal Nucleation in Organic Multilayer Formation, *Mol. Cryst. & Liq. Cryst.*, **322**, 161-166 (1998)

Irie S, Isoda S, Kuwamoto K, Miles M J, Kobayashi T and Yamashita Y: Monolayer Epitaxy of a Triangular Molecule on Graphite, *J. Cryst. Growth*, **198/199**, 939-944 (1999)

Ogawa T, Isoda S, Kobayashi T and Karl N: Crystal Structure Analysis of 3, 4, 9, 10-Perylenetetracarboxylic Dianhydride (PTCDA) by Electron Crystallography, *Acta Cryst.*, **B55**, 123-130 (1999)

Suga T, Isoda S and Kobayashi T: Structure and UV-VIS Spectrum of Dithallium Phthalocyanine Thin Film, *Technical Report of IEICE*, **OME99-61**, 55-60 (1999) (in Japanese)

Yaji T, Isoda S, Kobayashi T, Taguchi K, Takada K, Yasui M and Iwasaki F: Color Change Due to Phase Transition in N-(2,4-dinitrophenyl)-o-anisidine, *Mol. Cryst. & Liq. Cryst.*, **327**, 57-60 (1999)

Suga T, Isoda S and Kobayashi T: Characterization and Electric Conductivity of Dithallium Phthalocyanine (Tl_2Pc), *J. Porphyrins and Phthalocyanines*, **3**, 397-405 (1999)

Hashimoto S, Isdoa S, Kurata H, Lieser G and Kobayashi T: Molecular Orientation of Perfluoro-vanadyl-phthalocyanine Examined by Electron Energy-loss Spectroscopy, *J. Porphyrins and Phthalocyanines*, **3**, 585-591 (1999)

Tsujimoto M, Moriguchi S, Isoda S, Kobayashi T and Komatsu T: TEM Analysis of Pt-particles Embedded on TiO_2 Exhibiting High Photocatalytic Activity, *J. Electron Microscopy*, **48**, 361-366 (1999)

Suga T, Isoda S and Kobayashi T: Structure of Vacuum-deposited Tl_2Pc Film and its Optical and Electrical Properties, *J. Porphyrins and Phthalocyanines*, **3**, 647-653 (1999)

Moriguchi S, Isoda S and Kobayashi T: Measurement of and Compensation for the Difference between Voltage and Current Centers in HRTEM, *J. Electron Microscopy*, **48**, 437-441 (1999)

Ogawa T, Isoda S and Kobayashi T: Crystal Structure Analysis by Electron Microscopy, *Kessho-gakkai-shi*, **41**, 195-201 (1999) (in Japanese)

Tosaka M, Yamakawa M, Tsuji M, Kohjiya S, Ogawa T, Isoda S and Kobayashi T: Structural Studies on Polymer Whiskers by Transmission Electron Microscopy: I. Morphological and High-Resolution Observations, *Microscopy Resea. Tech.*, **46**, 325-333 (1999)

III. Polymer Condensed States Analysis

Yamanaka S, Yuguchi Y, Urakawa H, Kajiwara K and Kohjiya S: Polysiloxane Networks: Structural Characteristics and Formation Mechanism, *Network Polymer*, **20**, 157-163 (1999) (in Japanese)

Yamada N, Shoji S, Sasaki H, Nagatani A, Yamaguchi K, Kohjiya S and Hashim A S: Developments of High Performance Vibration Absorber from Poly(vinyl chloride)/Chlorinated Polyethylene/ Epoxidized Natural Rubber Blend, *J. Appl. Polym. Sci.*, **71**, 855-863 (1999)

Murakami K, Osanai S, Shigekuni M, Iio S, Tanahashi H, Kohjiya S and Ikeda Y: Silica and Silane Coupling Agent for in Situ Reinforcement of Acrylonitrile-Butadiene Rubber, *Rubber Chem. Technol.*, **72**, 119-129 (1999)

Urayama K, Yokoyama K and Kohjiya S: High Elogation of Deswollen Polysiloxane Networks, in *Wiley Polymer Networks Group Review Series Vol. 2*, Stokke B T and Elgsaeter A Ed., p.485-495, Wiley (1999)

Urayama K, Kircher O, Böhmer R and Neher D: Investigations of Ferroelectric-to-Paraelectric Phase Transition of Vinylidenefluoride Trifluoroethylene Copolymer Thin Films by Electromechanical Interferometry, *J. Appl. Phys.*, **86**, 6367-6375 (1999)

Urayama K, Kohjiya S: Ultra-High Extensibility of a Polymer Gel in the Deswollen State, *Ann. Rep. Res. Inst. Chem. Fib., Jpn.*, **56**, 49-56 (1999) (in Japanese)

Murakami S, Kohjiya S, Uchida T, Shimamura K: Structure of Extruded-Blown Film of High Density Polyethylene, *Kobunshi Ronbunshu*, **56**, 828-832 (1999) (in Japanese)

Tsujimoto J, Murakami S, Tsuji M and Kohjiya S: Structural Change during Uniaxial Drawing of Unoriented Poly (tetramethylene succinate) Films, *Sen'i Gakkaishi*, **55**, 361-368 (1999) (in Japanese)

Tsuji M, Tsujimoto J, Murakami S and Kohjiya S: Crystalline Phase Transition in Uniaxially Oriented Films of Poly (tetramethylene succinate) Induced by Tensile Extension, *Sen'i Gakkaishi*, **55**, 511-521 (1999) (in Japanese)

Tsuji M, Novillo L F A, Fujita M, Murakami S and Kohjiya S: Morphology of Melt-crystallized Poly(ethylene 2, 6-naphthalate) Thin Films Studied by Transmission Electron Microscopy, *J. Mater. Res.*, **14**, 251-258 (1999)

Shimizu T, Tsuji M and Kohjiya S: Crystalline Morphologies of Polychloroprene Thin Films as Revealed by Transmission Electron Microscopy Observation, *J. Mater. Res.*, **14**, 1645-1652 (1999)

Fujita M, Tsuji M and Kohjiya S: A TEM Study on Polyoxymethylene Edge-on Lamellae Crystallized Epitaxially on Alkali Halides, *Polymer*, **40**, 2829-2836 (1999)

Fujita M, Tsuji M, Kohjiya S, Wittmann J C: Perfectly Alternating Ethylene-Carbon Monoxide Copolymer Crystallized Epitaxially on Alkali Halides. 1. Morphological Observation by TEM, *Macromolecules*, **32**, 4383-4389 (1999)

Ito H, Sasaki H, Tsuji M and Kohjiya S: Penetration of Multifunctional Epoxide into Wool and Its Effect on Shrink Resistance, *Textile Res. J.*, **69**, 473-476 (1999)

Tsuji M, Shimizu T and Kohjiya S: TEM Studies on Thin Films of Natural Rubber and Polychloroprene Crystallized under Molecular Orientation, *Polym. J.*, **31**, 784-789 (1999)

Sakai Y, Imai M, Kaji K and Tsuji M: Tip-splitting Crystal Growth Observed in Crystallization from Thin Films of Poly(ethylene terephthalate), *J. Cryst. Growth*, **203**, 244-254 (1999)

Ikeda T, Yamada B, Tsuji M and Sakurai S: In situ Co-polymerization Behaviour of Zinc Dimethacrylate and 2-(N-Ethylperfluoro-octanesulphonamido)ethyl Acrylate in Hydrogenated Nitrile-Butadiene Rubber During Peroxide Crosslinking, *Polym. Int.*, **48**, 446-454 (1999)

Kawahara Y, Kikutani T and Tsuji M: Structural Analysis for Commercial Poly(ethylene terephthalate) Fiber with Longitudinal Thickness Fluctuation, *Sen'i Gakkaishi*, **55**, 336-340 (1999)

Yamaguchi S and Tsuji M: Fine Structure in the Poly(vinylidene fluoride) Thin Film Cast from N,N-Dimethylacetamide Solution, *Sen'i Gakkaishi*, **55**, 552-554 (1999) (in Japanese)

Fujita M, Tsuji M, Ihn K.J and Kohjiya S: Morphology of Polymer Crystals Grown from Solutions Epitaxially on Alkali Halides, *Kobunshi Ronbunshu*, **56**, 786-796 (1999) (in Japanese)

Tosaka M, Tsuji M, Kohjiya S, Cartier L and Lotz B: Crystallization of Syndiotactic Polystyrene in β-form. 4. Crystal Structure of Melt-Grown Modification, *Macromolecules*, **32**, 4905-4911 (1999)

Tosaka M, Yamakawa M, Tsuji M, Kohjiya S, Ogawa T, Isoda S and Kobayashi T: Structural Studies on Polymer Whiskers by Transmission Electron Microscopy. I. Morphological and High-Resolution Observations, *Microsc. Res. Tech.*, **46**, 325-333 (1999)

Tosaka M, Yamakawa M, Tsuji M, Murakami S, Kohjiya S: Structural Studies on Polymer Whiskers by Transmission Electron Microscopy. II. Unit Cell of Poly(*p*-hydroxybezoic acid) Whisker Crystal at Room Temperature, *J. Polym. Sci.: Part B: Polym. Phys.*, **37**, 2456-2462 (1999)

Tosaka M: Studies on Structure Formation of Polymer Crystals by High-resolution Transmission Electron Microscopy, *Sen'i Gakkaishi*, **55**, P-141 (1999) (in Japanese)

Tosaka M: High-resolution Transmission Electron Microscopy of Crystalline Polymers, *Recent Res. Devel. Macromol. Res.*, **4**, 45-56 (1999)

INERFACE SCIENCE

I. Solutions and Interfaces

Yamasaki Y, Enomoto H, Yamasaki N, and Nakahara M: Methanol Formation from Dichloromethane under Hydrothermal Conditions, *Chem. Lett*. **1999**, 83-84 (1999)

Nakahara M: Fundamental Knowledge of Supercritical Water and its Application to Polymer Chemistry, *Cellulose Comm.*, **6**, 60-66 (1999) (in Japanese)

Nakahara M *et al*. : Handbook of Sciences, **73**, National Observatory, Maruzen (1999) (in Japanese)

Nakahara M *et al*. : Handbook of the Properties of Water and Steam, 1-201, Japan Society of Mechanical Engineering, Maruzen (1999) (in Japanese)

Nakahara M and Matubayasi M: Properties and Structure of Supercritical Water, *Denki Kagaku oyobi Kougyou Butsuri Kagaku*, **67**, 988-993 (1999) (in Japanese)

Matsumoto M: Electrocapillarity and Double Layer Structure (Chapter 4), in "Electrical Phenomena at Interfaces," Ohshima H and Furusawa K, Eds., Marcel Dekker, New York, pp. 87-100 (1998)

Matubayasi M and Nakahara M: Reversible molecular dynamics for rigid bodies and hybrid Monte Carlo, *J. Chem. Phys.*, **110**, 3291-3301 (1999)

Matubayasi N, Wakai C, and M. Nakahara M: Structural Study of Supercritical Water. II. Computer simulations, *J. Chem. Phys.*, **110**, 8000-8011 (1999)

Tsujino Y, Wakai C, Matubayasi N, and Nakahara M: Noncatalytic Cannizzaro-type Reaction of Formaldehyde in Hot Water, *Chem. Lett*. **1999**, 287-288 (1999)

Miura Y, Kimura S, Imanishi Y, and Umemura J: Formation of Oriented Helical Peptide Layers on a Gold Surface Due to the Self-Assembling Properties of Peptides, *Langmuir*, **14**, 6935-6940 (1998)

Miura Y, Kimura S, Imanishi Y, and Umemura J: Oriented Helical Peptide Layer on the Carboxylate-Terminated Alkanethiol Immobilized on a Gold Surface, *Langmuir*, **15**, 1155-1160 (1999)

Umemura J, Murata Y, Tsunashima K, and Koizumi N: Polarized Infrared Spectra of Poled Aromatic Polyamide Films, *J. Ploymer Sci. Part B: Polymer Physics*, **37**, 531-538 (1999)

Hasegawa T, Kobayashi Y, Nishijo J, and Umemura J: The Effect of Surface Roughness on Infrared External Reflection Spectroscopy, *Vibr. Spectrosc.*, **19**, 199-203 (1999)

Hasegawa T, Lebranc R M, Nishijo J, and Umemura J: Hydrogen Bonding Network Formed Between Accumulated Langmuir-Blodgett Films of Barbituric Acid and Triminotriazine Derivatives, *J. Phys. Chem. B*, **103**, 7505-7513 (1999)

Okamura E and Nakahara M: NMR Study Directly Determining Drug Delivery Sites in Phospholipid Bilayer Membranes, *J. Phys. Chem. B*, **103**, 3505-3509 (1999)

Wakai C, Matubayasi N, and Nakahara M: Pressure Effect on Rotational Dynamics of Hydrophobic Hydration. Rotational Dynamics of Benzene, *J. Phys. Chem. A*, **103**, 6685-6690 (1999)

Bossev D P, Matsumoto M, and Nakahara M: ^{1}H and ^{19}F NMR Study of the Counterion Effect on the Micellar Structures Formed by Tetraethylammonium and Lithiu Perfluorooctylsulfonates. 1. Neat Systems, *J. Phys. Chem. B*, **103**, 8251-8258 (1999)

Murphy L R, Matubayasi N, Payne V A, and Levy R M: Protein Hydration and Unfolding - Insights from Experimental Partial Specific Volumes and Unfolded Protein Models, *Folding & Design*, **3**, 105-118 (1998)

Bossev D P, Matsumoto M, Sato T, Watanabe H, and Nakahara M: ^{1}H and ^{19}F NMR Study of the Counterion Effect on the Micellar Structures Formed by Tetraethylammonium and Lithiu Perfluorooctylsulfonates. 2. Mixed Systems, *J. Phys. Chem. B*, **103**, 8259-8266 (1999)

Okamura E, Kakitsubo R, and Nakahara M: NMR Determination of the Delivery Site of Bisphenol A in Phospholipid Bilayer Membranes, *Langmuir*, **15**, 8332-8335 (1999)

Okamura E, Fukushima N and Hayashi S: Molecular Dynamics Simulation of the Vibrational Spectra of Stearic Acid Monolayers at the Air/Water Interface, *Langmuir*, **15**, 3589-3594 (1999)

II. Molecular Aggregates

Mitsuya M and Sato N: Energy Shift for Core Electron Levels of Chemisorbed Molecules Observed by X-ray Photoelectron Spectroscopy in the Course of Monolayer Growth on a Si(111) Surface, *Langmuir*, **15**, 2099-2102 (1999)

Shirotani I, Inagaki Y, Sato N and Nishi H: Anomalous Absorption Spectra of Highly Oriented Thin Films of Triphenothiaselenazine, TPTS, *Chem. Phys. Lett*., **304**, 299-302 (1999)

Sato N, Kawamoto I, Sakuma T, Silinsh E A and Jurgis A J: A Molecular Design towards a Highly Amphoteric and Polar Molecule (HAPM) to Assemble Novel Organic Solid-State Structures, *Mol. Cryst. Liq. Cryst*., **333**, 243-258 (1999)

Asami K and Yamaguchi T: Electrical and Morphological Changes of Human Erythrocytes under High Hydrostatic Pressure Followed by Dielectric Spectroscopy, *Ann. Biomed. Eng.*, **27**, 427-435 (1999)

Asami K, Gheorghiu E and Yonezawa T: Real-Time Monitoring of Yeast Cell Division by Dielectric Spectroscopy, *Biophys. J.*, **76**, 3345-3348 (1999)

Higashiyama K, Sugimoto T, Yonezawa T, Fujikawa S, and Asami K: Dielectric Analysis for Estimation of Oil Content in the Mycelia of *Mortierella Alpina*, *Biotechnol. Bioeng.*, **65**, 537-541 (1999)

Asami K: Effect of Cell Shape on Dielectric Behavior of Fission Yeast, Biochim. *Biophys. Acta*, **1472**, 137-141 (1999)

Gheorghiu E, Balut C M, Asami K: Monitoring Cell Cycle Progression by Impedance Spectroscopy, *Med. Biol. Eng. Comput.*, **37**, 146-147 (1999)

III. Separation Chemistry

Yoshida Y, Matsui M, Shirai O, Maeda K and Kihara S: Evaluation of Distribution Ratio in Ion Pair Extraction Using Fundamental Thermodynamic Quantities, *Anal. Chim. Acta*, **373**, 213-225 (1998)

Yoshida Y, Matsui M, Maeda K and Kihara S: Physicochemical Understanding of the Selectivity at an Ion Selective Electrode of the Liquid Membrane Type and Relation between the Selectivity and Distribution Ratios in the Ion-pair Extraction, *Anal. Chim. Acta*, **374**, 269-281 (1998)

Hasegawa H, Matsui M, Okamura S, Hojo M, Iwasaki N and Sohrin Y: Arsenic Speciation Including "Hidden" Arsenic in Natural Water, *Appl. Organometal. Chem.*, **13**, 113-119 (1999)

Sasaki Y: Numeric Study on the Response of a Minimal Chemical Oscillator to an External Perturbation, *Bull. Chem. Soc. Japan*, **72**, 1465-1474 (1999).

Sasaki Y: Numeric Study on the Chaotic Response of Minimal Chemical Oscillator to a Sinusoidal Perturbation, *Bull. Chem. Soc. Japan*, **72**, 2607-2615 (1999).

Yamazaki S, Hanada M, Yanase Y, Fukumori C, Ogura K, Saeki T and Umetani S: A Simple Synthesis of Novel Extraction Reagents. 4-Acyl-5-pyrazolone-substituted Crown Ethers, *J. Chem. Soc., Perkin Trans. 1*, 693-696 (1999)

Tsurubou S, Umetani S and Komatsu Y: Quantitative Extraction Separation Systems of Alkali and Alkaline Earth Metal Ions Using Cryptands as Ion-size Selective Masking Reagents, *Anal. Chim. Acta*, **394**, 317-324 (1999)

Gao X, Cao H, Huang C, Umetani S, Chen G and Jiang P: Photoluminescence and Electroluminescence of a Series of Terbium Complexes, *Synthetic Metals*, **99**, 127-132 (1999)

Hojo M, Ueda T, Nishimura M, Hamada H, Matsui M and Umetani S: Higher Ion Aggregation in Higher Permittivity Solvents, *J. Phys. Chem. B*, **103**, 8965-8972 (1999)

SOLID STATE CHEMISTRY

I. Artificial Lattice Alloys

Ono T, Miyajima H, Shigeto K, Mibu K, Hosoito N and Shinjo T: Propagation of the Magnetic Domain Wall in Submicron Magnetic Wire Investigated by Using Giant Magnetoresistance Effect, *J. Appl. Phys.*, **85**, 6181-6183 (1999)

Shigeto K, Ono T, Miyajima H and Shinjo T: GMR Effect in a Single Trilayer Wire with Submicron Width, *J. Magn. Magn. Mater*. **198-199**, 58-60 (1999)

Ono T, Miyajima H, Shigeto K and Shinjo T: Dot-Arrays of Co/Pt Multilayers with Perpendicular Magnetic Anisotropy, *J. Magn. Magn. Mater*. **198-199**, 225-227 (1999)

Hamada S, Hosoito N, Ono T and Shinjo T: Spin Reorientation of the Micromagnetic Structure in Co/Au Multilayer Films with Moderate Perpendicular Anisotropy, *J. Magn. Magn. Mater.*, **198-199**, 496-499 (1999)

Sakurai J, Kuwai T, Miyake K, Ono T and Shinjo T: A Highly Sensitive Observation of Magneto-thermal Heat Production in Magnetization Process of Wires of Thin Magnetic Mono-layer, *J. Magn. Magn. Mater*, **198-199**, 578-580 (1999)

Mibu K, Tanaka S, Kobayashi T, Nakanishi A, Shinjo T: Magnetic Properties of Thin Cr Layers in Multilayer Systems Studied through ^{119}Sn Mössbauer Probes, *J. Magn. Magn. Mater.*, **198-199**, 689-691 (1999)

Shinjo T and Keune W: Mössbauer-effect Studies of Multilayers and Interfaces, *J. Magn. Magn. Mater.*, **200**, 598-615 (1999)

Hamada S, Hosoito N and Shinjo T: Use of the Mössbauer Effect to Probe Micromagnetic Structures in Co/Au Multilayers with ^{57}Fe, *J. Phys. Soc. Jpn.*, **68**, 1345-1352 (1999)

Hashizume H, Hosoito N and Ishimatsu N, Structure Study of Magnetic Multilayers by Resonant X-ray Magnetic Scattering, *Nippon Kesshou Gakkaishi*, **41**, 298-303 (1999) (in Japanese)

Kaneko K, Ono T, Miyajima H, Mibu K, Hosoito N and Shinjo T: Magnetism of Fe/Cr Multilayers Considered as Finite-Size Ferrimagnets, *Nippon Ouyou Jiki Gakkaishi*, **23**, 1353-1356 (1999) (in Japanese)

Ishimatsu N, Hashizume H, Hamada S, Hosoito N, Nelson C S, Venkataraman C T, Srajer G and Lang J C: Magnetic Structure of Fe/Gd Multilayers Determined by Resonant X-ray Magnetic Scattering, *Phys. Rev. B*, **60**, 9596-9606 (1999)

Ono T, Miyajima H, Shigeto K, Mibu K, Hosoito N and Shinjo T: Propagation of a Magnetic Domain Wall in a Submicrometer Magnetic Wire, *Science*, **284**, 468-470 (1999)

Shinjo T: Magnetic Properties of Multilayers and Interfaces by Mössbauer Spectroscopy, *Surf. Sci.*, **438**, 329-335 (1999)

Ono T and Shinjo T: Anisotropic Structure and Giant Magnetoresistance in Fe/Cr Multilayers on $SrTiO_3$(100) Substrates with Step Terraces, *Surf. Sci.*, **438**, 341-346 (1999)

II. Quantum Spin Fluids

Kimura H, Hirota K, Matsushita H, Yamada K, Endoh Y, Lee S-H, Majkrzak C F, Erwin R, Shirane G, Greven M, Lee Y S, Kastner M A and Birgeneau R J: Neutron-Scattering Study of Static Antiferromagnetic Correlations in $La_{2-x}Sr_xCu_{1-y}Zn_yO_4$, *Phys. Rev. B*, **59**, 6517-6523 (1999)

Birgeneau R J, Greven M, Kastner M A, Lee Y S, Wells B O, Endoh Y, Yamada K and Shirane G: Instantaneous Spin Correlations in La_2CuO_4, *Phys. Rev. B*, **59**, 13788-13794 (1999)

Wakimoto S, Shirane G, Endoh Y, Hirota K, Ueki S, Yamada, Birgeneau R J, Kastner M A, Lee Y S, Gehring P M and Lee S H: Observation of Incommensurate Magnetic Correlations at the Lower Critical Concentration for Superconductivity in $La_{2-x}Sr_xCuO_4$ (x=0.05), *Phys. Rev. B*, **60**, R769-772 (1999)

Kim Y J, Birgeneau R J, Kastner M A, Lee Y S, Endoh Y, Shirane G and Yamada K: Quantum Monte Carlo Study of Weakly Coupled Spin Ladders, *Phys. Rev. B*, **60**, 3294-3304 (1999)

Lee Y S, Birgeneau R J, Kastner M A, Endoh Y, Wakimoto S, Yamada K, Erwin R W, Lee S-H and Shirane G: Neutron-scattering Study of Spin-density Wave Order in the Superconducting State of Excess-oxygen-doped La_2CuO_{4+y}, *Phys. Rev. B*, **60**, 3643-3654 (1999)

Lee S-H, Majkrzak C F, Sinha S K, Stassis C, Kawano H, Lander G H, Brown P J, Fong H F, Cheong S-W, Matsushita H, Yamada K and Endoh Y: Search for Orbital Moments in Underdoped Cuprate Metals, *Phys. Rev. B*, **60**, 10405-10417 (1999)

Suzuki T, Oshima Y, Chiba K, Fukase T, Goto T, Kimiura H and Yamada K: Conventional Superconductorlike Behavior of the Superconducting Transition of $La_{2-x}Sr_xCuO_4$ (x~0.12) in Magnetic Fields, *Phys. Rev. B*, **60**, 10500-10503 (1999)

Kaneko N, Hidaka Y, Hosoya S, Yamada K, Endoh Y, Takekawa S and Kitamura K: Optimum Crucible Material for Growth of $Pr_{2-x}Ce_xCuO_4$ Crystal, *J. Cryst. Growth*, **197**, 818-824 (1999)

Sato T,. Yokoya T, Naitoh Y, Takahashi T, Yamada K and Endoh Y: Pseudogap of Optimally Doped $La_{1.85}Sr_{0.15}CuO_4$ Observed by Ultrahigh-Resolution Photoemission Spectroscopy, *Phys. Rev. Lett.*, **83**, 2254-2257 (1999)

Yamada K, Birgeneau R J, Endoh Y, Fukase T, Greven M, Fujita M, Hirota K, Hosoya S, Kastner M A, Kim Y M, Kimura H, Kurahashi K, Lee C H, Lee S H, Lee Y S, Matsushita H, Shirane G, Suzuki T, Ueki S and Wakimoto S: Static and Dynamical Incommensurate Spin Correlations in High-T_c Cuprates of $La_{2-x}Sr_xCuO_{4+y}$, *Physics and Chemistry of Transition-Metal Oxides (Springer-Verlag, Edits Fukuyama H and Nagaosa N)*, 182-191 (1999)

Yamada K, Kurahashi K, Endoh Y, Birgeneau R J and Shirane G: Neutron Scattering Study on Electron-hole Doping Symmetry of High-T_c Superconductivity, *J. Phys. & Chem. Solids*, **60**, 1025-1030 (1999)

Kimura H, Matsushita H, Hirota K, Endoh Y, Yamada K, Shirane G, Lee Y S, Kastner M A and Birgeneau R J: Neutron Scattering Study of Incommensurate Elastic Magnetic Peaks in $La_{1.88}Sr_{0.12}CuO_4$, *J. Phys. & Chem. Solids*, **60**, 1067-1070 (1999)

Matsushita H, Kimura H, Fujita M, Yamada K, Hirota K and Endoh Y: Sr Concentration Dependence of Incommensurate Elastic Magnetic Peaks in $La_{2-x}Sr_xCuO_4$, *J. Phys. & Chem. Solids*, **60**, 1071-1074 (1999)

Wakimoto S, Yamada K, Ueki S, Shirane G, Lee Y S, Lee S H, Kastner M A, Hirota K, Gehring P M, Endoh Y and Birgeneau R J: Neutron Scattering Study of Elastic Magnetic Signals in Superconducting $La_{1.94}Sr_{0.06}CuO_4$, *J. Phys. & Chem. Solids*, **60**, 1079-1081 (1999)

Kusano Y, Kikuchi T, Takada J, Fukuhara M, Ikeda Y and Hiroi Z: Phase Diagram of the Bao($BaCO_3$)-CaO-CuO System, *J. Am. Ceram. Soc.*, **82**, 1329-1332 (1999)

Nakanishi M, Yokoyama K, Kikuchi T, Fujiwara M, Fujii T, Takada J, Kusano Y, Ikeda Y and Takeda Y: Electrochemical Li Intercalation into the Li-Doped Bi-2212 Phase Prepared by Solid State Reaciton, *Funtai oyobi Funmatsu Yakin*, **46**, 990-993 (1999) (in Japanese)

Niinae T, Ikeda Y, Bando Y, Takano M, Kusano Y and Takada J: Synthesis, Thermal Stability, Structural Features, and Electromagnetic Properties of $Bi_{2+x}Sr_{2-x}CuO_{6+}$ (o *x* 0.4), *Physica C*, **313**, 29-36 (1999)

Kusano Y, Kikuchi T, Takada J, Fukuhara M, Ikeda Y and Takano M: Phase Diagram of BaO($BaCO_3$)-CaO-CuO System, *9th Cimtec-World Forum on New Materials, Symposium VI - Science*

and Engineering of HTC Superconductivity, Advances in Science and Technology (ed. Vincenzini P), Techna, **23**, 241-244 (1999)

Ikeda Y, Niinae T, Takeda Y, Kusano Y and Takada J: Reversible Crystal Transformation between Sheared Bi-2201 Phase and Layered Bi-2201 Phase, *9th Cimtec-World Forum on New Materials, Symposium VI - Science and Engineering of HTC Superconductivity, Advances in Science and Technology (ed. Vincenzini P), Techna*, **23**, 261-266 (1999)

Fujiwara M, Nakanishi M, Uwazumi Y, Fujii T, Takada J, Kusano Y, Takeda Y and Ikeda Y: Li Intercalation into Bi-2212 Phase by Electrochemical Method, *9th Cimtec-World Forum on New Materials, Symposium VI - Science and Engineering of HTC Superconductivity, Advances in Science and Technology (ed. Vincenzini P), Techna*, **23**, 301-304 (1999)

Kusano Y, Takada J, Fukuhara M, Ikeda Y and Takano M: Morphological Changes of Bi-Based Superconductors by Small Mechanical Force, *9th Cimtec-World Forum on New Materials, Symposium VI - Science and Engineering of HTC Superconductivity, Advances in Science and Technology (ed. Vincenzini P), Techna*, **23**, 329-332 (1999)

Nojiri H, Takahashi K, Fukuda T, Fujita M, Arai, M and Motokawa M: 25 T Repeating Pulsed Magnetic Fields System for Neutron Diffraction Experiments, *Physica B*, **241-243**, 210-212 (1998)

Fujita M, Frost C D, Arai M, Motokawa M, Fujita O, Akimitsu J and Bennington S M: Spin Dyanmics of the Spin-Peierls System $CuGeO_3$ at Various Temperatures, *Physica B*, **241-243**, 528-530 (1998)

Welz D, Nishi M, Fujita M, Kakurai K, Arai M, Akimitsu J and Fujii Y: Magnetic Excitations of Dimerized $CuGeO_3$: Continuum Scattering and Interchain Modulation, *Physica B*, **241-243**, 540-542 (1998)

III. Multicomponent Materials

Yamada T, Hiroi Z, Takano M, Nohara M and Takagi H: Synthesis and Magnetic Property of Cu_2GeO_4 Containing Edge-Sharing CuO_2 Chains, *Funtai oyobi Funmatsu Yakin*, **45**, 1136-1141 (1998) (in Japanese)

Suzuki C, Kawai J, Tanizawa J, Adachi H, Kawasaki S, Takano M and Mukoyama T: Local Spin Moment of $LaCoO_3$ Probed by a Core Hole, *Chemical Physics*, **241**, 17-27 (1999)

Terashima T and Bando Y: Growth of Films by MBE I- YBCO, *Kooncyodendotai to Ekizotikku Chodendotai, Kyoritsu Syuppan*, **3**, 174-181 (1999) (in Japanese)

Ohsugi S, Kitaoka Y, Tokunaga Y, Ishida K, Azuma M, Fujishiro Y and Takano M: Impurity Effect of the Spin-Ladder System $SrCu_2O_3$, *Physica B*, **259-261**, 1040-1041 (1999)

Niinae T, Ikeda Y, Bando Y, Takano M, Kusano Y and Takada J: Synthesis, Thermal Stability, Structural Features, and Electromagnetic Properties of $Bi_{2+x}Sr_{2-x}CuO_{6+\delta}$ ($0 \leqq x \leqq 0.4$), *Physica C*, **313**, 29-36 (1999)

Shirakami T, Takematsu M, Hirano A, Kanno R, Yamaura K, Takano M and Atake T: Spin Glass-Like Magnetic Properties of $LiNiO_2$, *Materials Science and Engineering B*, **54**, 70-72 (1998)

Takeda T, Nagata M, Kobayashi H, Kanno R, Kawamoto Y, Takano M, Kamiyama T, Izumi F and Sleight A W: High-Pressure Synthesis, Crystal Structure, and Metal-Semiconductor Transitions in the $Tl_2Ru_2O_{7-\delta}$ Pyrochlore, *J. Solid State Chem.*, **140**, 182-193 (1998)

Takeda T, Kanno R, Kawamoto Y, Takano M, Izumi F, Sleight A W and Hewat A W: Structure-Property Relationships in Pyrochlores: Low-Temperature Structures of $Tl_2Ru_2O_{7-\delta}$ (δ=0.00 and 0.05), *J. Mater. Chem.*, **9**, 215-222 (1999)

Takano M, Hiroi Z, Azuma M, Kawasaki S, Kanno R and Takeda T: Novel Transition Metal Oxides Prepared at High Pressure and Their Electronic Properties, *Physics and Chemistry of Transiton-Metal Oxides, Solid-State Sciences (ed. Fukuyama H and Nagaosa N), Springer-Verlag, Germany*, **125**, 279-288 (1999)

Koide T, Shidara T, Miyauchi H, Nakajima N, Fukutani H, Fujimori A, Kawasaki S, Takano M and Takeda Y: Soft X-Ray Magnetic Circular Dichroism in $La_{1-x}Sr_xMnO_3$ and $SrFe_{1-x}Co_xO_3$, *J. Magn. Soc. Japan*, **23**, 341-345 (1999)

Takano M: Superconductors Prepared under High Pressure, *Science of High Temperature Superconductivity (ed. Tachiki M and Fujita T), Shokabo*, 395-401 (1999) (in Japanese)

Terashima: T: Growth and Characterization of Thin Films, *Science of High Temperature Superconductivity (ed. Tachiki M and Fujita T), Shokabo*, 407-415 (1999) (in Japanese)

Hiroi Z and Takano M: $La_{1-x}Sr_xCuO_{2.5}$ Representing a Hole-Doped Spin Ladder System, *Physica B*, **259-261**, 1034-1035 (1999)

Kusano Y, Kikuchi T, Takada J, Fukuhara M, Ikeda Y and Takano M: Phase Diagram of $BaO(BaCO_3)$-CaO-CuO System, *9th Cimtec-World Forum on New Materials, Symposium VI - Science and Engineering of HTC Superconductivity, Advances in Science and Technology (ed. Vincenzini P), Techna*, **23**, 241-244 (1999)

Kusano Y, Takada J, Fukuhara M, Ikeda Y and Takano M: Morphological Changes of Bi-Based Superconductors by Small Mechanical Force, *9th Cimtec-World Forum on New Materials, Symposium VI - Science and Engineering of HTC Superconductivity, Advances in Science and Technology (ed. Vincenzini P), Techna*, **23**, 329-332 (1999)

Nishiyama M, Ogawa K, Chong I, Hiroi Z and Takano M: Scanning Tunneling Microscope Studies on the Atomic Structures in $Bi_2Sr_2CaCu_2O_{8+\delta}$ Highly Doped with Pb, *Physica C*, **314**, 299-307 (1999)

Takano M, Kanno R and Takeda T: A Chemical Contribution to the Search for Novel Electronic Properties in Transition Metal Oxides: $LiNiO_2$, *Mater. Sci. & Eng. B*, **63**, 6-10 (1999)

Kawasaki S, Takano M and Inami T: Synthesis, Structure, and Magnetic Properties of Ca_3BMnO_6 (B=Ni, Zn) and Ca_3ZnCoO_6 Crystallizing in the K_4CdCl_6 Structure, *J. Solid State Chem.*, **145**, 302-308 (1999)

Griend D A V, Boudin S, Caignaert V, Poeppelmeier K R, Wang Y, Dravid V P, Azuma M, Takano M, Hu Z and Jorgensen J D: $La_4Cu_3MoO_{12}$: A Novel Cuprate with Unusual Magnetism, *J. Am. Chem. Soc.*, **121**, 4787-4792 (1999)

Okamoto J, Mizokawa T, Fujimori A, Hase I, Nohara M, Takagi H, Takeda Y and Takano M: Correlation Effects in the Electronic Strucuture of $SrRuO_3$, *Phys. Rev. B*, **60**, 2281-2285 (1999)

Ishida T, Inoue K, Okuda K, Hiroi Z, Izumi M, Chong I and Takano M: Anisotropy of $Bi_{1.5}Pb_{0.7}Sr_{1.8}CaCu_2O_{8+\delta}$ Single Crystal, *Advances in Superconductivity XI: Proceedings of the 11th International Symposium on Superconductivity (ISS'98), Nov.*

16-19, 1998, Fukuoka (ed. Koshizuka N and Tajima S), Springer-Verlag Tokyo, 407-410 (1999)

Matsuno J, Mizokawa T, Fujimori A, Mamiya K, Takeda Y, Kawasaki S and Takano M: Photoemission and Hartree-Fock Studies of Oxygen-Hole Ordering in Charge-Disproportionated $La_{1-x}Sr_xFeO_3$, *Phys. Rev. B*, **60**, 4605-4608 (1999)

Kitaoka Y, Ishida K, Mukuda H, Mao Z Q, Ikeda S, Nishizaki S, Maeno Y, Kanno R and Takano M: NMR Prove of Magnetism and Superconductivity in Ruthenate Oxides, *Mater. Sci. & Eng. B*, **63**, 83-87 (1999)

Ohsugi S, Tokunaga Y, Ishida K, Kitaoka Y, Azuma M, Fujishiro Y and Takano M: Impurity-Induced Staggered Polarization and Antiferromagnetic Order in Spin-1/2 Heisenberg Two-Leg Ladder Compound $SrCu_2O_3$: Extensive Cu NMR and NQR Studies, *Phys. Rev. B*, **60**, 4181-4190 (1999)

Hiroi Z, Azuma M, Fujishiro Y, Saito T, Takano M, Izumi F, Kamiyama T and Ikeda T: Structural Study of the Quantum-Spin Chain Compound $(VO)_2P_2O_7$, *J. Solid State Chem.*, **146**, 369-379 (1999)

Saito T, Azuma M, Takano M, Hiroi Z, Narumi Y, Kindo K and Utsumi W: Magnetic Properties and Single Crystal Growth of a Spin Gapped Compound, High Pressure Phase of $(VO)_2P_2O_7$, *Funtai oyobi Funmatsu Yakin*, **46**, 1014-1019 (1999) (in Japanese)

Azuma M, Saito T, Fujishiro Y, Hiroi Z, Takano M, Izumi F, Kamiyama T, Ikeda T, Narumi Y and Kindo K: High-Pressure Form of $(VO)_2P_2O_7$: A Spin-1/2 Antiferromagnetic Alternating-Chain Compound with One Kind of Chain and a Single Spin Gap, *Phys. Rev. B*, **60**, 10145-10149 (1999)

Mukuda H, Ishida K, Kitaoka Y, Asayama K, Kanno R and Takano M: Spin Fluctuations in the Ruthenium Oxides RuO_2, $SrRuO_3$, $CaRuO_3$, and Sr_2RuO_4 Probed by Ru NMR, *Phys. Rev. B*, **60**, 12279-12285 (1999)

IV. Amorphous Materials

Sakida S, Hayakawa S and Yoko T: Part 1. ^{125}Te NMR Study of Tellurite Crystals, *J. Non-Cryst. Solids*, **243**, 1-12 (1999)

Sakida S, Hayakawa S and Yoko T: Part 2. ^{125}Te NMR Study of M_2O-TeO_2 (M=Li, Na, K, Rb and Cs) glasses, *J. Non-Cryst. Solids*, **243**, 13-25 (1999)

Sakida S, Hayakawa S and Yoko T: ^{125}Te NMR Study of MO-TeO_2 (M=Mg, Zn, Ba and Pb) glasses, *J. Ceram. Soc. Jap.*, **107**, 395-402 (1999)

Zhao G, Kozuka H, Kin H and Yoko T: Sol-Gel Preparation of $Ti_{1-x}V_xO_2$ Solid Solution Film Electrodes with Conspicuous Photoresponse in Visible Region, *Thin Solid Films*, **339**, 123-128 (1999)

Zhao G, Kozuka H, Lin H, Takahashi M and Yoko T: Preparation and Photo-Electrochemical Properties of $Ti_{1-x}V_xO_2$ Solid Solution Thin Film Photoelectrodes with Gradient Bandgap, *Thin Solid Films*, **340**, 125-131 (1999)

Uchino T and Yoko T: Sodium and Lithium Environments in Single- and Mixed-Alkali Silicate Glasses. An ab Initio Molecular Orbital Study, *J. Phys. Chem. B*, **103**, 1854-1858 (1999)

Uchino T and Yoko T: Structure and Low-Frequency Vibrational Properties of $(H_2O)_{10}$ Composed of a Ring Form of $(H_2O)_4$ and a Cage Form of $(H_2O)_6$, *Phys. Chem. Chem. Phys.*, **1**, 3473-3479 (1999)

Uchino T: Effect of Order on the Structure and Vibrational Properties of Glasses, *Chemistry and Chemical Industry*, **2**, 128-132 (1999) (in Japanese)

Takahashi M and Yoko T: Optical Nonlinearity in Homogenous Glasses, *New Glass*, **14**, 29 (1999) (in Japanese)

Takahashi M, Shigemura H, Kawamoto Y, Nishii J and Yoko T: Photochemical Reactions of Ge-related Defects in $10GeO_2$×$90SiO_2$ Glass Prepared by Sol-Gel Process, *J. Non-Cryst. Solids*, **259**, 149-155 (1999)

Takahashi M, Izuki M, Shojiya M, Qiu J, Kawamoto Y, and Kadono K: Preparation and Upconversion Properties of Er^{3+}-Doped Lead Fluorosilicate Glass-Ceramics, *J. Ceram. Soc. Japan*, **107**, 1175-1179 (1999) (in Japanese)

Kadono K, Shojiya M, Takahashi M, Higuchi H and Kawamoto Y: Radiative and Non-Radiative Relaxation of Rare-Earth Ions in Ga_2S_3×GeS_2×La_2S_3 Glasses, *J. Non-Cryst. Solids*, **259**, 39-44 (1999)

Higuchi H, Kanno R, Kawamoto Y, Takahashi M and Kadono K: EXAFS Study of the Er^{3+}- Containing Ga_2S_3-GeS_2-La_2S_3 Glass, *Phys. Chem. Glasses*, **40**, 122-125 (1999)

Shojiya M, Kadono K, Takahashi M, Kanno R and Kawamoto Y: Optical Transition Properties of Rare-Earth Ions in Nonfluoride-Halide Glasses, *Proc. SPIE - Int. Soc. Opt. Eng.*, **3280**, 23-30 (1999)

Fujiwara T, Takahashi M, Ohama M, Ikushima A J, Furukawa Y and Kitamura K: Comparison of Electro-Optic Effect between Stoichiometric and Congruent $LiNbO_3$, *Electron. Lett.*, **35**, 499-501 (1999)

Shigemura H, Kawamoto Y, Nishii J and Takahashi M: UV-Photosensitive Effect of Sol-Gel Derived GeO_2-SiO_2 Glasses, *J. Appl. Phys.*, **85**, 3413-3418 (1999)

Kawamoto Y, Ogura K, Shojiya M, Takahashi M and Kadono K: F1s XPS of Fluoride Glasses and Related Fluoride Crystals, *J. Fluorine Chem.*, **96**, 135-139, (1999)

Higuchi H, Kanno R, Kawamoto Y, Takahashi M and Kadono K: Physicochemical Properties and Structure of Ga_2S_3-GeS_2-La_2S_3-La_2S_3 Glasses (Ln=yttrium or lanthanoids), *Phys. Chem. Glasses*, **40**, 49-53 (1999)

FUNDAMENTAL MATERIAL PROPERTIES

I. Molecular Rheology

Inoue T, Onogi T and Osaki K: Viscoelasticity of Low Molecular Weight Polystyrene. Separation of Rubbery and Glassy Components., *J Polym Sci Polym Phys Ed*, **37**, 389-97 (1999)

Inoue T, Ryu D S, Osaki K and Takebe T: Viscoelasticity and birefringence of Syndiotactic polystyrene I. Dynamic measurement in supercooled state, *J Polym Sci Part B Polym Phys*, **37**, 399-404 (1999)

Inoue T and Osaki K: Comment on “Birefringence in the softening zone”, *Macromolecules*, **32**, 4725-7 (1999)

Inoue T: Birefringence of Polymers. *kobunshi*, **48**, 280-1 (1999)

Osaki K and Inoue T: A heuristic study on normal stress difference in oscillatory shear for permanent and temporary networks of polymer chains, *Nihon Reoroji Gakkaishi*, **27**, 117-9 (1999)

Watanabe H, Sato T, Hirose M, Osaki K, and Yao ML: Rheo-Dielectric Behavior of Low Molecular Weight Liquid Crystals. 1. Behavior of Nematic 5CB and 7CB, *Rheol. Acta*, **37**, 519-27 (1998)

Watanabe H: Nonlinear Rheology of Diblock Copolymer Micellar Dispersion. A Review of Recent Findings, *J. Non-Newtonian Fluid Mech.*, **82**, 315-29 (1999)

Watanabe H, Yao ML, Osaki K, Shikata T, Niwa H, and Morishima Y: Nonlinear Rheology of Concentrated Spherical Silica Suspensions. 3. Concentration Dependence, *Rheol. Acta*, **38**, 2-13 (1999)

Watanabe H, Sato T, Hirose M, Osaki K, and Yao ML: Rheo-Dielectric Behavior of Low Molecular Weight Liquid Crystal. 2. Behavior of 8CB in Nematic and Smectic States, *Rheol. Acta*, **38**, 100-07 (1999)

Kanaya T, Watanabe H, Matsushita Y, Takeda T, Seto H, Nagao M, Fujii Y, and Kaji K: Neutron Spin Echo Studies on Dynamics of Polymeric Micelles, *J. Phys. Chem. Solids*, **60**, 1367-69 (1999)

Cho YK, Watanabe H, and Granick S: Dielectric Response of Polymer Films Confined Between Mica Surfaces, *J. Chem. Phys.*, **110**, 9688-96 (1999)

Newstein MC, Wang H, Balsara NP, Lefebvre AA, Shnidman Y, Watanabe H, Osaki K, Shikata T, Niwa H, and Morishima Y: Microstructural Changes in a Colloidal Liquid in the Shear Thinning and Shear Tickening Regimes, *J. Chem. Phys.*, **111**, 4827-38 (1999)

Osaki K, Watanabe H, Inoue T: Stress Overshoot in Shear Flow of an Entangled Polymer with Bimodal Molecular Weight Distribution, *J. Soc. Rheol. Jpn*, **27**, 63-4 (1999)

Watanabe H, Sato T, Matsumiya Y, Inoue T, and Osaki K: Rheo-Dielectrics. Its Applicability, *J. Soc. Rheol. Jpn*, **27**, 121-25 (1999)

Matsumiya Y, Watanabe H, Sato T, and Osaki K: Synthesis and Linear Viscoelasticity of Model Comb Polymers, *J. Soc. Rheol. Jpn*, **27**, 127-28 (1999)

Watanabe H, Sato T, Osaki K, Matsumiya Y, and Anastasiadis SH: Effects of Spatial Confinement on Dielectric Relaxation of Block Copolymers Having Tail, Loop, and Bridge Conformations, *J. Soc. Rheol. Jpn*, **27**, 173-82 (1999)

Bossev DP, Matsumoto M, Sato T, Watanabe H, and Nakahara M: ^{1}H and ^{19}F NMR study of the Counterion Effect on the Micellar Structures Formed by Tetraethylammonium and Lithium Perfluorooctylsulfonates. 2. Mixed Systems, *J. Phys. Chem. B*, **103**, 8259-66 (1999)

Okamoto K, Takahashi M, Yamane H, Kashihara H, Watanabe H, and Masuda T: Shape Recovery of a Dispersed Droplet Phase and Stress Relaxation after Application of Step Shear Strains in a Polystyrene/Polycarbonate Blend Melt, *J. Rheol.*, **43**, 951-65 (1999)

II. Polymer Materials Science

Matsuba G, Kaji K, Nishida K, Kanaya T and Imai M: Conformational Change and Orientation Fluctuations Prior to Crystallization of Syndiotactic Polystyrene, *Macromolecules*, **32**, 8932-8937 (1999)

Matsuba G, Kaji K, Nishida K, Kanaya T and Imai M: Conformational Change and Orientational Fluctuations of Isotactic Polystyrene Prior to Crystallization, *Polym. J.*, **31**, 722-727 (1999)

Kaji K, Matsuba G, Nishida K, Kanaya T and Imai M: Structural Formation of sydiotactic Polystyrene during the Induction Period before Crystallization, *Kasen-Kouenshu*, **56**, 67-70 (1999) (in Japanese)

Nishida K, Kaji K, Kiriyama K and Kanaya T: Upper Concentration Limit of the Semidilute Region in Polyelectrolyte Solutions, Proceedings of Yamada Conference L, Polyelectrolytes, ed. Noda I and Kokufuda E, Yamada Science Foundation, 137-140 (1999)

Takeshita H, Kanaya T, Nishida K and Kaji K: Gelation Process and Phase Separation of PVA Solutions As Studied by a Light Scattering Technique, *Macromolecules*, **32**, 7815-7819 (1999)

Kanaya T, Kawaguchi T and Kaji K: Local Dynamics of Some Bulk Polymers above Tg As seen by Quasielastic Neutron Scattering, *Macromolecules*, **32**, 1672-1678 (1999)

Kanaya T, Hansen J, Tsukushi I, Nishida K, Kaji K, Yamamuro O, Tanaka K and Yamaguchi A: Fast Process in Glass-forming Polymers and Its Relation to Mechanical Properties, *J. Phys. Chem. Solids*, **60**, 1321-1323 (1999)

Kanaya T, Tsukushi I, Kaji K, Bartos J and Kristiak J: Microscopic basis of free volume concept as studied by quasielastic neutron scattering (QENS) and positron annihilation lifetime spectroscopy (PALS), *Phys. Rev.*, **E60**, 1906-1912 (1999)

Kanaya T, Watanabe H, Matsushita Y, Takeda T, Seto H, Nagao M, Fujii Y and Kaji K: Neutron Spin Echo Studies on Dynamics of Polymeric Micelles, *J. Phys. Chem. Solids*, **60**, 1367-1369 (1999)

Kanaya T, Tetaguchi M, Masuda T and Kaji K: Local Mobility of Substituted Polyacetylenes Measured by Quasielastic Neutron Scattering and its Relationship with Gas Permeability, *Polymer*, **40**, 7157-7161 (1999)

Tsukushi I, Yamamuro O, Yamamoto K, Takeda K, Kanaya T and Matsuo T: Neutron Scattering Study of Glassy Toluene: Dynamics of a Quasi-regid Molecular Glass, *J. Phys. Chem. Solids*, **60**, 1541-1543 (1999)

Tsukushi I, Kanaya T and Kaji K: Dynamical Heterogeneity of Glass-forming Polymers: Non-Gaussina Behavior. A Study on Distribution of Mean Square Displacement, Proceedings of The 8th Tohwa University International Symposium on Slow Dynamics in Complex Systems, ed. Tokuyama M., *AIP Conference Series*, **469**, 350-357 (1999)

Tsukushi I, Kanaya T, Yamamuro O, Matsuo T and Kaji K: Neutron Scattering Study of Amorphous Tri-O-methyl-b-cyclodextrin, *J. Phys. Chem. Solids*, **60**, (1999)

Tsukushi I and Kanaya T: Neutron Scattering Study of Dynamics in Glassy State, *High Pressure Science and Technology*, **9**, 126-133 (1999) (in Japanese)

Yamamuro O, Tsukushi I, Kanaya T and Matsuo T: Neutron Scattering Study of Boson Peak in Glassy 3-Methylpentane, *J.*

Phys. Chem. Solids, **60**, 1537-1539 (1999)

Nemoto N, K. Nakamura and Kanaya T: Structure and Dynamics of Ovalbumin Gels, Proceedings of Yamada Conference L, Polyelectrolytes, ed. Noda I. and Kokufuda E., Yamada Science Foundation, 319-322 (1999)

Kataoka M, Kamikubo H, Yunoki J, Tokunaga F, Kanaya T, Izumi Y, Shibata K: Low Energy Dynamics of Globular Proteins Studied by Inelastic Scattering, *J. Phys. Chem. Solids*, **60**, 1285-1289 (1999)

Ebisawa T, Yamazaki D, Tasaki S, Hino M, Kawai T, Iwata Y, Achiwa N, Kanaya T and Soyama K: A Modified Neutron Spin Echo Method Using Novel Spin Precession by Multilayer Spin Splitters Arranged in + + Configuration, *Phys. Lett.*, **A259**, 20-24 (1999)

Ebisawa T, Tasaki S, Hino M, Kawai T, Iwata Y, Yamazaki D, Achiwa N, Otake Y, Kanaya T and Soyama K: Cold Neutron Spin Interferometry and its Application to Modified Spin Echo Methods, *J. Phys. Chem. Solids*, **60**, 1569-1572 (1999)

III. Molecular Motion Analysis

Schacht J, Buivydas M, Gouda F, Komitov L, Stebler B, Lagerwall S T, Zugenmaier P and Horii F: Broad Band Dielectric Relaxation Spectroscopy of Molecular Reorientation in Smectic Liquid Crystalline Phases (SmA, SmB, and CrE), *Liquid Crystals*, **26**, No.6, 835-847 (1999)

Imai T, Sugiyama J, Itoh T and Horii F: Almost Pure I_α Cellulose in the Cell Wall of *Glaucocystis*, *J. Struct. Biol.*, **127**, 248-257 (1999)

lshida M, Oshima J, Yoshinaga K and Horii F: Structural Analysis of Core-Shell Type Polymer Particles Composed of Poly(butyl acrylate) and Poly(methyl methacrylate) by High-Resolution Solid-State ^{13}C NMR Spectroscopy, *Polymer*, **40**, 3323-3329 (1999)

Kuwabara K and Horii F: Solid-State ^{13}C NMR Analyses of the Orthorhombic-to-Hexagonal Phase Transition for Constrained Ultradrawn Polyethylene Fibers, *Macromolecules*, **32**, No.17, 5600-5605(1999)

Tsunashima Y, Kawanishi H, Nomura R and Horii F: Influence of Long-Range Interactions on Diffusion Behavior in Semidilute Solution: Dynamics of Cellulose Diacetate in Quiescent State, *Macromolecules*, **32**, No.16, 5330-5336 (1999)

Tsunashima Y and Kawanishi H: Shear Induced Fluctuations and Fluctuation-Length Transition in the Quasiflexible Polymer in a Solution of a Hydrogen-Bond Enhancing Solvent, *J. Chem. Phys.*, **111**, No.7, 3294-3301 (1999)

Tsunashima Y, Polymer Chain Dynamics in Dilute Solution under Couette Flow: Behavior of poly(a-methylstyrene) in Good Solvent, *J. Chem. Phys.*, **110**, No.24, 12211-12217 (1999)

Masuda K, Kaji H and Horii F: ^1H CRAMPS Measurements of Different Types of OH Groups in Poly(vinyl alcohol) Films, *Polymer J.*, **31**, No.1, 105-107 (1999)

Ishida H and Horii F: Solid-State ^{13}C NMR Analyses of the Structure and Chain Conformation of Thermotropic Liquid Crystalline Polyether Crystallized from the Melt through the Liquid Crystalline State, *Polymer*, **40**, No.13, 3781-3786 (1999)

Schacht J, Buivydas M, Gouda F, Komitov L, Stebler B, Lagerwall S T, Horii F and Zugenmaier P: Slow Molecular Reorientation in Higher-Ordered Liquid Crystalline Phases of a Homologous Series of Stilbenes, Slow Dynamics in Complex Systems: Eighth Tohwa University International Symposium, Tokuyama M and Oppenheim I, Eds., Am. Inst. Phys., 1999, pp. 128-133.

ORGANIC MATERIALS CHEMISTRY

I. Polymeric Materials

Takaragi A, Minoda M, Miyamoto T, Liu H-Q and Zhang L-N: Reaction Characteristics of Cellulose in the LiCl/1,3-Dimethyl-2-Imidazolidinone Solvent System, *Cellulose*, **6**, 93-102 (1999)

Minoda M, Zhou Q and Miyamoto T: Development of Cellulose-Based Functional Materials: *Kobunshi-Kako*, **48**, 355-360 (1999) (in Japanese)

Goto A and Fukuda T: Kinetic Study on Nitroxide-Mediated Free Radical Polymerization of tert-Butyl Acrylate, *Macromolecules*, **32**, 618-623 (1999)

Goto A and Fukuda T: Determination of the Activation Rate Constants of Alkyl Halide Initiators for Atom Transfer Radical Polymerization, *Macromol. Rapid Commun.*, **20**, 633-636 (1999)

Fukuda T: Kinetic Characterization of Living Radical Polymerization: *Kobunshi*, **48**, 498-501 (1999) (in Japanese)

Fukuda T: Stable-Radical-Mediated Living Radical Polymerization, in *Rajikaru-Jugo Handbook*, NTS, 107-114 (1999) (in Japanese)

Ohno K, Izu Y, Yamamoto S, Miyamoto T and Fukuda T: Nitroxide-Controlled Free Radical Polymerization of a Sugar-Carrying Acryloyl Monomer, *Macromol. Chem. Phys.*, **200**, 1619-1625 (1999)

Yamada K, Minoda M and Miyamoto T: Controlled Synthesis of Amphiphilic Block Polymers with Pendant N-Acetyl-D-Glucosamine Residues and Their Interaction with WGA Lectin, *Macromolecules*, **32**, 3553-3558 (1999)

Wataoka I, Urakawa H, Kobayashi K, Ohno K, Fukuda T, Akaike T and Kajiwara K: Molecular Specification of Homopolymer of Vinylbenzyl-Lactose-Amide in Aqueous Solution, *Polymer J.*, **31**, 590-594 (1999)

Wataoka I, Urakawa H, Kobayashi K, Akaike T, Manfred S and Kajiwara K: Structural Characterization of Glycoconjugate Polystyrene in Aqueous Solution, *Macromolecules*, **32**, 1816-1821 (1999)

Ohno K and Fukuda T: Sugar-Carrying Polymers, *Rajikaru-Jugo Handbook*, NTS, 567-583 (1999) (in Japanese)

Ide N and Fukuda T: Nitroxide-Controlled Free-Radical Copolymerization of Vinyl and Divinyl Monomers. 2. Gelation, *Macromolecules*, **32**, 95-99 (1999)

Yamada K, Miyazaki M, Ohno K, Fukuda T and Minoda M: Atom Transfer Radical Polymerization of Poly (vinyl ether) Macromonomers, *Macromolecules*, **32**, 290-293 (1999)

Okamura H, Minoda M, Fukuda T, Miyamoto T and Komatsu K: Solubility Characteristics of C_{60} Fullerenes with Two Well-Defined Polystyrene Arms in a Polystyrene Matrix, *Macromol. Rapid. Commun.*, **20**, 37-40 (1999)

Okamura H, Miyazono K, Minoda M and Miyamoto T: Preparation of Water-Soluble Pullulans Bearing Pendant C60 and Their Aqueous Solubility, *Macromol. Rapid. Commun.*, **20**, 41-45 (1999)

Ohno K, Fujimoto K, Tsujii Y and Fukuda T: Synthesis of a Well-Defined Anthracene-Labeled Polystyrene by Atom Transfer Radical Polymerization, *Polymer*, **40**, 759-763 (1999)

Horinaka J, Ito S, Yamamoto M, Tsujii Y and Matsuda T: Influence of a Fluorescent Probe on the Local Relaxation Times for a Polystyrene Chain in the Fluorescence Depolarization Method, *Macromolecules*, **32**, 2270-2274 (1999)

Miyamoto T, Minoda M and Tsujii Y: Controlled Synthesis of Amphiphilic Block Polymers Having Glucose Residues and Their Structure Formation, *Chinese J. Polym. Sci.*, **17**, 21-26 (1999)

Oyane A, Minoda M, Miyamoto T, Takahashi R, Nakanishi K, Kim H. -M, Kokubo T and Nakamura T: Apatite Formation on Ethylene-Vinyl Alcohol Copolymer Modified with Silanol Groups, *J. Biomed. Mater. Res.*, **47**, 367-373 (1999)

Tsujii Y, Ejaz M, Yamamoto S, Fukuda T and Miyamoto T: Precise Control of Surface Graft Polymerization, *Kasen-Kouenshu*, **56**, 9-14 (1999) (in Japanese)

Fukuda T and Goto A: Kinetics of Controlled Radical Polymerization: *Polym. Prepr. (Div. Polym. Chem., Am. Chem. Soc.)*, **40** (2), 311-312 (1999)

Goto A, Sato K, Fukuda T, Moad G, Rizzardo E and Thang S H: Mechanism and Kinetics of Reversible Addition-Fragmentation Chain Transfer-Based Controlled Radical Polymerization of Styrene, *Polym. Prepr. (Div. Polym. Chem., Am. Chem. Soc.)*, **40** (2), 397-398 (1999)

Minoda M, Yamada K, Miyazaki M, Endo M, Ohno K and Fukuda T: Atom Transfer Radical Polymerization of Poly(vinyl ether) Macromonomers: *Polym. Prepr. (Div. Polym. Chem., Am. Chem. Soc.)*, **40** (2), 399-400 (1999)

Yamamoto S, Ejaz M, Ohno K, Tsujii Y, Matsumoto M and Fukuda T: Preparation of Well-Defined Polymer Brushes on Silicon Substrate by the Surface-Initiated ATRP Technique and their Characterization, *Polym. Prepr. (Div. Polym. Chem., Am. Chem. Soc.)*, **40** (2), 401-402 (1999)

II. High-Pressure Organic Chemistry

Davydov VA, Kashevarova LS, Rakhmanina AV, Agafonov V, Allouchi H, Ceolin R, Dzyabchenko AV, Senyavin VM, Szwarc T, Tanaka T, Komatsu, K: Polymerization of C_{60} at 1.5 GPA, *Fullerenes: Recent Advances in the Chemistry and Physics of Fullerenes and Related Materials*, **5**, 731-742 (1998)

Nagel P, Pasler V, Lebedkin S, Meingast C, Sundqvist B, Tanaka T, Komatsu K: Intermolecular Bond Stability of C_{60} Dimers and 2D Pressure-Polymerized C_{60}, *Electronic Properties of Novel Materials - Progress in Molecular Nanostructures*, **442**, 194-197 (1998)

Burger B, Kuzmany H, Komatsu K: Catalytic C_{120} - Vibrational Spectra and Stability, *Electronic Properties of Novel Materials - Progress in Molecular Nanostructures*, **442**, 211-214 (1998)

Matsuura A, Nishinaga T, Komatsu K: Synthesis, Structure and Properties of Naphthalene Fully Annelated with Bicyclo[2.2.2]octene Frameworks, *Tetrahedron Lett*, **40**, 123-126 (1999)

Ohtsuki T, Masumoto K, Tanaka T, Komatsu K: Formation of Dimer, Trimer, and Tetramer of C_{60} and C_{70} by -Ray, Charged-Particle Irradiation, and Their HPLC Separation, *Chem. Phys. Lett.*, **300**, 661-666 (1999)

Davydov VA, Kashevarova LS, Rakhmanina AV, Agafonov V, Allouchi H, Ceolin R, Dzyabchenko AV, Senyavin VM, Szwarc T, Tanaka T, Komatsu: Particularities of C_{60} Transformation at 1.5 GPa, *J. Phys. Chem.B*, **103**, 1800-1804 (1999)

Murata Y, Kato N, Fujiwara K, Komatsu K: Solid-State [4+2] Cycloaddition of Fullerene C_{60} with Condensed Aromatics Using a High-Speed Vibration Milling Technique, *J. Org. Chem.*, **64**, 3483-3488 (1999)

Nishinaga T, Wakamiya A, Komatsu K: 1,4-Dithiin Annelated with Bicyclo[2.2.2]octene Units: Experimental and Theoretical Evidence for the Aromaticity in 1,4-Dithiin Dication, *Chem. Commun.*, **1999**, 777-778.

Nishinaga T, Wakamiya A, Komatsu K: The First Isolation of the Hexafluoroantimonate Salt of a 1,4-Dithiin Radical Cation Stabilized by Bicyclo[2.2.2]octene Annelation, *Tetrahedron Lett.*, **40**, 4375-4378 (1999)

Komatsu K, Murata Y, Wang G-W, Tanaka T, Kato N, Fujiwara K: The Solid-State Mechanochemical Reaction of Fullerene C_{60}, *Fullerene Sci. Tech.*, **7**, 609-620 (1999)

Tanaka T, Komatsu K: Synthesis of the Singly Bonded Fullerene Dimer $C_{120}H_2$ and the Difullerenylacetylene $C_{122}H_2$, and Generation of the All-Carbon Dianion C_{122}^{2-}, *J. Chem. Soc., Perkin 1*, **1999**, 1671-1676

Okamura H, Minoda M, Fukuda T, Miyamoto T, Komatsu K: Solubility Characteristics of C_{60} Fullerenes with Two Well-Defined Polystyrene Arms in a Polystyrene Matrix, *Macromol. Rapid Commun.*, **20**, 37-40 (1999)

Komatsu K, Fujiwara K, Murata Y, Braun T: Aqueous Solubilization of Crystalline Fullerenes by Supramolecular Complexation with γ-Cyclodextrin and Sulfocalix[8]arene under Mechanochemical High-Speed Vibration Milling, *J. Chem. Soc., Perkin 1*, **1999**, 2963-2966.

Kudo K, Komatsu K: Reduction of Alkali Metal Carbonate to Methane with Water in the Presence of Raney Alloy, *J. Mol. Cat. A*, **415**, 159-167 (1999)

Kudo K, Komatsu K: Selective Formation of Methane in Reduction of CO_2 with Water by Raney Alloy Catalyst, *J. Mol. Cat. A*, **415**, 257-264 (1999)

Kudo K, Komatsu K: Methanation of Alkali Metal Carbonate and CO_2 with Water in the Presence of Raney Fe-Ru/C Mixed Catalyst, *Sekiyu Gakkaishi*, **42**, 157-164 (1999)

Fujitsuka M, Luo C, Ito O, Murata Y, Komatsu K: Triplet Properties and Photoinduced Electron-Transfer Reactions of C_{120}, the [2+2] Dimer of Fullerene C_{60}, *J. Chem. Phys.*, **103**, 7155-7160 (1999)

Tsubaki K, Murata Y, Komatsu K, Kinoshita T, Fuji K: The Supramolecular Structure of 1, 4-Bis(9-fluorenyl)-1, 4-dihydro[60]fullerene with Hexahomotrioxacalix[3]arene in the Solid State, *Heterocycles*, **51**, 2553-2556 (1999)

Komatsu K: Cyclic -Conjugated Systems Annelated with Bicycloalkene Frameworks, *Eur. J. Org. Chem.*, **1999**, 1495-1502

Wan TSM, Leung GNW, Tso TSC, Komatsu K, Murata Y: Separation of Fullerenes with Non-aqueous Capillary Electrophoresis, *Separation of Fullerenes by Liquid Chromatography*, **1999**, 161-176

Komatsu K: Fullerene Dimer; Nucleophilic Addition to Fullerene; Chemistry of Fullerenes, the Third Allotrope of Carbon, *Kikan Kagaku-Sosetsu*, **43**, 42-47, 85-93 (1999)

SYNTHETIC ORGANIC CHEMISTRY

I. Synthetic Design

Yamaguchi S, Jin R-Z, Itami Y, Goto T, Tamao K: The First Synthesis of Well-Defined Poly (2,5-silole), *J. Am. Chem. Soc*. **121**, 10420-21 (1999)

Kawachi, A, Tanaka Y, Tamao K: Synthesis and Structures of a Series of Ge-M (M = C, Si, and Sn) Compounds Derived from Germyllithium Containing Three 2-(Dimethylamino)phenyl Groups on Germanium, *J. Organomet. Chem.*, **590**, 15-24 (1999)

Tamao K, Asahara M, Saeki T, Toshimitsu A: Reaction of Hypercoordinate Dichlorosilanes Bearing 8-(Dimethylamino)-1-naphthyl Group(s) with Magnesium: Formation of 1,2-Disilaacenaphthene Skeleton Accompanied by Amino Group Migration from Carbon to Silicon, *Angew. Chem., Int. Ed.*, **38**, 3316-18 (1999)

Kawachi A, Maeda H, Mitsudo K, Tamao K: Optical Resolution and Epimerization of Fluorosilane Having an Optically Active Amino Group: A New Convenient Access to Optically Active Organosilicon Compounds, *Organometallics*, **18**, 4530-33 (1999)

Yamaguchi S, Jin R-Z, Tamao K: Silole Polymer and Cyclic Hexamer Catenating through the Ring Silicons, *J. Am. Chem. Soc*. **121**, 2937-38 (1999)

Tamao K, Asahara M, Saeki T, Toshimitsu A: Wurtz-type Coupling Reaction of Pseudo-penacoordinate Halodisilanes Using Magnesium: Enhanced Reactivity of the Silicon-Halogen Bond by Intramolecular Amine-coodination to Silicon, *Chem. Lett*. **1999**, 335-36

Yamaguchi S, Ishii H, Tamao K: A New Chiral Molecular Square with *D4* Symmetry Composed of Enantiomerically Pure Spirosilane, *Chem. Lett.*, **1999**, 309-10

Yamaguchi S, Akiyama S, Tamao K: Effect of Countercation Inclusion by [2.2.2] Cryptand upon Stabilization of Potassium Organofluorosilicates, *Organometallics*, **18**, 2851-54 (1999)

Kawachi A, Tanaka Y, Tamao K: Reaction of {Tris[2-(dimethylamino)phenyl]germyl}lithium with Elemental Selenium: Formation of 2,2,4,4-Tetrakis[2-(dimethylamino) phenyl]-1,3,2,4-diselenadigermetane, *Chem. Lett.*, **1999**, 21-22.

Kawachi,A, Tanaka Y, Tamao K, Distorted Germyllithium Induced by Intramolecular Coordination of an Amino Group: Synthesis and Structures of {Tris[2-(dimethylamino)phenyl] germyl}lithium, *Eur. J. Inorg. Chem.* **1999**, 461-64

Tamao K, Asahara M, Sun G-R, Kawachi A, Synthesis, Structure, and Reactivity of 1, ω-Bis(pseudo-pentacoordinated) 1, -difluoro-oligosilanes Bearing 8-(Dimethylamino)-1-naphthyl Groups, *J. Organomet. Chem.* (Okawara issue) **574**, 193-205 (1999)

Tamao K, Kawachi A, Asahara M, Toshimitsu A: Recent Developments in the Silicon Interelement Linkage: The Case of Functionalized Silyllithium, Silylenoid, and Sila-ylide, *Pure Appl. Chem.*, **71**, 393-400 (1999)

Tamao K: Invitation to the Chemistry of the Inter-Element Lincage, Gendai-Kagaku, No.10, 24-31 (1999) (in Japanese)

Noyori R, Shibasaki M, Suzuki K. Tamao K. Nakasuji K, and Narasaka K, Eds.: Organic Chemistry I, Tokyo Kagaku Doujin, 1999 (in Japanese)

II. Fine Organic Synthesis

Lakshmaiah G, Kawabata T, Shang M and Fuji K: Total Synthesis of (-)-Horsfiline via Asymmetric Nitoroolefination, *J. Org. Chem.*, **64**, 1699-1704 (1999)

Chen J, Kawabata T, Ohnishi H, Shang M and Fuji K: Lewis Acid-Promoted Nitroolefination of Enol Silyl Ethers via an Addition Elimination Process, *Chem. Pharm. Bull.*, **47**, 394-397 (1999)

Fuji K, Furuta T, Otsubo T and Tanaka K: Hydrogen-bonded Network with a Unique Structural Unit Having Zeolite-like Properties, *Tetrahedron Lett.*, **40**, 3001-3004 (1999)

Fuji K, Tsubaki, K, Tanaka K, Hayashi N, Otsubo T and Kinoshita T: Visualization of Molecular Length of -Diamines and Temperature by a Receptor Based on Phenolphthalein and Crown Ether, *J. Am. Chem. Soc.*, **121**, 3807-3808 (1999)

Tanaka K, Nuruzzaman M, Yoshida M, Asakawa N, Yang X, Tsubaki K and Fuji K: Use of 1,1'-Binaphthalene-8,8'-diol as a Chiral Auxiliary for Asymmetric Michael Addition. Application to the Synthesis of Turmeronol A and B, *Chem. Pharm. Bull.*, **47**, 1053-1055 (1999)

Tanaka K, Watanabe T, Shimamoto K, Sahakitpichan P and Fuji K: Asymmetric Olefination of Metallic arene or Diene Complexes to form Planar Chiral Complexes, *Tetrahedron Lett.*, **40**, 6599-6602 (1999)

Fuji K, Watanabe Y, Ohtsubo T, Nuruzzaman M, Hamajima Y and Kohno M: Synthesis of Extremely Simplified Compounds Possessing the Key Pharmacophore Units of Taxol, Phenylisoserine and Oxetane Moieties, *Chem. Pharm. Bull.*, **47**, 1334-1337 (1999)

Fuji K, Yang X-S, Ohnishi H, Hao X-J, Obata Y and Tanaka K: A Highly Efficient Method for the Resolution of 8,8'-Dihydroxy-1,1'-biphenyl, *Tetrahedron: Asymmetry*, **10**, 3243-3248 (1999)

Fuji K, Kinoshita N and Tanaka K: Et_2Zn as a base: zinc enolate free from other metals significantly enhances the enantiomeric excess in palladium-catalyzed allylic alkylation, *Chem. Commun.*, 1895-1896 (1999)

Ikeda H, Fuji K, Tanaka K, Iso Y and Yoneda F: DNA Oligomers Having a Diazapyrenium Dication (DAP^{2+}); Synthesis and DNA Cleavage Activities, *Chem. Pharm. Bull.*, **47**, 1455-1463 (1999)

Tsubaki K, Murata Y, Komatsu K, Kinoshita T and Fuji K: The Supramolecular Structure of 1,4-Bis(9-fluorenyl)-1,4-dihydro [60]fullerene with Hexahomotrioxacalix[3]arene in the Solid State, *Heterocycles*, **51**, 2553-2556 (1999)

Fuji K, Kinoshita N, Tanaka K and Kawabata T: Enantioselective Allylic Substitution Catalyzed by an Iridium Complex: Remarkable Effects of Cation, *Chem. Commun.*, 2289-2290 (1999)

Fuji K: Development of New Asymmetric Reactions Utilizing *Carbanions*, *Yakugakuzasshi*, **119**, 114-125 (1999) (in Japanese)

Fuji K: Artificial Catalysts That Differentiate Enantiomers, *Farumashia*, **35**, 1211-1213 (1999) (in Japanese)

BIOORGANIC CHEMISTRY

I. Bioorganic Reaction Theory

Fujii M, Yasui S, and Nakamura K: Silica gel catalyzed selective reductions by NAD(P)H models, *Rev. Heteroat. Chem.*, **20**, 167-205 (1999)

Kawai Y, Hida K, and Ohno A: Reduction of β-Keto Esters with a Reductase: Construction of Plural Stereocenters Remote from the Reaction Center, *Bioorganic Chemistry*, **27**, 3-19 (1999)

Kawai Y, Hida K, Tsujimoto M, Kondo S, Kitano K, Nakamura K, and Ohno A: Asymmetric Reduction of α-Keto Esters and α-Diketones with a Bakers' Yeast Keto Ester Reductase, *Bull. Chem. Soc. Jpn.*, **72** (1), 99-102 (1999)

Kawai Y and Ohno A, Highly efficient asymmetric reduction with a novel enzyme, *Yuki Gosei Kagaku Kyokaishi*, **57**, 798-804 (1999) (in Japanese)

Kawasaki M, Nakamura K, and Kawabata S: Lipase-catalyzed enantioselective deacetylation of *ortho*-substituted phenyl acetates with 1-butanol in organic solvents, *J. Mol. Catal. B: Enzym.*, **6**, 447-451 (1999)

Kimura T, Kawai Y, Ogawa S, and Sato R: First Preparation and Structural Determination of Optically Pure Cyclic Polysulfides, 6,10-Diethyl Trithiolo[*h*]benzopentathiepin Monooxides, *Chem. Lett.*, 1305-1306 (1999)

Kitayama T, Okamoto T, Hill R K, Kawai Y, Takahashi S, Yonemori S, Yamamoto Y, Ohe K, Uemura S, and Sawada S: Chemistry of Zerumbone I. Simple Isolation, Conjugate Addition Reactions, and a Unique Ring Contracting Transannular Reaction of Its Dibromide, *J. Org. Chem.*, **64**, 2667-2672 (1999)

Nakajima N, Ishihara K, Hamada H, Yamane S, Nakamura K, and Furuya T: Multi-enzymatic Glucosylation Using Eucalyptus UDP-Glucosyltransferase Coupled UDPglucose-Fermentation by Bakers' Yeast, *Biosci., Biotechnol., Biochem.*, **63**, 934-936 (1999)

Nakajima N, Sugimoto M, Ishihara K, Nakamura K, Hamada H: Further Characterization of Earthworm Serine Proteases: Cleavage Specificity Against Peptide Substrates and on Autolysis, *Biosci., Biotechnol., Biochem.*, **63**, 2031-2033 (1999)

Nakamura K, Inoue Y, Matsuda T, and Misawa I: Stereoselective Oxidation and Reduction by Immobilized *Geotrichum candidum* in an Organic Solvent, *J. Chem. Soc., Perkin Trans. 1*, 2397-2402 (1999)

Ogawa S, Kikuchi M, Kawai Y, Niizuma S, and Sato R: Synthesis, Structure, and Redox Reactions of New Crowded Benzodithiolium Salt: First Isolation and Characterization of Stable Dithiolyl Radical with 7 π-Electron Framework, *Chem. Commun.*, 1891-1892 (1999)

Ogawa S, Sugawara M, Kawai Y, Niizuma S, Kimura T, and Sato R: Novel Photochemical Ring Contraction of 1,4,7,10-Tetraisopropyldibenzo[c,g][1,2,5,6] tetrachalcogenocins: Efficient Synthesis, Structure, and Redox Reactions of 1,4,6,9 Tetraisopropylchalcogenanthrenes, *Tetrahedron Lett.*, **40**, 9101-9106 (1999)

Ohno A: Designed syntheses of chiral compounds mediated by biocatalysts: production of a desired stereoisomer, *Rev. Heteroat. Chem.*, **20**, 29-68 (1999)

Ohno A, Oda S, and Yamazaki N: $NAD(P)^+$-NAD(P)H models. 89. Effect of magnesium ion on the stereochemistry in oxidation of NAD(P)H analog, *Tetrahedron Lett.*, **40**, 4577-4580 (1999)

Ohta M, Nakamura K, Tsuchiya H, Takama K, and Suzuki T: Effect of Several Solutions Including Mineral-encaging Zeolites on the Restoration of Cell Motility of Tributyltin-intoxicated *Euglena gracilis* Z, *Biosci. Biotechnol. Biochem.*, **63**, 1691-1696 (1999)

Oki M, Hirose T, Kataoka Y, Ogata T, Toyota S, Matsuo T, Kawai Y, and Ohno A: Reactivities of Stable Rotamers. XLI. Reactions of 1-(9-Fluorenyl)-2-(1 methylethenyl)naphthalene Rotamers with Chalcogenyl Halides and Observation of Coloration During the Reaction of Methanesulfenyl Chloride and the *ap*-Rotamer, *Bull. Chem. Soc. Jpn.*, **72**, 63-72 (1999)

Yasui S, Shioji K, Tsujimoto M, and Ohno A: Kinetic study on the reaction of tributylphosphine with methylviologen. Reactivity of the phosphine radical cation intermediate towards nucleophiles, *J. Chem. Soc., Perkin Trans. 2*, 855-862 (1999)

II. Bioactive Chemistry

Takahashi T, Tanaka H, Matsuda A, Doi T, Yamada H, Matsumoto T, Sasaki D and Sugiura Y: DNA Cleaving Activities of 9-Membered Masked Enediyne Analogues Possessing DNA Intercalator and Sugar Mieties. *Bioorg. Med. Chem.Lett.*, **8**, 3303-3306 (1998)

Aizawa Y and Sugiura Y, Morii T: Comparison of the Sequence-Selective DNA Binding by Peptide Dimers with Covalent and Noncovalent Dimerization Domains. *Biochemisty*, **38**, 1626-1632 (1999)

Aizawa Y, Sugiura Y, Ueno M, Mori Y, Imoto K, Makino K and Morii T: Stability of the Dimerization Damain Effects the Cooperative DNA Binding of Short Peptides. *Biochemistry*, **38**, 4008-4017 (1999)

Inoue T, Sugiura Y, Saitoh J, Ishiguro T and Otsuka M: Fluorescence Property of Oxazola Yellow-linked Oligonucleotide. Triple Helix Formation and Photocleavage of Double-stranded DNA in the Presence of Spermine. *Bioorg. Med. Chem.*, **7**, 1207-1211 (1999)

Sugiura Y: Chemistry in Biological and Medical Sciences. *Chemistry*, **54**, 20-21 (1999) (in Japanese)

Futaki S, Aoki M, Ishimawa T, Kondo F, Asahara T, Niwa M, Nakaya Y, Yagami T and Kitagawa K: Chemical Ligation to Obtain Proteins Comprising Helices with Individual Amino Acid Sequences. *Bioorg. Med. Chem.*, **7**(1), 187-192 (1999)

Kamada M, Yamamoto S, Takikawa M, Kunimi K, Maegawa M, Futaki S, Ohmoto Y, Aono T, Samuel S. Koide: Identification of the Human Sperm Protein that Interacts with Sperm-Immobilizing Antibodies in the Sera of infertile Women. *Fertil. Steril.*, **72**(4), 691-695 (1999)

Futaki S, Omote M, Sugiura Y, Fukuda M and Niwa M: Modulation of Alamethicin Assembly by Hybridization. *Peptide Science 1998 Ed by M. Kondo, Protein Research Foundation* (405-408) 1999

III. Molecular Clinical Chemistry

Banasik M and Ueda K: Dual Inhibitory Effects of Dimethyl Sulfoxide on Poly(ADP-ribose) Synthetase, *J. Enz. Inhib*, **14**, 239-250 (1999)

Okamoto H, Takano E, Sugao T, Kage K, Okamoto E, Nishimura N and Ueda K: Direct Amplification of *Escherichia coli* O157 Vero Toxin Genes from Human Feces by the Polymerase Chain Reaction, *Ann. Clin. Biochem*, **36**, 642-648 (1999)

Ueda K, Tanaka S, Matoh N, Takehashi M and Masliah E: Molecular Diagnosis of Alzheimer Disease in Relation to Parkinson Disease, *Clin. Chem. Lab. Med*, **37**, S156 (1999)

Takano E, Okamoto H, Sugao T, Okamoto E, Nishimura N and Ueda K: Direct Amplification of *Escherichia coli* O157 Vero Toxin Genes from Human Feces by Polymerase Chain Reaction, *Clin.Chem. Lab. Med*, **37**, S156 (1999)

Ikemoto M, Tsunekawa S, Murayama H, Kasai Y, Totani M and Ueda K: Development of an Excellent ELISA for Human Liver-type Arginase using Monoclonal Antibodies and its Clinical Usefulness, *Clin. Chem. Lab. Med*, **37**, S468 (1999)

Ariumi Y, Masutani M, Copeland T D, Mimori T, Sugimura T, Noda M, Shimotohno K, Ueda K and Hatanaka M: Suppression of Poly(ADP-ribose) Polymerase Activity by DNA-dependent Protein Kinase, *Oncogene*, **18**, 4616-4625 (1999)

Takehashi M, Tanaka S and Ueda K: NACP/α-synuclein is a Synaptic Protein Phosphorylated by Serine/threonine Kinase(s), *6th IUBMB Conference*, Abstructs, 104 (1999)

Tanaka S, Takehashi M, Matoh N and Ueda K: NAC Interacts with Aβ Protein in Amyloid Formation and Induces Neuronal Cell Injury, *International Symposium on Dementia: From Molecular Biology to Therapentics*, Program & Abstracrs, 22 (1999)

Takehashi M, Tanaka S and Ueda K: α-Synuclein is a Synaptic Protein Phosphorylated by Serine/threonine Kinase(s), *International Symposium on Dementia: From Molecular Biology to Therapentics*, Program & Abstracrs, 29 (1999)

Adachi, Y: HIV-1 Infection and Nucleocytoplasmic Transport, *In "Dynamism of Intracellular Traffic" (Yoneda Y and Nakano A, eds), Springer-Verlag Tokyo*, 32-39 (1999)

MOLECULAR BIOFUNCTION

I. Functional Molecular Conversion

Wada S, He P, Watanabe N, Sakata K and Sugimoto K: Suppression of d-Galactosamine-Induced Rat Liver Injury by Glycosidic Flavonoids-Rich Fraction from Green Tea, Biosci. *Biotechnol. Biochem.*, **63**, 570-572 (1999)

Sakata K, Watanabe N, Usui T: Molecular Basis of Alcoholic Aroma Formation During Tea Processing, In *Food for Health in the Pacific Rim*, Proceedings of 3rd International Conference of Food Science and Technology, Ed. By Whitaker JR, Norman FH, Shoemaker CF, Singh P, Food & Nutrition Press, Trumbull, Connecticut, 1999, pp 93-105.

Sakata K, Guo W and Moon J-H: Tea Chemistry Part II. With Special Reference to Tea Aroma Precursors, in *Global Advances in Tea Science*, Ed. by Jain NK et al., Aravali Books International, Delhi, 1999, pp. 691-704.

Sakata K: Molecular Basis of Floral Aroma Formation during Oolong Tea Manufacturing, *Kagaku to Seibutsu* (in Japanese), **37**, 20-27 (1999)

Tokutake N, Hiratake J, Irie T, Yamano A and Oda J: The Absolute Configuration of an Intermediate Cyclic Sulfoximine in the Asymmetric Synthesis of Transition-State Analogue Inhibitors of γ-Glutamylcysteine Synthetase, *Acta Crystallogr.*, **C55**, 1598-1599 (1999)

Koizumi M, Hiratake J, Nakatsu T, Kato H and Oda J: A Potent Transition-State Analogue Inhibitor of *Escherichia coli* Asparagine Synthetase A, *J. Am. Chem. Soc.*, 121, 5799-5800 (1999)

Inoue M, Hiratake J and Sakata K: Synthesis and Characterization of Intermediate and Transition-state Analogue Inhibitors of γ-Glutamyl Peptide Ligases, *Biosci. Biotechnol. Biochem.*, **63**, 2248-2251 (1999)

Hiratake J: Probing the Function of Biocatalysts and Their Applications by Organic Synthetic Methods, *Nippon Nõgei Kagaku Kaishi* (in Japanese), **73**, 1261-1272 (1999)

Koiwa H, Kato H, Nakatsu T, Oda J, Yamada Y and Sato F: Crystal Structure of Tobacco PR-5d Protein at 1.8 Å Resolution Reveals a Conserved Acidic Cleft Structure in Antifungal Thaumatin-like Proteins, *J. Mol. Biol.*, **286**, 1137-1145 (1999)

Yamashita A, Kato H, Wakatsuki S, Tomizaki T, Nakatsu T, Nakajima K, Hashimoto T, Yamada Y and Oda J: Structure of Tropinone Reductase-II Complexed with $NADP^+$ and Pseudotropine at 1.9 Å Resolution: Implication for Stereospecific Substrate Binding and Catalysis, *Biochemistry*, **38**, 7630-7637 (1999)

Nakajima K, Kato H, Oda J, Yamada Y and Hashimoto T: Site-directed Mutagenesis of Putative Substrate-binding Residues Reveals a Mechanism Controlling the Different Stereospecificities of Two Tropinone Reductases, *J. Biol. Chem.*, **274**, 16563 - 16568 (1999)

Kato H: Four-dimensional Structural Analysis of Enzymes, *Farumasia* (in Japanese), **35**, 29-32 (1999)

Fukuchi-Mizutani M, Mizutani M, Tanaka Y, Kusumi T and Ohta D: Microsomal Electron Transfer in Higher Plants: Cloning and Heterologous Expression of NADH-Cytochrome b_5 Reductase from Arabidopsis, *Plant Physiol.*, **119**, 353-361 (1999)

Ohta D, Mizutani M: Cytochrome P450 in Higher Plants: Molecular Diversity and Gene Expression, *Kagaku to Seibutsu* (in Japanese), **37**, 128-134 (1999)

Nakatsu, T: Crystal Structure of Aparagine Synthetase —Evolutional Relationship to Class II Aminoacyl-tRNA Synthetase, *Journal of the Crystallographic Society of Japan* (in Japanese), **41**, 129-135 (1999)

Nakatsu, T: Similarity in Structure and Function vs. Non-homology in Amino Acid Sequence, *Kagaku to Seibutsu* (in Japanese), **37**, 487-491 (1999)

II. Molecular Microbial Science

Watanabe A, Kurokawa Y, Yoshimura T, Kurihara T, Soda K and Esaki N: Role of Lysine39 of Alanine Racemase from *Bacillus stearothermophilus* That Binds Pyridoxal 5'-Phosphate: Chemical Rescue Studies of Lys39→Ala Mutant, *J. Biol. Chem.*, **274** (7), 4189-4194 (1999)

Mihara H, Maeda M, Fujii T, Kurihara T, Hata Y, Esaki, N: A

*nif*S-like Gene, *csd*B, Encodes an *Escherichia coli* Counterpart of Mammalian Selenocysteine Lyase, *J. Biol. Chem.*, **274** (21), 14768-14772 (1999)

Nardi-Dei V, Kurihara T, Park C, Miyagi M, Tsunasawa S, Soda K and Esaki N: DL-2-Haloacid Dahalogenase from *Pseudomonas* sp. 113 Is a New Class of Dehalogenase Catalyzing Hydrolytic Dehalogenation Not Involving Enzyme-Substrate Ester Intermediate, *J. Biol. Chem.*, **274** (30), 20977-20981 (1999)

Kulalova L, Galkin A, Kurihara T, Yoshimura T and Esaki N: Cold-Active Serine Alkaline Protease from the Psychrotrophic Bacterium *Shewanella* Strain Ac10: Gene Cloning and Enzyme Purification and Characterization, *Appl. Environ. Microbiol.*, **65** (2), 611-617 (1999)

Galkin A, Kulakova L, Ashida H, Sawa Y and Esaki N: Cold-Adapted Alanine Dehydrogenases from Two Antarctic Bacterial Strains: Gene Cloning, Protein Characterization, and Comparison with Mesophilic and Thermophilic Counterparts, *Appl. Environ. Microbiol.*, **65** (9), 4014-4020 (1999)

Okubo Y, Yokoigawa K, Esaki N, Soda K and Kawai H: Characterization of Psychrophilic Alanine Racemase from *Bacillus psychrosaccharolyticus. Biochem. Biophys. Res. Com.*, **256** (2), 333-340 (1999)

Bae H-S, Lee S-G, Hong S-P, Kwak M-S, Esaki N, Soda K and Sung M-H: Production of Aromatic D-Amino Acids from α-Keto Acids and Ammonia by Coupling of Four Enzyme Reactions, *J. Mol. Catal. B: Enzymatic 6*, 241-247 (1999)

Kawata Y, Tamura K, Yano S, Mizobata T, Nagai J, Esaki N, Soda K, Tokushige M and Yumoto N: Purification and Characterization of Thermostable Aspartase from *Bacillus* sp. YM55-1, *Arch. Biochem. Biophys.*, **366** (1), 40-46 (1999)

Watanabe A, Kurokawa Y, Yoshimura T and Esaki N: Role of Tyrosine 265 of Alanine Racemase from *Bacillus stearothermophilus, J. Biochem.*, **125** (6), 987-990 (1999)

Watanabe A, Yoshimura T, Mikami B and Esaki N: Tyrosine 265 of Alanine Racemase Serves as a Base Abstracting α-Hydrogen from L-Alanine: The Counterpart Residue to Lysine 39 Specific to D-Alanine. *J. Biochem.*, 126 (4), 781-786 (1999)

MOLECULAR BIOLOGY AND INFORMATION

I. Biopolymer Structure

Fujii T and Hata Y: Analysis of a Reaction Mechanism for the Dehalogenase by its Quasi-four-dimensional Structure, *Baiosaiensu To Indasutori*, **57**, 37-38 (1999) (in Japanese)

Fujii T, Maeda M, Mihara H, Kurihara T, Esaki N and Hata Y: Crystal Structure of a NifS-like Protein from *Escherichia coli*, *Acta Cryst.*, **A55 Supplement**, Abstract P06.04.036 (1999)

Fujii T, Kurihara T, Esaki N and Hata Y: X-ray Crystal Structure Analysis of Each Reaction Step of Dehalogenase Enzyme, *Spring-8 User Experiment Report*, **3**, 207 (1999)

Hata Y, Li Y.-F., Fujii T, Kurihara T and Esaki N: Crystal Structure of an Ester Intermediate Formed between L-2-Haloacid Dehalogenase and L-2-Chlorobutyrate, *Photon Factory Activity Report*, **16**, 275 (1998)

Hata Y, Li Y.-F., Fujii T, Kurihara T and Esaki N: X-ray Crystallographic Analysis of the Catalytic Mechanism of L-2-Haloacid Dehalogenase, *Acta Cryst.*, **A55 Supplement**, Abstract P06.04.037 (1999)

Hiragi Y, Ichimura K, Higurashi T and Kawata Y: SAXS Observation of Denaturation and Renaturation of *Escherichia coli* Chaperonin Proteins GroEL and GroES, *Photon Factory News*, **17**, 15-20 (1999) (in Japanese)

Matsumoto T: Membrane destabilizing activity of influenza virus heamagglutinin-based synthetic peptide: implications of critical glycine residue in fusion peptide, *Biophys. Chem.*, **79**, 153-162 (1999)

Mihara H, Maeda M, Fujii T, Kurihara T, Hata Y and Nobuyoshi E: A *nif*S-like Gene, csdB, Encodes an *Escherichia coli* Counterpart of Mammalian Selenocysteine Lyase. Gene Cloning, Purification, Characterization and Preliminary X-ray Crystallographic Studies, *J. Biol. Chem.*, **274**, 14768-14772 (1999)

Sakai H, Fujii T, Kawata Y and Hata Y: Crystallographic Studies of Thermostable Aspartase from *Bacillus* YM55, *Photon Factory Activity Report*, **16**, 259 (1998)

II. Molecular Biology

Aoyama T, Ohgishi M, Muramoto T, Tukuda M, and Oka A: Artifical Regulation of Transcription Factors in Transgenic Plants. *Proceedings of the second BRAIN Seminar: Cytochrome P450 and Plant Genetic Engineering* pp. 20-23 (1999)

Steindler C, Matteucci A, Sessa G, Weimar T, Ohgishi M, Aoyama T, Morelli G, and Ruberti I: Shade Avoidance Responses are Mediated by the ATHB-2 HD-Zip Protein, a Negative Regulator of Gene Expression. *Development*, **126**, 4235-4245 (1999)

Kobayashi Y, Kaya H, Goto K, Iwabuchi M, and Araki T: A Pair of Related Genes with Antagonistic Roles in Mediating Flowering Signals. *Science*, **286**, 1960-1962 (1999)

Sawa S, Watanabe K, Goto K, Kanaya E, Morita EH, and Okada K: *FILAMENTOUS FLOWER*, a Meristem and Organ Identity Gene of *Arabidopsis*, Encodes a Protein with a Zinc Finger and HMG-Related Domains. *Genes & Dev.*, **13**, 1079-1088 (1999)

III. Biological Information Science

Ogata H, Goto S, Sato K, Fujibuchi W, Bono H and Kanehisa M: KEGG: Kyoto Encyclopedia of Genes and Genomes, *Nucleic Acids Res.*, **27**, 29-34 (1999)

Kawashima S, Ogata H and Kanehisa M: AAindex: amino acid index database, *Nucleic Acids Res.*, **27**, 368-389 (1999)

Goto S, Nishioka T and Kanehisa M: LIGAND database for enzymes, compounds, and reactions, *Nucleic Acids Res.*, **27**, 377-379 (1999)

Wackett L P, Ellis L B M, Speedie S M, Hershberger C D, Knackmuss H-J, Spormann A M, Walsh C T, Forney L J, Punch W F, Kazic T, Kanehisa M and Berndt D J: Predicting microbial biodegradation pathways, *ASM News*, **65**, 87-93 (1999)

Kanehisa M: KEGG: From genes to biochemical pathways, In "*Bioinformatics: Databases and Systems*" (Letovsky S, ed.), pp. 63-76, Kluwer Academic Publishers (1999)

Tomii K and Kanehisa M: Systematic detection of protein structural motifs, In "*Pattern Discovery in Biomolecular Data*" (Wang J T L, Shapiro B A and Shasha D, eds.), pp.97-110, Oxford Univ. Press (1999)

Bono H, Nakao M and Kanehisa M: Cluster analysis of genome-wide expression profiles to predict gene functions with KEGG, *Nature Genetics*, **23** (3s), 33-34 (1999)

Fujibuchi W and Kanehisa M: Gene cluster analysis, *Suuri Kagaku*, **432**, 12-18 (1999) (in Japanese)

Goto S: Simulation of metabolic network, *bit*, **31** (6), 18-23 (1999) (in Japanese)

Kawashima S and Kanehisa M: Knowledge base of biological function based on genome information, *Iden*, **53**(8), 28-31 (1999) (in Japanese)

Kanehisa M: GenomeNet, *bit*, **31**(8), 28-33 (1999) (in Japanese)

Kawashima S and Kanehisa M: Pathway database - Making a database of biological activities in a cell, *bit*, **31**(9), 63-70 (1999) (in Japanese)

Goto S: Bioinformatics, *Chemistry Today*, **344**, 50-55 (1999) (in Japanese)

Nakao M, Bono H, Kawashima S, Kamiya T, Sato K, Goto S and Kanehisa M: Genome-scale gene expression analysis and pathway reconstruction in KEGG, *Genome Informatics*, **10**, 94-103 (1999)

Goto S, Shiraishi K, Okamoto K, Ishida H, Nakatani T, Deno T and Kanehisa M: Ortholog identifiers for integration of genomic and pathway information in KEGG, *Genome Informatics*, **10**, 204-205 (1999)

Park K-J and Kanehisa M: Prediction of nuclear localization signals by HMM, *Genome Informatics*, **10**, 261-262 (1999)

Hattori M and Kanehisa M: Detection of apoptotic domains against KEGG database by the HMM search, *Genome Informatics*, **10**, 267-268 (1999)

Kawashima S, Kawashima T, Nishida H, Makabe K W and Kanehisa M: MAGEST: ESTs and gene expression pattern database for *Halocynthia roretzi* maternal cDNA, *Genome Informatics*, **10**, 274-275 (1999)

Sato K X, Goto S and Kanehisa M: Unit-based de novo drug design using a library of protein-ligand interaction sites, *Genome Informatics*, **10**, 320-321 (1999)

NUCLEAR SCIENCE RESEARCH FACILITY

I. Particle and Photon Beams

II. Beams and Fundamental Reaction

Ao H, Iwashita Y, Shirai T and Noda A: High power model fabrication of Disk-and-Washer cavity, Proc. 24th Linear Accelerator Meeting in Japan, Sapporo, 254-256 (1999) (in Japanese)

Ao H, Iwashita Y, Shirai T, Noda A, Inoue M: Biperiodic Disk-and-Washer Cavity for Electron Acceleration, Proc. of the 1998 Linear Accelerator Conference, Chicago 1998, 255-257 (1998).

Inoue M : Status of Accelerators in Japan, Proc. of the first Asian Particle Accelerator Conference APAC98, 23-27 (1999)

Kawase Y, Shiroya S, Inoue M: An Accelerator-Assisted Nuclear Fuel Assembly for a Future Project at KURRI, Proc. of the 1998 Linear Accelerator Conference, Chicago 1998, 300-302 (1998).

Iwashita Y, Noda A, Shirai T, Morita A, Tadokoro M, Hirota J.I., Umezawa M and Hiramoto K: Novel Design for Electromagnet with Wide Excitation Range, Jpn. J. Appl. Phys., 38, 895-897 (1999)

Iwashita Y: Beam Tracking in Inflector Septum Magnet of KSR, Beam Science and Technology, 4, 20 (1998)

Iwashita Y: Oscillating Gaussian Distribution, Beam Science and Technology, 4, 21-22 (1998)

Iwashita Y: Multi-Harmonic Impulse Cavity, Proc. of the 1999 Particle Accelerator Conference, New York, March 29- April 2, 3645-3647 (1999)

Iwashita Y, Morita A: MULTI-HARMONIC IMPULSE CAVITY, Proc of the 24th Linear Accelerator Meeting in Japan, July 7-9 Sapporo, Japan 262-264 (1999) (in Japanese)

Iwashita Y, Morita A: High Gradient Field Generation by Multi-Harmonic Superposition, Proc. of the 12th Symposium on Accelerator Science and Technology, Oct. 27-29, Wako, Japan, 215-217 (1999)

Iwashita Y: RF Cavity Design, Text for OHO'99 High Energy Accelerator Seminar, Aug. 31-Sep. 3, KEK, Japan, IIB-1-13 (1999) (in Japanese)

Iwashita Y: 2.5D Cavity Code with High Accuracy, Proc. of the 1998 Linear Accelerator Conference, Chicago 1998, 136-138 (1998).

Urakabe E, Hiramoto K, Inoue M, Iwashita Y, Kanazawa M, Morita A, Nishi M, Norimine T, Noda A, Noda K, Ogawa H, Shirai T, Torikoshi M, Umezawa M, Yamada S, Fujita Y: Beam Profile Control with Use of the Octupole Magnet, Jpn. J. Appl. Phys., 38, 6145-6149 (1999)

Urakabe E, Kanai T, Kanazawa M, Kitagawa A, Suda M, Iseki Y, Tomitani T, Shimbo M, Torikoshi M, Noda K, Futami Y, Mizota M, Noda A: The Spot Scanning Irradiation with 11C Beams, Proceedings of the Second JAPAN-KOREA Joint Meeting on Medical Physics, 188-191 (1999)

Kapin V, Inoue M, Iwashita Y, Noda A: Design Considerations for Multiple-Beam RFQ Structures, Proc. of the 1998 Linear Accelerator Conference, Chicago 1998, 591-593 (1998).

Kihara T, Okamoto H, Iwashita Y, Oide K, Lamanna G, and Wei J: Three-dimensional laser cooling method based on resonant linear coupling, Phys. Rev. E, **59**, 3594-3604 (1999)

Kishimoto Y, Tada M, Shibata M, Kominato K, Ooishi C, Funahashi H, Yamamoto K, Masaike A, and Matsuki S: The CARRACK-2 axion experiment, Proceedings of the second international workshop on the identification of dark matter eds. N. J. C. Spooner and V. Kudryavtsev, 636 - 641 (1999)

Shirai T, Sugimura T, Iwashita Y, Fujita H, Tonguu H, Noda A: Commissioning of an Electron Ring, KSR at Kyoto University, Science and Technology, Wako, Japan, 180-182 (1999)

Shirai T, Sugimura T: Control System for the Electron Linac, Beam Science and Technology, 4, 23-25 (1999)

Shirai T, Sugimura T, Iwashita Y, Fujita H, Tonguu H, Noda A: First Beam Circulation Test of an Electron Storage/Stretcher Ring, KSR, Proc. of the 1999 Particle Accelerator Conference, New York, 1999, 3110-3112 (1999).

Andreev V, Bissofi G, Comunian M, Lombardi A, Pisent A, Porcellato A.M, Shirai T: Scale Room Temperature Model of the Superconducting RFQ1 for the PIAVE Linac Proc. of the 1998 Linear Accelerator Conference, Chicago 1998, 965-967 (1998).

Sugimura T, Morita A, Shirai T, Iwashita Y, Fujita H, Tonguu H, Noda A: Extraction system of the electron storage and stretcher ring, KSR, Science and Technology, Wako, Japan, 165-167 (1999)

Tada M, Kishimoto Y, Kominato K, Shibata M, Funahashi H, Yamamoto K, Masaike A, Matsuki S: CARRACKII - a new large-scale experiment to search for axions with Rydberg-atom cavity detector, Nuclear Physics 72B (1999) 164 -168.

Tongu H, Shirai T, Fujita H, Sugimura T, Iwashita Y, Noda A: Present status of the Vacuum System of KSR, Proc. of the 12th symposium on Accelerator Science and Technology, Wako, Japan, 290-292 (1999)

Tongu H, Noda A, Fujita H, Inoue M, Sugimura T, Shirai T, Iwashita Y: Vacuum System of beam transport section for KSR, Beam Science and Technology, 4, 31-32 (1999)

Noda A: Accelerator Complex of Ion and Electron Storage Rings with their Booster Synchrotron, Beam Science and Technology, 4, 26-30 (1999)

Noda A, Shirai T, Tonguu H, Sugimura T, Iwashita Y, Morita A and Inoue M: Slow Beam Extraction at KSR with Combination of Third Order Resonance and RFKO, Proc. of the 1999 Particle Accelerator Conference, New York, 1999, 1294-1296 (1999).

Noda A, Ao H, Iwashita Y, Urakabe E, Kihara T, Sugimura T, Shirai T, Tonguu H, Fujieda M, Fujita H, and Morita A : Activities of Accelerator and Beam Physics Research at Nuclear Science Research Facility, ICR, Kyoto University, Proc. of the 12th Symposium on Accelerator Science and Technology, Wako, Japan, 1999, 51-53 (1999).

Matsui J, Ishi Y, Itano A, Tsunematsu T, Sako K, Kanazawa M, Torikoshi M, Noda K, Yamada S, Hosono K, Noda A, and Sato K : Magnet System of the Synchrotron for Hyogo Hadron Therapy Center, Proc. of the 12th Symposium on Accelerator Science and Technology, Wako, Japan, 1999, 302-304 (1999).

Sawada K, Sakata T, Okanishi K, Miyazaki H, Uno K, Akiyama M, Harada H, Itano A, Higashi A, Akagi T, Kitagawa A, Noda K, Yamada S, Torikoshi M, Noda A, and Hosono K : Design Manufacture and Performance Test of the Injector for Hyogo Hadrontherapy Center, Proc. of the 12th Symposium on Accelerator Science and Technology, Wako, Japan, 1999, 367-369 (1999).

Kokubo T, Ueda S, Itano A, Yamada S, Torikoshi M, Noda K, Noda A, and Sato K: The Accelerator Control System for the Hyogo Hadrontherapy Center, Proc. of the 12th Symposium on Accelerator Science and Technology, Wako, Japan, 1999, 447-449 (1999).

Noda A, Morita A, Noda K, Kumada M, Hiramoto K and Kubo K : Effect of phase relation between ripples of ring dipole and quadrupole magnets on time structure of the slow extracted beam, Proc. of the 12th Symposium on Accelerator Science and Technology, Wako, Japan, 1999, 456-458 (1999).

Yanamoto U, Itano A, Arakawa M, Sakai A, Hosono K, Kanazawa M, Noda A, Noda K, Sato K, Torikoshi M, and Yamada S: Beam Position Monitor of the Synchrotron at Hyogo Hadron Therapy Center, Proc. of the 12th Symposium on Accelerator Science and Technology, Wako, Japan, 1999, 507-509 (1999).

Fujieda M, Iwashita Y, Noda A, Mori Y, Ohmori C, Sato Y, Yoshii M, Blaskiewicz M, Brennan J M, Roser T, Smith K S, Spitz R and Zaltsmann A: Barrier bucket experiment at the AGS, Phys. Rev. ST Accel. Beams 2, 122001 (1999)

Fujieda M, Iwashita Y, Noda A, Mori Y, Ohmori C, Sato Y, Yoshii M, Blaskiewicz M, Brennan J M, Roser T, Smith K S, Spitz R and Zaltsmann A: MAGNETIC ALLOY LOADED RF CAVITY FOR BARRIER BUCKET EXPERIMENT AT THE AGS, Proc. of the 1999 PAC, 857-859 (1999)

Ohmori C, Ezura E, Fujieda M, Mori Y, Muramatsu R, Nakayama H, Sato Y, Takagi A, Toda M, Uesugi T, Yamamoto M, Yoshii M, Kanazawa M and Noda K: HIGH FIELD-GRADIENT CAVITIES LOADED WITH MAGNETIC ALLOYS SYNCHROTRONS, Proc. of the 1999 PAC, 413-417 (1999)

Muramatsu R, Fujieda M, Mori Y, Nakayama H, Ohmori C, Sato Y, Takagi A, Uesugi T, Yamamoto M, Yoshii M, Kanazawa M and Noda K: THE FIRST BEAM ACCELERATION TEST USING HIGH GRADIENT CAVITY AT HIMAC, Proc. of the 1999 PAC, 798-799 (1999)

Yamamoto M, Fujieda M, Hashimoto Y, Mori Y, Muramatsu R, Ohmori C, Sato Y, Takagi A, Uesugi T and Yoshii M: BEAM LOADING EFFECTS ON HIGH GRADIENT MA-LOADED CAVITY, Proc. of the 1999 PAC, 860-862 (1999)

Yamamoto M, Fujieda M, Mori Y, Muramatsu R, Ohmori C, Sato Y, Takagi A, Uesugi T, Yoshii M, Kanazawa M and Noda K: MULTI-HARMONIC ACCELERATION WITH HIGH GRADIENT MA CAVITY AT HIMAC, Proc. of the 1999 PAC, 863-865 (1999)

Sato Y, Fujieda M, Mori Y, Nakayama H, Ohmori C, Muramatsu R, Uesugi T, Yamamoto M, Toda M, Takagi A, Yoshii M, Taniguchi Y and Ohta K: WIDE-BAND PUSH-PULL AMPLIFIER FOR HIGH GRADIENT CAVITY, Proc. of the 1999 PAC, 1007-1009 (1999)

Koba K, Arakawa D, Fujieda M, Ikegami K, Ishi Y, Kanai Y, Kubota C, Machida S, Mori Y, Ohmori C, Shinto K, Shibuya S, Takagi A, Toyama T, Uesugi T, Watanabe T, Yamamoto M, Yokoi T and Yoshii M : LONGITUDINAL IMPEDANCE TUNER USING HIGH PERMEABILITY MATERIAL, Proc. of the 1999 PAC, 1653-1655 (1999)

Ueno R, Matoba M, Adachi T, Fujieda M, Ishi S, Koba K, Machida S, Mori Y, Muramatsu R, Ohmori C, Sakai I, Sato Y, Uesugi T, Umezawa K, Yamamoto Y, Yoshii M, Noda K, Kanazawa M and Yamada S : MULTI-ORBIT SYNCHROTRON WITH FFAG FOCUSING FOR ACCELERATION OF HIGH INTENSITY HADRON BEAMS, Proc. of the 1999 PAC, 2271-2273 (1999)

Blaskiewicz M, Brennan J M, Roser T, Smith K, Spitz R, Zaltzman A, Fujieda M, Iwashita Y, Noda A, Yoshii M, Mori Y, Ohmori C and Sato Y: BARRIER CAVITIES IN THE BROOKHAVEN AGS, Proc. of the 1999 PAC, 2280-2282 (1999)

Muramatsu R, Fujieda M, Mori Y, Ohmori C, Sato Y, Yamamoto M, Kanazawa M, Noda K: Bunch Rotation using Sawtooth RF, Proc. of the 12th Symposium on Accelerator Science and Technology, 102-103 (1999)

Fujieda M, Iwashita Y, Noda A, Mori Y, Muramatsu R, Ohmori C, Sato Y, Yamamoto M, Yoshii M: Study of Adiabatic Condition on Beam Compression with Barrier Bucket, Proc. of the 12th Symposium on Accelerator Science and Technology, 251-253 (1999)

Koba K, Arakawa D, Fujieda M, Ikegami K, Ishi Y, Kanai Y, Kubota C, Machida S, Mori Y, Ohmori C, Shinto K, Shibuya S, Takagi A, Toyama T, Uesugi T, Watanabe T, Yamamoto M, Yokoi T, Yoshii M : Longitudinal impedance tuner using new material FINEMET, Rev. Sci. Inst., Vol.70, No.7, 2988-2992 (1999)

Matsuki S, Tada M, Kishimoto Y, Shibata M, Kominato K, Ooishi C, Funahashi H, Yamamoto K, and Masaike A: Progress in Kyoto axion search experiment, Proceedings of the second international workshop on the identification of dark matter eds. N. J. C. Spooner and V. Kudryavtsev, 441 - 446 (1999)

Yamamoto K, and Matsuki S: Quantum analysis of the Rydberg atom cavity detector of dark matter axions, Nuclear Physics 72B 132 -136 (1999)

Yamamoto K and Matsuki S: Quantum analysis of Rydberg atom cavity detector for dark matter axion search, Proceedings of the second international workshop on the identification of dark matter eds. N. J. C. Spooner and V. Kudryavtsev, 474 - 479 (1999)

Morita A, Noda A, Inoue M, Shirai T, Iwashita Y, Hiramoto K, Katane M, Tadokoro M, Nishi M and Umezawa M: A Compact Proton Synchrotron With Combined-Function Lattice Dedicated For Cancer Therapy, Proc of the 1999 Particle Accelerator Conference, 2528-2530 (1999)

Morita A, Noda A, Iwashita Y, Tadokoro M and Umezawa M: Combined Function Magnet for Compact Proton Synchrotron, Proc. of the 12th Symposium on Accelerator Science and Technology, 305-306 (1999)

RESEARCH FACILITY OF NUCLEIC ACIDS

Kawashima S, Ogata H and Kanehisa M: AAindex: amino acid index database, Nucleic Acids Res., 27, 368-9 (1999)

Kawashima S and Kanehisa M: Knowledge base of biological function based on genome information, Iden, 53(8), 28-31 (1999) (in Japanese)

Kawashima S and Kanehisa M: Pathway database; Making a database of biological activities in a cell, bit, 31(9), 63-70 (1999) (in Japanese)

Nakao M, Bono H, Kawashima S, Kamiya T, Sato K, Goto S and Kanehisa M: Genome-scale gene expression analysis and pathway reconstruction in KEGG, Genome Informatics, 10, 94-103 (1999)

Kawashima S, Kawashima T, Nishida H, Makabe K W and Kanehisa M: MAGEST: ESTs and gene expression pattern database for Halocynthia roretzi maternal cDNA, Genome Informatics, 10, 274-5 (1999)

SEMINARS

Doctor Raul Oscar Barrachina
Centro Atomico Bariloche Comision Nacional de Energia Atomica, Rio Negro, Argentina
"Thomas Mechanism in Electron Capture to the Continuum"
Thursday 29 July 1999

Professor Burkhard Fricke
Department of Physics, University of Kassel, Kassel, Germany
"Single and Double Ionization Cross Section Calculations with the fully Coupled Channel Method"
Thursday 29 July 1999

Professor Shuji Sakabe
Institute of Laser Engineering, Osaka University, Osaka, Japan
"Symmetric Charge-Transfer Cross Sections of Transition Elements in the Impact-Energy Range 30-1000 eV"
Thursday 29 July 1999

Professor Jhon A. Tanis
Department of Physics Kalamazoo, Western Michigan University, MI, U.S.A.
"Double-K-Shell Vacancy Production in Atomic Li"
Thursday 29 July 1999

Doctor Bela Sulik
Institute of Nuclear Research of the Hungarian Academy of Sciences (ATOMKI), Debrecen, Hungary
"Hot Electrons in Relatively Slow (150-250 keV/u) Ion-Atom Collisions"
Thursday 29 July 1999

Professor James H. McGuire
Department of Physics, Tulane University, New Orleans, LA, U.S.A.
"Sequencing in Multielectron Transitions"
Thursday 29 July 1999

Doctor Nikolaus Stolterhoft
Hahn-Meistner Institut Bereich Schwerionenphysik, Berlin, Germay
"Two-K-Vacancy Production by Multielectron Correlation in 95 MeV/u Ar^{18+} + Li Collisions"
Thursday 29 July 1999

Professor Ladislau Nagy
Faculty of Physics, Babes-Bolyai University, Kogalniceanu, Romania
"Electron Correlation in One- and Two-Electron Transitions Induced by Fast Charged Particles"
Thursday 29 July 1999

Professor Horst Schmidt-Bocking
Institut fur Kernphysik, Universitat Frankfurt, Frankfurt, Germany
"A Kinematically Complete Differential Electron Cross Sections in Slow He^{2+} + He: Transfer Ionization"
Thursday 29 July 1999

Doctor Yoh Itoh
Josai University, Tokyo, Japan
"Absolute Photoionization Cross Section Measurement of Xe^{+} Ions in the 4d-Threshold Energy Region"
Thursday 29 July 1999

Professor Steven T. Manson
Department of Physics and Astronomy, Georgia State University, Atlanta, Georgia, U.S.A.
"Photoionization of Ions (Theor)"
Thursday 29 July 1999

Doctor Yoshiro Azuma
Institute of Materials Structure Science High Energy Accelerator Organization, Tsukuba, Japan
"Single, Double, and Triple Photoionization of Lithium"
Thursday 29 July 1999

Professor Winthrop W. Smith
Physics Dept, University of Connecticut, CT, U.S.A
"Electron emission processes in a dense laser-exited Na beam"
Thursday 29 July 1999

Doctor Henning Schmidt
Department of Physics, Stockholm University, Stockholm, Sweden
"Collision Experiments performed at the Cryring Gas-Jet"
Thursday 29 July 1999

Professor Jean-Pierre Briand
Eris University Pierre et Marie Curie, Paris, France
"X Rays from Hollow Atoms"
Thursday 29 July 1999

Professor Kenji Kimura
Department of Engineering Physics and Mechanics, Kyoto University, Kyoto, Japan
"Electron Emission from Surfaces"
Thursday 29 July 1999

Professor Martin Stockli
Kansas State University
"X-Ray Emission by Highly Charged Ar Impact on SiO_2"
Thursday 29 July 1999

Professor Hiroyuki Torii
University of Tokyo
"Capillary Transmission of Highly Charged Ions"
Thursday 29 July 1999

Doctor John Gillaspy
National Institute of Standards and Technology (NIST), MD, U.S.A
"Atomic Resolution STM Image of HOPG"
Thursday 29 July 1999

Doctor Baerbel Siegmann
Fakultat fur Physik, Universitat Bielefeld, Bielefeld, Germany
"Ion-Impact Ionization and Fragmentation of Molecules"
Friday 30 July 1999

Professor Bernd Huber
CEA, Grenoble, France

"Heavy-Ion Cluster Collisions"
Friday 30 July 1999

Professor Kazuhiko Okuno
Department of Physics, Tokyo Metropolitan University, Tokyo, Japan
"Fragmentation of Diatomic Molecules in Slow Multiply Charged Ion Collisions"
Friday 30 July 1999

Professor Kazuhiro Yabana
Graduate School of Science and Technology, Niigata University, Niigata, Japan
"Ion-Cluster Collisions: Theory and Experiment"
Friday 30 July 1999

Doctor Gerald Gwinner
Max-Planck-Institute fur Kernphysik, Heidelberg, Germany
"Electron-Ion Recombination at Very Low Energies"
Friday 30 July 1999

Professor Dirk Schwalm
Max-Planck-Institute fur Kernphysik, Heidelberg, Germany
"Collisional Break-Off of Molecules"
Friday 30 July 1999

Professor Tohru Kinugawa
JCT, Chofu, Tokyo
"Performance of the Tokyo EBIT for the Collision Experiments with Highly Charged Ions"
Friday 30 July 1999

Doctor John Gillaspy
National Institute of Standards and Technology (NIST), MD, U.S.A
"Photon Emission by the Ion Cloud in the NIST EBIT"
Friday 30 July 1999

Doctor Jose R. Crespo-Lopez-Urrutia
Department of Physics, Universitat Freiburg, Freiburg, Germany
"Status of the Freiburg Electron Beam Ion Trap FreEBIT: A New Source for High-Z Hydrogenic Ions"
Friday 30 July 1999

Professor Tatsuaki Kanai
NIRS, Chiba
"Topics in Heavy-Ion Radiotherapy"
Friday 30 July 1999

Professor Chii-Dong Lin
Department of Physics, Kansas State University, KS, U.S.A
"p^+/p^- and e^+/e^- Collisions with Negative Ions at Low Energies"
Friday 30 July 1999

Doctor Brett D. DePaola
Department of Physics, Kansas State University, KS, U.S.A
"Progress in the MOTRIMS Project: Ion-Atom Collisions with a MOT Target"
Friday 30 July 1999

Professor Itzik Ben
Department of Physics, Kansas State University, KS, U.S.A
"Charge Transfer in very slow (milli-eV) $H^+ + D(1s)$ collisions"
Friday 30 July 1999

Professor Wah Chiu
National Center for Macromolecular Imaging, Baylor College of Medicine, USA
"Electron Crystallography of Biological Particles"
Thursday 25 March 1999

Dr. Yoshihide Fukahori
Materials Develop Department, Bridgestone Corporation, Yokohama, Japan
"Fracture and Fatigue of Polymeric Materials"
Friday 22 January 1999

Dr. Bernard Lotz
Institut Charles Sadron (CNRS-ULP), Strasbourg, France
"Frustrated Polymer Crystal Structures"
Saturday 30 January 1999

Prof. Jean-Marc di Meglio
Department of Applied Mathematics, Australian National University, Australia
"Micromanipulation of Absorbed Polymer Chains Using an Atomic Force Microscope (AFM)"
Monday 15 March 1999

Dr. Yoshihide Fukahori
Materials Develop Department, Bridgestone Corporation, Yokohama, Japan
"Reinforcement of Polymeric Materials"
Wednesday 17 March 1999

Dr. Regina Valuuzi
Biotechnology Center, Tufts University, Boston, USA
"Structural Study of Silk"
Friday 2 April 1999

Dr. Mary Anne Mehta
Faculty of Engineering, Shizuoka University, Hamamatsu, Japan
"Polymer Solid Electrolytes - A Miscellany"
Wednesday 26 May 1999

Prof. Kuang SHIN-JUN
Pulp and Paper Industrial Research Institute of China, Beijing, China
"The Development of Non-Wood Fiber in Pulp and Paper Industry"
Thursday 3 June 1999

Prof. Kazuyoshi Iwata
Faculty of Engineering, Fukui University, Fukui, Japan
"New Theoretical Approach for Entanglement Couplings in Polymers - Rubber Elasticity and Polymer Crystallization"
Thursday 2 September 1999

Prof. Tomoo Shiomi
Faculty of Engineering, Nagaoka University of Technology, Nagaoka, Japan
"Crystallization Behavior in Multi-phase Systems of

Polymers”
Friday 26 November 1999

Dr. Bruce A. Moyer
Oak Ridge National Laboratory, U.S.A.
“Crown Ethers for Selective Extraction of Metal Ions: From Fundamental to Applied Chemistry”
Saturday 4 December 1999

Professor Ingrid Mertig
Institüt für Theoretische Physik, Technische Universität Dresden, Germany
“Microscopic Origin of XMR(X=G, T)”
Monday 22 February 1999

Doctor Claude Chappert
Institut d’Électronique Fondamentale Université Paris Sud, Orsay, France
“Ion Beam Irradiation and Magnetic Nanostructures”
Friday 26 March 1999

Professor Werner Keune
Laboratorium für Angewandte Physik, Gerhard-Mercator-Universität, Duisburg, Germany
“Recent Development of Mössbauer Spectroscopic Studies on Multilayers and Interfaces”
Friday 8 October 1999

Doctor Pierre Beauvillain
Institut d’Électronique Fondamentale Université Paris Sud, Orsay, France
“Recent Results on Spectroscopic Magneto-optics and Non-linear Magnetic-optics”
Monday 25 October 1999

Doctor Lech Tomasz Baczewski
Institute of Physics, Polish Academy of Sciences, Warsaw, Poland
“Magnetic and Magnetotransport Properties of Epitaxial MBE-Grown Co/Cu Multilayers”
Tuesday 16 November 1999

Dr. Masayasu Takeda
Department of Physics, Tohoku University
“Magnetic Artificial Lattice Studied by Polarized Neutron Reflection”
Friday 13 November 1998

Dr. Hitoshi Ohta
Department of Physics, Kobe University
“ESR Measurement under High Magnetic Field and Magnetic Transition in the
Low-dimensional Magnetic System”
Wednesday 10 Febrary 1999

Dr. Masaaki Matsuda
The Institute of Physical and Chemical Research
“Study of the Low-dimensional Copper Oxide by Neutron Scattering”
Wednesday 10 Febrary 1999

Professor Y. J. Uemura
Department of Physics, Columbia University, USA
“μ SR Studies of Doped and Undoped Spin Gap Systems”
Monday 11 January 1999

Professor H. Takagi
Department of Advanced Materials Science and Graduate School of Frontier Sciences,
University of Tokyo
“Heavy Fermion like behaviors in LiV2O4 Spinel”
Wednesday 24 March 1999

Dr. N. D. Zhigadl
National Institute for Research in Inorganic Materials
“Homologous series of high-Tc superconductors (Cu,C)Sr2Can-1CunOy and (Cu,N,C)Sr2Can-1CunOy Synthesized under high pressure”
Thursday 25 March 1999

Professor Paul Hagenmuller
Universite de Bordeaux I
“Solid State Chemistry and Material Science”
Monday 11 November 1999

Professor Thomas P. Seward III
Alfred University
“Fundamental and Technological Problems in Glass Industry”
Monday 5 July 1999

Professor Evaristo Riande
Institute of Science and Technology of Polymers,
National Council of Scientific Research (CSIC),
Madrid, Spain
Theoretical Predictions of the Equilibrium and Dynamic Dielectric Properties of Polymers
Thursday 30 September 1999

Professor John F. Brady
Division of Chemistry and Chemical Engineering,
California Institute of Technology,
Pasadena, CA 91125, USA
Stress Relaxation in Colloidal Dispersions
Thursday 9 December 1999

Associate Professor Hervé Marand
Department of Chemistry and Materials Science and Engineering, Virginia Polytechnic Institute and State University, Virginia, USA
“Equilibrium Melting Temperature and Crystal Growth Rate Analyses of Flexible Chain Polymers”
Friday 14 May 1999

Dr. Jozef Kristiak
Institute of Physics, Slovak Academy of Science, Slovak Republic
“Does Positronium Feel Dynamics of Polymer Chains?”
Monday 21 June 1999

Professor Junji Watanabe
Department of Polymer Chemistry, Tokyo Institute of Technology, Tokyo Japan
“Structure of Liquid Crystalline Polymers and their Formation Processes”
Monday 6 September 1999

Professor David C. Bassett
J. J. Thomson Physical Laboratory, University of Reading, Reading, UK
“Advanced Polyolefine Fibers and Self-Composites: New Materials and New Science”

Friday 10 September 1999

Professor Bernd Ewen
Max-Planck-Institute für Polymerforschung, Mainz, Germany
"Single and Many Chain Behaviour in Melts of Short Chain Homopolymers and Related Binary Blends as Observed by Static and Dynamic Neutron Scattering"
Friday 29 October 1999

Professor Francisco J. Baltá Calleja
Consejo Superior de Investigaciones Científicas, Madrid, Spain
"Application of Synchrotron Radiation to Time-Resolved Scattering of Polymers"
Monday 1 November 1999

Professor Chi Wu
Department of Chemistry, The Chinese University of Hong Kong, Shatin, N. T. Hong Kong
"Internal Motion of Linear Chains and Spherical Microgels in Solution"
Tuesday 2 November 1999

Professor Hajime Tanaka
Institute of Industrial Science, University of Tokyo, Tokyo, Japan
"Slow Dynamics in Complex Fluids"
Thursday 16 November 1999

Professor Yoshio Inoue
Tokyo Institute of Technology, Japan
"Structure, Properties, and Biodegradation of Bacterial Polyesters"
Monday 18 January 1999

Dr. Giichi Tanabe
National Institute of Materials and Chemical Research, Japan
"Possibilities of Polysilanes as Advanced Materials"
Thursday 11 March 1999

Professor Toshio Nishi
The University of Tokyo, Japan
"Structure Formation in Crystalline Polymer Blends"
Tuesday 16 March 1999

Prof. Eduardo Humeres
Universidade Federal de Santa Catarina
"Supermolecular Catalysis by Water Induced by Polysaccharides. p-Nitrobenzyl Amyloses Xanthate"
Monday 4 October 1999

Dr. Andrew K. Wittaker
University of Queensland, Australia
"NMR and MRI Studies of Swellable Polymer Devices"
Monday 1 November 1999

Professor Dax Kukulf
University of Warwick, UK
"Snthesis of Functional Polymers by Living Radical Polymerization"
Wednesday 3 February 1999

Professor Kanji Kajiwara
Faculty of Engineering and Design, Kyoto Institute of Technology, Kyoto, Japan
"Structure Formation of Glycopolymers in Solution"
Friday 26 February 1999

Professor Krzysztof Matyjaszewski
Carnegie Mellon University, USA
"Comparison of Several Controlled Radical Polymerization Systems"
Wednesday 21 July 1999

Professor Leonardus W. Jenneskens
Utrecht University, Utrecht, The Netherlands
"The Case of Imperfect Combustion; (non)-Alternant PAH, Soot and Carbon Allotropes"
Thursday 20 May 1999

Professor Yves Rubin
Department of Chemistry and Biochemistry, University of California, Los Angeles,
Los Angeles, U.S.A.
"Very Recent Advances in the Chemistry of C_{60} and Approaches to Endohedral Metallofullerenes"
Saturday 5 June 1999

Professor Herbert Mayr
Department of Organic Chemistry, Ludwig Maximilians University of Munich, Munich, Germany
"Reactivity Scales for Predicting Polar Organic and Organometallic Reactions"
Thursday 14 October 1999

Professor Philip E. Eaton
Department of Chemistry, University of Chicago, Chicago, U.S.A.
"Octanitrocubane: Challenge and Rewards"
Thursday 21 October 1999

Professor Yitzhak Apeloig
Technion-Israel Institute of Technology, Israel
"Low-coordination Silicon Compounds. Experiment and Theory"
(mostly about silylene, disilenes, triple bouds and silyl radicals)
Monday 12 April 1999

Professor Dainis Dakternieks
Deakin University, Australia
"Organotin Chemistry - Pathways to New Materials and Chirotechnology"
Wednesday 21April 1999

Professor Michael Brook
McMaster University, Canada
"New Materials from Silicones and Biopolymers"
Tuesday 1 June 1999

Professor Peter Jutzi
University Bielefelt, Germany
"Cyclopendadienyl ñ Metal Complexes"
Tuesday 1 June 1999

Professor Robert West
University of Wisconsin, Madison, USA
"Low-Coordinate Silicon Compounds - Some Recent Results"
Tuesday 1 June 1999

Professor Emeritus Akira Nakamura
Osaka University, Osaka, Japan
"Polymerization of Olefins Catalyzed by Organotantalum Compounds"
Monday 21 June 1999

Professor Konrad Seppelt
Free University, Berlin
"Small Molecules Made from Electronegative Elements"
Thursday 30 September 1999

Professor Guy Bertrand
Paul Sabatier University, France
"Stable Carbenes and Related Species"
Thursday 7 October 1999

Professor Yoshito Tobe
Department of Fundamental Chemical Engineering, Osaka University
"Enthalpy-Entropy Compensation in Chiral Molecular Recognition"
Tuesday 12 January 1999

Professor Kenji Koga
Nara Institute of Science and Technology
"Synthesis of Lithium Amide and Approach to Asymmetric Catalysis"
Thursday 4 February 1999

Professor Masahiro Hirama
Graduate School of Science, Tohoku University
"Paramagnetic Chromoprotein Antibiotics Mechanism and Synthesis"
Tuesday 16 March 1999

Professor Mugio Nishizawa
Faculty of Pharmaceutical Sciences, Tokushima Bunri University
"Olefin Cyclization Using Mercury Triflate"
Tuesday 16 March 1999

Associate Professor Katsuhiko Tomooka
Department of Chemical Engineering, Tokyo Institute of Technology
"Development and Progress in Carbanion [1,2]-Rearrangement"
Friday 23 April 1999

Professor Gerrit-Jan Koomen
University of Amsterdam
"Biomimetic Synthesis of Nitraria Alkaloids"
Thursday 27 May 1999

Professor Peter M·tyus
Semmelweis University, Hungary
"Synthesis of Novel 4,5-Fused Pyridazines with Biological Interest"
Saturday 29 May 1999

Dr. Ganesh Pandey
National Chemical Laboratory, India
"Newer Synthetic Designs Involving Non-Stabilized Azomethine Ylides"
Tuesday 5 October 1999

Professor Volker Jäger
University of Stuttgart, Germany
"Synthesis of New Carbo-and Heterocyclic Structures and Their Biological Evaluation as Glyosidase Inhibitors"
Thursday 11 November 1999

Professor Daniel Bellus
Fribourg University, Germany
"Synthetic Successes and Surprises with Cyclobutane"
Friday 26 November 1999

Dr. Michel Miesch
Directeur de Recherche CNRS, Strasbourg, France
"Strain Assisted Total Synthesis of Natural Products"
Friday 26 November 1999

Professor Yoshimitsu Nagao
Faculty of Pharmaceutical Science, The University of Tokushima
"Development of New Reactions and Medicines based on Non-covalent Interactions"
Wednesday 15 December 1999

Professor Hiroshi Terada
Faculty of Pharmaceutical Science, The University of Tokushima
"Dynamics of Transmitting Fuction of Transporter and its Mechanism for Recognition of Medicines"
Wednesday 15 December 1999

Prof. K. S. Feldman
Pennsylvania State Univeristy
"Ellagitannin Chemistry"
Friday 9 April 1999

Dr. Roland Furstoss
CNRS, Marseille, France
"Biocatalysis in fine organic synthesis: some illustrative applications"
Monday 15 November1999

Professor Joanna Strosznajder
Laboratory of Cellular Signaling, Medical Research Center, Polish Academy of Sciences,Warsaw, Poland
"Nitric Oxide in Adult and Aged Brain: Effect of Aβ"
Wednesday 17 March 1999

Dr. Robert Strosznajder
Department of Neurophysiology, Medical Research Center, Polish Academy of Sciences,Warsaw, Poland
"Aggregated beta amyloid 1-40 decreases Ca^{2+} and cholinergic receptor-mediated phosphoinositides degradationby alteration of membrane and cytosolic phospholipase C in brain cortex"
Wednesday 21 April 1999

Dr. Yoshihiko Hirose
Pharmaceutical Enzyme Division, Amano Pharmaceutical Co., Ltd. Japan
"Approach towards the Applications of Biocatalytic Reactions"
Monday 18 January 1999

Professor Peter Schreier
Department of Food Chemistry, University of Wüzburg, Germany
"Biocatalysis and Flavour Formation"

Monday 6 September 1999

Professor Taichi Usui
Department of Agriculture, Shizuoka University, Japan
"Glycotechnological Studies on Oligosaccharide-Chain Library Preparation and Their Functionalization"
Monday 27 September 1999

Professor Yutaka Ebizuka
Graduate School of Pharmaceutical Sciences, The University of Tokyo, Japan
"Structure and Function of Synthetic Enzymes of Natural Products"
Friday 10 December 1999

Professor Shigeo Yoshida
Plant Functions Laboratory, The Institute of Physical and Chemical Research (RIKEN)
"Prospects for the Plant Regulation Science Towards the 21st Century"
Monday 20 December 1999

Professor Jennifer Littlechild
University of Exeter, UK
Structural Studies on Enzymes Important in Biotransformation Reactions
Saturday 5 June 1999

Dr. Jiri Damborsky
Masaryk University, Czech Republic
"Application of Computer Modelling and Bioinformatics for Study of the Microbial Degradation of Xenobiotic Compounds"
Friday 15 October 1999

Professor Chris Bowler
Molecular Plant Biology Laboratory, Stazione Zoologica, Napoli, Italy
"Molecular Genetic Dissection of Light Signal Transduction in Tomato"
Wednesday 18 February 1999

Dr. Tamaki Watanabe
High Energy Accelerator Research Organization (KEK), Japan
"Heavy Ion Cooler Storage Ring, TARN II"
Wednesday 6 January 1999

Professor Satoru Yamada
National Institute of Radiological Sciences, Japan
"HIMAC and Related Science"
Thursday 21 January 1999

Dr. Kimikazu Sasa
Research Laboratory for Nuclear Reactors, Tokyo Institute of Technology, Japan
"Plasma Generation by High Intensity Ion Beam using RFQ Linac"
Wednesday 24 February 1999

Professor Kazuhisa Nakajima
High Energy Accelerator Research Organization (KEK), Japan
"High Brightness laser and Beam-Plasma Interaction"
Wednesday 30 June 1999
Thursday 1 July 1999

Dr. Jean- Michel Lagniel
CEA- Saclay, DSM/ DAPNIA/ SEA, France
"High Intensity Linac Studies in France"
Thursday 9 September 1999

Dr. Eric Esarey
Lawrence Berkeley National Laboratory, USA
"Laser synchrotron light via Thomson scattering and applications"
Wednesday 20 October 1999

MEETINGS AND SYMPOSIUMS

Germany-Japan Joint Seminar on Polymer Materials

29 September 1999

1. New materials via ring opening polymerization
   H. Höcker
   Technische Hochschule Aachen

2. Rotaxanes with Cucurbituril and α-cyclodextrin
   E. Schollmeyer
   Deutsches Textilforschungszentrum Nord-West e.V.

3. New polymer materials synthesized by controlled radical polymerizations
   T. Fukuda
   ICR, Kyoto University

4. New inisurfs and surfmers for core-shell particles
   H.-J. P. Adler
   Technische Universität Dresden

5. Dynamical heterogeneity of amorphous polymers
   T. Kanaya
   ICR, Kyoto University

6. Association of AB-blockcopolymers in nematic solvents
   H. Finkelmann
   Universität Freiburg

7. Rheology of diblock copolymer micelles
   H. Watanabe
   ICR, Kyoto University

8. Layered silicates: anisotropic fillers for improved mechanical properties of polymers
   W. Gronski
   Universität Freiburg

9. Fine structures in crystalline polymer materials as revealed by transmission electron microscopy
   M. Tsuji
   ICR, Kyoto University

10. Structure and properties of blown cellulose films
    H.-P. Fink
    Fraunhofer Institut Angewandte Polymerforschung

11. Melt spinning - a special process of polymer processing under different view points
    R. Beyreuther
    Institut für Polymerforschung Dresden

THESES

YAMAGUCHI, Koichiro
D Sc, Kyoto University
“The regularization of the basic x-ray absorption spectrum fine structure equation via the wavelet-Galerkin method”
Supervisor: Professor Mukoyama T
Tuesday 23 March 1999

Osawa, Daisuke
D Sc, Kyoto University
“K-shell internal ionization and excitation in b decay of ^{35}S”
Supervisor: Professor Mukoyama T
Wednesday 24 November 1999

IRIE, Satoshi
D Sc, Kyoto University
"The Effects of Molecular Shape on Organic Monolayer Epitaxy"
Supervisor: Professor Kobayashi T
24 May 1999

KAWASAKI, Shuji
D Sc, Kyoto University
"High Pressure Synthesis and Physical Properties of Fe^{4+}-containing Perovskite Type Oxide with Charge-transfer type Electronic structure"
Supervisor: Professor Takano M
23 March 1999

SAKIDA, Shinichi
D Eng, Kyoto University
“Studies on Structure of Tellurite Glasses”
Supervisor: Yoko T
23 March 1999

OHNO, Kohji
D Eng, Kyoto University
“Synthesis and Properties of Novel Types of Glycopolymers”
Supervisor: Professor Miyamoto T
23 March 1999

YAMADA, Kenji
D Eng, Kyoto University
“Controlled Synthesis of Glycopolymers by Living Polymerization Techniques”
Supervisor: Professor Miyamoto T
23 March 1999

TSUBAKI, Kazunori
D Pharm Sci, Kyoto University
“Creation of Functional Molecules Possessing Cyclic Polyether Moiety”
Supervisor: Professor Fuji K
25 January 1999

WATANABE, Toshiyuki
“Studies on Asymmetric Olefination Using Optically Active Phosphonate Reagents”
Supervisor: Professor Fuji K
23 March 1998

TANAKA, Akira
“Syntheses and Structure-Activity Relationship of New Type of ACAT Inhibitors”
Supervisor: Fuji K
24 September 1998

HIDA, Kouichi
D Sc, Kyoto University
"Synthesis of Optically Active Alcohols Using Reductase from Bakers' Yeast"
Supervisor: Associate Professor Nakamura K
23 July 1999

KEURA, Yoshinori
D Pharm Sci, Kyoto University
“Studies on Syntheses and Stereochemistry of New Inhibitors of Tachykinun NK, Receptor”
Supervisor. Professor Sugiura Y
25 January 1999

INOUE, Teruhiko
D Pharm Sci, Kyoto University
“Chemical Clarification and Model Assembly of Cellular Signal Transmission and Transcription Reaction”
Supervisor, Professor Sugiura Y
23 March 1999

AIZAWA, Yasunori
D Pharm Sci, Kyoto University
“Recognition Mechaniom of DNA Swquences by Dimer Proteins”
Supervisor, Professor Sugiura Y
23 March 1999

KUSAKABE, Tetsuya
D Pharm Sci, Kyoto University
“DNA Recognition and Strand Scission by Enediyne Antitumor Antibiotic Dynemicin A”
Supervisor. Professor Sugiura Y
24 May 1999

SATAKE, Honoo
D Pharm Sci, Kyoto University
“Gene Sequences and Gene Expression of Bioactive Peptides from Mollusca and Annelida”
Supervisor. Professor Sugiura Y
24 November 1999

ASADA, Shinichi
D Med, Kyoto University
“The Effect of HSP47 on Prolyl 4-hydroxylation of Collagen Model Peptides”
Supervisor: Professor Nagata K
24 September 1999

NISHIYAMA, Akira
D Med, Kyoto University
“Identification of Thioredoxin-Binding Protein 2/Vitamin D_3 Up-regulated Protein 1 as a Negative Regulator of Thioredoxin Function and Expression”
Supervisor: Professor Yodoi J
24 November 1999

FUCHIKAMI, Yoshihiro
Enzymological Studies of Fragmentary D-Amino Acid Aminotransferases

D Agr, Kyoto University
Supervisor: Professor Esaki N
23 July 1999

MIHARA, Hisaaki
Enzymological Studies of Cysteine Desulfurase and Selenocysteine Lyase
D Agr, Kyoto University
Supervisor: Professor Esaki N
24 September 1999

WATANABE, Akira
Mechanistic Studies of Alanine Racemase from *Bacillus stearothermophilus*
D Agr, Kyoto University
Supervisor: Professor Esaki N
24 September 1999

KIHARA, Daisuke
D Sci, Kyoto University
Development of Method for Predicting Membrane Proteins and Analysis of Their Distribution in Genomes
Supervisor: Professor Kanehisa M
24 May 1999

WATANABE, Tamaki
D Sci, Kyoto University
"Study of Beam Orbit and Development of High Sensitivity Beam-Position Monitor for Orbit Correction at the Heavy Ion Cooler Synchrotron TARN II"
Supervisor: Professor Noda A
23 March 1999

ORGANIZATION AND STAFF

INSTITUTE FOR CHEMICAL RESEARCH
KYOTO UNIVERSITY

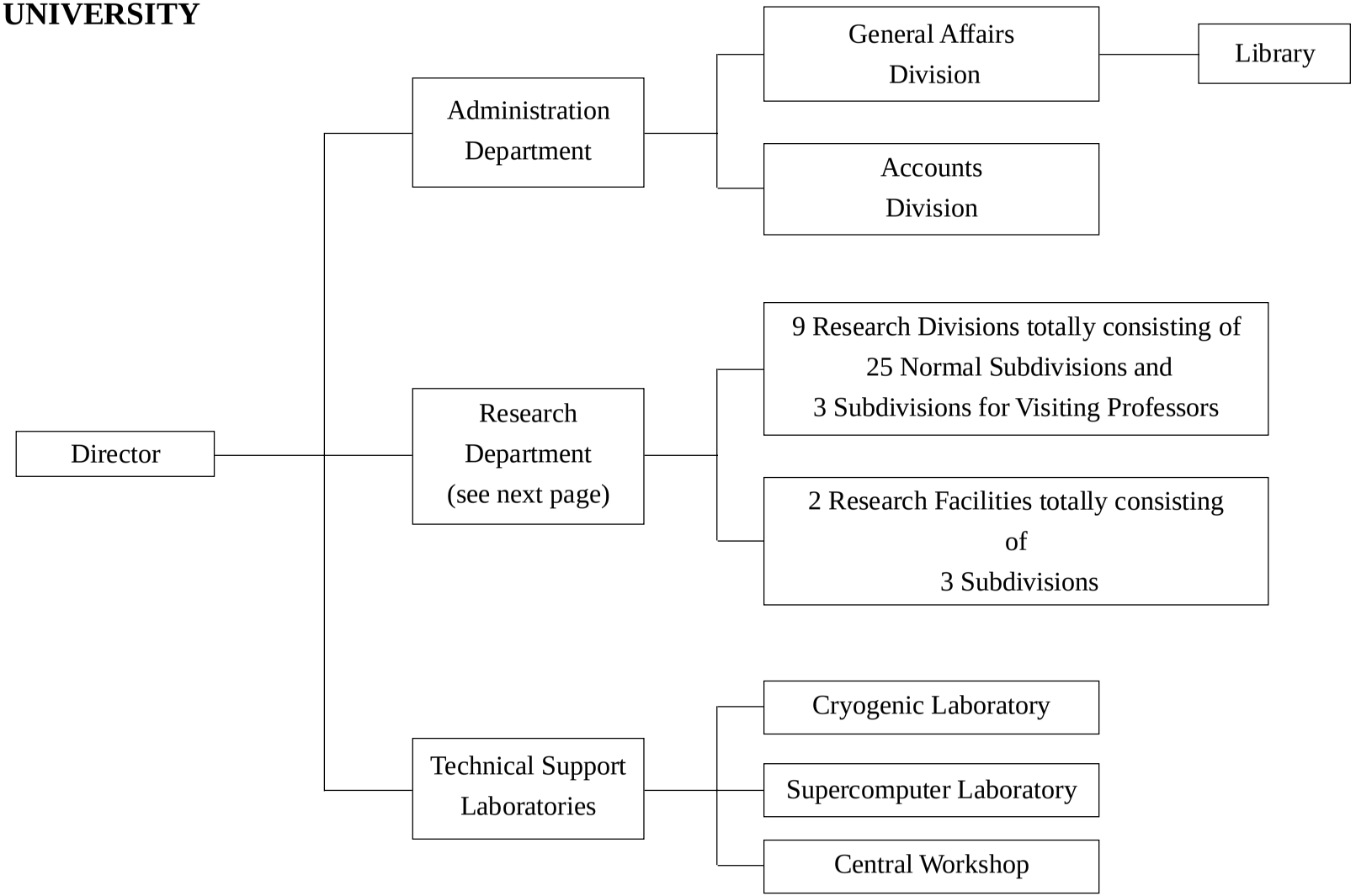

INSTITUTE FOR CHEMICAL RESEARCH, KYOTO UNIVERSITY As of 31 December 1999

RESEARCH DIVISION (G: Laboratory for Visiting Professors)

	Research Division	**Subdivision (Laboratory)**	**Related Graduate School** *Graduate School of / Division of*	**Professor**	**Associate Professor**	**Instructor**
Director SUGIURA, Yukio	States and Structure	I. Atomic and Molecular Physics	*Science / Physics I*	MUKOYAMA, Takeshi	ITO, Yoshiaki	KATANO, Rintarou NAKAMATSU, Hirohide
		II. Crystal Information Analysis	*Science / Chemistry*	KOBAYASHI, Takashi	ISODA, Seiji	OGAWA, Tetsuya NEMOTO, Takashi
		III. Polymer Condensed States	*Engineering / Polymer Chemistry*	KOHJIYA, Shinzo	TSUJI, Masaki	URAYAMA, Kenji TOSAKA, Masatoshi MURAKAMI, Syozo
	Interface Science	I. Solutions and Interfaces	*Science / Chemistry*	NAKAHARA, Masaru	UMEMURA, Junzo	MATSUMOTO, Mutsuo MATSUBAYASHI, Nobuyuki
		II. Molecular Aggregates	*Science / Chemistry*	SATO, Naoki	ASAMI, Koji	KITA, Yasuo YOSHIDA, Hiroyuki
		III. Separation Chemistry	*Science / Chemistry*		UMETANI, Shigeo	SASAKI, Yoshihiro HASEGAWA, Hiroshi
	Solid State Chemistry	I. Artificial Lattice Alloys	*Science / Chemistry*	SHINJO, Teruya	HOSOITO, Nobuyoshi	
		II. Quantum Spin Fluids	*Science / Chemistry*	YAMADA, Kazuyoshi	MIBU, Ko	IKEDA, Yasunori
		III. Multicomponent Materials	*Science / Chemistry*	TAKANO, Mikio	TERASHIMA, Takahito	AZUMA, Masaki
		IV. Amorphous Materials	*Engineering / Molecular Engineering*	YOKO, Toshinobu	UCHINO, Takashi	TAKAHASHI, Masahide
		G. Structure Analysis		MAEKAWA, Sadamichi	HOSONO, Hideo	
	Fundamental Material Properties	I. Molecular Rheology	*Engineering / Molecular Engineering*	OSAKI, Kunihiro	WATANABE, Hiroshi	INOUE, Tadashi
		II. Polymer Materials Science	*Engineering / Polymer Chemistry*	KAJI, Keisuke	KANAYA, Toshiji	NISHIDA, Koji
		III. Molecular Dynamic Characteristics	*Engineering / Molecular Engineering*	HORII, Fumitaka	TSUNASHIMA, Yoshisuke	KAJI, Hironori
		G. Composite Material Properties		MATSUURA, Kazuo HANABUSA, Kenji		
	Organic Materials Chemistry	I. Polymeric Materials	*Engineering / Polymer Chemistry*	MIYAMOTO, Takeaki	FUKUDA, Takeshi	TSUJII, Yoshinobu MINODA, Masahiko
		II. High-Pressure Organic Chemistry	*Engineering / Energy & HC Chemistry*	KOMATSU, Koichi		MORI, Sadayuki MURATA, Yasujiro NISHINAGA, Tohru
	Synthetic Organic Chemistry	I. Synthetic Design	*Engineering / Energy & HC Chemistry*	TAMAO, Kohei	TOSHIMITSU, Akio	KAWACHI, Atsushi YAMAGUCHI, Shigehiro
		II. Fine Organic Synthesis	*Pharmaceutical Sci. / Pharmac. Chem.*	FUJI, Kaoru	KAWABATA, Takeo	TSUBAKI, Kazunori
		G. Synthetic Theory		TANAKA, Hirokaza	TOMOOKA, Katsuhiko	
	Bioorganic Chemistry	I. Bioorganic Reaction Theory	*Science / Chemistry*		NAKAMURA, Kaoru	KAWAI, Yasushi SUGIYAMA, Takashi
		II. Bioactive Chemistry	*Pharmaceutical Sci. / Drug System*	SUGIURA, Yukio	FUTAKI, Shiro	NAGAOKA, Makoto
		III. Molecular Clinical Chemistry	*Medicine / Internal Medicine*	UEDA, Kunihiro	TANAKA, Seigo	ADACHI, Yoshifumi
	Molecular Biofunction	I. Functional Molecular Conversion	*Agriculture / Agricul. Chem.*	SAKATA, Kanzo	HIRATAKE, Jun	MIZUTANI, Masaharu
		II. Molecular Microbial Science	*Agriculture / Agricul. Chem.*	ESAKI, Nobuyoshi	YOSHIMURA, Tohru	KURIHARA, Tatsuo
	Molecular Biology and Information	I. Biopolymer Structure	*Science / Biophysics*		HATA, Yasuo	HIRAGI, Yuzuru FUJII, Tomomi AKUTAGAWA, Tohru
		II. Molecular Biology	*Science / Biophysics*	OKA, Atsuhiro	AOYAMA, Takashi	GOTO, Koji
		III. Biological Information Science	*Science / Biophysics*	KANEHISA, Minoru	GOTO, Susumu	
	Nuclear Science Research Facility	I. Particle and Photon Beams	*Science / Physics II*	NODA, Akira	IWASHITA, Yoshihisa	SHIRAI, Toshiyuki
		II. Beams and Fundamental Reaction	*Science / Physics II*		MATSUKI, Seishi	
	Research Facility of Nucleic Acids		*Science / Biophysics*	KANEHISA, Minoru	SUGISAKI, Hiroyuki	KAWASHIMA, Shuichi

PERSONAL

Obituary

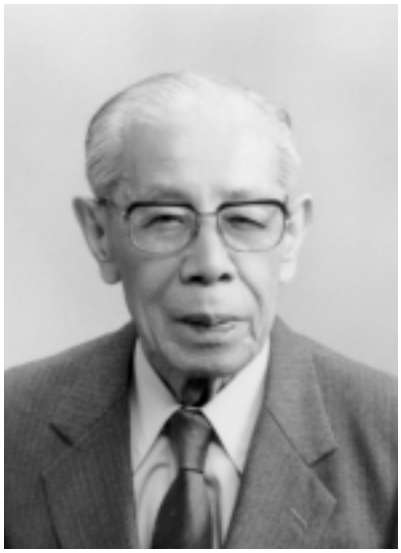

Professor Emeritus
Dr. Waichiro Tsuji (1911 - 1999)

Professor Dr. Waichiro Tsuji, Professor Emeritus of Kyoto University passed away on January 27, 1999 in Kyoto.

Dr. Tsuji was born on February 24, 1911 in Kyoto. He entered the Department of Mechanical Engineering, Faculty of Engineering, Kyoto Imperial University in 1932, and moved to the Department of Industrial Chemistry, Faculty of Engineering in 1935. After the graduation, he went to the Graduate School of Engineering, and got a Doctor degree of Engineering from Kyoto University in 1948. Dr. Tsuji was appointed to Associate Professor of a newly founded Department, the Department of Fiber Chemistry, Faculty of Engineering, Kyoto Imperial University in 1945, and promoted to a full Professor of the Institute for Chemical Research, Kyoto University in 1950 to direct the Laboratory of Fiber Chemistry (presently the Laboratory of Polymer Material Science, Division of Fundamental Material Properties II). From 1967 to 1970 he was elected as the Director of the Institute for Chemical Research, and greatly contributed to the administration of the Institute, especially at the move of the Institute from Takatsuki, Osaka to Uji, Kyoto and in settling the campus disturbances which occurred during this period. He retired from Kyoto University in 1974, honored with the title of Professor Emeritus of Kyoto University. After the retirement, he moved to the Faculty of Home Economics (presently the Graduate School of Human Environmental Science), Mukogawa Women's University as a full Professor in 1974. He was elected as the Dean of the Faculty in 1976, and the Chair of the Graduate School of Human Economics in 1982. Dr. Tsuji retired from Mukogawa Women's University in 1984.

His research field was mainly concerned with fiber chemistry and polymer chemistry. He started his scientific life as a student in the laboratory of Professor Ichiro Sakurada in 1939. At that time Professor Sakurada and his collaborators succeeded in preparing water-insoluble poly(vinyl alcohol) (PVA) fiber, which was given the general name 'vinylon' in Japan in 1948 and later named 'vinal' in the United States. In the beginning, therefore, his research was closely related to vinylon. First, he improved the vinylon fiber and developed a modified vinylon, named vinylon S. Then he invented an emulsion-mixture spinning method where PVA is used as one component to produce a two component composite fiber; using this method a fire retardant fiber of PVA and poly(vinyl chloride) mixture was later developed and industrially produced. He also invented and developed membranes and fibers of polyelectrolyte complex. Furthermore, his research was extended to improvement of properties of fibers. He succeeded in improving several natural fibers by chemical modifications, developing an amorphizing method of fibers, providing hydrophilic properties to hydrophobic fibers by a graft-polymerization method and modifying fibers by chemical cross-linking. In order to test properties of those fibers and fabrics, he developed several testing machines as well; of these, a rotational drum type measuring instrument of electrostatic propensity is noteworthy, which is still now used as a standard testing method in the Japan Industrial Standard (JIS).

Dr. Tsuji devoted himself to the Society of Fiber Science and Technology, Japan. He served as the Manager of Kansai Branch from 1964 to 1972, and then he was elected as the Vice-President of the Society from 1970 to 1972 and as the President from 1972 to 1974. During this period, he organized two investigating commissions as Coordinator, "Study Team of European Chemical Fibers (1971)" and "Study Team of European Non-Woven Fabric Technology (1973)". Dr. Tsuji participated in establishing the Kansai Branch of the Society of Polymer Science, Japan, serving as the Vice-Manager from 1952 to 1963. He was also elected as the Vice-President of the Adhesion Society of Japan from 1965 to 1968. Owing to these efforts, he won the Award for Distinguished Service from the Society of Fiber Science and Technology, Japan in 1980 and also from the Adhesion Society of Japan in 1983. Dr. Tsuji was awarded the Second Class of the Order of the Sacred Treasure for his great academic and educational contributions in 1983.

Retirement

Professor Takeshi Mukoyama (Atomic and Molecular Physics, Division of States and Structure)

On the 31st of March, 2000, Dr.Takeshi Mukoyama retired from Kyoto University after 35 years of service to the University and was honored with the title of Professor Emeritus of Kyoto University.

Dr.Mukoyama was born in Hyogo on the 21th of February, 1937. After graduation from Faculty of Science, Kyoto University in 1959, he continued his studies as a graduate student of the Department of Nuclear Engineering, Faculty of Engineering. He was employed by the Sumitomo Electric Industries, Co. Ltd for 2 years from 1962. In 1964, he was appointed an instructor of the Laboratory of Nuclear Radiation, Institute for Chemical Research, Kyoto University. Under the supervision of the Emeritus Professor Sakae Shimizu, he was granted a doctoral degree from Kyoto University in 1969 for his studies on Radiationless Annihilation of Positrons. On a leave of absence in the year 1977 to 1978, he worked on the Experimental Study of Ion-Atom Collisions in cooperation with Professor D.Berenyi at Institute for Nuclear Research of the Hungarian Academy of Sciences (ATOMKI) in Hungary. In 1988, Dr.Mukoyama was appointed full Professor of Kyoto University and directed the Laboratory of Nuclear Radiation (present name, States and Structure I), Institute for Chemical Research. He took part in Japan-US collaboration on ion-atom collisions and was a principal investigator of Japan-Hungarian collaboration on inner-shell ionization phenomena. He chaired the XVI International Symposium on Ion - Atom Collision, 1999. At the Graduate School of Science, Kyoto University, he gave lectures on High Energy Atomic Spectroscopy and supervised the dissertation works of many graduate students. His sincere and warmhearted character has been admired by his friends, colleagues and students.

During the past 35 years, his research interest encompassed a wide array of atomic physics, radiation physics, and molecular physics. His contribution to the Institute through both academic and administrative activities is hereby gratefully acknowledged, and his academic achievements are briefly described below.

Following his early studies on the interaction between atomic electrons and nucleus, he worked on positron annihilation with K-shell electrons, inner-shell ionization processes in atoms and molecules, ion-atom collisions, and chemical effect in x-ray spectra. He developed a theory which includes exactly the relativistic effect in order to calculate the probability of inner-shell ionization by atomic collisions in heavy elements. Moreover, he quantitatively explained the experimental data with the aid of his developed theory by taking into account of the higher-order processes.

He studied chemical effects in the x-ray spectra, especially the $K\beta$:$K\alpha$ x-ray intensity ratios in Mn and Cr compounds, both theoretically and experimentally. From the observed and calculated results, he first suggested that the difference of the coordination numbers around metal ions affects the $K\beta$:$K\alpha$ ratios for the compounds.

Owing to his international academic efforts, he was honored with the Degree of Honorary Doctor (Doctor Honoris Causa) of Lajos Kossuth University in Hungary in 1994.

NAME INDEX

KEYWORD INDEX